SRC/SEMATECH Engineering Research Center
for Environmentally Benign Semiconductor Manufacturing

2008 ANNUAL REPORT

Core and Selected Customized Projects

February 2008

Section 1

Core Projects

LIST OF CORE PROJECTS

SRC Task # 425.012
CMOS Biochip for Rapid Assessment of New Chemicals

SRC Task # 425.013
Non-PFOS/non-PFAS Photoacid Generators: Environmentally Friendly Candidates for Next Generation Lithography

SRC Task # 425.014
Environmentally Benign Electrochemically Assisted Chemical Mechanical Planarization (E-CMP)

SRC Task # 425.015
Reductive Dehalogenation of Perfluoroalkyl Surfactants in Semiconductor Effluents

SRC Task # 425.016
EHS Impact of Electrochemical Planarization Technologies

SRC Task # 425.017
Environmentally Benign Vapor Phase and Supercritical CO(2) Processes for Patterned Low k Dielectrics

SRC Task # 425.018
Destruction of Perfluoroalkyl Surfactants in Semiconductor Process Waters using Boron Doped Diamond Film Electrodes

SRC Task # 425.019
Low Environmental Impact Processing of sub-50 nm Interconnect Structures

SRC Task # 425.020
An Integrated, Multi-Scale Framework for Designing Environmentally-Benign Copper, Tantalum and Ruthenium Planarization Processes

SRC Task # 425.021
Low-Water and Low-Energy Rinsing and Drying of Patterned Wafers, Nano-Structures, and New Materials Surfaces

SRC Task # 425.022
Environmentally-Friendly Cleaning of New Materials and Structures for Future Micro-and Nano-Electronics Manufacturing

SRC Task # 425.023
ESH Assessment: Materials, Structures and Processes for Nano-Scale MOSFETs with High-Mobility Channel

CMOS Biochip for Rapid Assessment of New Chemicals

(*Task Number: 425.012*)

PIs:

- **David L. Mathine, Optical Sciences, UA**
- **Raymond B. Runyan, Department of Anatomy and Cell Biology, UA**

Graduate Students:

- **None**

Undergraduate Students:

- **None**

Other Researchers:

- **Jadrian Rusche, Department of Anatomy and Cell Biology, UA**
- **Matt Scholz, Department of Plant Sciences, UA**

Cost Share (other than core ERC funding):

- **None**

Objectives

- **Develop a tool for the assessment of toxicity of chemicals.**
- **Develop a cell based biosensor**
  - **Use various mamilian cell lines**
  - **Construct a microscale reaction chamber**
  - **Genetically engineer cells for use as harbingers of toxicity**
- **Validate the device with the known toxin TCE and then evaluate new chemicals.**

ESH Metrics and Impact

1. *Current best technology involves animal studies to determine toxicity of new chemicals.*

2. *Current approaches to solve the problem centers around reduced usage of toxic materials.*

3. *The goal of this work is to determine the toxicity of new chemicals. This work hopes to define standards for toxicity.*

4. *Chemicals will be evaluated prior to introduction into a manufacturing environment.*

Rapid Assessment of Chemicals and Process Chemistries

- *Rapid assessment of chemicals and process chemistries*
- *A smart CMOS substrate is used to monitor cell activity*
- *A first step towards an on-line ESH monitor.*

Mammalian Cells

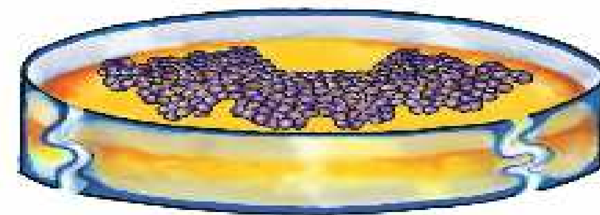

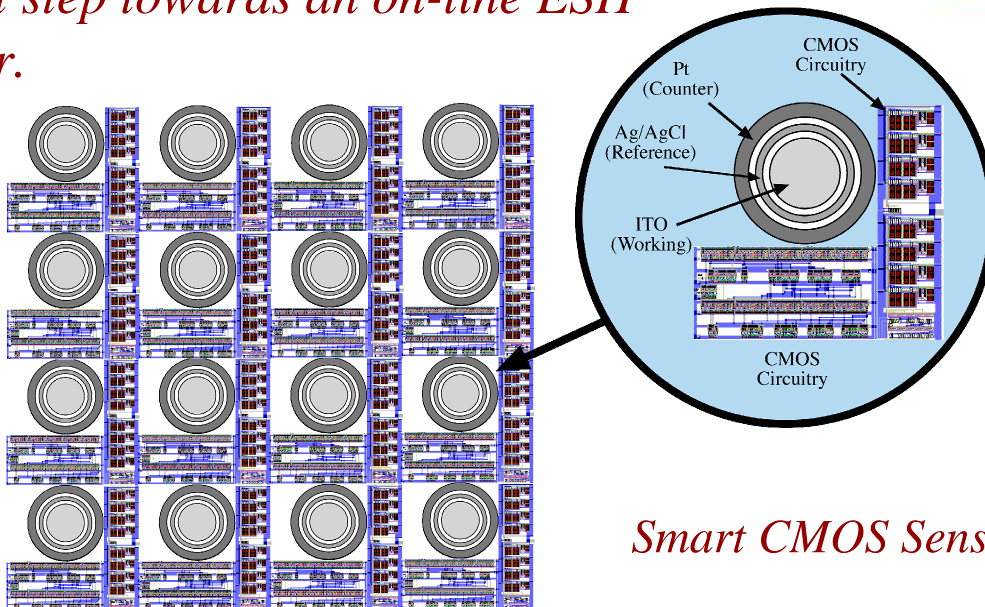

Smart CMOS Sensor

Sensor for Monitoring Cells

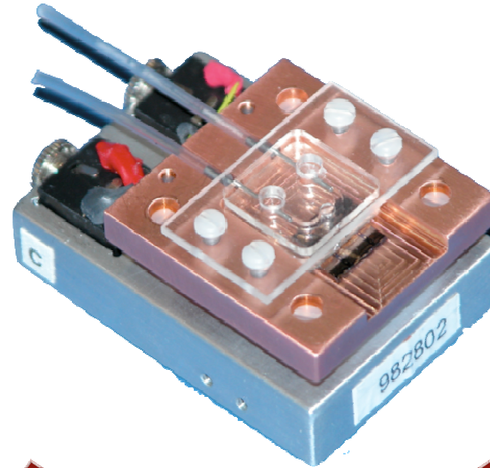

Capacitance Sensor

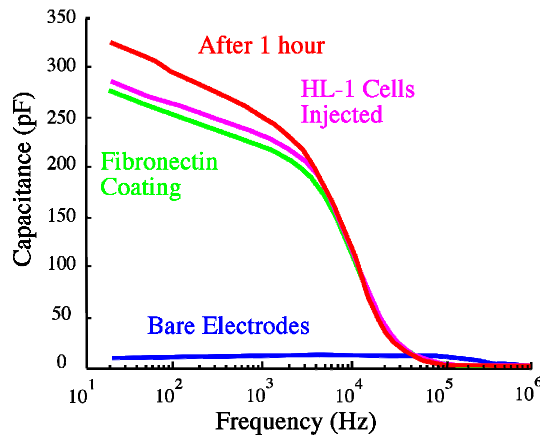

Chemical Sensor

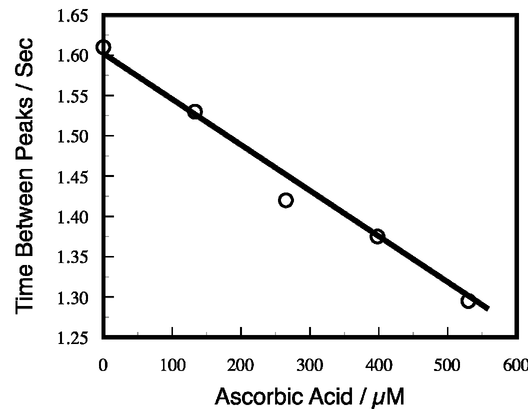

Optical Sensor

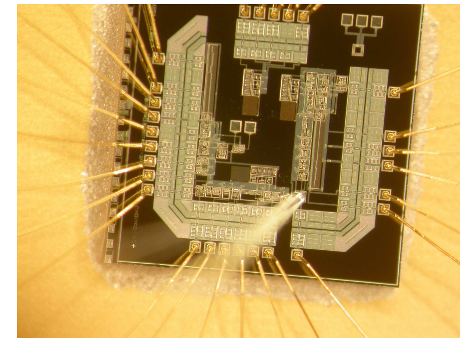

Phenol Red Sensor Development

Nichia LED Emission

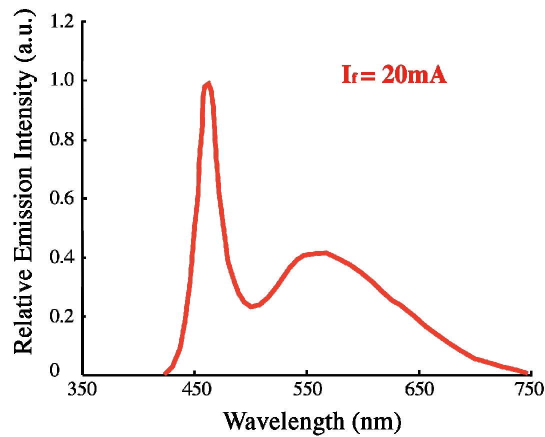

Phenol Red Absorption

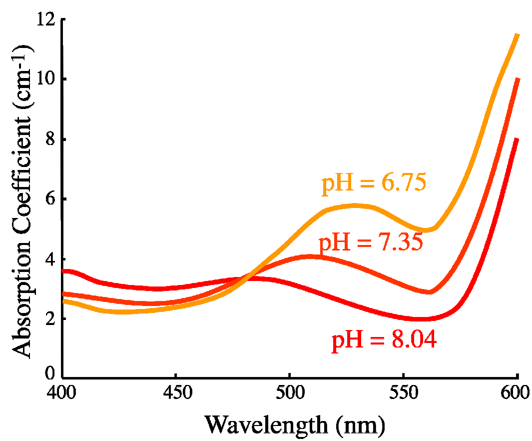

CMOS Photodetector

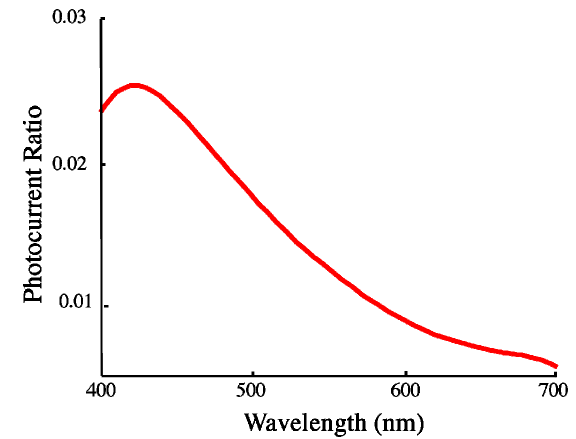

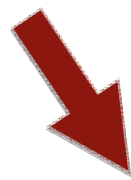

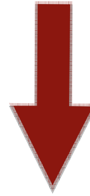

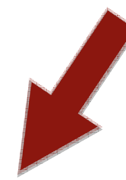

$$S = \frac{\int E(\lambda) e^{-\alpha(\lambda)t} \frac{I_2(\lambda)}{I_1(\lambda)} d\lambda}{\int E(\lambda) e^{-\alpha(\lambda)t} d\lambda}$$

Phenol Red Sensor Development

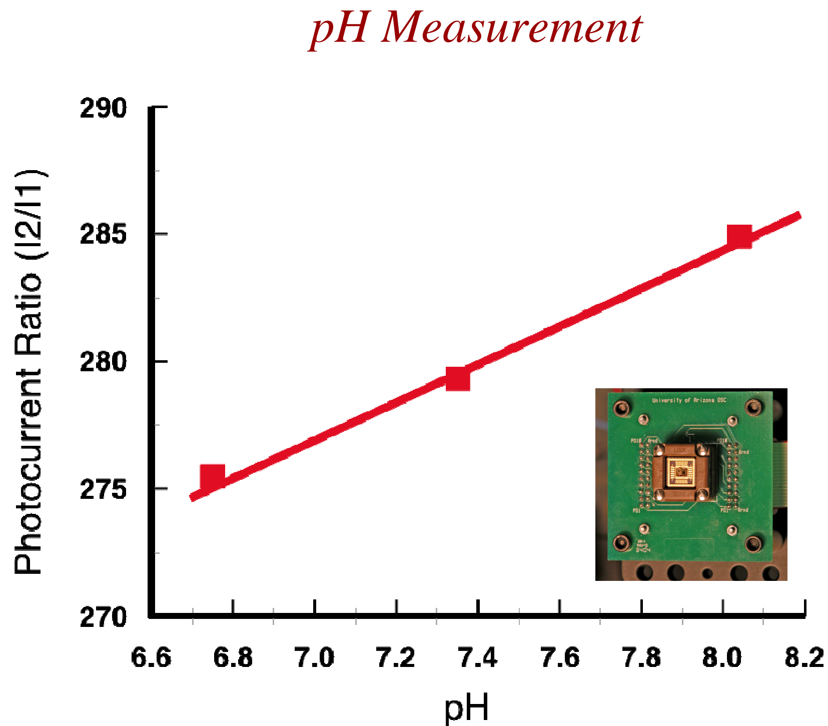

- *Optical determination of pH demonstrated*
- *Shows validity of CMOS photodetectors for use in biological measurements*
- *Readily integratable into biochip sensor*

Measurement of Florescence Labeled Yeast

Argon Laser Source

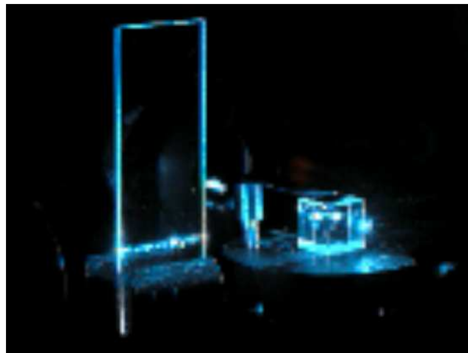

GFP Florescence Spectra

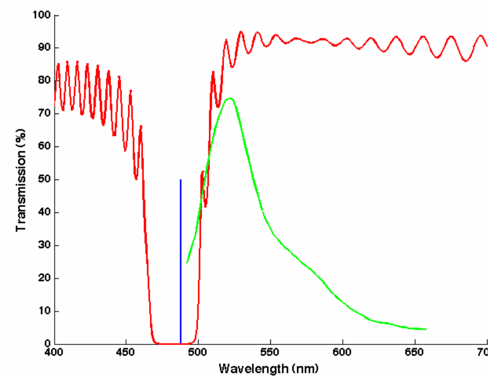

Integrated Optical Filter

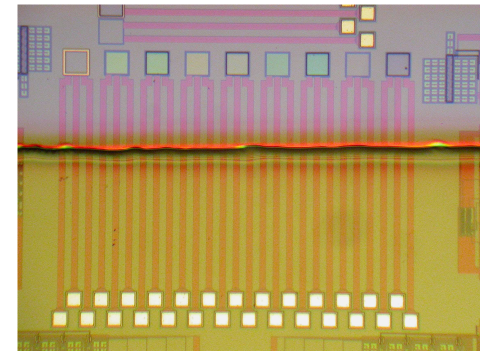

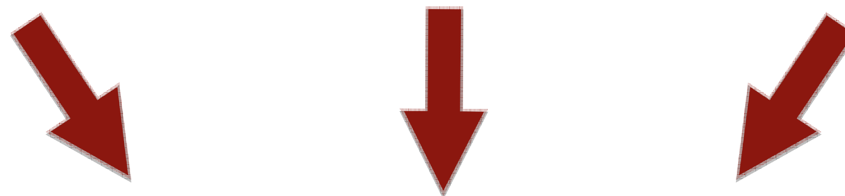

$$S = \frac{\int E(\lambda)F(\lambda)\frac{I_2(\lambda)}{I_1(\lambda)}d\lambda}{\int E(\lambda)F(\lambda)d\lambda}$$

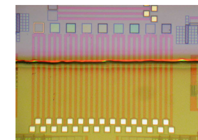

Measurement of Florescence Labeled Yeast

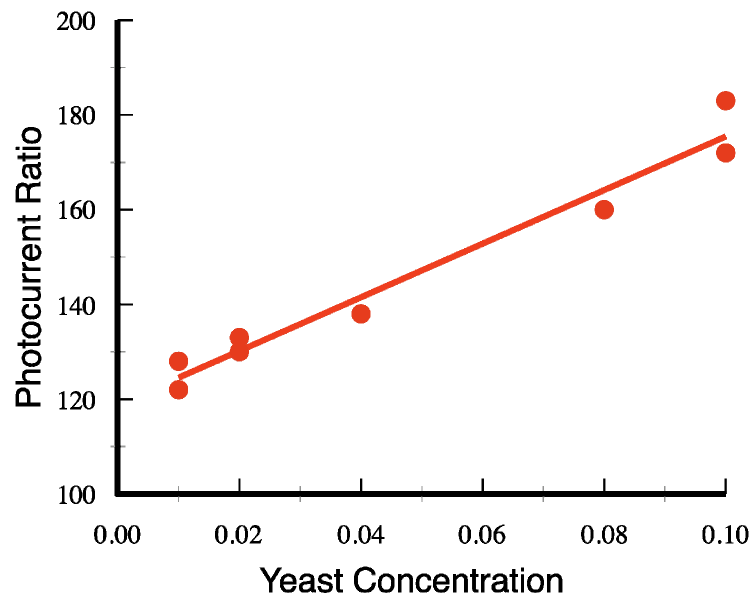

- *Optical determination of pH demonstrated*
- *Shows validity of CMOS photodetectors for use in biological measurements*
- *Sensor is easily integrated into biochip sensor*

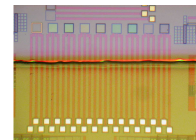

Attachment of Cells to Dielectric Surfaces

Cellular Response

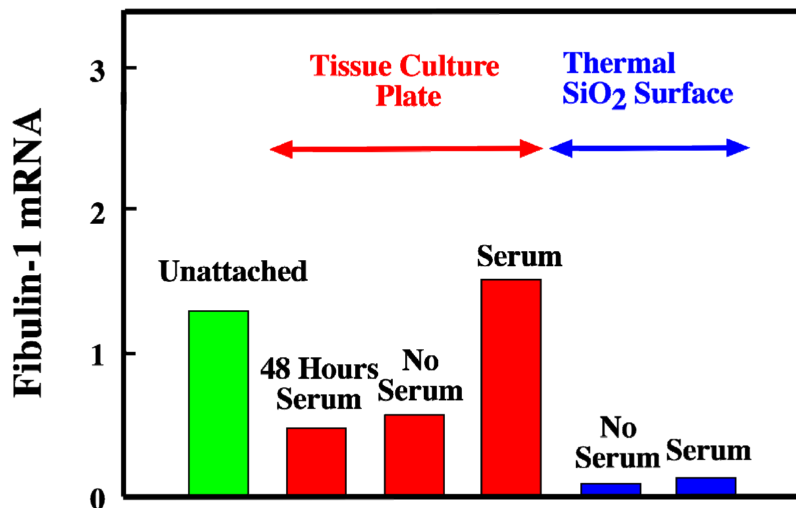

- *The extracellular matrix protein Fibulin-1 was monitored from COS-7 cells.*
- *COS-7 cells attached to SiO_2 surfaces with minimal stimulus.*
- *Mammilian cells show attachment to a variety of common semiconductor manufacturing materials.*

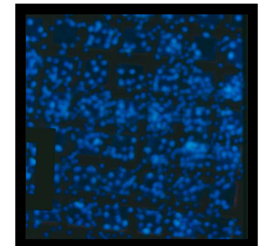

Develop New Techniques for Toxicity Testing

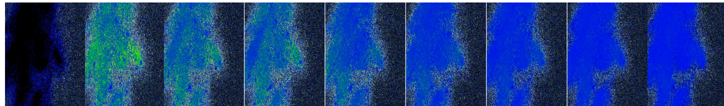

Control for 10ppb/100ppb TCE cells @ 10nM VP

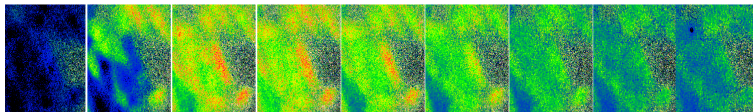

Treated: 10ppb TCE cells @ 10nM VP

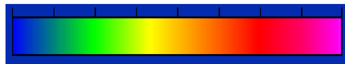

Low Calcium flow High Calcium flow

- *Developed novel technique for toxicity determination*
- *Demonstrated on the known toxic TCE*
- *Next step it to evaluate new chemicals*

Industrial Interactions and Technology Transfer

- **His-An Kwong, Freescale Seminconductor Inc.**
- **Phil Naughton, SEMATECH**
- **Thomas S. Roche, Freescale Semiconductor Inc.**
- **Dawn Speranza, SEMATECH**
- **Walter F. Worth SEMATECH**

Future Plans

Next Year Plans

- Determine Toxicity of New Chemicals
- Integrate Multiple Sensors on CMOS Chip
- Demonstrate Hand Held Sensor
- Move this Tool Toward Commercialization

Long-Term Plans

- Commercialize this Tool

Publications, Presentations, and Recognitions/Awards

- **D. J. O'Connell, A. J. Molinar, A. Luiz Pasqua Tarares, D. L. Mathine, R. B. Runyan, and J. J. Bahl, "Cell Attachment to Selected Cell Based Biosensor Surfaces,"** ***Life Sciences*** **80 (2007) 1395.**
- **P.T. Caldwell, P. A. Thorne, S. Boitano, R. B. Runyan, P. D. Johnson, and O. Selmin," "Tricholoroethylene Disrupts Cardiac Gene Expression and Calcium Homeostasis in Rat Myocytes,"** ***Enviromental Health Perspectives*****, Revised December 29, 2007.**
- **D. L. Mathine, T. Hoda, D. J. O'Connell, J. J. Bahl, and R. B. Runyan, "A Colorimetric pH Sensor for Use in a Cell-Based Biosensor," Submitted to** ***Sensors and Actuators B: Chemical.***
- **D. L. Mathine, J. Rusche, T. Hoda, and R. B. Runyan, "A CMOS Spectroscopic Duel Photodetector for Determination of Green Fluorescent Protein Labeled Yeast," Submitted to** ***Lab on a Chip***
- **D. L. Mathine, J. J. Bahl, R. B. Runyan, "CMOS Photodetectors for a Cell Based Biosensor," Photonincs North, Ottawa, Ontario, Canada, June 2007 (Invited Talk)**

Non-PFOS/non-PFAS Photoacid Generators: Environmentally Friendly Candidates for Next Generation Lithography

(Task Number: 425.013)

PIs:

- **Christopher K. Ober, Materials Science and Engineering, Cornell University**
- **Reyes Sierra, Chemical and Environmental Engineering, UA**

Graduate Students:

- **Victor Gamez, PhD candidate, Chemical and Environmental Engineering, University of Arizona**

Other Researchers:

- **Yi Yi, Postdoctoral Fellow, Materials Science and Engineering, Cornell University**

Cost Share (other than core ERC funding):

- **$25k from Rohm and Haas Microelectronics**

Objectives

- **Develop PFOS free photoacid generators for chemically amplified resist application with superior imaging performance**
- **Evaluate lithographic performance in selected model 193 nm and EUV resists**
- **Evaluate the environmental aspects of new PFOS free photoacid generators**

ESH Metrics and Impact

1. *Reduction in the use or replacement of ESH-problematic materials*

   Complete replacement of perfluorooctanesulfonate (PFOS) structures including metal salts and photoacid generators in photoresist formulations

2. *Reduction in emission of ESH-problematic material to environment*

   Develop new PAGs that can be readily disposed of in ESH friendly manner

3. *Reduction in the use of natural resources (water and energy)*

   All of the non-PFOS PAG compounds were prepared using simple, energy reduced chemistry (within 4 steps) in high yields and purity, which reduces water use and the use of organic solvents.

4. *Reduction in the use of chemicals*

   By preparing non-PFOS PAG compounds using simple chemistry (within 4 steps) in high yields and purity, we have reduced the use of fluorinated chemicals.

Bioaccumulation of PFOS

Global Distribution of PFOS in Wildlife

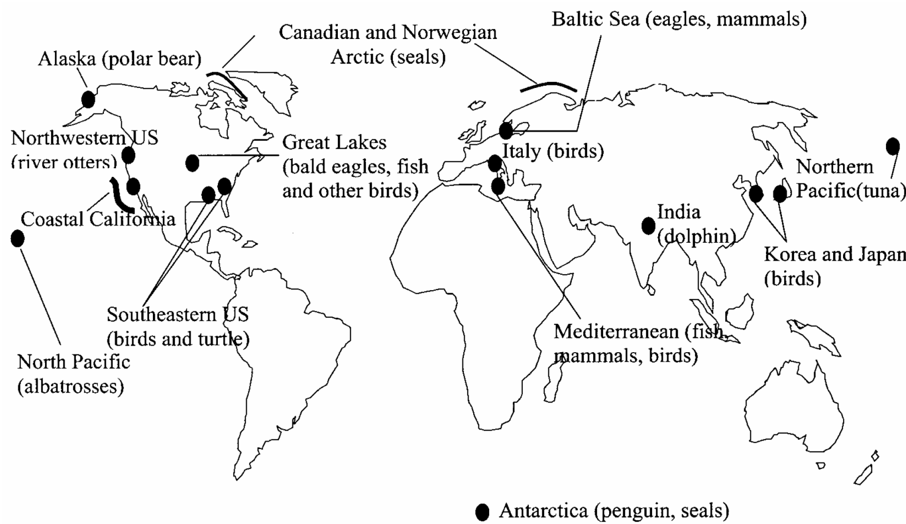

Environ. Sci. Technol. **2001,** ***35*****, 1339.**

Accumulation of PFOS in Marine Mammals

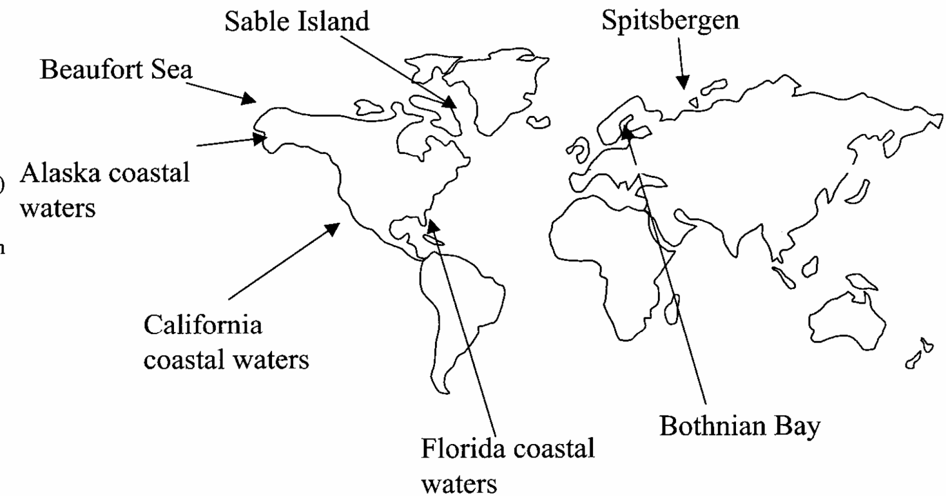

Environ. Sci. Technol. **2001,** ***35*****, 1593.**

The EPA proposed a significant new use rule (SNUR) for PFOS in 2000.

Next Generation PAGs — environmentally friendly, no bioaccumulation

PFOS PAG Performance Issues

"Segregation or non-uniform distribution of PAG"

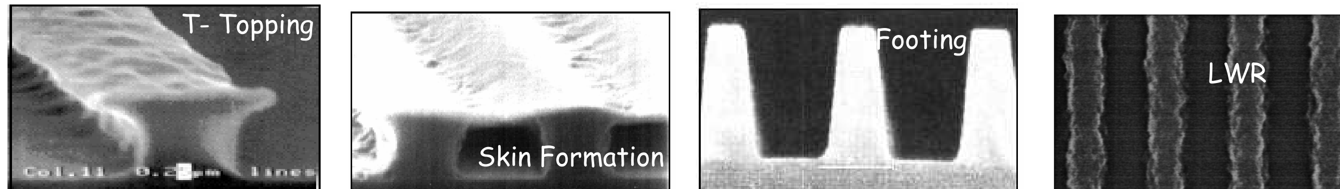

"Surface segregation increases with increase in fluorine content"

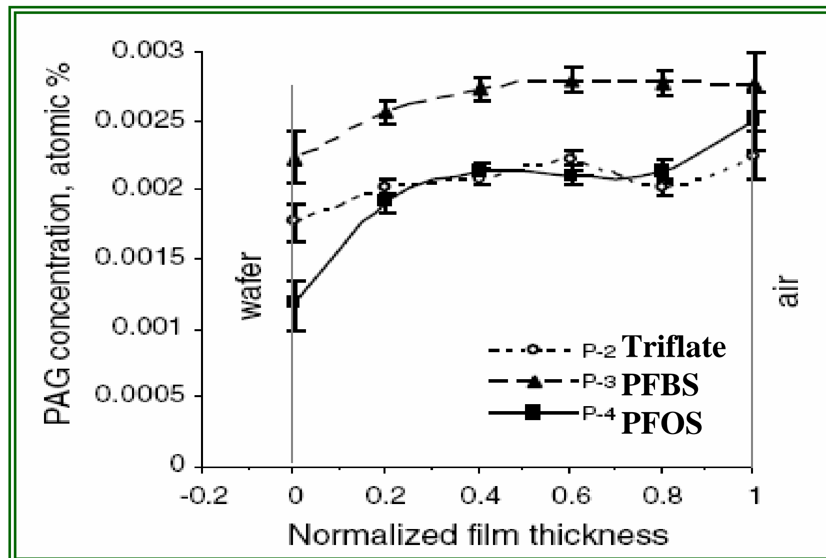

RBS Depth Profile of polar PAGs in a IBMA-MMA-MAA-t-BMA matrix

"PAG leaching Surface Phenomena"

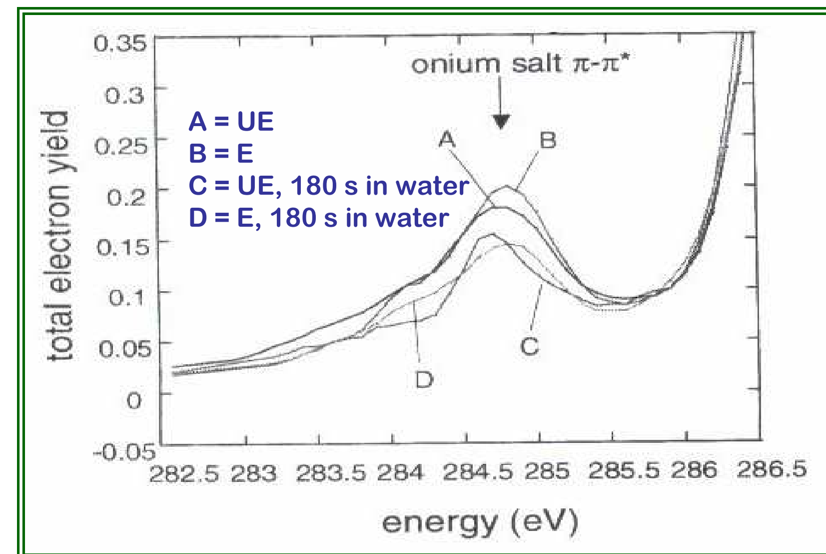

NEXAFS spectra of polar PFOS in a IBMA-MMA-MAA-t-BMA matrix

C.K. Ober et al., *JPST* (1999); J. L. Lenhart et al., Langumir, (2005); W. Hinsberg et al., SPIE, 2004; M. D. Stewart et al., *JVSTB* (2002)

Molecular Design of New Acids:

Environmentally Safe, Better Performance

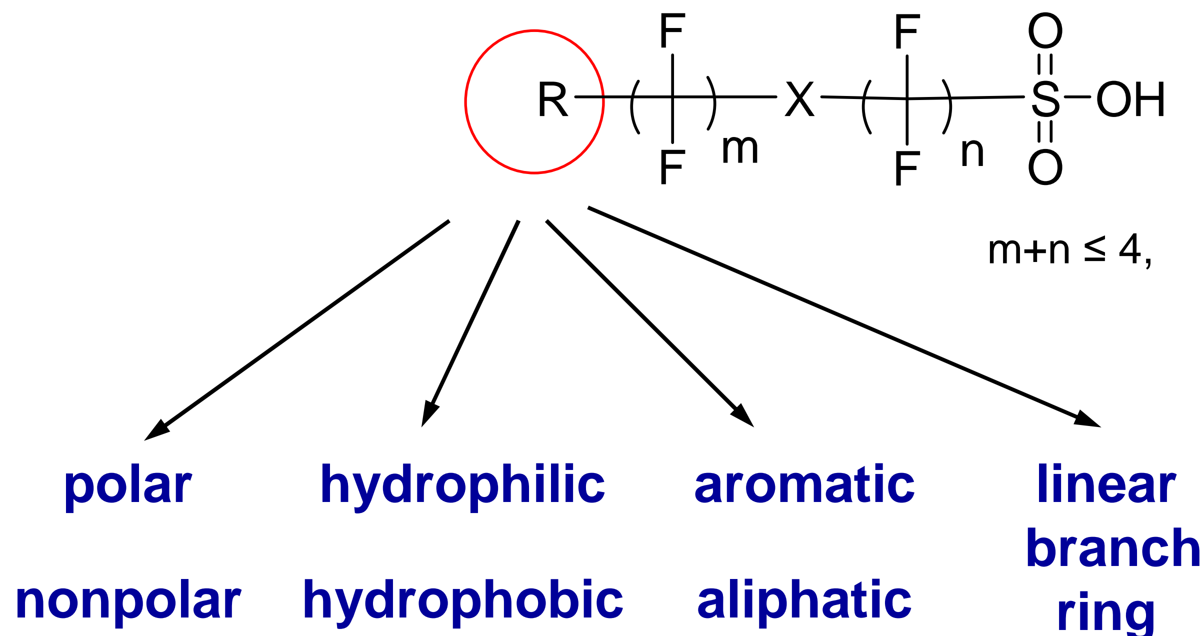

Practical synthetic chemistry considerations:

- **Simple chemistry — low cost & less time**
- **Efficient reactions — high yield & high purity**

XPS Analysis: New PAGs Mix Better with Resists

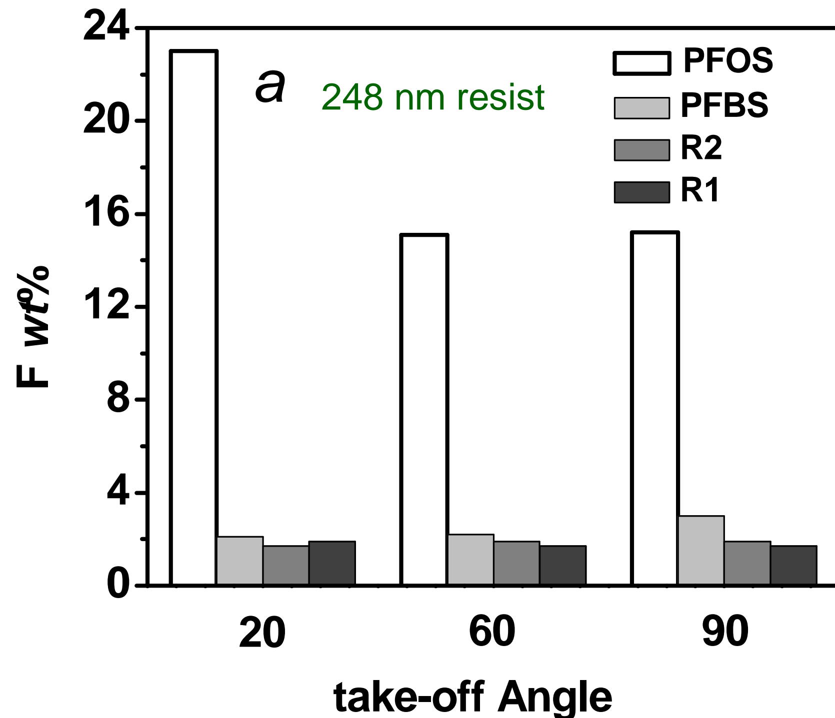

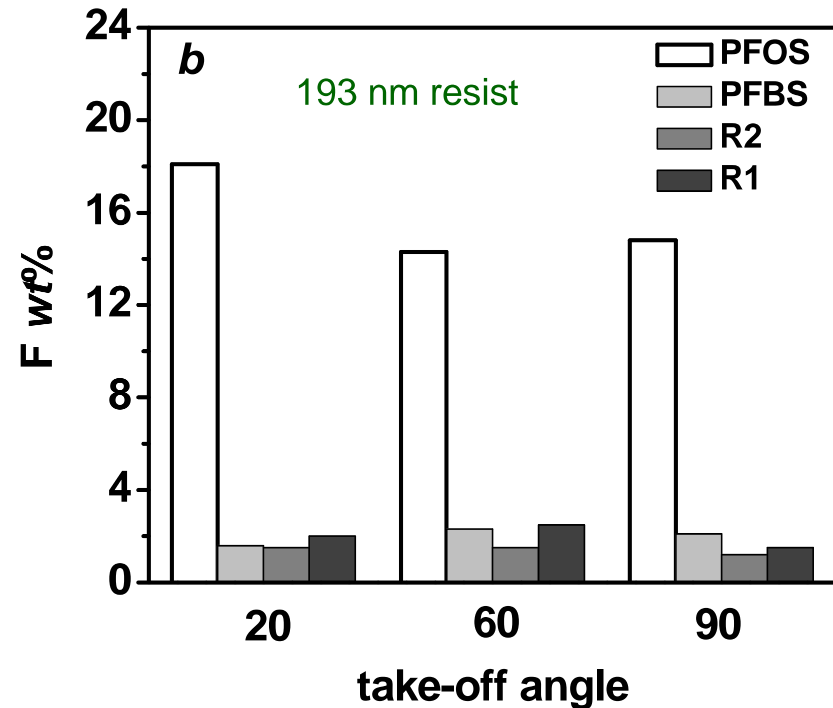

- **Heavy surface segregation of TPS PFOS**
- **Homogeneous distribution and better performance of non-PFOS PAGs (R1 & R2)**

Better Line Edge Roughness @ EUV

Less LER, better performance

Cao H. et al. *Proc. SPIE* Vol. 5376, p757, 2004.

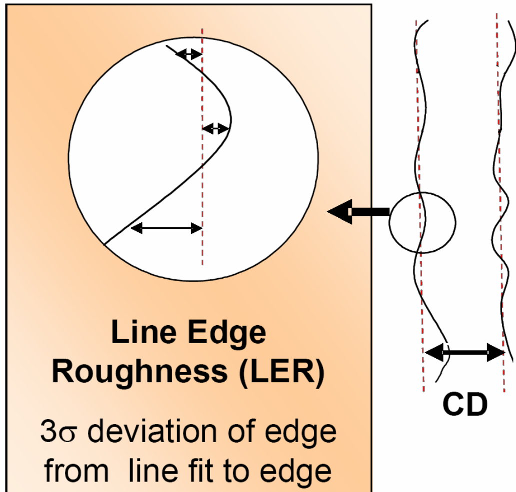

100 nm (1: 1) lines

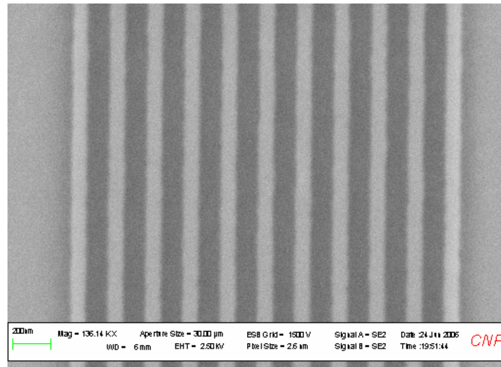

LER calculated by SuMMIT software

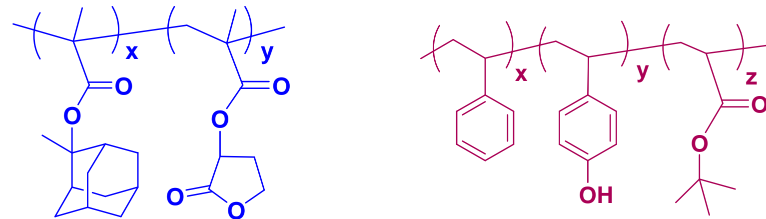

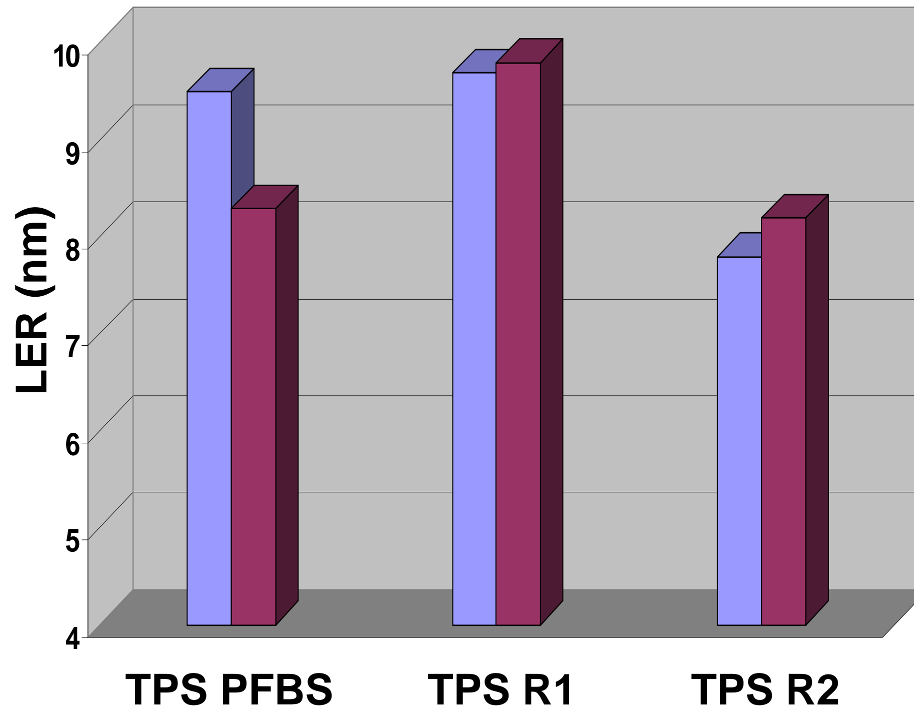

The non-PFOS PAGs (R1 & R2) demonstrate better or similar LER performance as PFBS PAG.

Outstanding Non-PFOS PAG Performance @ EUV

TPS R1

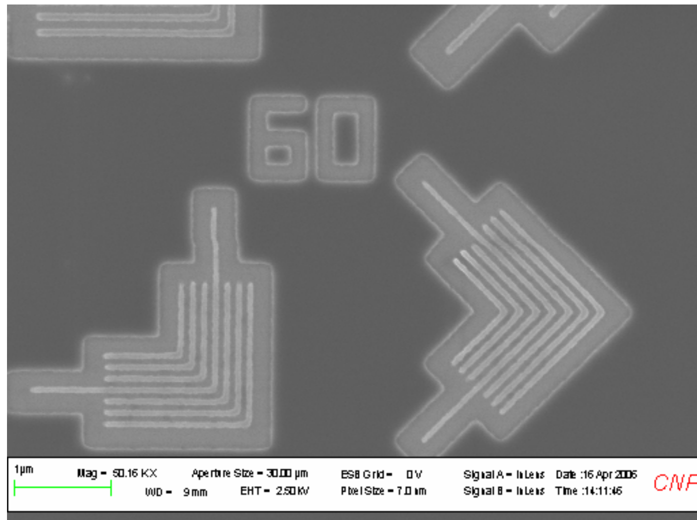

TPS R2

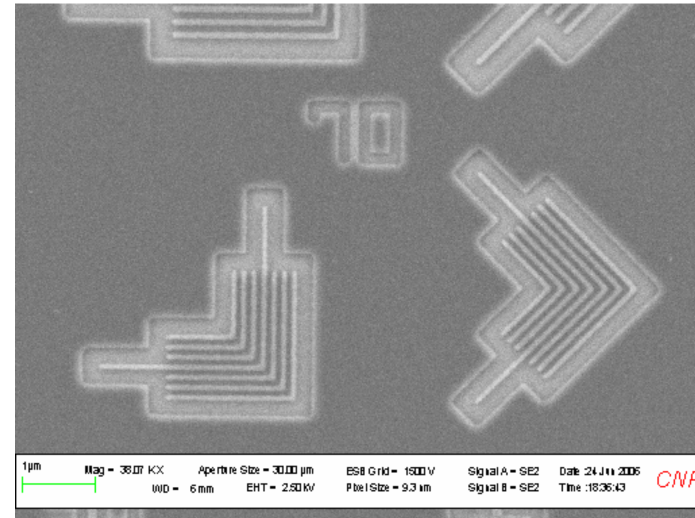

Non-PFOS PAGs easily reach sub-100 nm resolution with ESCAP resist under non-optimized conditions.

Industrial Interactions and Technology Transfer

- Collaboration with Rohm & Haas Electronic Materials for photolithography tests of non-PFOS photoacid generators
- Samples provided to Rohm & Haas Electronic Materials
- Samples provided to TOK
- Samples provided to AZ Microelectronics
- Performance at 193 nm and EUV evaluated with the assistance of International Sematech
- Interactions with Intel on LER issues

Future Plans

Next Year's Plans

- Prepare new generation non-PFOS photoacid generators
- Environmental evaluation of new non-PFOS photoacid generators
- Compare environmental toxicity of different iodonium/sulfonium cations
- Summarize previous studies and submit several manuscripts for transfer of know-how to technical community

Long-Term Plans

- Establish the relationship between photoacid generators' structure and their environmental properties
- Use advanced analytical tools to evaluate photoacid generators' environmental properties

Publications, Presentations, and Recognitions/Awards

Publications

•Ayothi R., Yi Y., Cao H. B., Wang Y., Putna S., Ober C. K. "Arylonium Photoacid Generators Containing Environmentally Compatible Aryloxyperfluoroalkanesulfonate Groups" *Chem. Mater.* 2007, 19, 1434.
•Ober C. K., Yi Y., Ayothi R. "Photoacid generator compounds and compositions" *PCT Application* WO2007124092, April 2007.

Presentations

•IBM Self-assembly Workshop, Almaden, CA, Jan. 15, 2008. "Photopatternable Block Copolymers: Chemically Active BCP Resists", invited talk.
•International Symposium on Advanced Materials and Nano-materials with Precisely Designed Architectures, October 4th – 6th in Sapporo, Japan. "Studies in the biological-materials interface", invited talk.
•European Polymer Congress, Portorož, Slovenia, 2 – 6 July, 2007. "Building and Patterning the Biology-Materials Interface", invited talk.
•Humboldt University, Berlin, Germany, 17 June, 2007. "Building and Patterning the Biology-Materials Interface", invited talk.
•IUMACRO-07, Brooklyn, NY, June 10 – 13, 2007. "Tailoring Surfaces to Resist Non-Specific Binding"
•BIOS Conference Series, University of Pisa, Pisa, Italy, May 31, 2007. "Tailoring the Material-Biology Interface", invited talk.
•Conference on Nanomaterials for Defense Applications, San Diego, CA, April 24 – 26, 2007. Lithography and Biology: 2D and 3D Patterning for the Biology-Materials Interface, invited talk.

Recognitions/Awards

•2007 Humboldt Research Prize for C.K. Ober

Non-PFOS/non-PFAS Photoacid Generators: Environmentally Friendly Candidates for Next Generation Lithography

(*Task Number: 425.013*)

Subtask: Assessment of the environmental compatibility of new PFOS-free photoacid generators

PIs:

- **Chris K. Ober, Materials Science and Engineering, Cornell University**
- **Reyes Sierra, Chemical and Environmental Engineering, UA**

Graduate Students:

- **Victor M Gamez, PhD candidate, Chemical and Environmental Engineering, UA**

Undergraduate Students:

- **Matthew West, Chemical and Environmental Engineering, UA**

Other Researchers: ---

Cost Share (other than core ERC funding):

UA/NASA undergraduate fellowship (to M West)

Objectives

- **To characterize the environmental behavior of novel PFOS-free (and PFAS-free) photoacid generators (PAGs).**

- **To investigate the treatability of novel PFOS-free (and PFAS-free) PAGs using conventional physico-chemical and biological treatment methods.**

ESH Metrics and Impact

1. *Reduction in emission of ESH-problematic materials to environment: 100% removal of PFOS utilized as PAG in photolithography.*

Chemical structures of the novel PAGs (I)

Non-ionic compounds

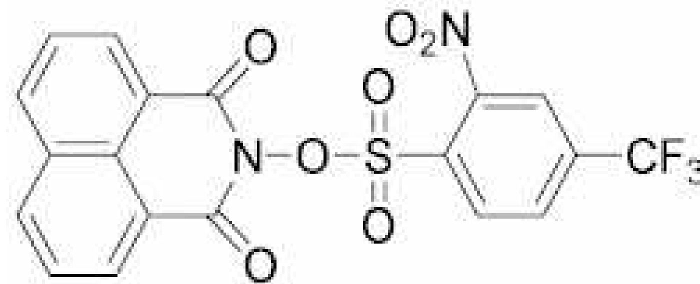

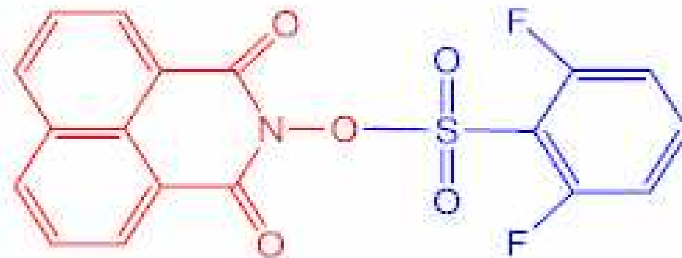

Chemical structures of the novel PAGs (II): Ionic Compounds

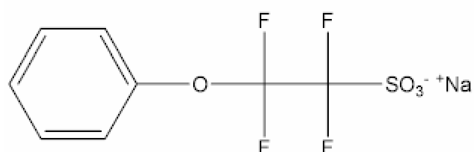

SF1

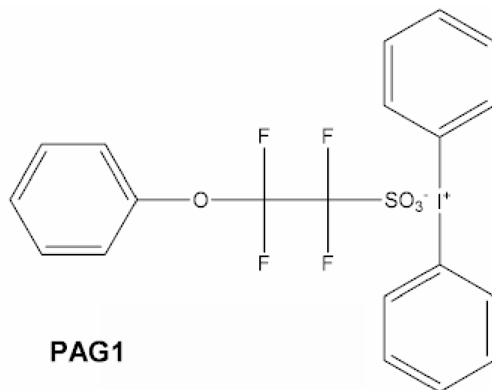

PAG1

PF1 (Na+ salt)

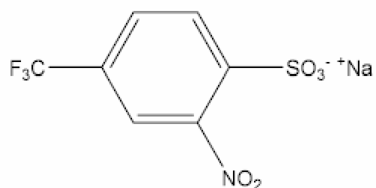

SF2

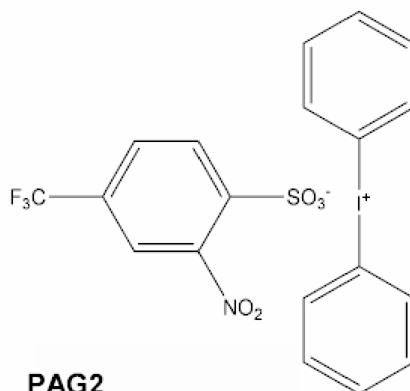

PAG2

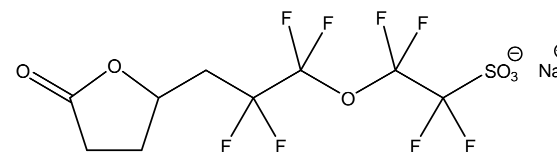

Lactone-PAG (Na+ salt)

Chemical structures of the PAG counterions: Diphenyliodonium (DPI) and triphenylsulfonium (TPS)

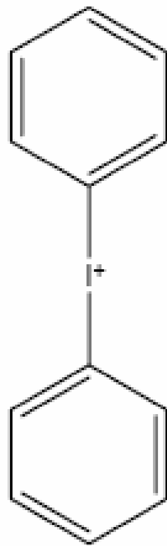

Diphenyliodonium

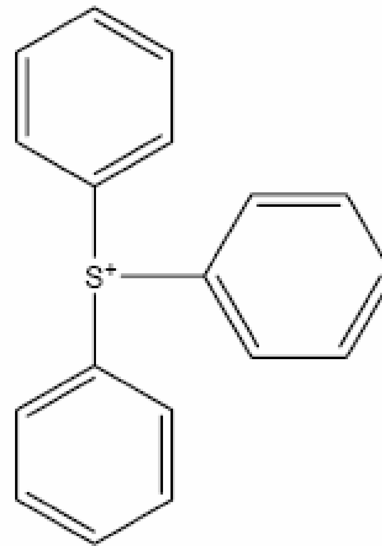

Triphenylsulfonium

Method of Approach

Toxicity testing:

Toxicity was evaluated in assays employing common indicator organisms, *i.e.,*

- Microtox assay
- Methanogenic microorganisms in anaerobic wastewater treatment sludge, i.e.,
  - H_2-degrading methanogens
  - Acetate-utilizing methanogens

Cytotoxicity was also monitored using:

- The mitochondrial toxicity test (MTT).

Microbial degradation:

Microbial degradation was investigated under different redox conditions, *i.e.,*

- Aerobic degradation as sole carbon source
- Aerobic cometabolism, and
- Anaerobic reductive dehalogenation.

Method of Approach

Persistence-Bioaccumulation-Toxicity prediction:

- The EPA **PBT (Persistence-Bioaccumulation-Toxicity) Profiler** (available at http://esc.syrres.com/pbt/) was utilized to estimate the persistence, bioaccumulation, and chronic fish toxicity potential of the various PAGs.

- The **applicability** of the PBT Profiler to surfactants, highly fluorinated compounds and reactive compounds is known to be very limited. Predictions obtained using this screening method should be used with caution.

Results

Microbial Toxicity and Cytotoxicity

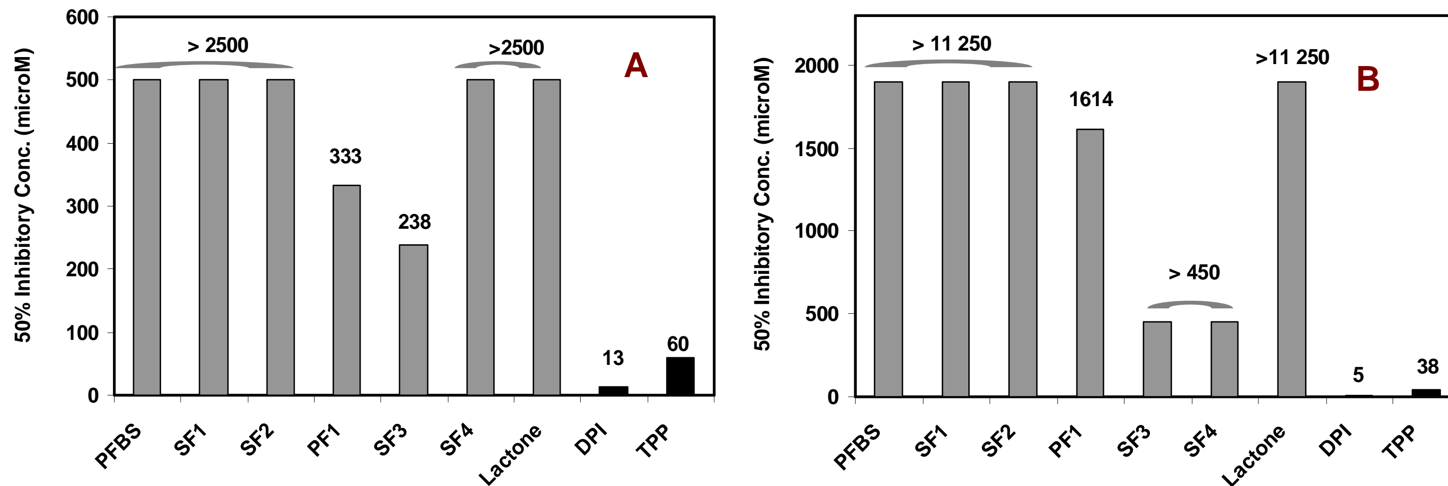

*Toxic response of the novel PAGs (nonionic and Na+ salt of ionic compounds) and PAG counterions in the MTT assay (**A**) and the Microtox assay (**B**).*

The toxicity of the novel PAGs (non-ionic PAGs and Na^+ salts of ionic PAGs) is very low compared to that of the PAG counterions, diphenyliodonium and triphenylsulfonium.

Results

Microbial Biodegradation of novel PAGs

- With the exception of SF2, PAGs were not biodegraded under any of the redox conditions evaluated.

- SF2 was rapidly degraded under anaerobic conditions. The nitro compound was transformed to the corresponding aromatic amine, which was persistent even after extended incubation.

- Further research will evaluate the cooxidation potential of the new PAGs under nitrifying conditions. Nitrifiers possess ammonia monooxygenases, which are known to attack lower halogenated hydrocarbons.

Results

Persistence-Bioaccumulation-Toxicity Prediction using EPA PBT-Profiler

PBT Profiler Estimate	PBT Color code[1]	Persistence[2]	Bioaccumulation[3]	Fish- Chronic Toxicity[4]
PAG anions				
SF1	PBT	+	—	—
SF2	PBT	+	—	—
PF1	PBT	+	—	—
PFBS	PBT	+	—	—
PFOS	PBT	+	—	—
SF3	PBT	++	—	Not calculated
SF4	PBT	++	—	Not calculated
Counter ions				
Diphenyliodonium (K^+)	PBT	+	--	+
Triphenylsulfonium (K^+)	PBT	+	+	++

Orange or **red** implies that the corresponding EPA criterium has been exceeded. (--) No concern, (+) concern; (++) high concern.

Results

Environmental fate properties predicted for the PAG counterions using EPA PBT-Profiler

Persistence			Bioaccumulation	Toxicity
Media	Half-Life (days)	Percent in each medium	BCF	F_ChV* (mg/l)
Potassium triphenylsulfonium				
Water	38	6%	3,000	0.028
Soil	75	61%		
Sediment	340	33%		
Air	12	0%		
Potassium diphenyliodonium				
Water	38	12%	100	1.4
Soil	75	87%		
Sediment	340	1%		
Air	5.8	0%		

* F ChV= Chronic Fish toxicity values

The PBT *Profiler* estimated that triphenylsulfonium (TPS) may be a PBT pollutant.

Conclusions

- The novel PAGs exert no/low toxicity and are not bioaccumulative. However, they are resistant to microbial degradation.

- Improved PAG substitutes which are more prone to biodegradation still need to be developed.

- Diphenyliodonium and triphenylsulfonium, two common PAG counterions, should be replaced by more environmentally benign alternatives. Both counterions were highly toxic in assays with microbial and human cells.

Industrial Interactions and Technology Transfer

Industrial liaisons:

Jim Jewett (jim.jewett@intel.com), Intel Corporation

Future Plans

Next Year Plans

- Evaluate the environmental compatibility of new generation PAGs.
- Continue the evaluation of the treatability of the most promising PAGs using conventional physico-chemical and biological methods.
- Evaluate the environmental fate properties of the new PAGs using a commercial prediction engine (CATABOL)* known to be suited for fluorinated compounds. The applicability of the EPA PBT profiler for these compounds is limited.

Long-Term Plans

- Establish the main chemical features for enhancing biodegradation potential of PAG compounds and facilitate design of environmentally compatible chemistries.

* Dimitrov et al. (2004) Predicting the biodegradation products of perfluorinated chemicals using CATABOL. SAR QSAR Environ Res. 15(1):69-82).

Publications, Presentations, and Recognitions/Awards

- **Presentations**

Gamez, V.M., Ober, C. and Sierra-Alvarez, R. 2007. "Non-PFOS/non-PFAS Photoacid Generators: Environmentally Friendly Candidates for Next Generation Lithography". Teleseminars of the SRC/Sematech Environmental Research Center for Environmentally Benign Semiconductor Manufacturing. June 18.

Environmentally Benign Electrochemically-Assisted Chemical Mechanical Planarization (E-CMP)

(*Task Number: 425.014*)

Subtask 1: Novel Chemistries and Novel E-CMP Pads

PI:

- **Srini Raghavan, Department of Materials Science and Engineering, UA**

Graduate Student:

- **Ashok Muthukumaran: Ph. D. candidate, Department of Materials Science and Engineering, UA**

Cost Share (other than core ERC funding):

- **In-kind donation (patterned wafers) from Intel :$10,000**

Objectives

- **Optimize dihydroxybenzene sulfonic acid (DBSA) based chemical system for electrochemical mechanical removal of Ta with a 1:1 selectivity with respect to copper**
- **Evaluate DBSA based chemical system for the removal of TaN under ECMP conditions**

ESH Metrics and Impact

- **Basis of comparison**:
  - ➢ Conventional slurry based Copper CMP
    - Requires slurries with higher solid content
    - Higher polishing pressure
    - Higher polish time during bulk copper removal
- **Manufacturing Metrics**:
  - ➢ The use of ECMP will reduce the polish time, polishing pressure and the amount of waste generated by a typical slurry based CMP
- **ESH Impact:**

Goals	Usage Reduction		Waste Reduction	
	Chemicals	Abrasives	Solid	Liquid
Using full sequence ECMP	N/A	> 90%	> 99%	N/A

Current Year Activities

➢ During the last contract year, Di-hydroxybenzene Sulfonic acid (DBSA) was shown to have promise as a chemical agent suitable for ECMP of Ta

➢ In the current contract year, optimization of DBSA based chemical system has been done to yield a Ta removal rate of ~ 200 Å/min with a 1:1 selectivity with respect to Cu

- Variables Optimized
  - Peroxide concentration
  - pH
  - Current density

➢ Additionally, the use of the chemical system for electrochemical mechanical removal of TaN has been investigated

Effect of Peroxide Concentration on Ta Removal

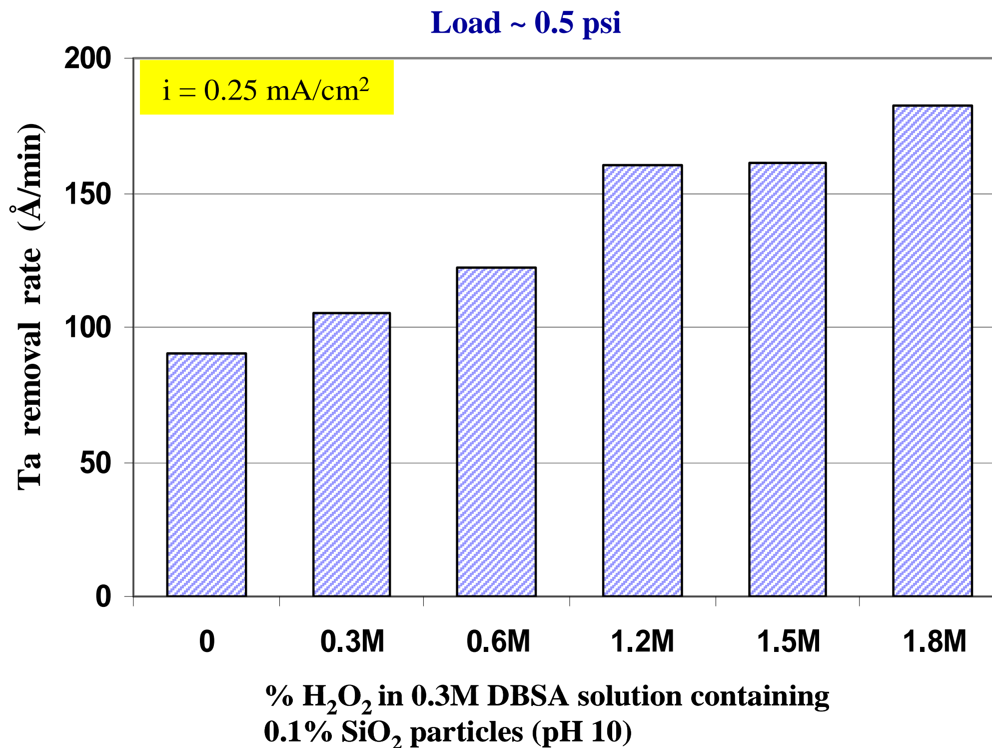

- 0.3M DBSA solution (pH 10) containing 0.1% of 80 nm SiO_2 particles ; current density = 0.25 mA/cm^2
- Removal rate of tantalum is 90 Å/min in the absence of peroxide
- Addition of 1.2M peroxide, increases the removal rate to 160 Å/min
- Peroxide concentration greater than 1.2M increases the removal rate only marginally

Removal Rate of Cu and Ta as a Function of pH

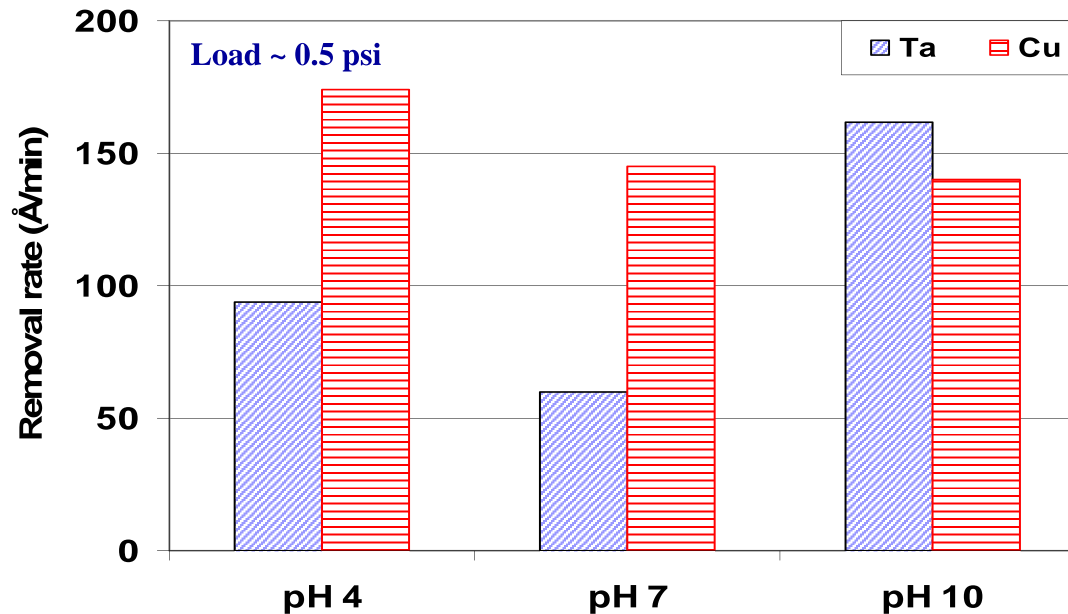

- 0.3 M DBSA solution + 1.2M H_2O_2 + 0.1% SiO_2 at a current density of **0.25 mA/cm²**
- Ta removal
  - Highest removal rate of 160 Å/min obtained at pH 10
- Cu removal
  - Removal rate at pH 10 is 140 Å/min; rates decrease slightly with increase in pH

Effect of Current Density

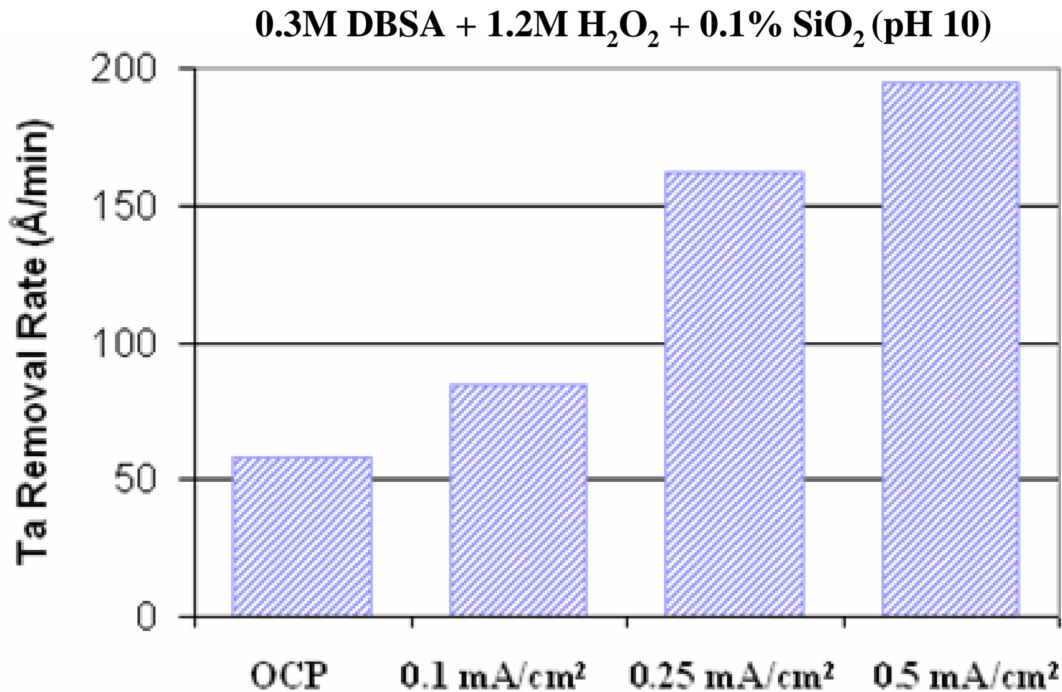

- Removal rate of Ta increases linearly with increasing applied current density
- Removal rate of ~ 200 Å/min for 0.5 mA/cm^2 (corresponding to 1 V overpotential)

Note: AFM surface roughness (R_a)

- Bare Ta surface cleaned in dil.HF: R_a *~ 40 Å*
- Ta surface polished in optimized solution at a current density of 0.5 mA/cm^2: R_a *reduced to 8 Å*
- CDO surface after complete removal of Ta: R_a *~ 5 Å*

Selectivity (Ta/Cu)

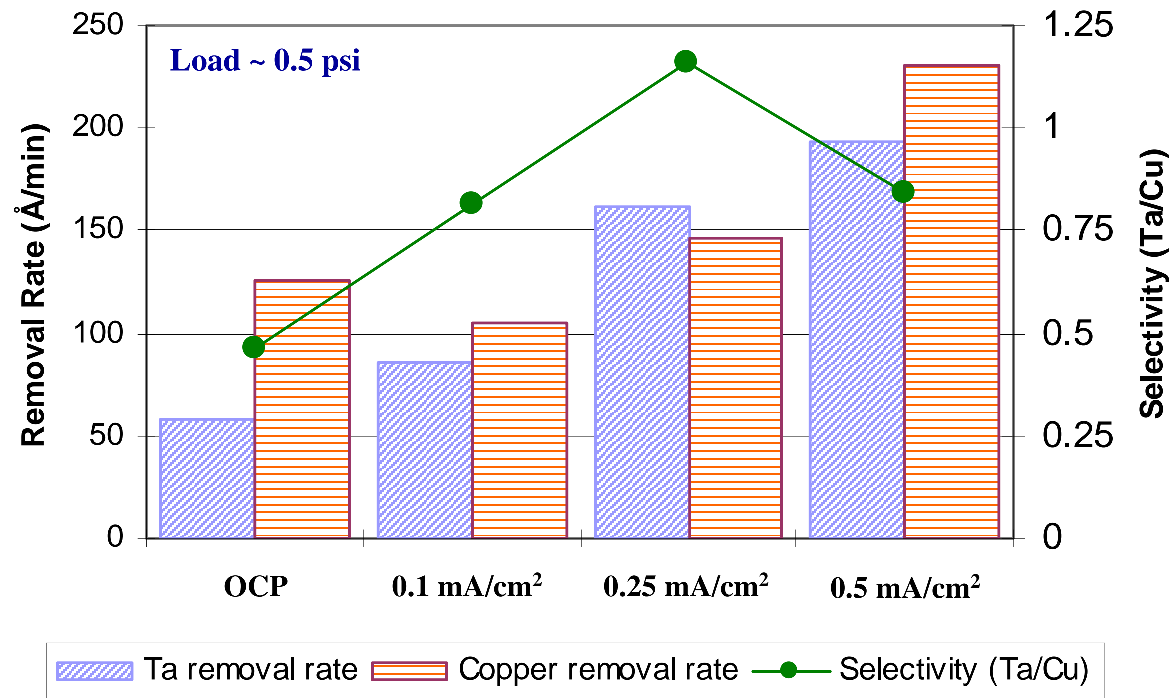

$$Selectivity = \frac{Removal\ rate\ of\ Ta}{Removal\ rate\ of\ Cu}$$

- 0.3 M DBSA solution + 1.2M H_2O_2 + 0.1 % SiO_2 (pH 10)
- **Selectivity of 0.85:1 (Ta/Cu) at 0.5 mA/cm^2**

Proposed Mechanism and Current Efficiency

➢MECHANISM OF Ta REMOVAL

- Ta undergoes an interfacial 2 e^- transfer reaction forming TaO on the surface

$$Ta + H_2O \rightarrow TaO(surface) + 2H^+ + 2e^-$$

- TaO is further oxidized and dissolved by H_2O_2 and DBSA in the bulk solution to form complexes of the type,

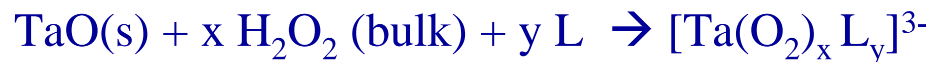

$$TaO(s) + x\ H_2O_2\ (bulk) + y\ L \rightarrow [Ta(O_2)_x\ L_y]^{3-}$$

where x = {1,2,3} with corresponding y ={6,4,2}

Applied current density (mA/cm^2)	Estimated removal rate (Å/min) of tantalum based on $2e^-$ transfer	Actual removal rate of tantalum (Å/min) in 0.3M DBSA + 1.2M H_2O_2 + 0.1% SiO_2 (pH 10)	Calculating current efficiency (%) after correcting for OCP removal rate
OCP	-	60	-
0.1	34	85	80
0.25	85	160	109*
0.5	169	195	81

Note: * Current efficiency greater than 100% due to analytical error ??

Comparison of DBSA and MSA Based Chemical Systems for Ta Removal

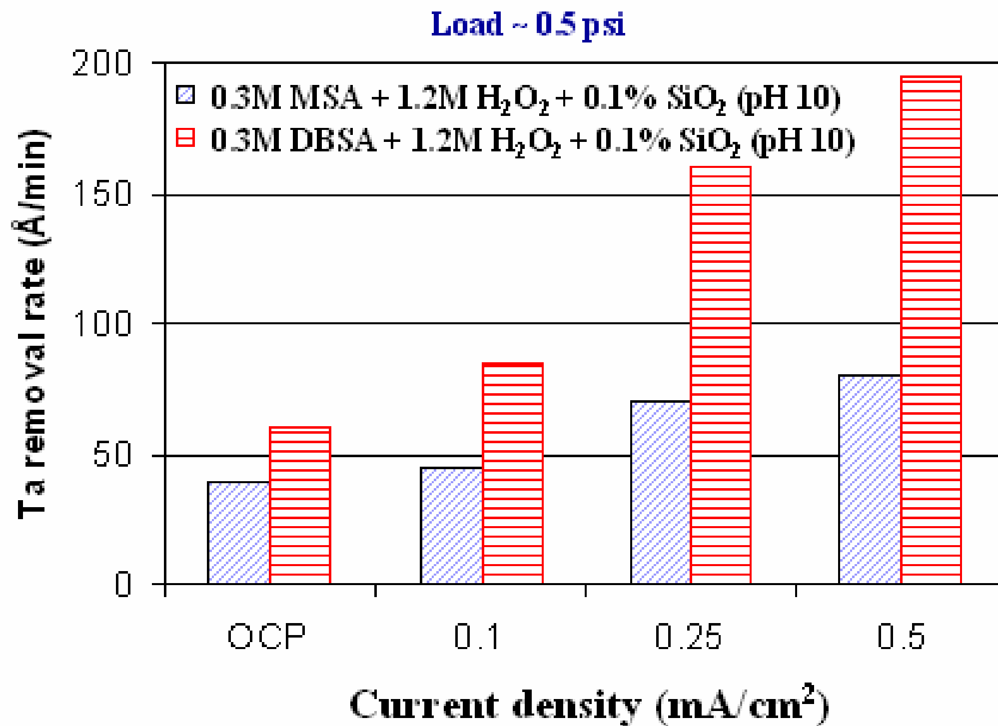

- 0.3M Methane sulfonic acid (MSA) + 1.2M H_2O_2 + 0.1 % SiO_2 (pH 10)
  - Under OCP condition, the removal rate of Ta is 40 Å/min
  - Highest removal rate of 80 Å/min obtained at a current density of 0.5 mA/cm^2; this is roughly one half of that obtained with DBSA

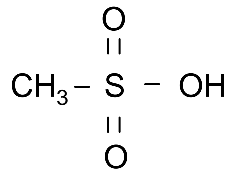

Methanesulfonic acid

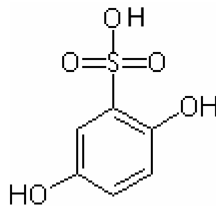

Dihydroxy benzene sulfonic acid

Evaluation of DBSA Based Chemical System for TaN Removal

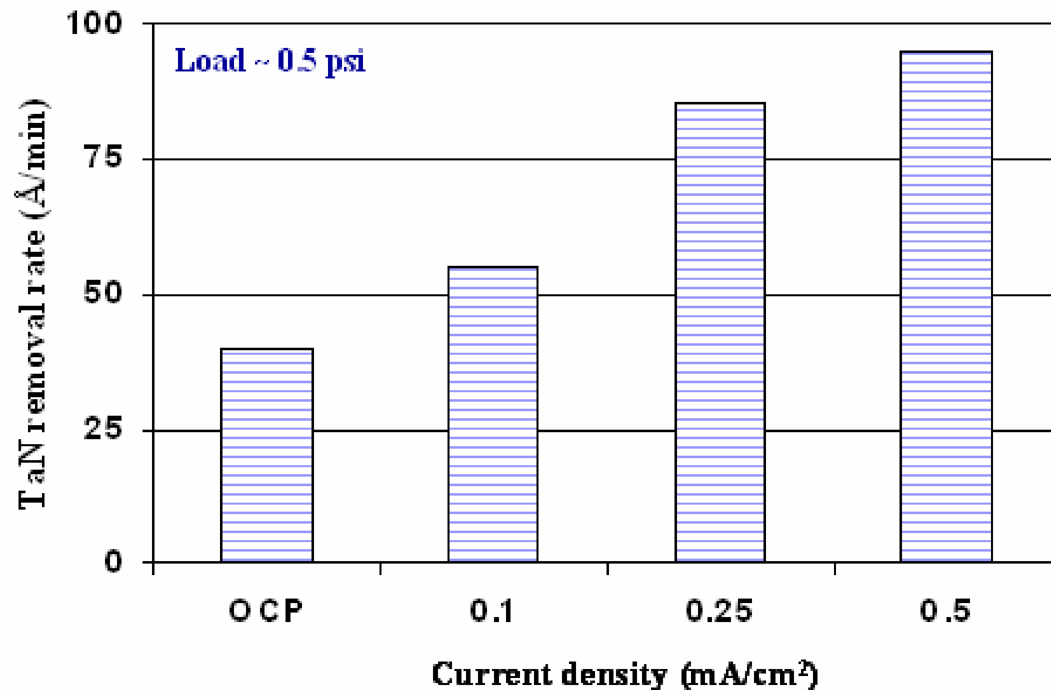

- 0.3 M DBSA solution + 1.2M H_2O_2 + 0.1 % SiO_2 (pH 10)
- Under OCP condition, the removal rate of TaN is 40 Å/min
- Removal rate increases to 95 Å/min at an applied current density of 0.5 mA/cm^2; this is roughly one half the RR of Ta

Patterned Test Structure for ECMP

(Fabricated at Intel D2 with the assistance of Michael Ru, Liming Zhang and Zhen Guo)

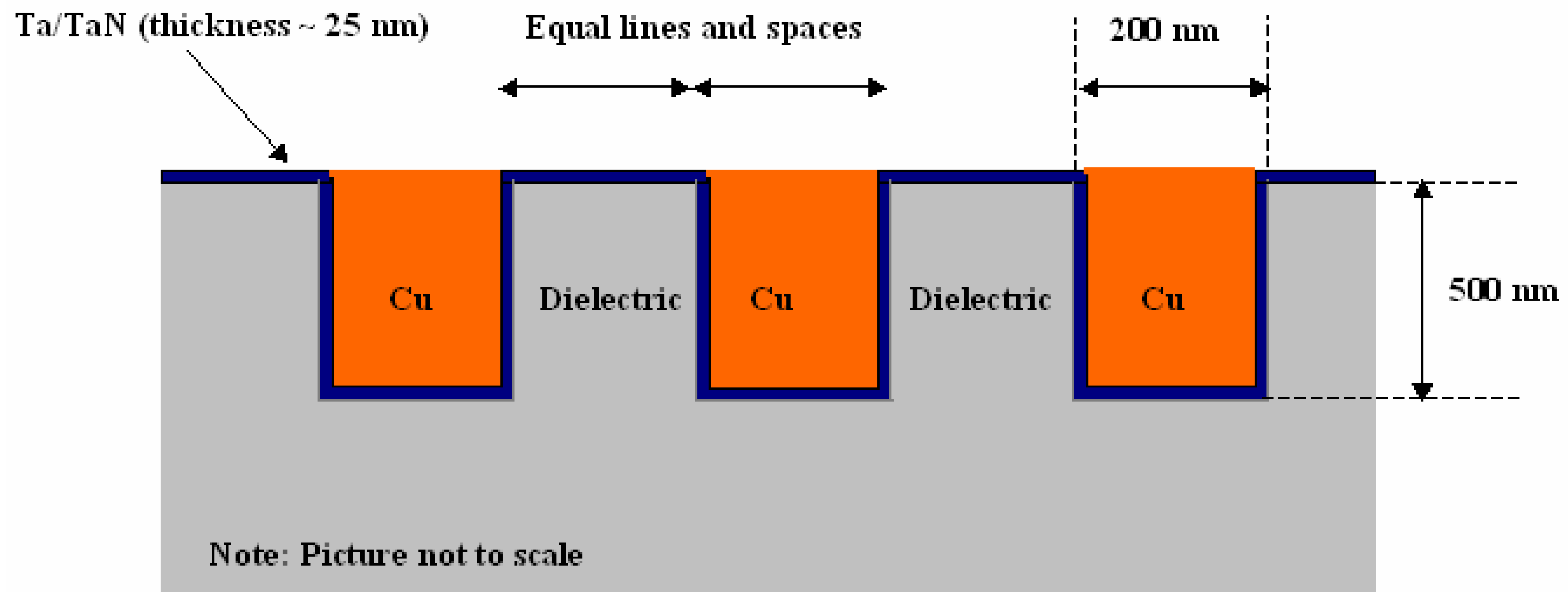

- This test structure will be used to test the 1:1 selectivity between Ta and Cu

Summary

- Ta removal rate of ~ 200Å/min obtained in 0.3 M DBSA solution containing 1.2M H_2O_2 and 0.1% SiO_2 (pH 10) at a current density of 0.5 mA/cm^2
- Ta/Cu selectivity of ~ 1:1 observed at pH 10 at a current density of 0.5 mA/cm^2 (oxide removal rate in the formulation ~ 30 Å/min)
- Performance of DBSA is better than that of MSA
- DBSA is not effective for TaN as it is for Ta

Industrial Interactions and Technology Transfer

- Work on Ta ECMP was presented at Applied Materials in August 2007; the seminar was hosted by Dr. Tom Osterheld
- Interacted with Dr. Liming Zhang, Dr.Raghu Gorantla, Dr. Michael Ru and Dr. Zhen Guo of Intel Corporation, Santa Clara (to design test structures)

Future Plans

Next Year Plans

- Develop chemical systems for the removal of other barrier layers (WN, Ru)
- Electrochemical end point detection for barrier layer-low k transition

Long-Term Plans

- Near neutral chemical system for one step removal of Cu and barrier layer
- Design of pads for ECMP

Publications/Presentations

- A.Muthukumaran, N. Venkataraman and S. Raghavan, "Evaluation of Sulfonic Acid Based Solutions for Electrochemical Mechanical Removal of Tantalum," accepted for publication in ***J. Electrochem. Soc***., 155 (3), 5 pp (2008).
- A.Muthukumaran, N. Venkataraman, S. Tamilmani and S. Raghavan, "Anodic Dissolution of Copper in Hydroxylamine Based Solutions with Special Reference to Electrochemical Planarization (ECMP)," ***Proceedings of The Corrosion Control 007 Conference***, Australia, Paper 105, 8 pp (2007).
- A.Muthukumaran and S. Raghavan, "Sulfonic Acid Based Chemistries for Electrochemical Mechanical Removal of Tantalum," ***TECHCON***, Texas, Sep 10-12 (2007).
- A.Muthukumaran, N. Venkataraman, V. Lowalekar and S. Raghavan, "Sulfonic Acid Based Chemistries for Electrochemical Mechanical Removal of Tantalum," ***The Electrochemical Society - The 6th International Semiconductor Technology Conference***, China, March 18-20 (2007).

Environmentally Benign Electrochemically Assisted Chemical Mechanical Planarization (E-CMP)

(*Task Number: 425.014*)

Subtask 2: Modeling, Optimization and Control

PI:

- **Duane Boning, Electrical Engineering and Computer Science, MIT**

Graduate Students:

- **Daniel Truque, EECS, MIT, graduated with M.S. degree in June 2007**
- **Wei Fan, Ph.D. candidate, EECS, MIT**
- **Joy Johnson, M.S. candidate, EECS, MIT**

Undergraduate Student:

- **Zhipeng Li, EECS, MIT**

Other Researcher:

- **Ed Paul, Visiting Professor, Stockton College**

Cost Share (other than core ERC funding):

- **Experimental support, Albany Nanotech**

Objectives

- **Develop models for ECMP (bulk copper, full copper, and barrier removal steps) at the**
  - **wafer-scale**
  - **chip-scale**
  - **feature-scale**
- **Develop control and optimization strategies utilizing integrated models**
  - **minimize process time, consumables usage**
  - **maximize uniformity, yield**

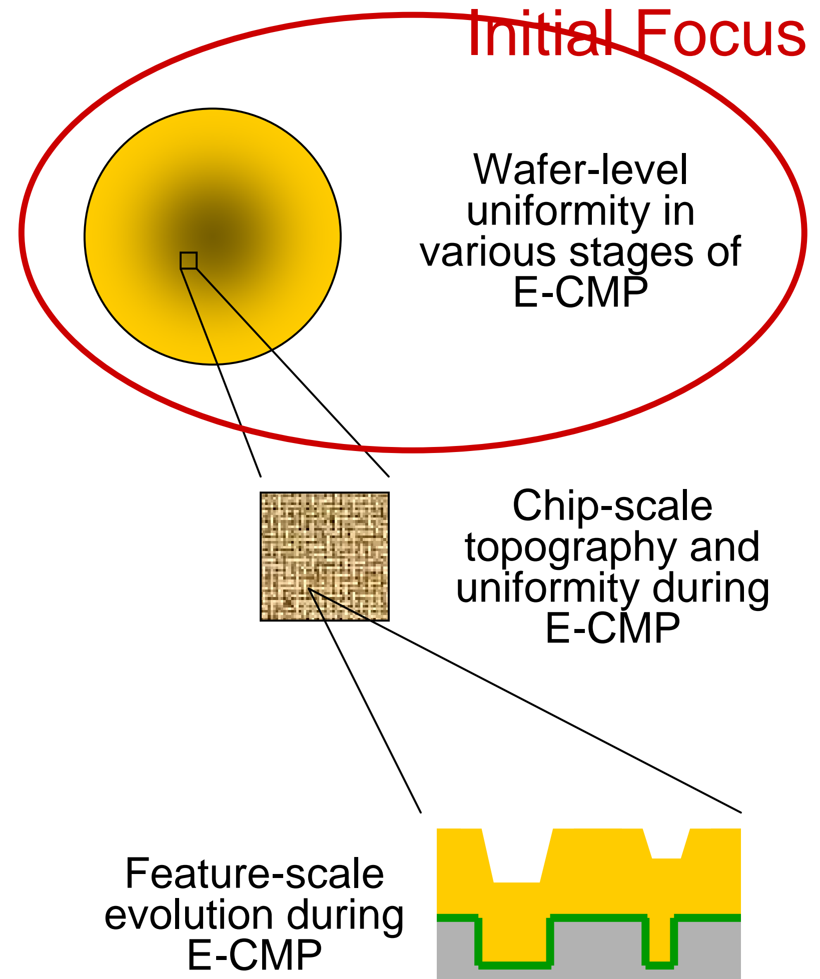

ESH Metrics and Impact

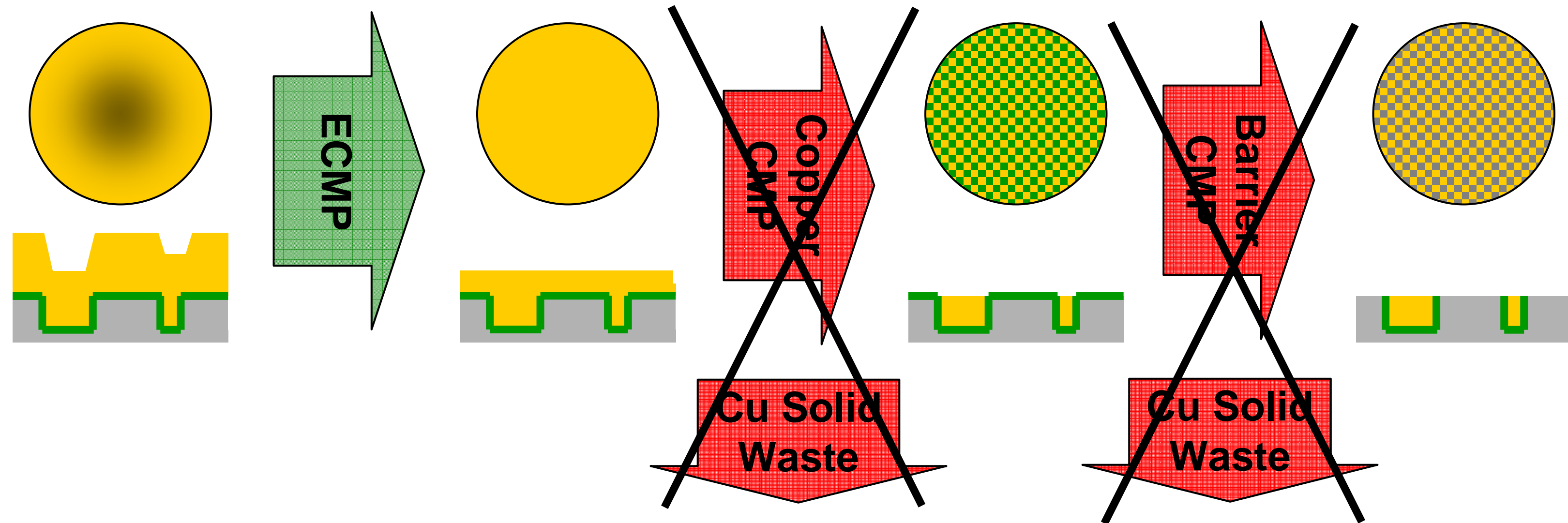

1. ***Reduction in the use or replacement of ESH-problematic materials***
2. ***Reduction in emission of ESH-problematic material to environment***
   - **Reduce or eliminate solid slurry particle waste**
     - Eliminate copper touch-down CMP (eliminate ~20% of planarization cycle)
     - Lower solid content barrier ECMP (~80% solids reduction in this step)
3. ***Reduction in the use of natural resources (water and energy)***
   - **Shorten process cycle time by ~20%**
   - **Increase in pad lifetime (5X)**
4. ***Reduction in the use of chemicals***
   - **Replace CMP slurry with ECMP electrolyte**

ECMP – Wafer Scale Modeling Approach

- **Cu removal rate across wafer as function of:**
  - **Initial copper thickness (e.g. nonuniform plating profile)**
  - **Applied voltages in multiple zones in ECMP tool**
  - **Tool/process parameters: geometry of electrical contact to wafer, velocity, pressure**
- **Semi-physical model**
  - **Model structure based on physics of process**
  - **Fit to experimental characterization data**
- **Two models considered:**
  - **Ohmic: voltage drops vertically/laterally in electrolyte**
  - **Nonlinear: include electrochemical dependence at electrode**

Ohmic ECMP Model

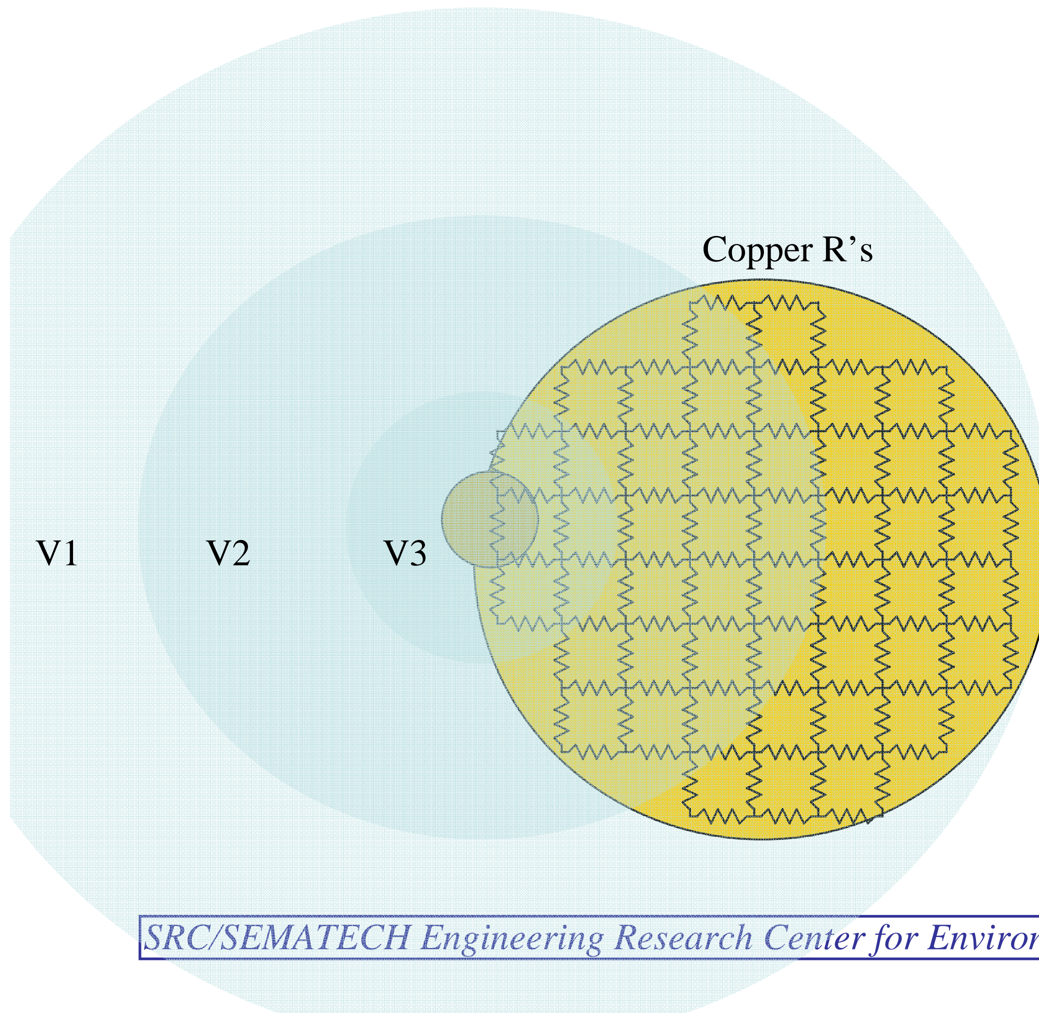

Pad voltage zones

Wafer Contact

V3 V2 V1

Electrolyte n^{th} level

Electrolyte First level

Copper level

i_n

Ohmic ECMP Model Approach

- **Calculate static current density to calculate removal**

$$I\left[\frac{C}{sec}\right]\cdot\frac{1}{\text{area }[cm^2]}\cdot\frac{1\,atom_{Cu}}{2e^-[C]}\cdot\frac{1\,mole_{Cu}}{N_A\,atoms_{Cu}}\cdot\frac{63.546\,g_{Cu}}{1\,mole_{Cu}}\cdot\frac{1\,cm^3}{8.941\,g_{Cu}}\cdot\frac{10^7\,nm}{1\,cm}\cdot\frac{60\,sec}{1\,min}=RR\left[\frac{nm}{min}\right]$$

$$area_{wafer}=683.4cm^2\rightarrow\frac{RR}{I}=31.02\frac{nm}{A\cdot\min}$$

- **Average radially and calculate removal rate**
- **Add static etch rate and calculate time interval's amount removed**
- **Update thickness and iterate**

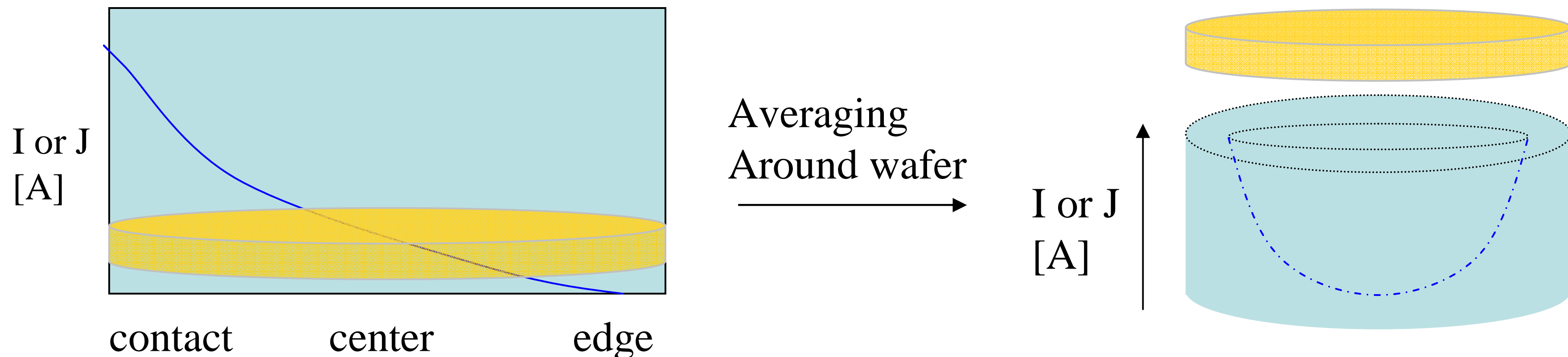

Ohmic ECMP Model Results: t = 10 sec

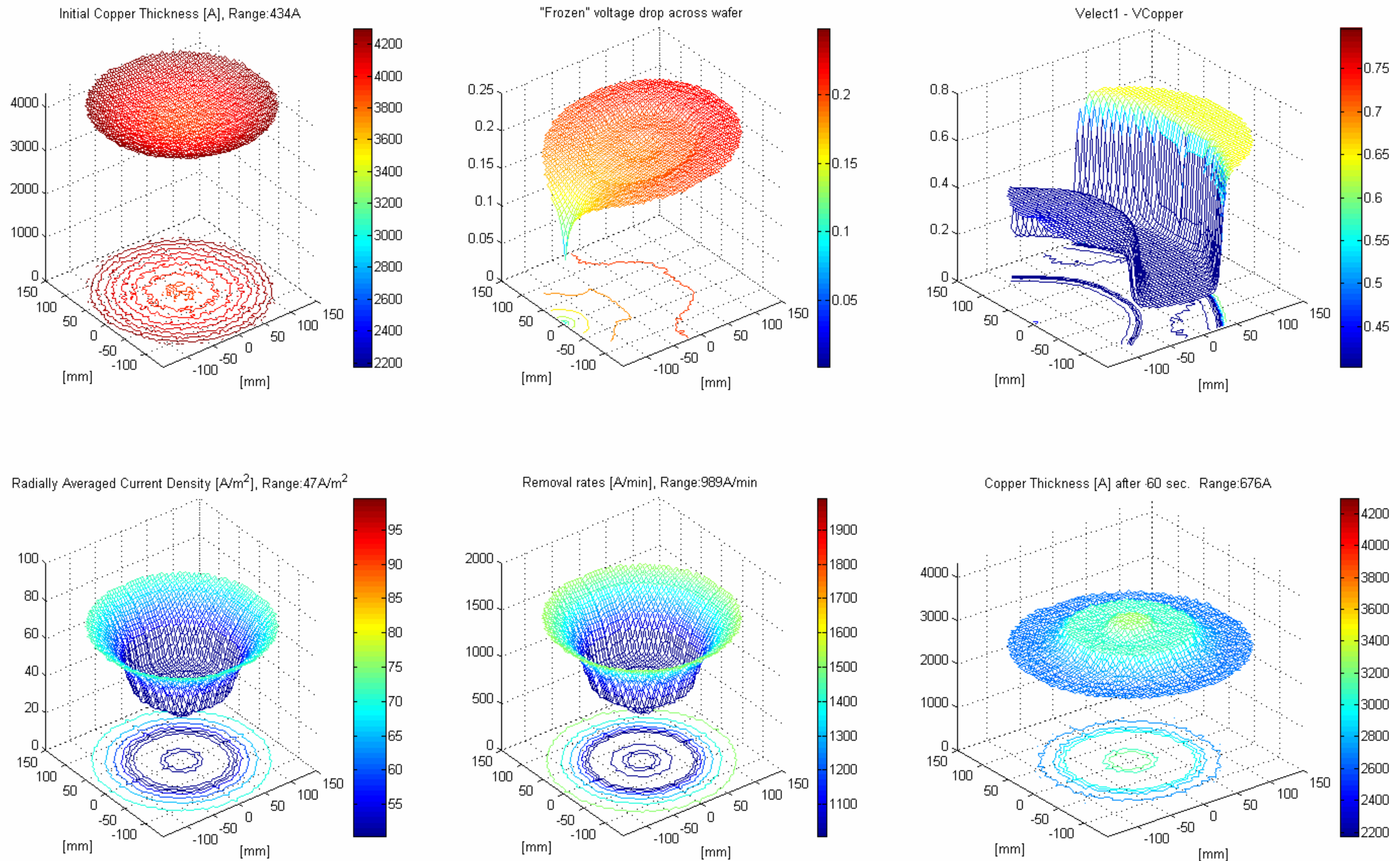

Try Ohmic Model with More Experiments

- **Collaboration with Albany Nanotech**
- **Experiment:**
  - **Different voltages on different zones – intentionally introduce nonuniformity to aid in modeling**
  - **Measure before and after Cu thicknesses on blanket films**
  - **With and without head sweep (to better localize kinematics)**
- **Revised numerical implementation of model**
  - **Better handling of zero-current boundary conditions**
- **Results: Model accuracy limitations**
  - **Nonlinear voltage dependence**
  - **Does not fit well near center of wafer**
  - **Edge region – difficult to fit**

Ohmic Model – Different Voltages in Each Zone

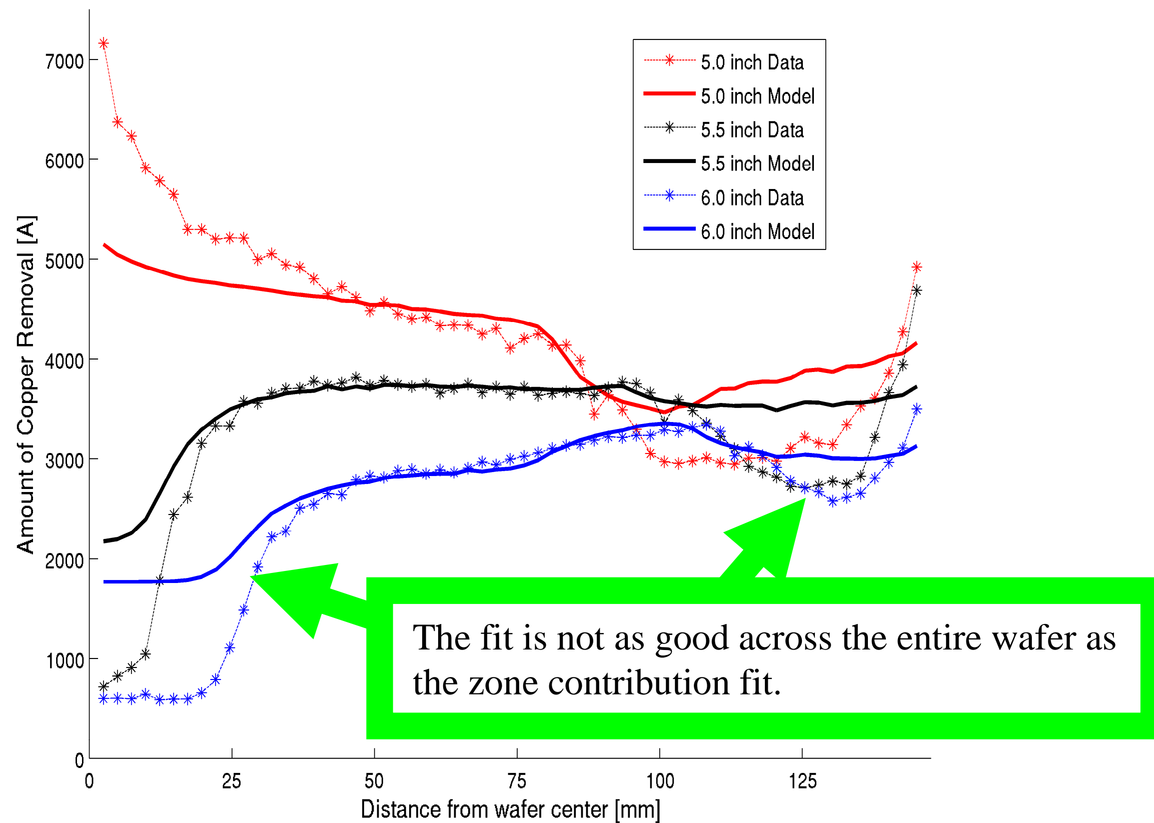

Amount of copper removal for head position L of 5.0, 5.5, and 6.0 inches, and voltage zone settings of *V1, V2, V3* = 2, 1, 3 V. Basic ohmic model versus data. The RMS error of this fit is 531 Å.

Nonlinear Removal in Applied Voltage

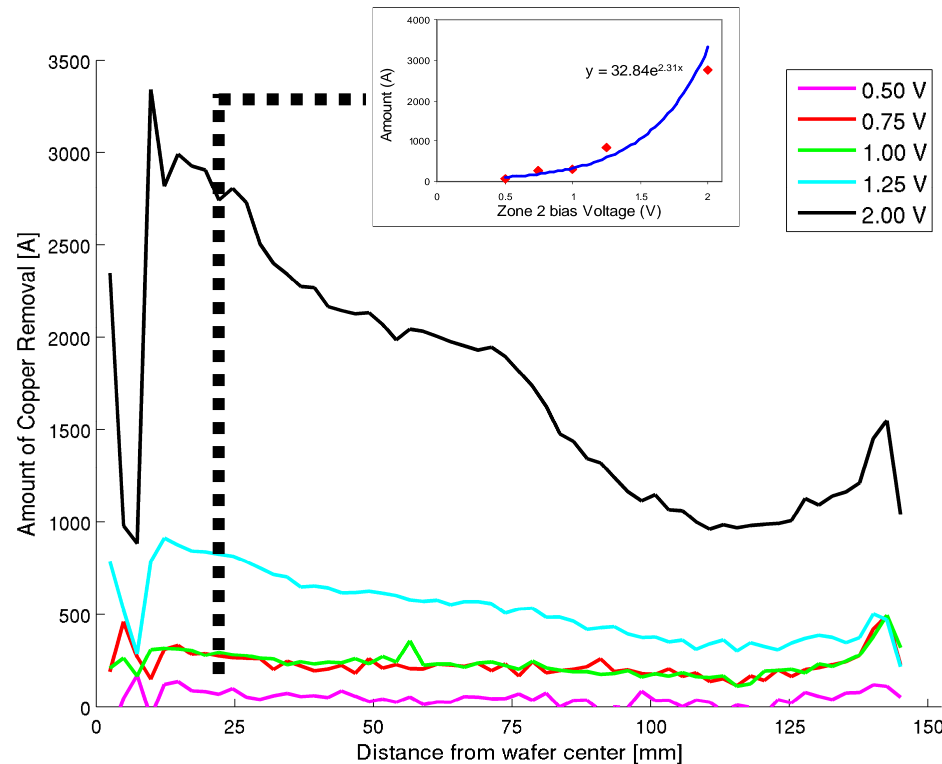

Experimentally measured copper removal for five different values of *V2* (with *V1* = *V3* = 0V, L = 6.0inch). Figure inset shows the observed nonlinear relationship between *V2* and the removal amount (current density) for one selected wafer radius.

Extension: Non-Ohmic Model

- **Account for nonlinear (exponential) Butler-Volmer electrochemical dependence at the wafer surface using a simple diode model**
- **1D implementation**
  - **Neglect voltage drop across wafer (highly conductive copper film)**
  - **Neglect lateral coupling and current flow in the electrolyte**

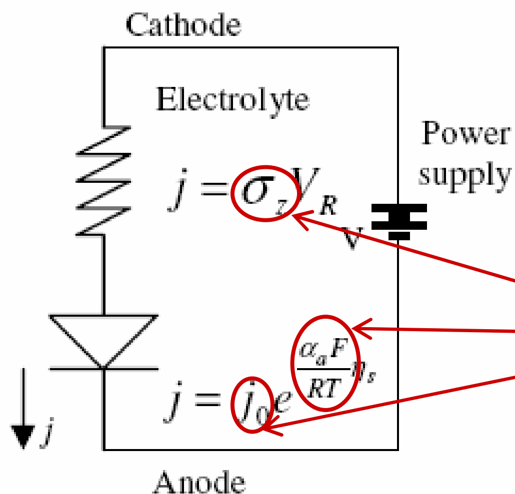

Assumptions:
1. Conduction and Faradic current are equal
2. Instantaneous /complete removal of surface layer
3. Removal of passivation layer by zone
4. "Best fit" values for V_o, J_o, & σ
5. No lateral current

Removal Rate (J,t) -> $t \cdot \frac{J \cdot C}{s \cdot cm^2} \cdot \frac{1Cu}{2e^-} \cdot \frac{1molCu}{N_A \cdot Cu} \cdot \frac{63.54gCu}{1mols} \cdot \frac{cm^3}{8.96g} \cdot \frac{1e^-}{1.67 \times 10^{-19} C} \cdot \frac{10^7 nm}{1cm} = nm$

Non-Ohmic Model Results

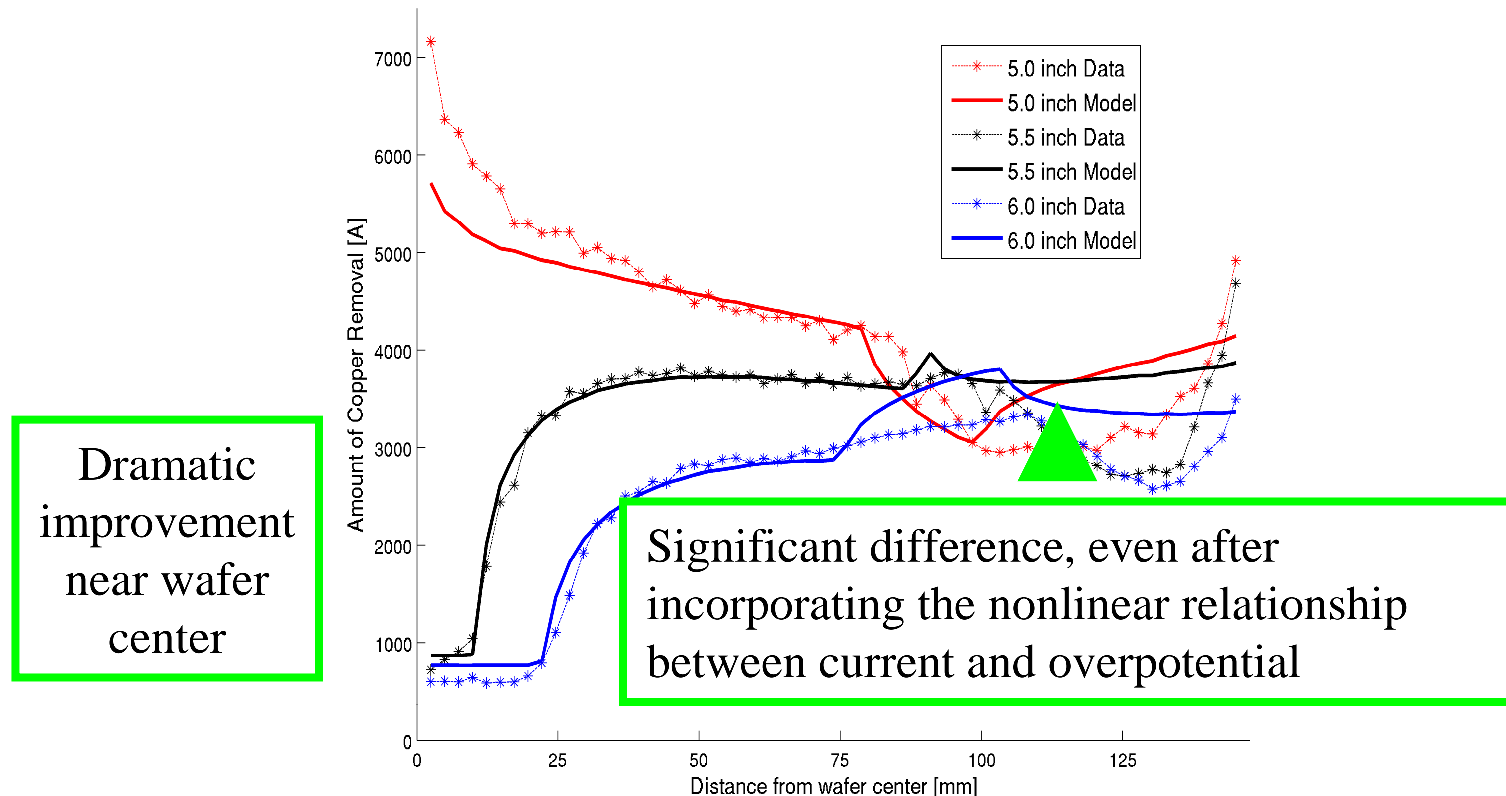

Amount of copper removal for L = 5.0, 5.5, 6.0 inch, and voltage zone settings of *V1, V2, V3* = 2, 1, 3 V. Non-ohmic model versus data. The RMS error of this fit is 412 Å, a 22% improvement.

Possible Passivation Kinetics Effects

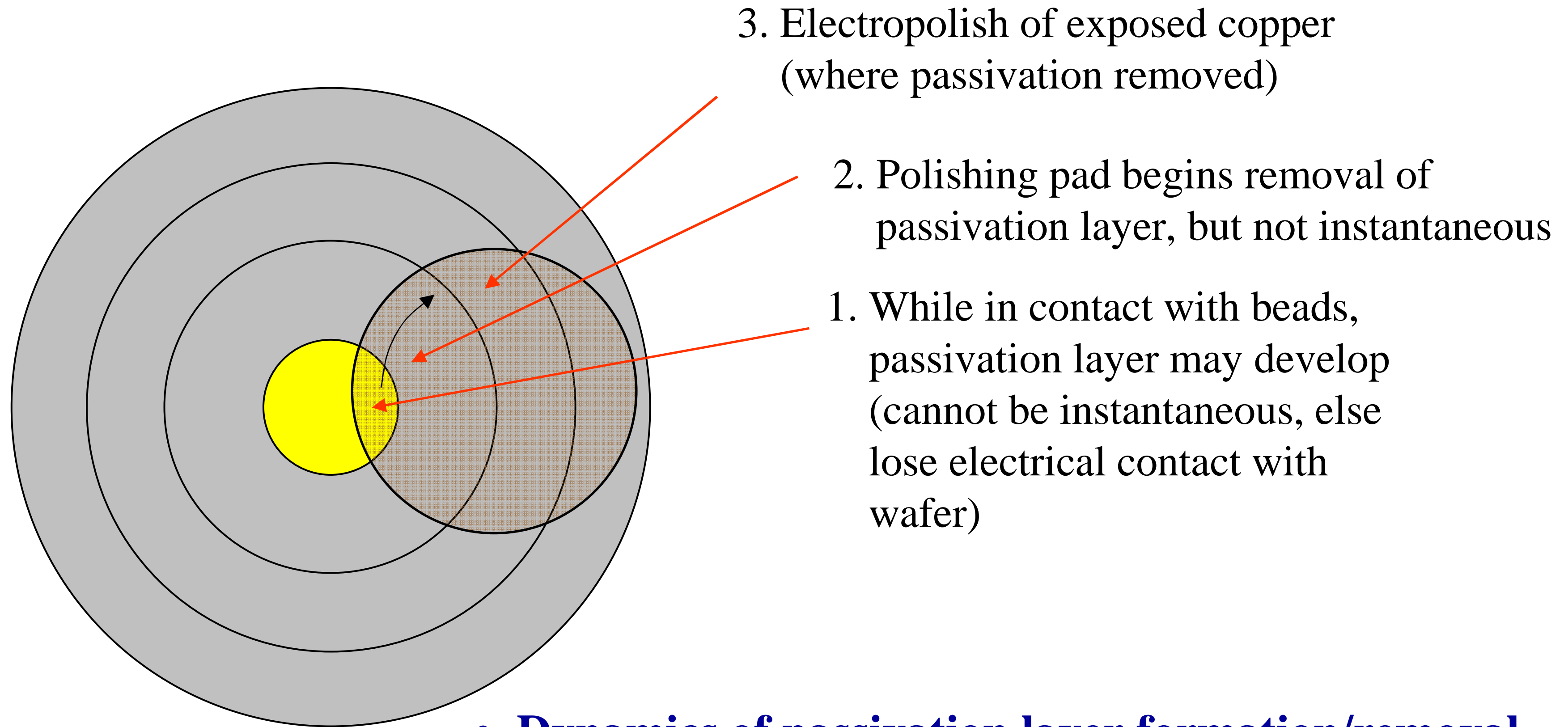

- **Dynamics of passivation layer formation/removal may affect the time-averaged voltage & current that different regions on the wafer experience**
  - **Explain model prediction errors near wafer edge?**

Industrial Interactions and Technology Transfer

- **Albany Nanotech (Chris Borst)**
  - **ECMP experiments on blanket wafer copper removal**
  - **Modeling for wafer-scale ECMP as a function of position, zonal electrical bias**

Future Plans

Next Year Plans

- Improve wafer scale ECMP model physics
  - Two electrode model with electrochemistry
  - Consider dynamics of protective film formation/removal
- Implement 2D/3D version of wafer scale model
  - Cross-coupling in electrolyte; thin film resistance for full copper removal case
- Analysis of conductive pad configuration
- Begin feature/chip-scale ECMP model development

Long Term Plans

- Integrated feature, chip and wafer-scale ECMP model
- Optimization and control strategies for maximized uniformity and minimized process consumption/time

Publications, Presentations, and Recognitions/Awards

- **D. Truque, X. Xie, and D. Boning, "Wafer Level Modeling of Electrochemical-Mechanical Polishing (ECMP)," CMP Symposium, MRS Spring Meeting, April 2007.**
- **Z. Li, D. Truque, D. Boning, R. Caramto, and C. Borst, "Modeling Wafer Level Uniformity in Electrochemical-Mechanical Polishing (ECMP)," Advanced Metallization Conference, Albany, NY, Oct. 2007.**

Reductive Dehalogenation of Perfluoroalkyl Surfactants in Semiconductor Effluents

(*Task Number: 425.015*)

PIs:

- Reyes Sierra, Chemical and Environmental Engineering, UA
- Neil Jacobsen, Chemistry Department, UA
- Vicki Wysocki, Chemistry Department, UA

Graduate Students:

- Valeria Ochoa, PhD candidate, Chemical and Environmental Engineering, UA

Undergraduate Students:

- Chandra Khatri, Chemical and Environmental Engineering, UA

Other Researchers:

- Antonia Luna, Postdoc, Chemical and Environmental Engineering, UA

Cost Share (other than core ERC funding):

UA/NASA grant (to C. Khatri)

Objectives

- **Investigate the feasibility of reductive dehalogenation of PFOS and related perfluorinated compounds using two different approaches:**
  - Chemical biomimetic treatment by vitamin B_{12} and Ti(III) citrate.
  - Anaerobic microbial degradation.
- **Optimize the kinetics of reductive dehalogenation.**
- **Enhancing catalysis with zeolites and other reactive surfaces.**
- **Characterize the mechanisms and products of reductive dehalogenation.**

ESH Metrics and Impact

1. **Reduction in emission of ESH-problematic materials to environment: ≈ 100% removal of PFOS from aqueous waste streams.**

2. **Reduction in the use of natural resources involved in alternative treatment methods (energy):**

   Considerable reduction in energy consumption compared to alternative treatment methods such as reverse osmosis, ultrasonic treatment, etc.

3. **New strategies to design biodegradable PFAS.**

Method of Approach

- ***Optimization of chemical reductive dehalogenation:***

  Technical PFOS with vitamin B_{12}/ Ti(III)

  Temperature, pH, [vitamin B_{12}] and [Ti (III) citrate]

- ***Mechanisms of reductive dehalogenation***

  Role of vitamin B_{12} on chemical reductive dehalogenation

  Electron Paramagnetic Resonance (EPR) – radical mechanism

- ***Enhanced Vitamin B_{12} catalysis via reactive surfaces***

  Solid supports

  Zeolites and activated carbon.

- ***Monitoring of PFOS and PFOS degradation products***

  Analytical approaches

  Removal of PFOS, fluoride release, HPLC, LC-MS-MS, and F-NMR

Results

Chemical *vs.* Microbial Reductive Dehalogenation

- PFOS is reductively dehalogenated by vitamin B_{12}/Ti(III) citrate.
- PFOS is highly resistant to microbial reductive degradation by natural mixed inocula after long periods of incubation

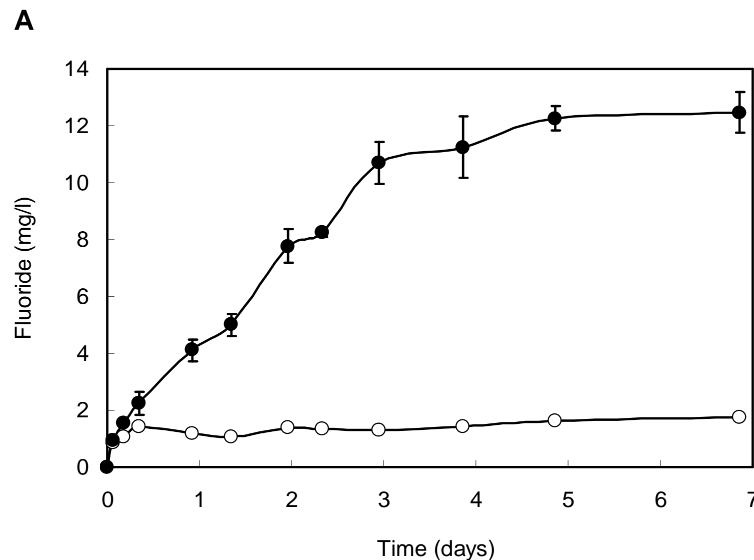

Time course of fluoride release in: (○) PFOS + Ti(III) citrate; (●) PFOS + vit. B12 + Ti(III) citrate) during the chemical reductive defluorination of PFOS by vit. B12 (260 µM) and Ti(III) citrate (36 mM). Samples were incubated at 70ºC and pH 9.0.

Results

Chemical Reductive Dehalogenation

- Technical PFOS contains 20-30% (w/w) branched isomers.
- Branched PFOS isomers are more susceptible to reductive dehalogenation compared to the linear PFOS isomer.

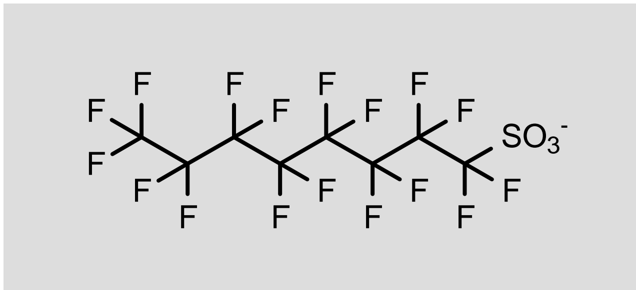

Linear isomer

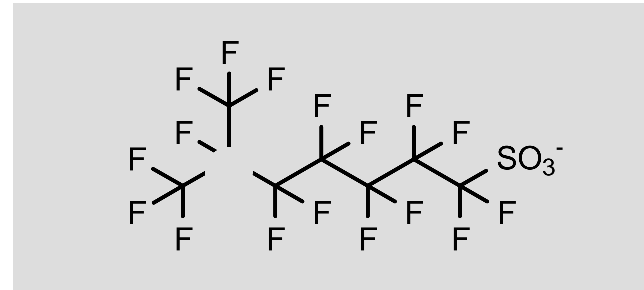

Branched isomer

Results

Optimization of Chemical Reductive Dehalogenation

The impact of temperature and pH, as well as vitamin B_{12} and Ti(III) citrate dosage on the rate of PFOS dehalogenation was assessed:

- The degradation rate increased 37-fold with increasing temperature from 30º to 70ºC.
- A 5.9-fold rate enhancement was attained by increasing the reaction pH from 7.5 to 9.0.
- An optimal vitamin B_{12} dosage of 393 μM was determined
- The rate increased 21-fold by raising the molar ratio Ti(III)/PFOS from 27 to 110.
- The impact of adding co-solvents to improve compound availability is being investigated

Reductive Dehalogenation of PFOS

Effect of Vitamin B12 Dosage

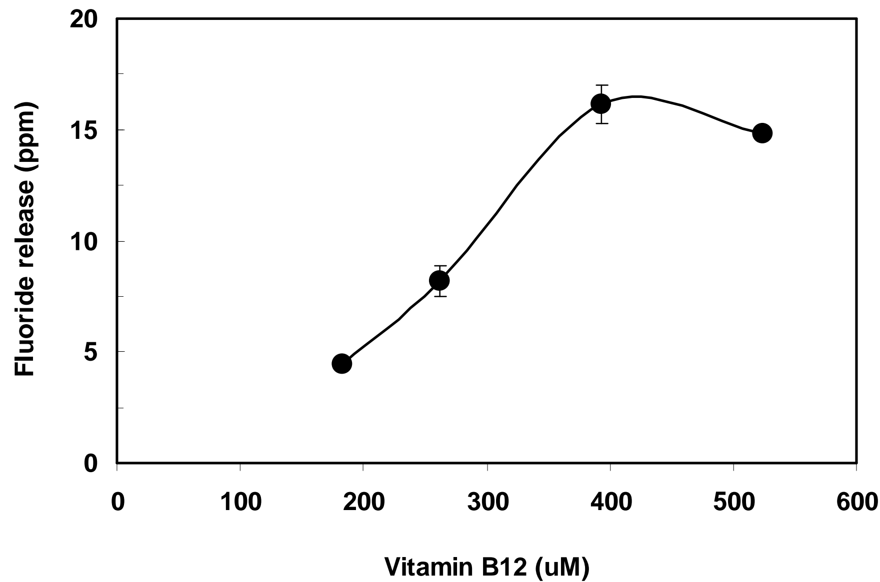

Fluoride release during the reductive dehalogenation of technical PFOS after 1 day (dotted bars) and 7 days (gray bars). For experimental conditions see Slide #5.

Enhancement Catalysis Vitamin B_{12} with Reactive Surfaces

Catalytic effect of Zeolite and Granular Activated Carbon (GAC)

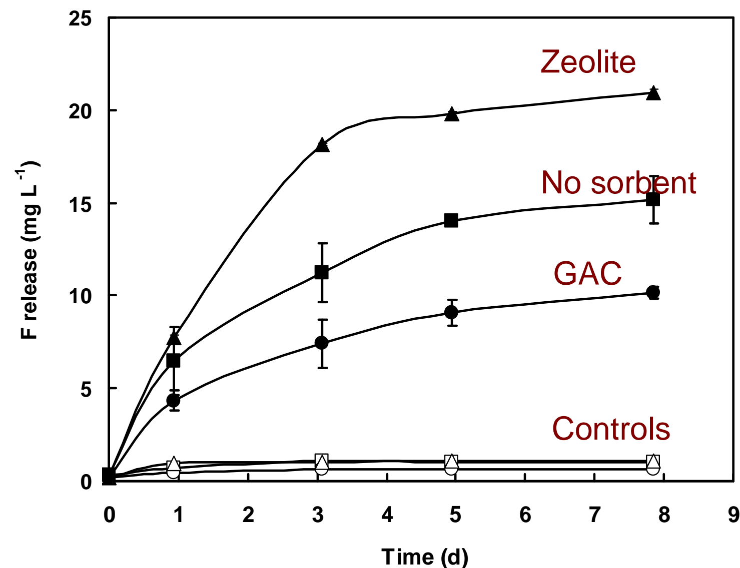

Time course of fluoride release during reductive dehalogenation of PFOS in the presence of different sorbents.

Controls: *PFOS with: (□) Ti(III) cit.; Δ) Ti(III) cit./ zeolite; (○) Ti(III) cit./ GAC .*
Treatments: *PFOS with: (■) Ti(III) cit./ B12; (▲) Ti(III) cit./ B12 /zeolite; (●) Ti(III) cit/ B12/ GAC.*

- Faujasite zeolite enhances the rate and extent of PFOS dehalogenation.

Proposed Mechanism of Biomimetic Reductive of PFOS with Vitamin B_{12}/Ti(III)

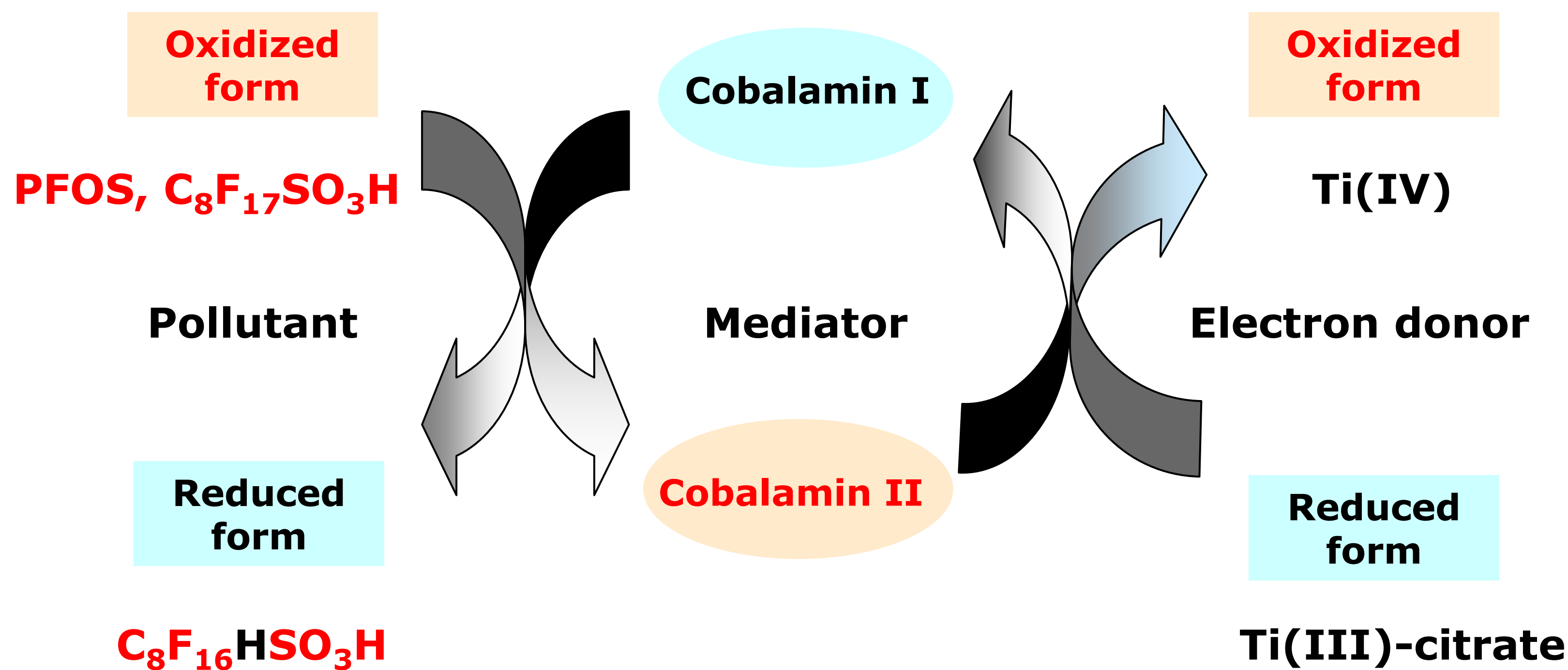

Mechanism of Reductive Dehalogenation of PFOS with Vitamin B_{12}/Ti(III)

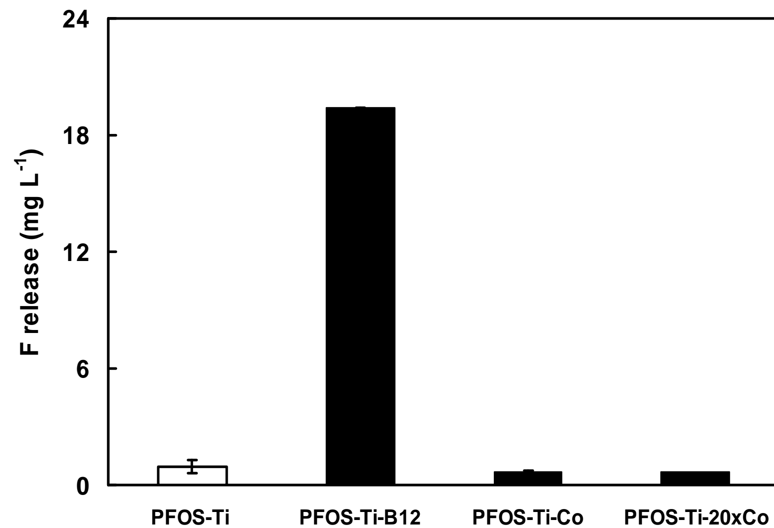

Effect of catalyst on the biomimetic reductive dehalogenation of technical PFOS on day 7. Control samples (white bars) and treatment samples (black bars).

- Vitamin B12 (cobalamine) is responsible for PFOS dehalogenation.
- PFOS was not degraded when Co(II) was used in lieu of vitamin B12.
- Electron paramagnetic resonance (EPR) results confirmed the involvement of a radical-mediated mechanism.

Results:

Identification of Degradation Products

- LC-MS/MS, solid and liquid F-NMR and GC/MS studies were conducted to identify the products of the PFOS dehalogenation.
- No PFOS degradation products were detected either in the reaction solution or in the gas phase.
- Fluorinated compounds were not detected in the insoluble/colloidal fraction
- Organic acids and CO_2 still need to be explored.

Conclusions I

- **PFOS is susceptible to chemical reductive dehalogenation by vitamin B12/Ti(III).**

- **Branched PFOS isomers are more susceptible to reductive dehalogenation than the linear PFOS isomer.**

  Branched PFOS better ESH characteristics (more prone to biodegradation in anaerobic sediments).

- **Reductive dehalogenation of PFOS involves a radical mechanism.**

Conclusions II

- **Optimized temperature and pH greatly enhances PFOS reductive dehalogenation kinetics.**

    T = 70°C ; pH = 9

- **Catalysis of vitamin B12 enhanced by reactive surfaces.**

    Certain zeolites increase defluorination rates

- **PFOS is highly recalcitrant to microbial dehalogenation.**

    No F^- release in 2 years from technical PFOS

Industrial Interactions and Technology Transfer

Industrial liaisons:

- Walter Worth - Sematech
- Tim Yeakley – TI

Future Plans

Next Year Plans

- **Evaluate treatment conditions to promote the chemical reductive dehalogenation of PFOS and reduce treatment costs:**
  - **Use of zeolites as catalyst.**
  - **Use of co-solvents to improve PFOS availability.**
  - **Replacement of the catalyst and the electron donor:**

    Alternatives to vitamin B12: eg. Ni- and Fe-cofactors (F_{430}, hematin, etc.)

    Alternatives to Ti(III) citrate: dithiotreitol, etc.

- **Complete the identification of key products of reductive dehalogenation.**
  - **Explore CO_2 and organic acids.**

- **Evaluate the reductive dehalogenation of PFOS by microorganisms that biosynthesize high levels of vit. B12 (eg. *Methanosarcina barkerii*).**

Future Plans

Long-Term Plans

- Build and evaluate a prototype treatment system and test it on real PFAS containing wastewaters generated during semiconductor manufacturing.
- Make treatment costs competitive by replacing chemical catalysts/e-donor with microbial catalysts.

Publications, Presentations, and Recognitions/Awards

- **Publications**

  Ochoa-Herrera et al. "Reductive defluorination of perfluorooctane-sulfonate (PFOS). (Under review).

- **Awards**

  Ochoa-Herrera, V. Outstanding teaching assistant of the Dept. Chemical and Environmental Engineering, academic year 2006/2007.

EHS Impact of Electrochemical Planarization Technologies

(*Task Number: 425.016*)

PI:

- **Alan West, Chemical Engineering, Columbia University**

Graduate Student:

- **Kristin Shattuck, PhD candidate, Chemical Engineering, Columbia University**

Undergraduate Student:

- **Neha Solanki, Chemical Engineering, Columbia University**

Other Researcher:

- **Jeng-Yu Lin, Visiting Scholar, Chemical Engineering, National Tsing-Hua University**

Objectives

- Develop methods for planarization that optimize the use of electrochemistry and improve aspects of current technologies
- Develop a method to predict feature scale planarization through the use of planarization factors
- Test planarization capabilities of novel ECMP electrolytes using patterned structures
  - Phosphate based electrolytes containing BTA inhibitors
- Develop electrolytes for polishing liner materials
  - Ruthenium
- Study galvanic corrosion between Cu and Ru
  - Potentially utilizing microfluidics

ESH Metrics and Impact

1. *Development of a more environmentally benign polishing electrolyte*
    - *Improve process yield*
    - *Potential elimination of slurry particles*
    - *Reduction or elimination of complexing agents and oxidizers in solution, facilitating waste treatment*

2. *Potential reduction in electrolyte volume*
    - *Reduce waste generation*

3. *Extend lifetime of consumables*
    - *polishing pads*

Method

1. *Screen ECMP electrolytes using an RDE*
   - *Potassium phosphate based electrolytes investigated*

2. *Use custom built ECMP tool to evaluate electrolytes for their planarization capabilities*
   - *Compare results with RDE predictions to develop a potential screening technique and model for planarization*

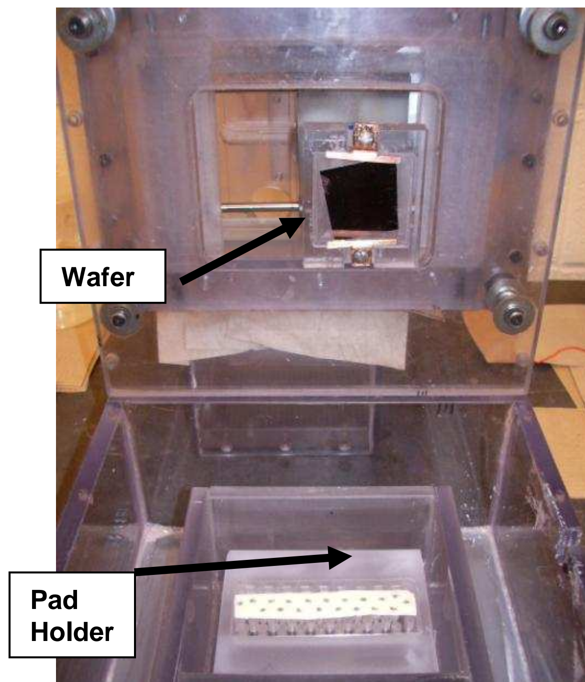

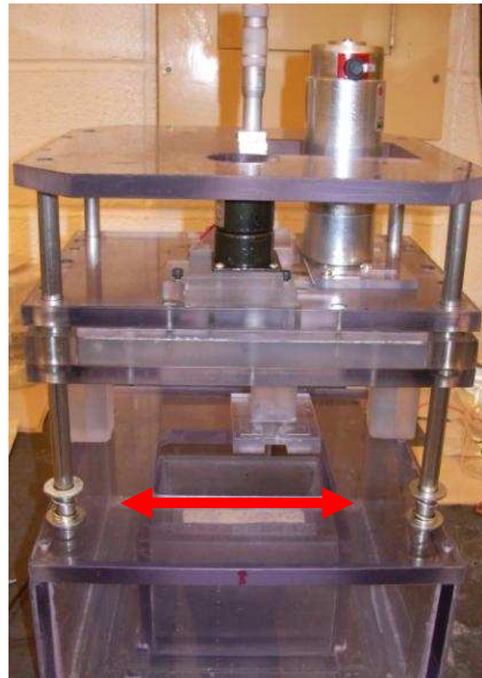

Design features:

- ***2D linear motion***
- ***Apply and control low downforces (<1 psi)***
- ***Ease of changing between various electrolytes and pads***
- ***Operate in contact and non-contact modes***

Method

1. *Cu Electrolytes*
    - *pH*
    - *Salt concentration*
    - *BTA concentration*

2. *Cu ECMP*
    - *IC1000/1010*
    - *Suba*
    - *Politex*
    - D100

3. *Patterned Wafers*
    - *Cu electrodeposition performed on wafers*
    - *Blanket Cu wafer patterned with lithography*
    - *Features created by multiple etching steps post lithography*
    - *Profilometry used to characterize polishing results Before/After*

4. *Ru Electrolytes*
    - *Potassium phosphate based electrolytes*
        - *pH*
        - *BTA concentration*
    - *Ceric ammonium nitrate (CAN) containing electrolytes*

Approach

- *To determine planarization capabilities of electrolytes, a planarization factor,* ε, *was defined assuming validity of Faraday's law*

$$\varepsilon = \frac{s_o - s_f}{\lambda_{avg}} \approx \frac{i_t - i_b}{i_{avg}} \longrightarrow \varepsilon_{RDE} = \frac{i_{no} - i_{BTA}}{i_{no}}$$

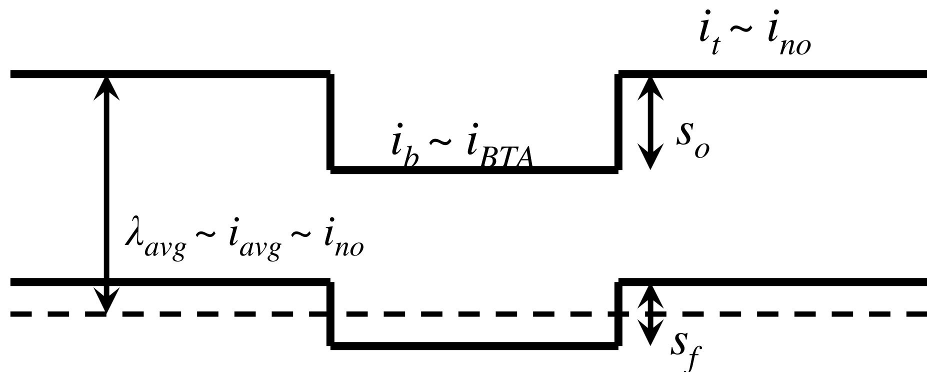

$$\varepsilon_{ECMP} = \frac{i_{pad} - i_{no-pad}}{i_{pad}}$$

Results

- *Anodic polarization curves for oxidation of a Cu RDE*
  - *Rotation speed:100 RPM*

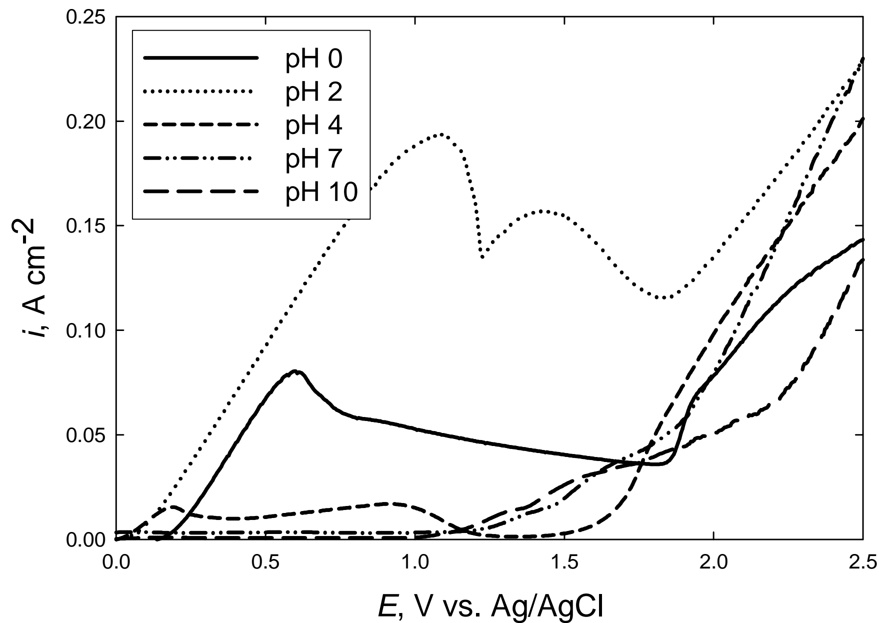

Five pH values shown for a 1 M KH_2PO_4 based electrolyte, all electrolytes contain No BTA

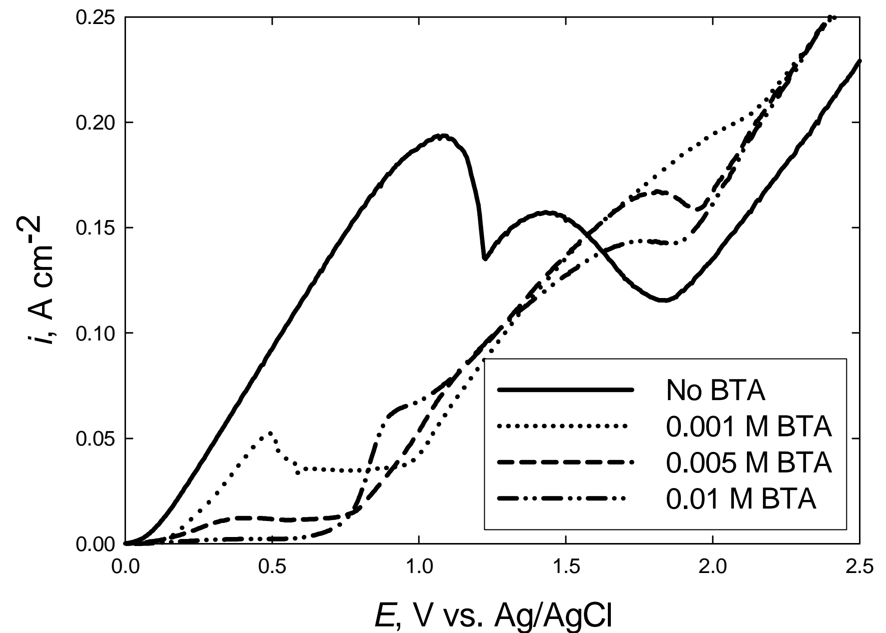

1 M KH_2PO_4 electrolyte with pH 2 containing three different BTA concentrations

Results

- *Planarization factors, ε, for an RDE and ECMP tool*
  - *Good correlation between ε_{RDE} and ε_{ECMP} is observed*

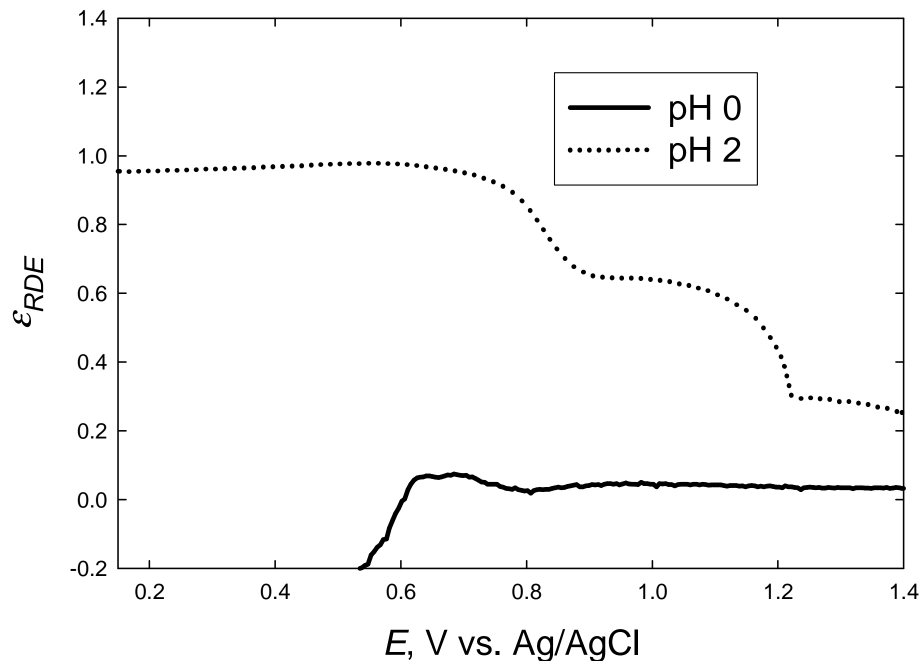

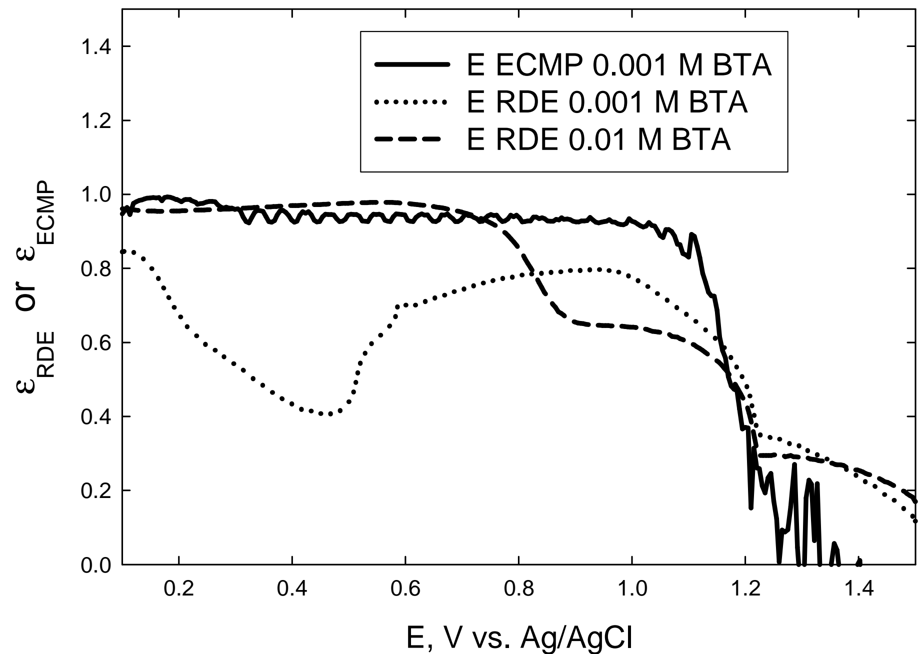

ε_{RDE} of concentrated phosphoric acid (pH ~0) and pH 2, no BTA present

ε_{RDE} and ε_{ECMP} of electrolytes with pH 2, using various BTA concentrations

Results

No BTA, No Contact

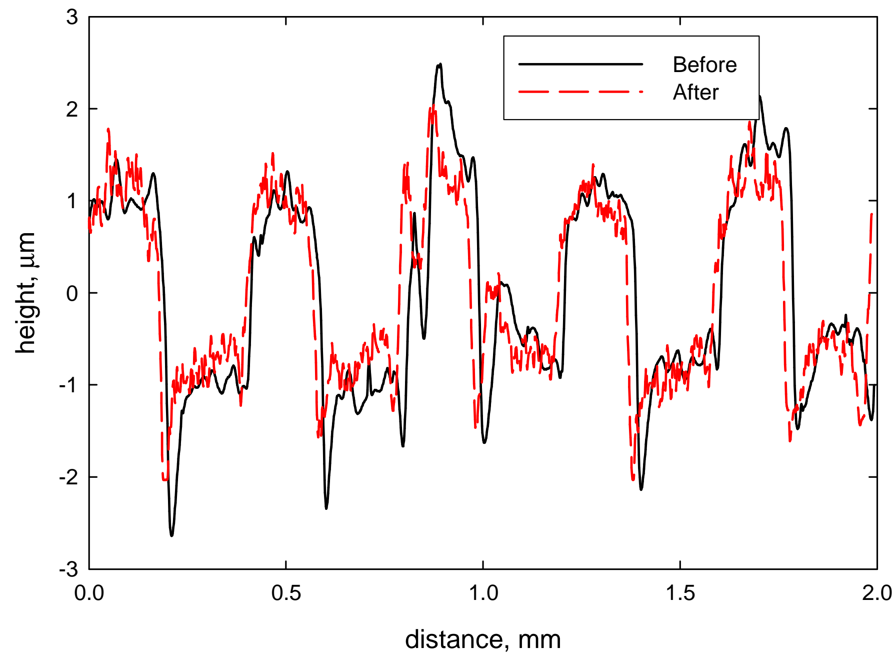

0.001 M BTA, With Contact

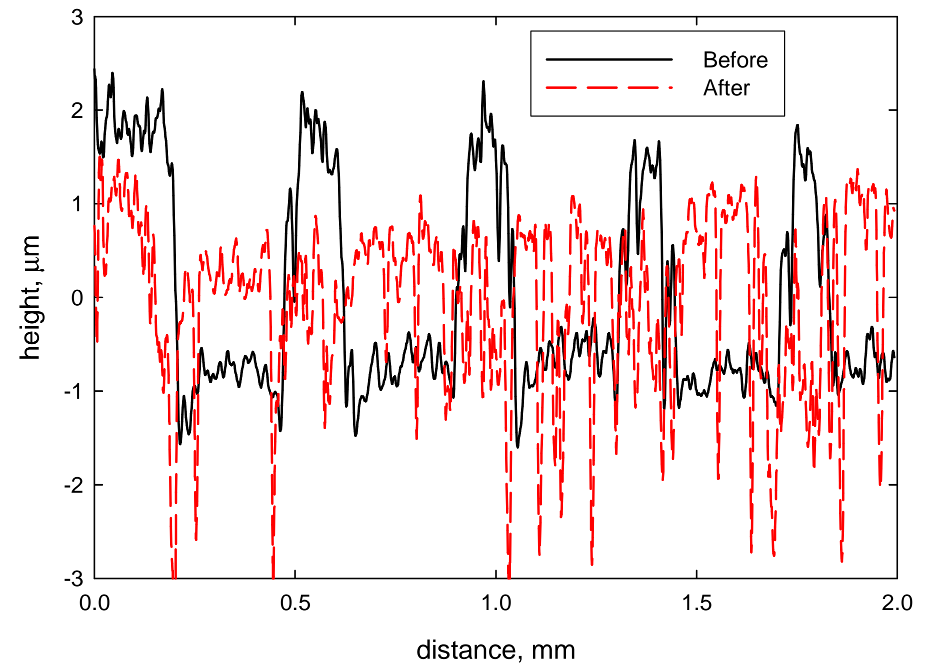

- 0.5 V vs. Ag/AgCl
- time: 300 s

- 0.5 V vs. Ag/AgCl
- time: 210 s

Results

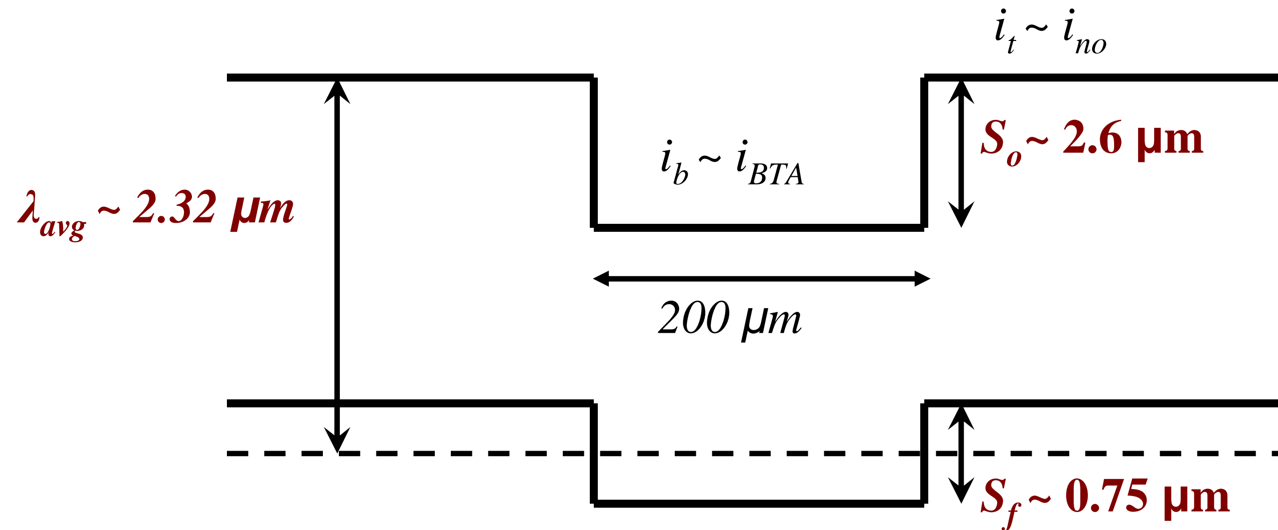

$$\varepsilon = \frac{s_o - s_f}{\lambda_{avg}} \sim \frac{2.60 - 0.75}{2.32} \sim 0.80$$

Results

- *Polishing Ru liners*
  - *Initially investigating*
    - *Potassium phosphate based electrolytes*
    - *Electrolytes containing CAN, ceric ammonium nitrate*

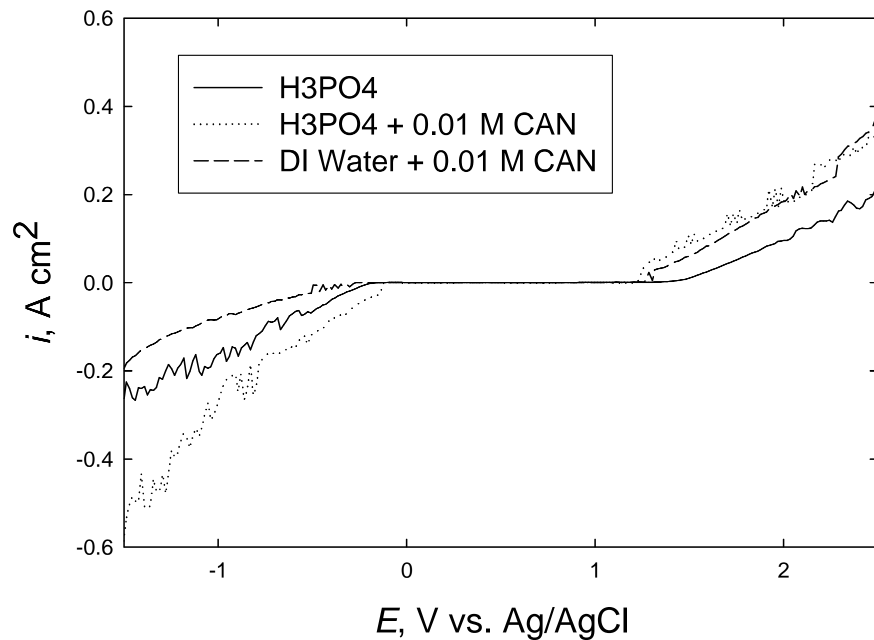

Scan rate: 10 mV s^{-1}

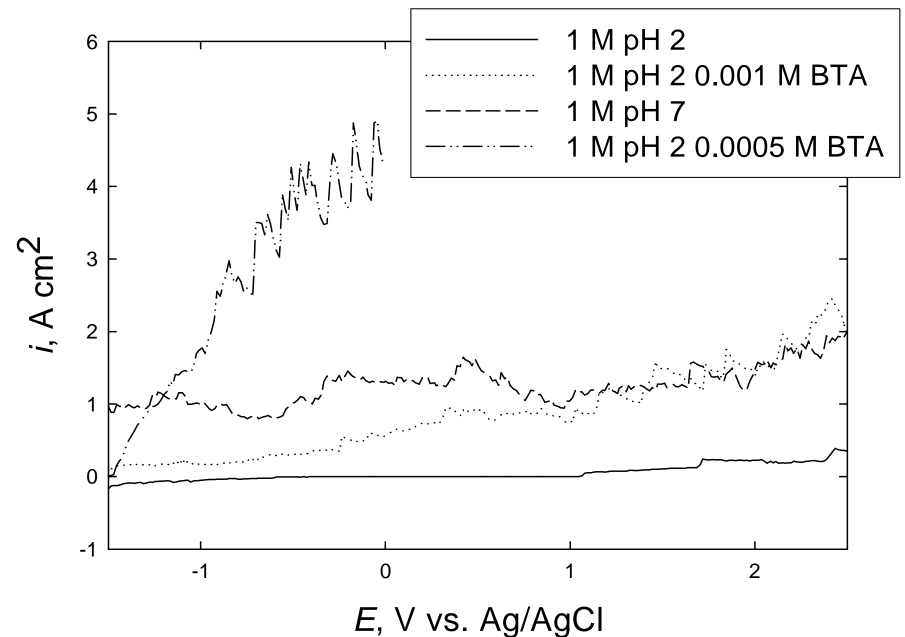

Scan rate: 10 mV s^{-1}

Industrial Interactions and Technology Transfer

- **Industry mentors/contacts**
  - **Intel**
  - **Novellus**
  - **Texas Instruments**

- **Polishing Pads**
  - **Cabot**
  - **Rohm & Haas**

- **Wafers**
  - **IBM**
  - **Novellus**

Future Plans

Next Year Plans

- Finish planarization studies on Cu ECMP
  - Establish appropriate model to predict planarization
- Continue investigation of polishing liner materials
  - Ru
- Begin microfluidic studies to investigate galvanic corrosion between Ru and Cu

Long-Term Plans

- Optimize pad / chemistry
- Demonstrate on Cu/Ru/Ta structures
- Collaborate with industry/university to perform wafer-scale ECMP tool experiments

Publications, Presentations, and Recognitions/Awards

- **K. G. Shattuck, J. Y. Lin, and A. C. West, Characterization of Phosphate Electrolytes for use in Cu Electrochemical Mechanical Planarization, Electrochimica Acta, (*Submitted*)**

- **K. G. Shattuck, J. Y. Lin, and A. C. West, Planarization Studies of Phosphate Based Electrolytes for use in Cu ECMP, (*Pending*)**

- **J. Y. Lin, A. C. West, and C. C. Wan, Adsorption and Desorption Studies of Glycine and Benzotriazole during Cu Oxidation in a Chemical Mechanical Polishing Bath, Journal of the Electrochemical Society, (*Submitted*)**

- **J. Y. Lin, A. C. West,and C. C. Wan, Evaluation of Post-Cu CMP Cleaning of Organic Residuals Using a Microfluidic Device, Electrochemistry Communication, (*Submitted*)**

Environmentally Benign Vapor Phase and Supercritical CO_2 Processes for Patterned Low k Dielectrics

(*Task Number: 425.017*)

PIs:

- **Karen K. Gleason, Department of Chemical Engineering, MIT**

Graduate Students:

- **Salaman Baxamusa: PhD Candidate, Department of Chemical Engineering, MIT (NSF Fellow)**
- **Shannan O'Shaughnessy, PhD: Department of Chemical Engineering, MIT (Graduated 5/07)**
- **Nathan J. Trujillo: PhD: CEP Candidate, Department of Chemical Engineering, MIT (Started 9/07)**

Cost Share (other than core ERC funding):

- **$70k (NSF Fellowship for Sal Baxamusa)**

Objectives

- **Develop new methods to deposit, pattern, and process low k materials to meet roadmap goal of dielectric constant less than 2.0.**
- **Process step reduction through EHS focused approach for selectively deposited low k dielectric**

ESH Metrics and Impact

1. *Resist-free photolithography would eliminate use of photoresist. Approximately 25,000 liters of photoresist materials is used annually in typical semiconductor foundries, at a cost of about $1,600 per liter. Through spin-on process approximately 95% of resist is wasted and disposed as toxic material [1] .*

2. *Common positive tone resist developer tetramethyl ammonium hydroxide poses health hazards when handled[2] . Acute aquatic toxicity testing of neutralized solution has been shown to be highly toxic to organisms. High resolution features were developed using IPA which is biodegradable, not likely to bioconcentrate, and has low potential to affect organisms.*

3. *Typical iCVD process requires between .02-.12 W/cm^2 [3] for polymer deposition compared to conventional PECVD which uses 0.4-2.1 W/cm^2[4,5] . No plasma etch eliminates additional >7.1 W/cm^2[6] power requirement.*

[1] Percin et al., IEEE Transactions on Semiconductor Manufacturing (2003) 16 (3)
[2] Lee et al., J. Micromech. Microeng. (2005) 15
[3] Martin et al.Surf. Coating Tech. (2007) 201
[4]Castex et al. Microelec. Eng. (2005) 82
[5]Wong et al. Thin Sol. Films 462–463 (2004)
[6]Berruyer et al. J. Vac. Sci. Technol. A. 16.3 (1998)

iCVD Process Chemistry

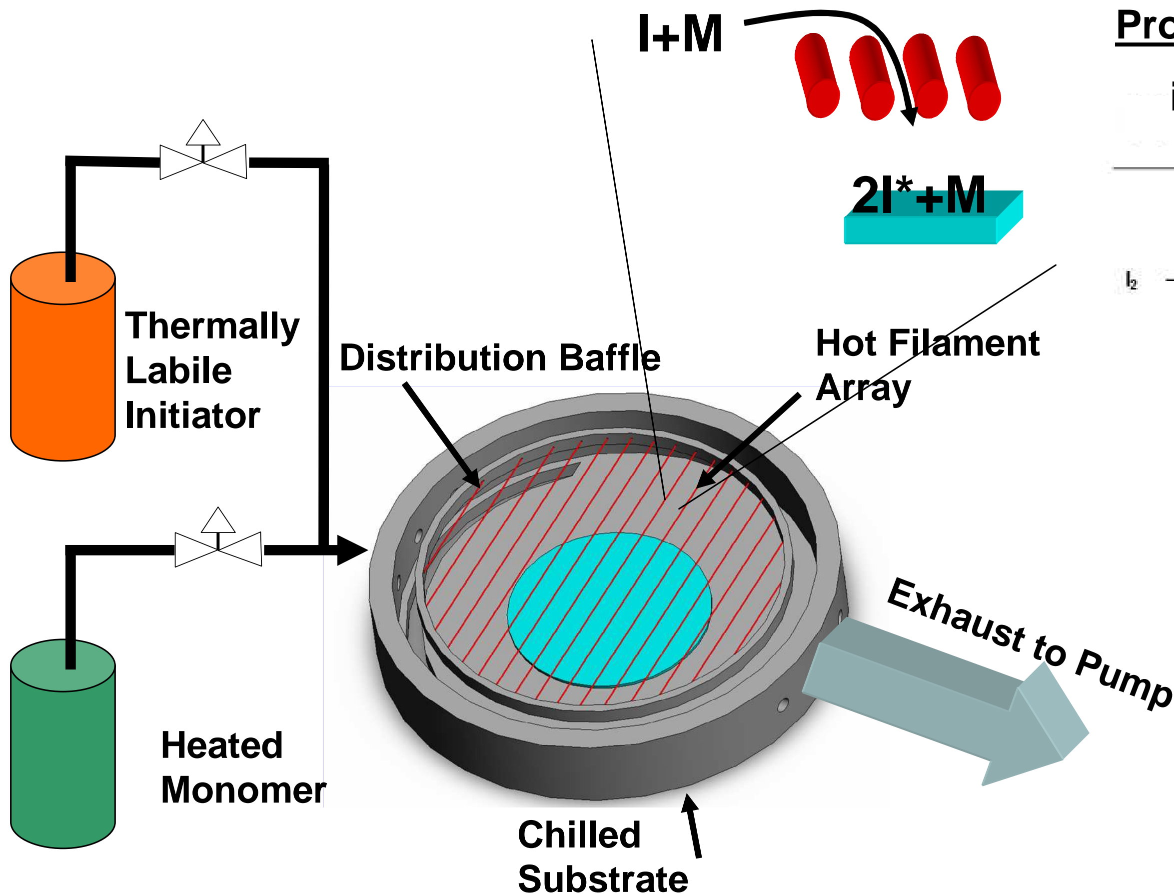

Proposed Polymerization Mechanisms

iCVD (novel low energy process)

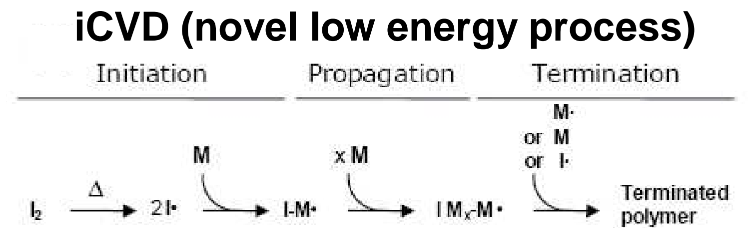

PECVD (conventional process)

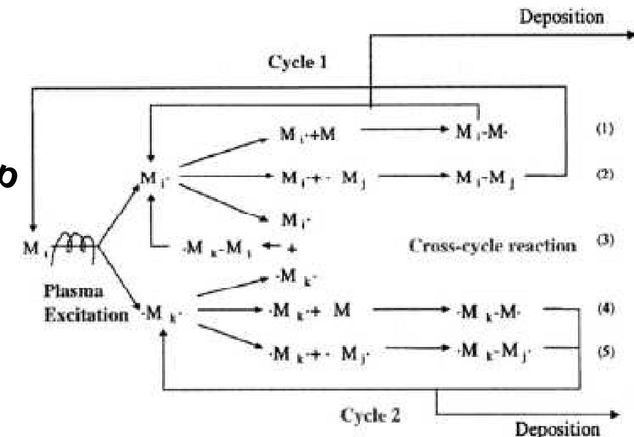

New Low-k iCVD Precursor V4D4

- Free volume of siloxane ring for low-k
- Four vinyl groups make ideal for free radical polymerization via iCVD
- No need for cross linker
- 3-D network from "puckered" ring
- Plasma polymerization gives k as low as 2.5

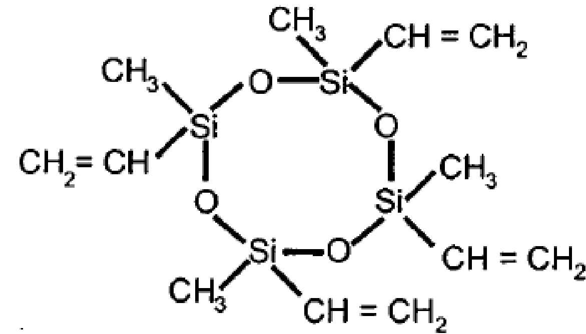

1,3,5,7-TETRAVINYLTETRAMETHYLCYCLOTETRASILOXANE

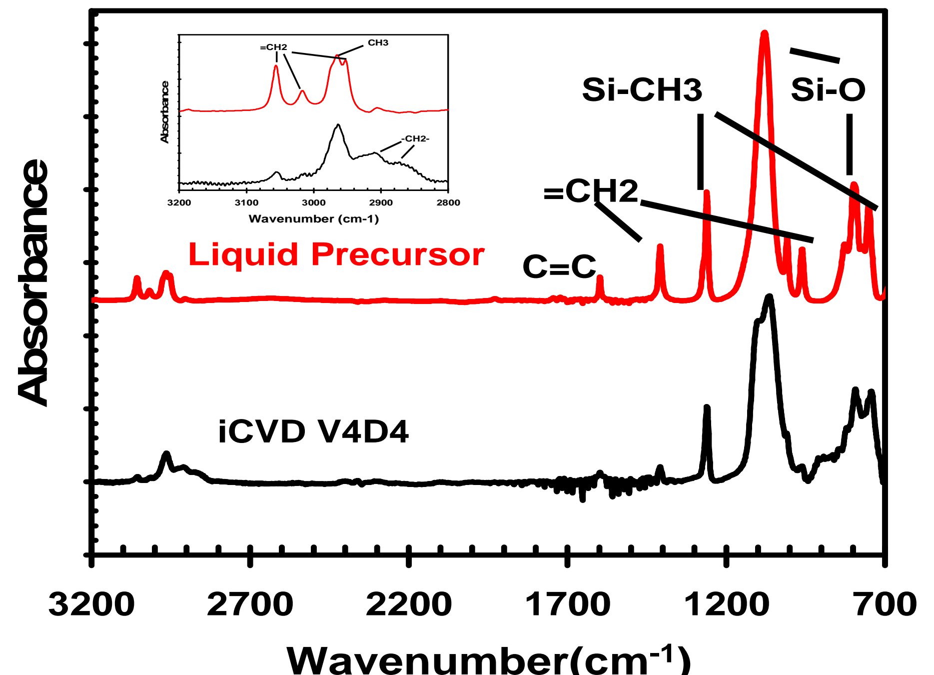

Additive Polymer Patterning Using Self Assembled Mask (no traditional lithography)

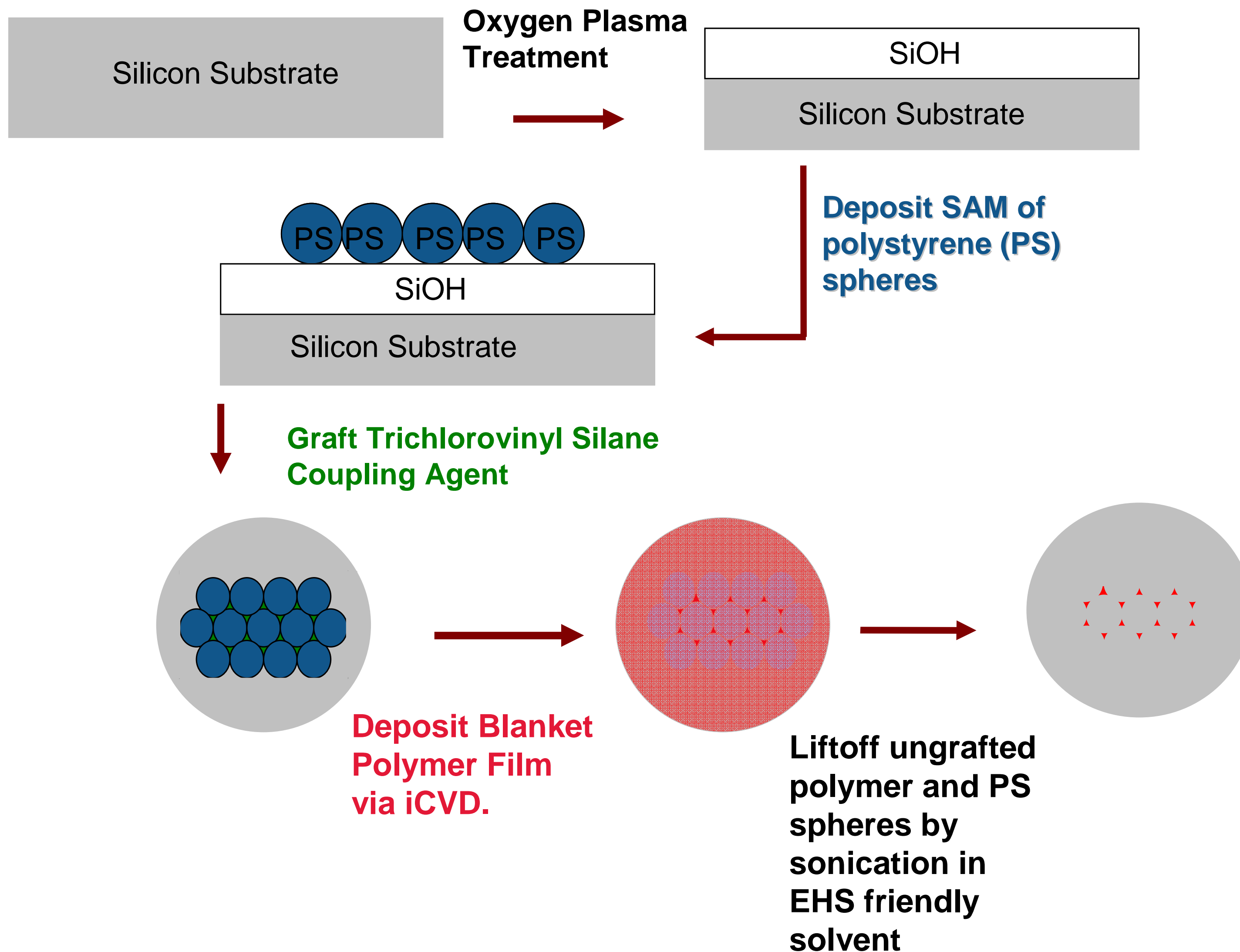

Low-k Lift-Off With IPA

- iCVD V4D4 Pattern with 1 μm spheres
- Very well-ordered patterns achieved
- Lift-off after sonicating in IPA for 1 hr
- Achieved full lift-off with environmentally friendly solvent
- Up to 700 nm in height

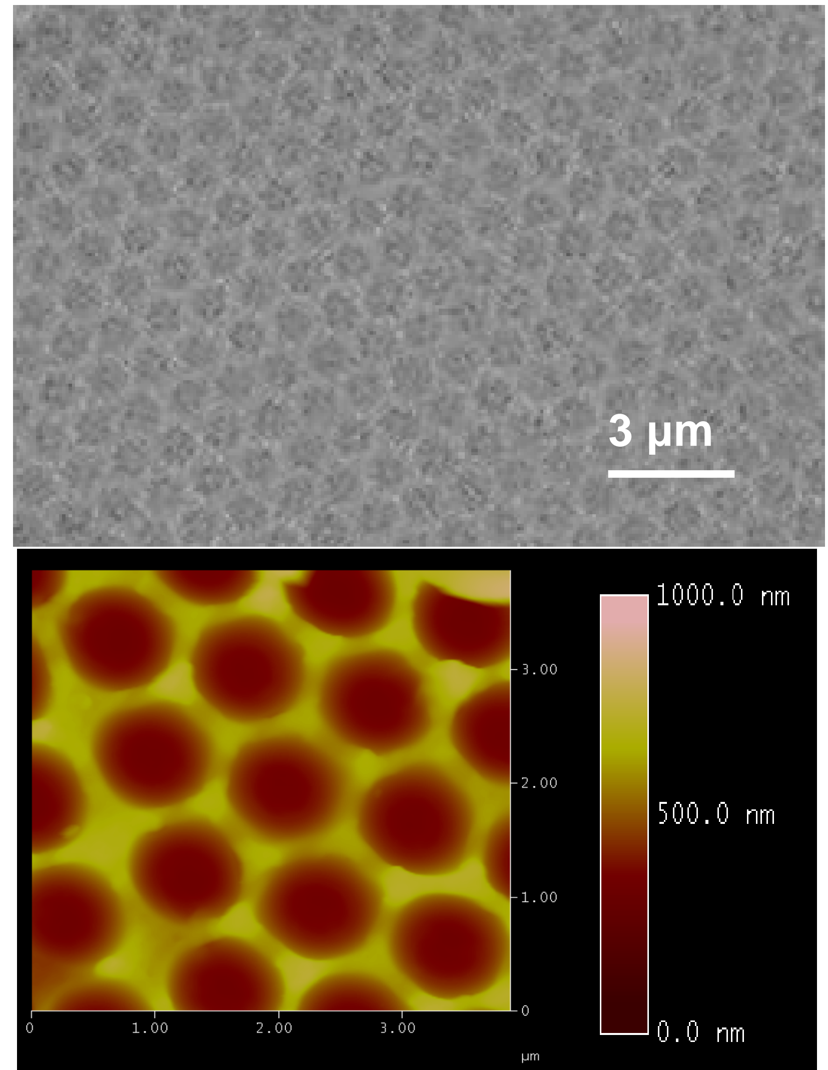

Environmentally Friendly 75 nm Low-k Pattern

- Used 200nm spheres for pattern
- Very well ordered patterns achieved from IPA lift-off
- Smallest features about 75 nm wide and about 100 nm in height
- Excellent substrate adhesion:10 minute sonication in THF

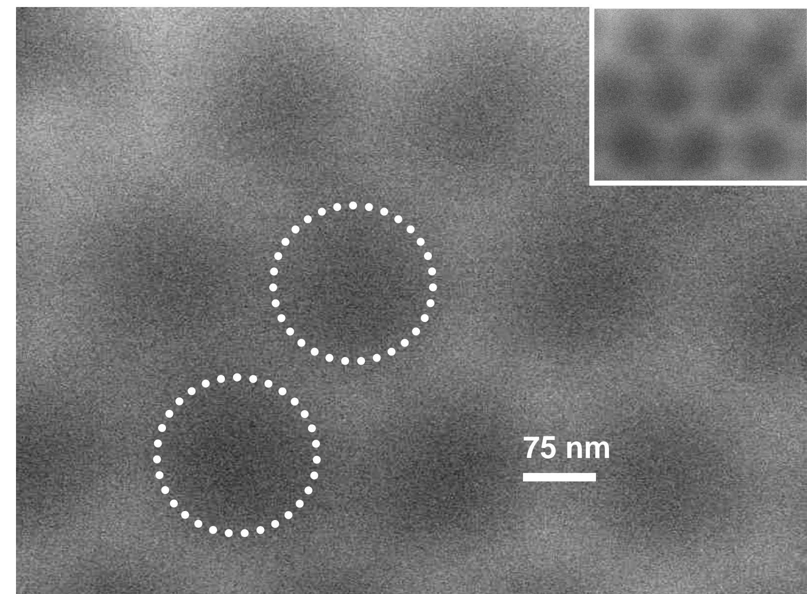

Resistless Patterning Prevents Waste

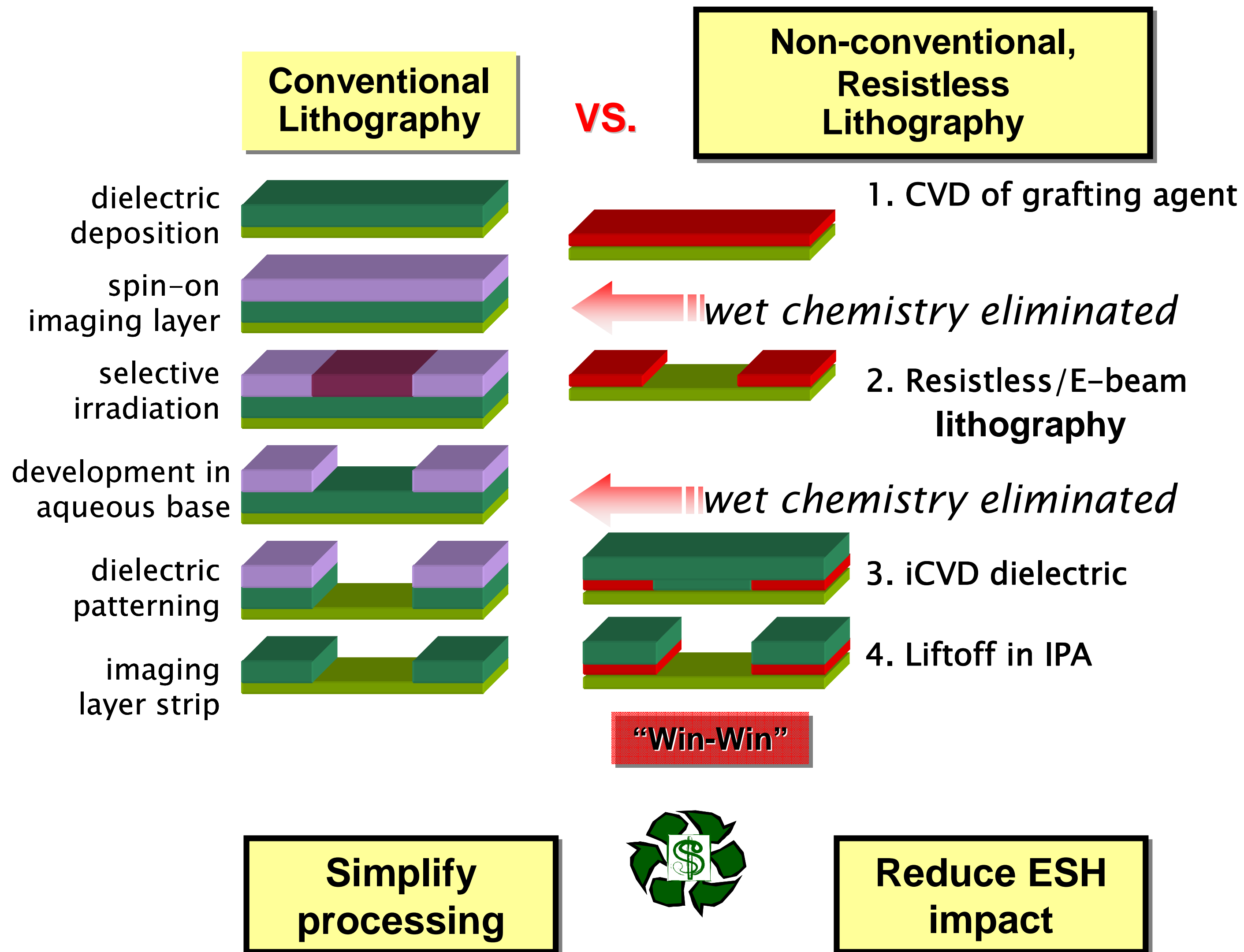

Resist-Free Photo Lithography

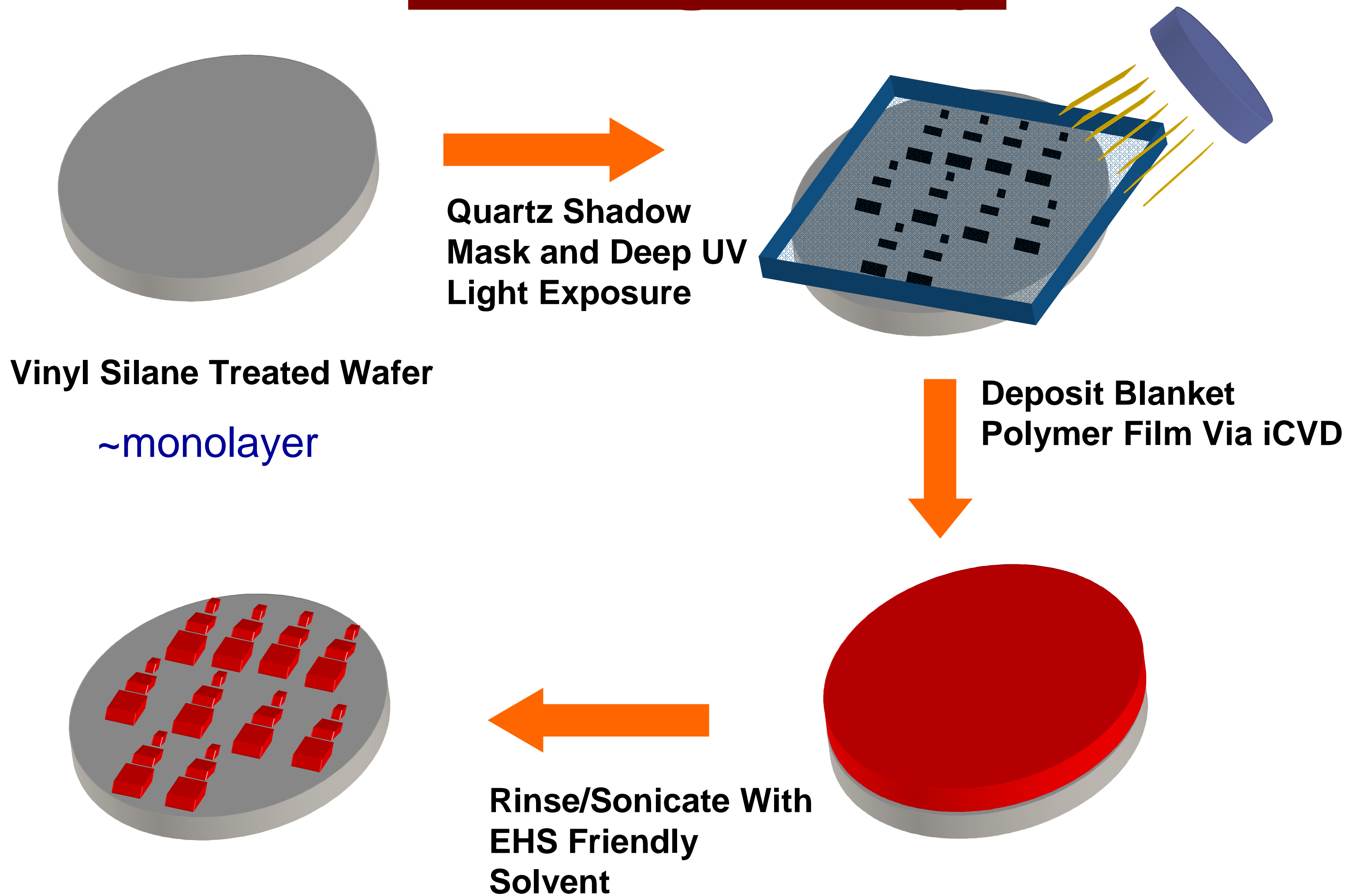

Photolysis of Trichlorovinylsilane

•Exposing grafted vinyl silane monolayer to 193 nm light photolyzes vinyl bonds and removes ability to tether iCVD polymer. Can use lithography masks to define exposure pattern.

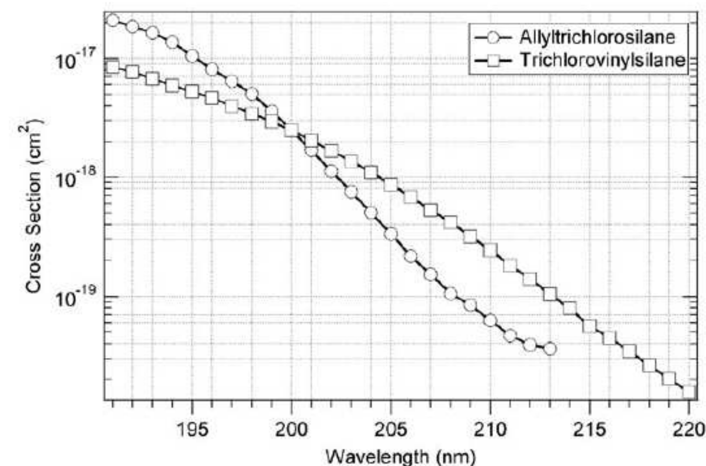

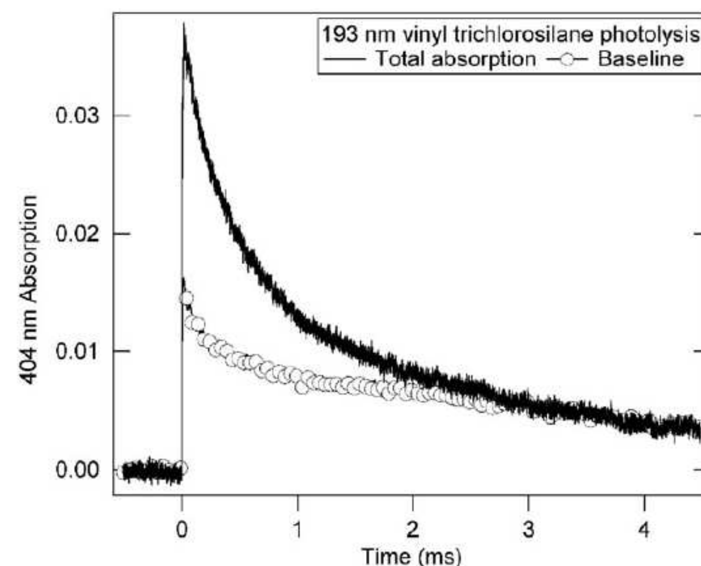

DeSain et al., *Phys. Chem. Chem. Phys,* (2006), 8

Environmentally Friendly 193 nm Photolithography

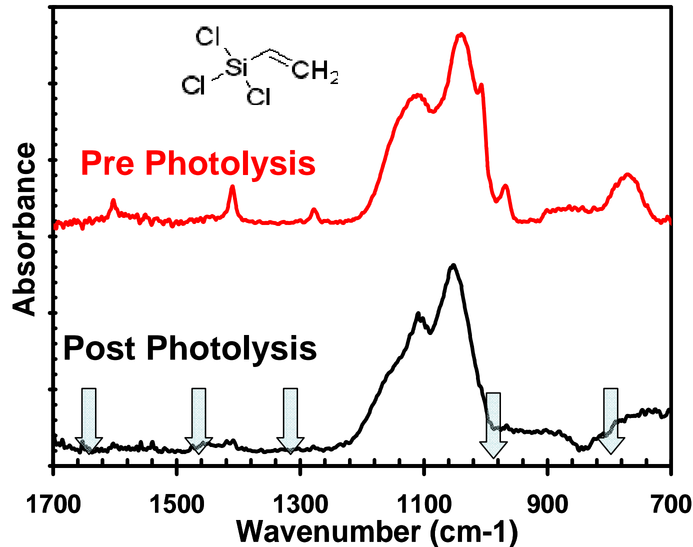

Thickness 28nm	Contact Angle 97º
Thickness 26nm	Contact Angle 50º

Loss of organic moieties and hydrophilic contact angle indicate destruction of vinyl monolayer

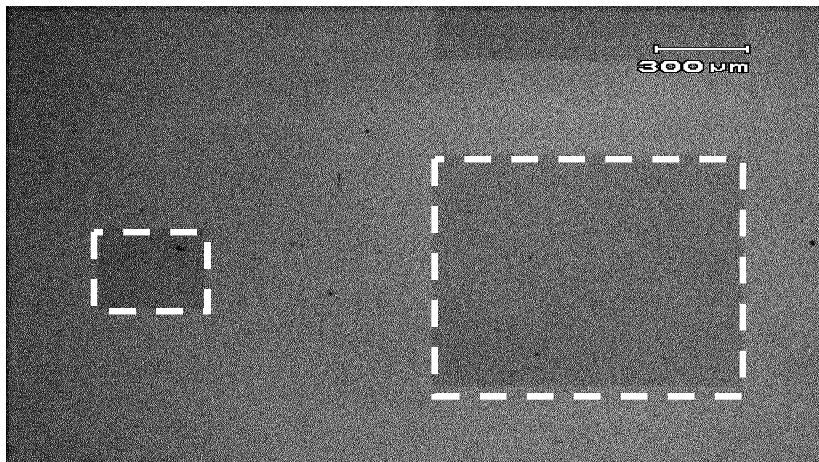

Grafted polymer pattern

Pre Deposition	Post Deposition
Thickness 35 nm	Thickness 53 nm
Contact Angle 68º	Contact Angle 105º

Grafting only in unexposed area!

Industrial Interactions and Technology Transfer

- **Harry Levinson, Manager Strategic Lithography Technology and Senior Fellow: AMD Harry.Levinson@amd.com**

- **Qingguo Wu, Technologist: Novellus Systems Inc. Qingguo.Wu@novellus.com**

- **Dorel Toma, Director, US Technology Development Center, Tokyo Electron Limited.**

Future Plans

Next Year Plans

- Incorporate porogens into additively patterned low k material
- Study mechanical and thermal stability of low k material
- Perform resist free patterning with wafers patterned by e-beam at Cornell
- Create higher resolution patterns using resist-free photolithography

Long-Term Plans

- Perform resist free photolithography using commercial patterning equipment

Publications, Presentations, and Recognitions/Awards

PUBLICATIONS

- W. Shannan O'Shaughnessy, Sal Baxamusa, Karen K. Gleason, "Additively Patterned Polymer Thin Films by Photo-Initiated Chemical Vapor Deposition (piCVD)",Chem. Mater. 19, 5836–5838 (2007).
- W. S. O'Shaughnessy, S. K. Murthy, D. J. Edell, and K. K. Gleason; Stable Insulation Synthesized by Initiated Chemical Vapor Deposition of Poly(1,3,5-trivinyltrimethylcyclotrisiloxane) Biomacromolecules, 8, 2564-2570 (2007).
- O'Shaughnessy, W.S.; Mari-Buye, N.; Borros, S.; and Gleason, K.K.; Initiated Chemical Vapor Deposition (iCVD) of a surface modifiable copolymer for covalent attachment and patterning. Macromol. Rapid Commun. 28, 1877–1882 (2007).
- Tyler P. Martin, Kenneth K.S. Lau, Kelvin Chan, Yu Mao, Malancha Gupta, W. Shannan O'Shaughnessy, Karen K. Gleason, Initiated chemical vapor deposition (iCVD) of polymeric nanocoatings, Surface And Coatings Technology, 201, 9400-9405 (2007).
- Ph.D. Thesis, W. Shannan O'Shaughnessy, Dept. of Chemical Engineering, MIT

PRESENTATIONS

- K.K. Gleason, Polymeric Nanocoatings by Chemical Vapor Deposition, Pall Corporation, 2/6/2007
- K.K. Gleason, Design of CVD processes for low k dielectrics and air gap formation, 2007 MRS Spring Meeting:Symp. B, San Francisco, CA 4/11/2007 (invited)
- K.K. Gleason, Initiated chemical vapor deposition (iCVD) of polymeric nanocoatings, 16th European Conference on Chemical Vapor Deposition, Den Haag, Netherlands, 9/20/2007 (invited).
- K.K. Gleason, Chemical Vapor Deposition of Polymeric Nanocoatings, U. Calgary, Dept. Chemical Engineering, 10/5/2007 (invited).
- K.K. Gleason, Conformal Polymeric Thin Films via Initiated Chemical Vapor Deposition, AVS Seattle, WA, 10/15/2007 (invited)
- K.K. Gleason, Engineering Polymeric Nanocoatings by Vapor Deposition 31th Annual Symposium of the Macromolecular Science and Engineering Program at the University of Michigan., Ann Arbor, MI, 10/25/2007 (invited).
- Nathan J. Trujillo and Karen K. Gleason, ERC TeleSeminar, "Additive Patterning of Low Dielectric Constant Polymer Using iCVD", December 13, 2007

Environmentally Benign Vapor Phase and Supercritical CO_2 Processes for Patterned Low k Dielectrics

(Task Number: 425.017; Ober sub-task)

PIs:

- **Christopher K. Ober, Cornell University**
- **Karen K. Gleason, Massachusetts Institute of Technology**
- **James J. Watkins, University of Massachusetts, Amherst**

Graduate Students:

- **Nelson M. Felix, Cornell University, Chemical Engineering (graduated 1/08)**
- **Jing Sha, Cornell University, Materials Science & Engineering**
- **Katy Bosworth, Cornell University, Chemistry (other support)**

Cost Share (other than core ERC funding):

- **IBM Fellowship ($80k), KB**
- **NSF Support ($80k), JS**

Objectives

- **Understand the fundamental solubility characteristics of resist molecules in supercritical (sc) CO_2**
  - **scCO_2 is an environmentally friendly, non-polar high performance solvent**
- **Demonstrate the high-resolution patternability and development of non-polar materials in scCO_2**
  - **scCO_2 has performance attributes that may make it ideal as a high resolution resist developer**
- **Provide lithography expertise and patterning capabilities to Gleason and Watkins groups**
- **Provide needed specialty materials to Gleason and Watkins groups**

ESH Metrics and Impact

Goals/Possibilities	Usage Reduction			Emmision Reduction			
	Energy	Water	Chemicals	PFCs	VOCs	HAPs	Other
Reduce organic solvents used in processing materials	No energy used to purify and treat water	Eliminate need for water usage	Up to 100% reduction of organic solvents used	N/A	Minimal use of organic solvents	Up to 100% reduction of HAPs	N/A
Reduce processing time / temperature	Reduce anneal process costs	N/A	N/A	N/A	N/A	N/A	N/A
Additive processing	N/A	N/A	Eliminate waste of costly material	N/A	Minimal use of organic solvents	N/A	N/A

- **Eliminates water usage in development**
- **Eliminates need for organic solvents**
- **Recyclable**

Why a New Developer Solvent?:

Environmental and Performance Advantages of $scCO_2$

- Environmentally friendly, zero VOC solvent
- Highly tunable solvating power
  - ρ(T,P)
  - Leaves no residue
  - Clean separations
- One-phase fluid
  - Zero surface tension
  - Transport, viscosity between that of liquid and gas
- Nonpolar, inert character
- Potential to reduce LER and eliminate pattern collapse

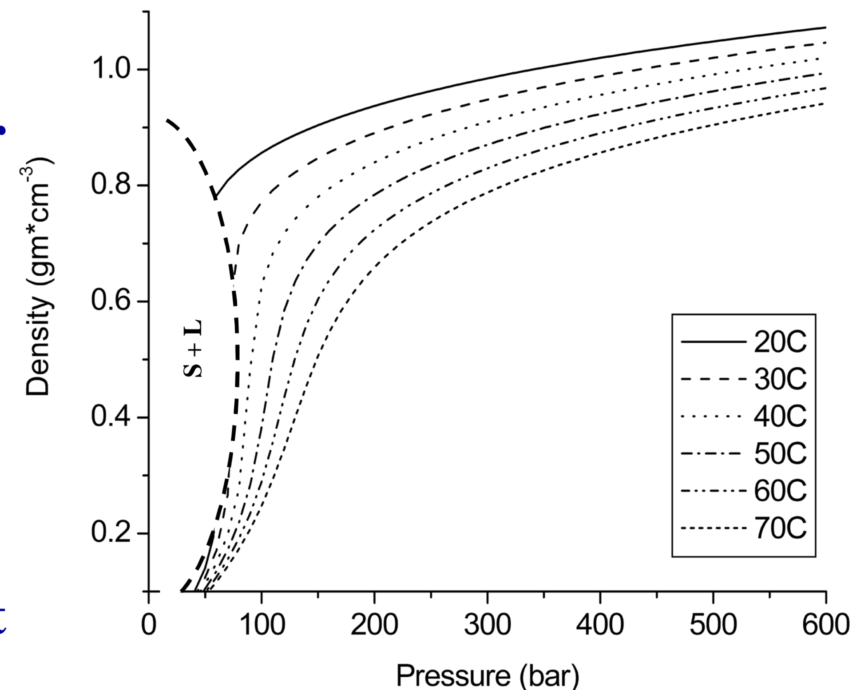

Molecular Glasses as Patternable Materials

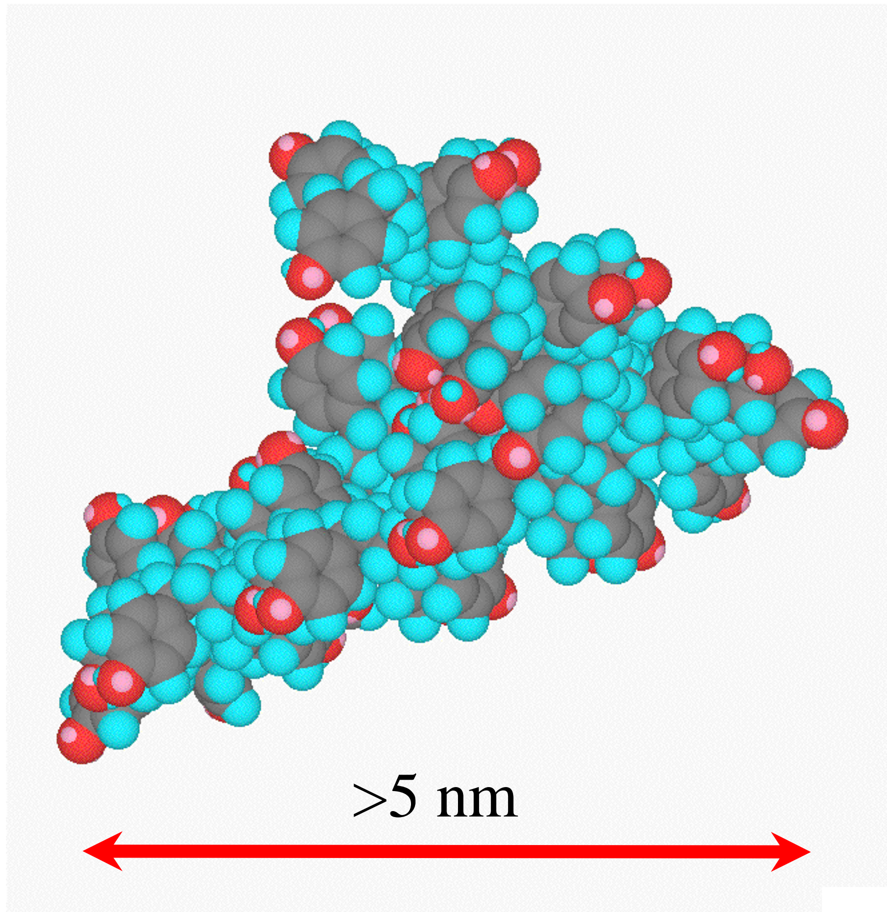

- Molecular glasses uniform, small size
- Potential low k precursors
- Possibility of vapor deposition
- Processing in untraditional solvents

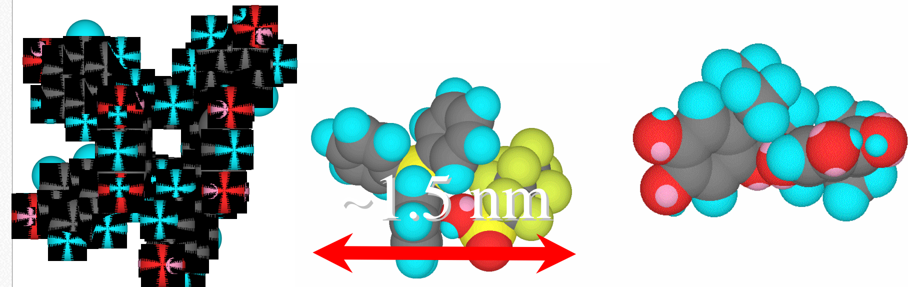

Molecular glass components

Keys to Solubility Control in $scCO_2$

- **Increasing polarity decreases solubility in $scCO_2$**
- **Increasing molecular size decreases solubility**

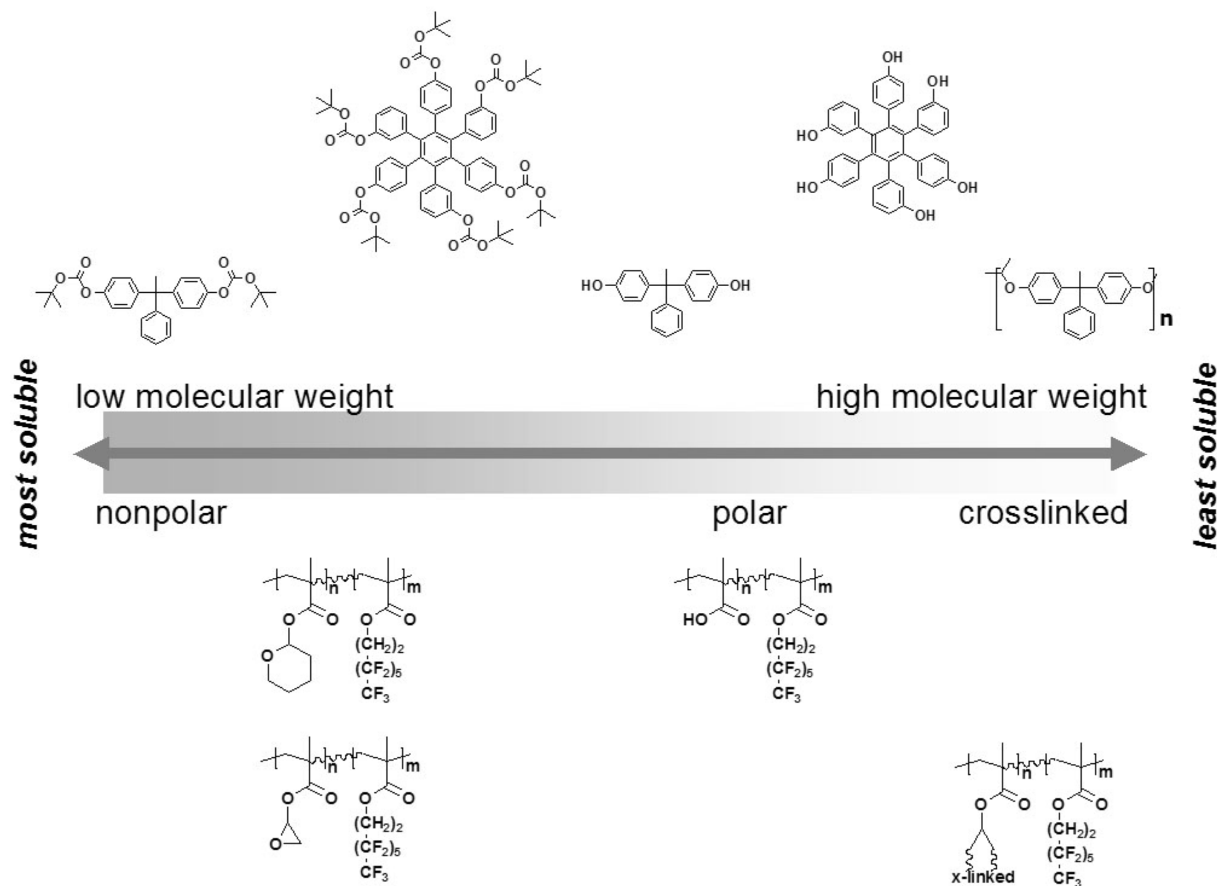

Effects of Polarity: More Polar, Less Soluble

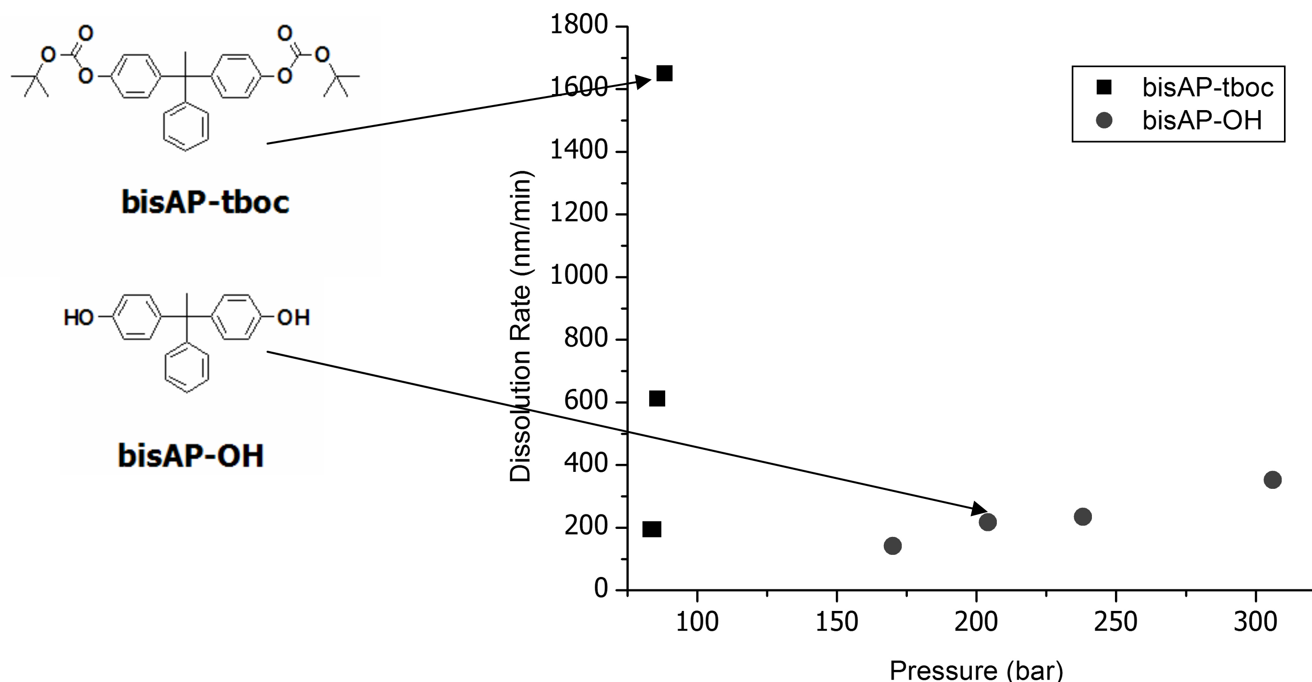

- **Study using Cornell dissolution rate monitor**
- **Molecules with less than 3 –OH groups still significantly soluble.**
- **Effect more pronounced at lower temperatures.**
- **Indicative of contrast between exposed and unexposed regions.**

Effect of Molecular Weight and Tg

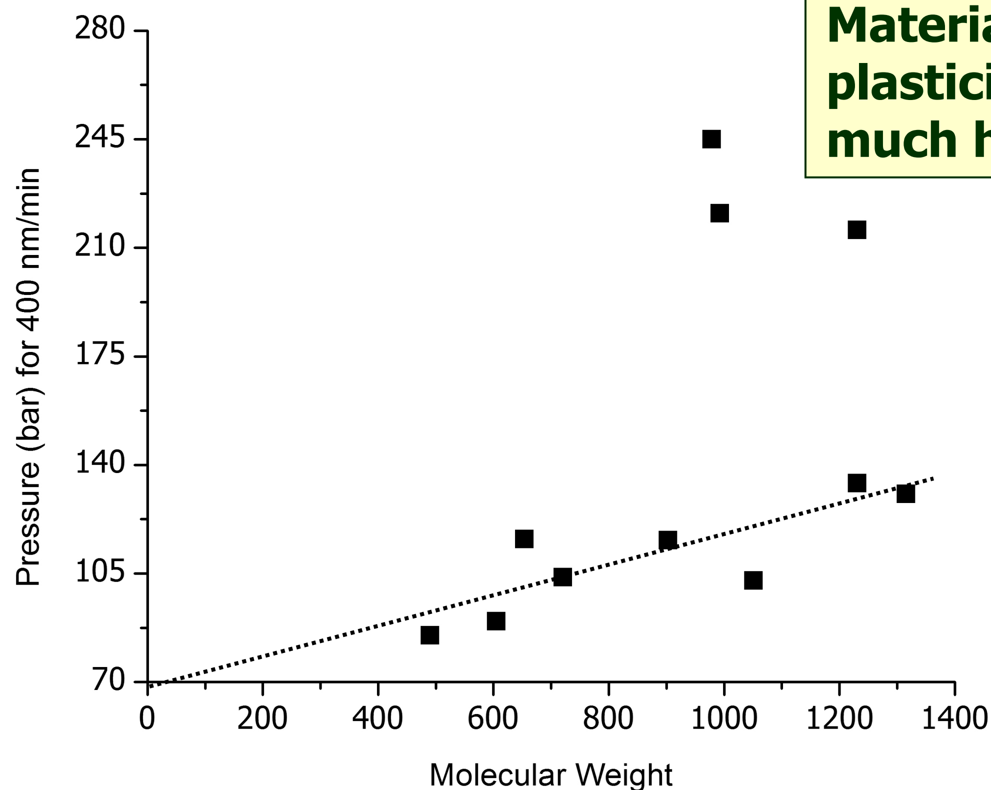

Materials that resist plasticization require much higher pressures.

Necessary pressure to achieve dissolution rate increases predictably with larger MW.

However, photoresists approaching 2000 g/mol still soluble in $scCO_2$!

Felix, N. M, et al., *J. Mat. Chem.*, **17**, (2007) 4598-4604.

Calix[4]resorcinarenes:

Tunable Dissolution Rates, Soluble with no fluorine

calix-tboc

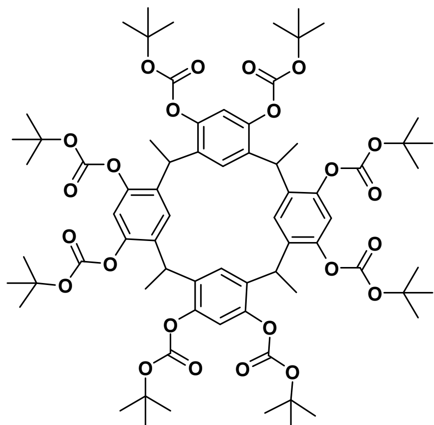

4hp-calix-tboc

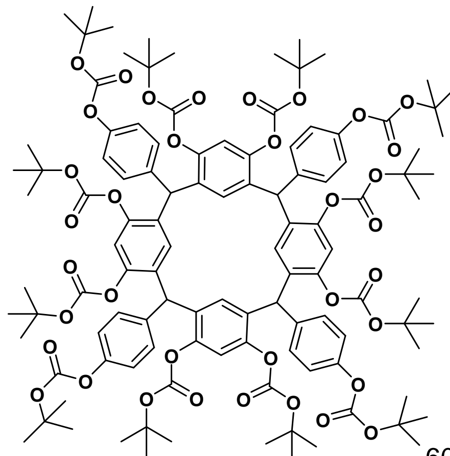

4tb-calix-tboc

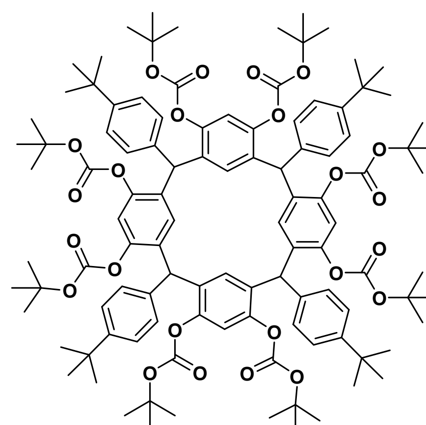

si-calix-tboc

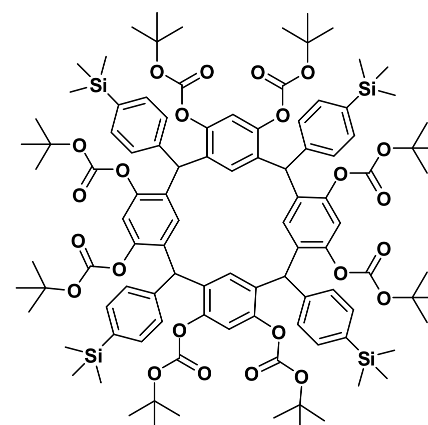

Felix, N. M, et al., *Adv. Mater.*, in press.

	Tg (C)
calix-tboc	107
4hp-calix-tboc	84
4tb-calix-tboc	110
4si-calix-tboc	140

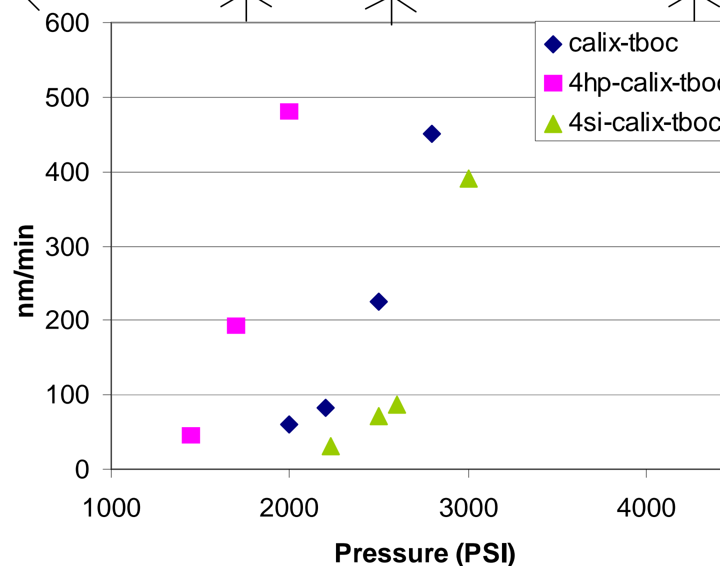

Patterning of Molecular Glasses in $scCO_2$

Developed at 37 °C, 2500psi (e-beam exposure)

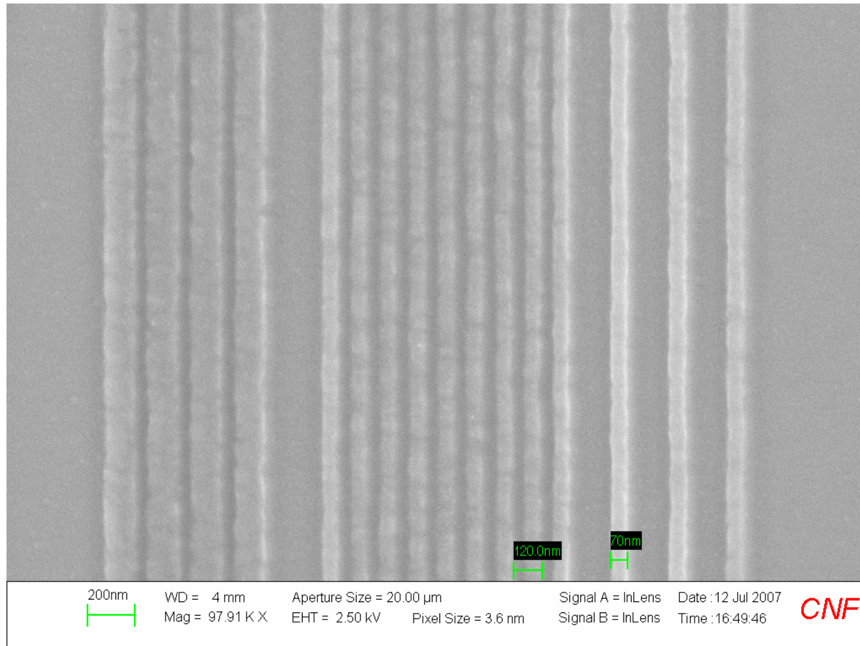

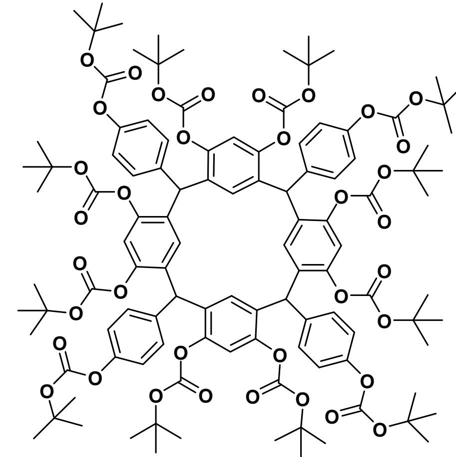

- Calixarenes provide information about patterning non-polar molecular building blocks for a variety of applications

- Sub-100nm performance shown with calix[4]resorcinarenes developed in $scCO_2$
- Model systems for low k glasses

Chain Scission Resists for Positive-tone $scCO_2$ Processing

- **PMMA is classical positive tone resist**
  - **High resolution e-beam, EUV resist with low LER**
  - **Problem: low sensitivity**

- **Acid catalyzed chain scission**
  - **Improved sensitivity**
  - **Use acetal bonds to crosslink otherwise $scCO_2$ soluble species**

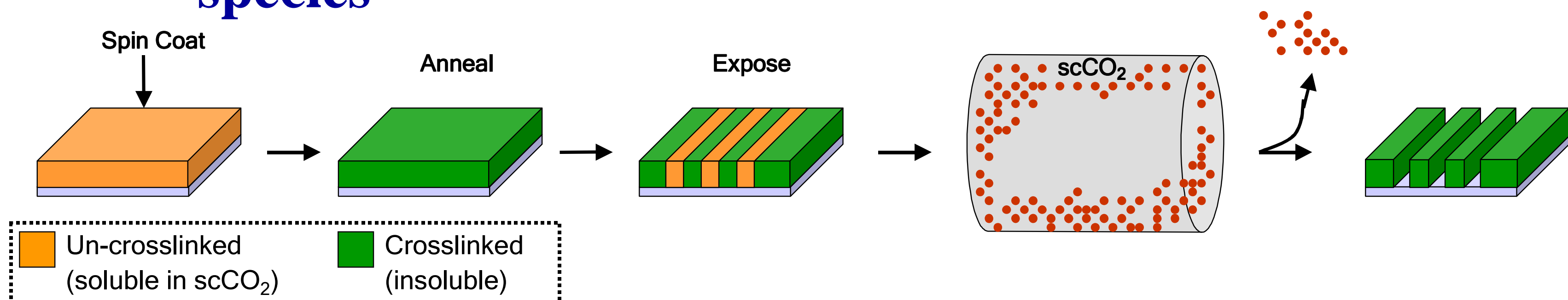

Positive Tone Patterning:

- Electron-beam patterning, 100kV, Cornell
- Develop in $scCO_2$: 40 °C, 2000 psi (140 bar)
- First intrinsic positive-tone system for $scCO_2$ development!
- Either aqueous base (wet) or $scCO_2$ (dry) development possible

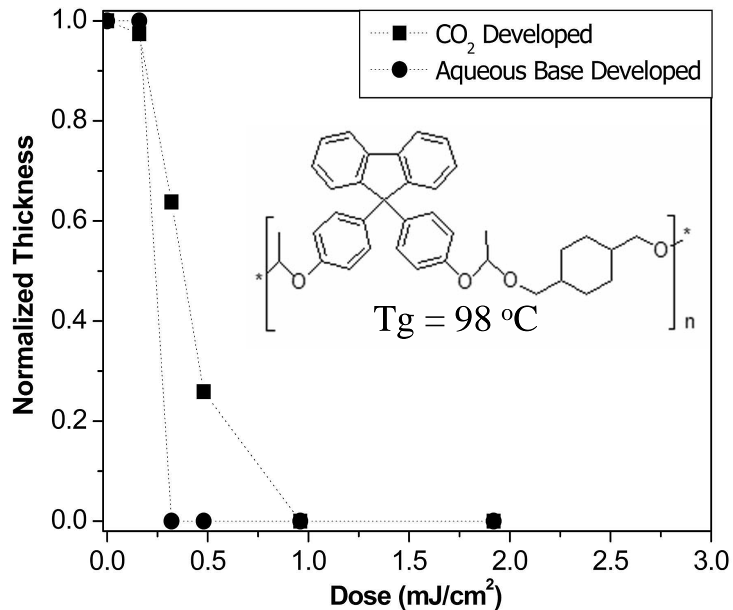

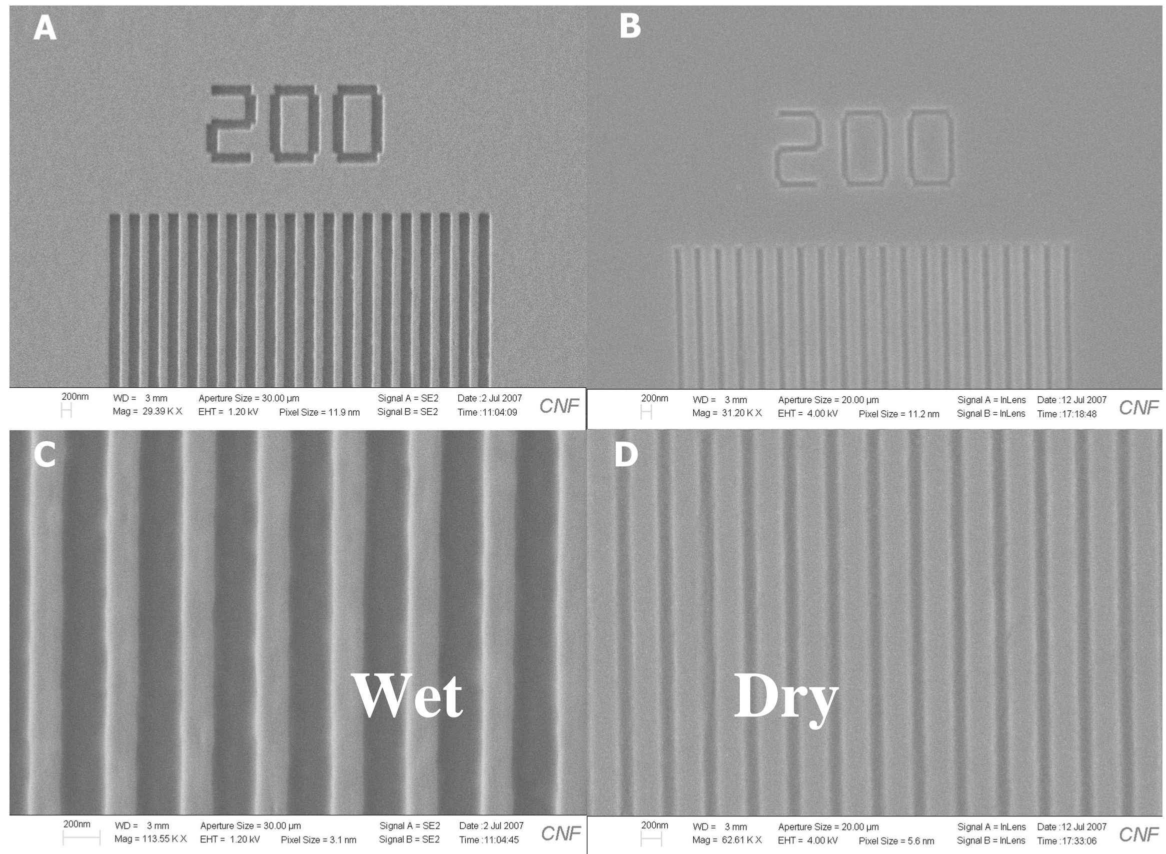

SRC/SEMATECH Engineering Research Center for Environmentally Benign Semiconductor Manufacturing

Cornell University

Photoinitiated CVD

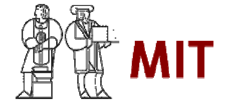

- Photoinitiated CVD can grow low k polymer material by initiating free radical chemistry from the patterned surface with potential to directly produce patterned thin films
- Patterned high resolution initiator films supplied to Gleason group

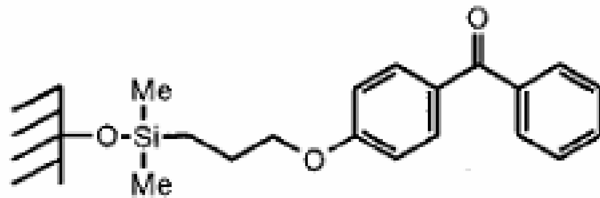

Surface initiator for piCVD

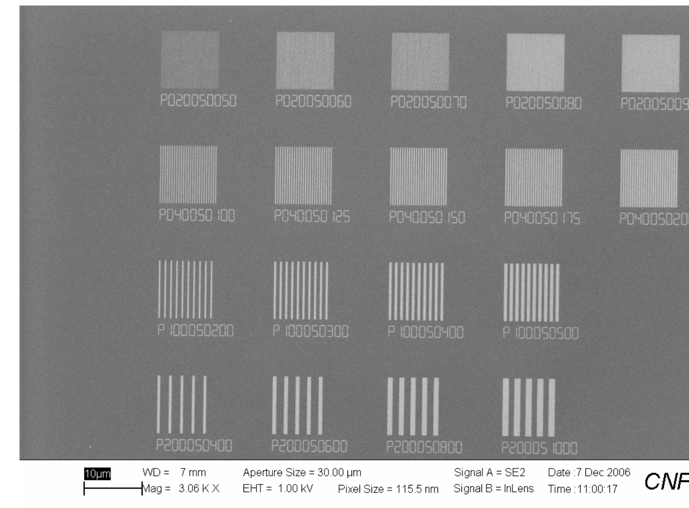

Examples of patterned initiator (down to 80nm zones)

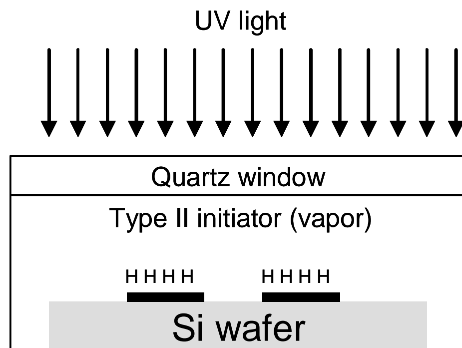

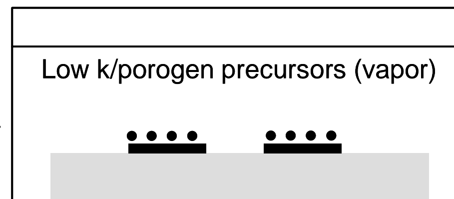

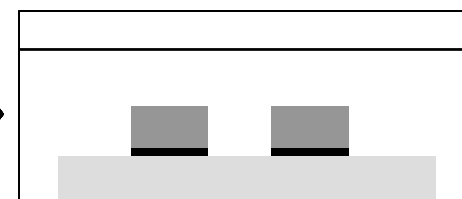

Self-Assembling Polymers

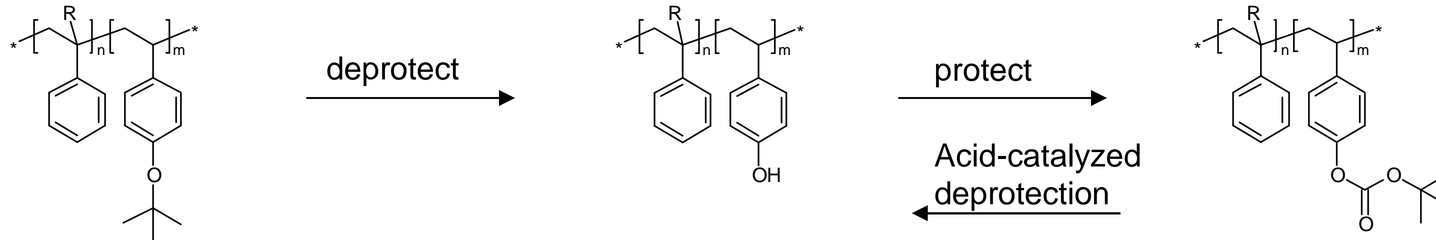

R = -H

PS-PtBuOS	PS-PHOST	PS-PtBOCOS
34K-29K	**34K-20K**	**34K-36K**

R = $-CH_3$

PαMS-PtBuOS	PαMS-PHOST	PαMS-PtBOCOS
7K-25K	**7K-17K**	
7K-21K	**7K-14K**	
7K-23K	**7K-16K**	**7K-29K**
18K-64K	**18K-35K**	**7K-64K**

Block coolymers used as template by Watkins for patternable low k materials

Black: have been synthesized; Red: polymers provided to Watkins group

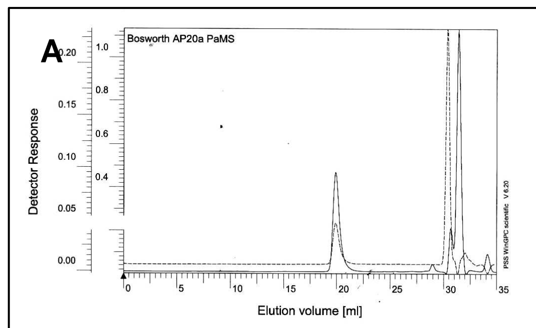

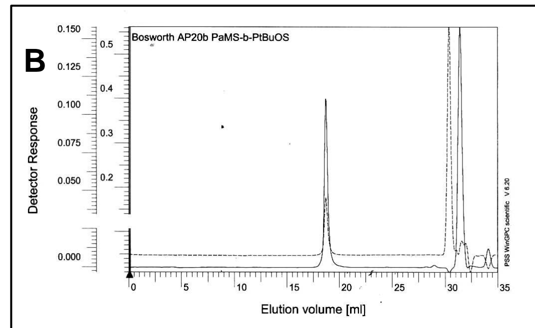

GPC traces of synthesized polymer, including UV (solid) and IR (dotted) traces. a) PαMS block, 7.0 kg/mol, D. 1.10; b) PαMS-b-PtBuOS, 28 kg/mol, D 1.10 (from UV traces). This corresponds with PαMS-PHOST 7K-14K

Industrial Interactions and Technology Transfer

- AZ Microelectronics has hired Nelson Felix

- Interactions with IBM Almaden Research Center
- Discussions with Rohm and Haas Microelectronics
- Interactions with Intel

- Collaboration with International Sematech for EUV exposures

  - Kim Dean, Sematech
  - Kevin Orvek, Intel / Sematech
  - Will Conley, Freescale / Sematech

Future Plans

Next Year Plans

- Assess use of $scCO_2$-soluble materials as low-k precursors
- Continue synthesis efforts for low-k porogens and precursors
- Demonstrate of vapor deposition of low-k precursors with dry $scCO_2$ processing

Long-Term Plans

- Explore use of $scCO_2$ in ordering / assembly of low-k materials
- Continue to demonstrate new chemistries for patternability and functionality of small, nonpolar molecules

Publications, Presentations, and Recognitions/Awards

Publications

- Frauke Pfeiffer, Nelson Felix, Christian Neuber, Christopher K. Ober, Hans-Werner Schmidt, "Physical Vapor Deposition of Chemically Amplified Photoresists: A New Route to Patterning Molecular Glass Resists", Adv. Func. Mater., in press.
- Frauke Pfeiffer, Nelson M. Felix, Christian Neuber, Christopher K. Ober, and Hans-Werner Schmidt, "Towards Environmentally Friendly, Dry Deposited, Water Developable Molecular Glass Photoresists", Advanced Materials, in press.
- Nelson M. Felix, Anuja De Silva, Camille Man Yin Luk and Christopher K. Ober, "Dissolution Phenomena of Phenolic Molecular Glass Photoresist Films in Supercritical CO2", J. Mater. Chem., (2007), 17(43), 4598-4604.
- Anuja De Silva, Jin Kyun Lee, Xavier André, Nelson M. Felix, Heidi B. Cao, Hai Deng and Christopher K. Ober, "Study of the Structure-Properties Relationship of Phenolic Molecular Glass Resists for Next Generation Photolithography", Chem. Mater., in press.
- Nelson Felix and Christopher K. Ober, "Acid-Labile, Chain-Scission Polymer Systems Used as Positive-Tone Photoresists Developable in Supercritical CO2", Chem. Mater., submitted.
- Nelson M. Felix, Anuja De Silva, and Christopher K. Ober, "Calix[4]resorcinarene Derivatives as High Resolution Photoresist Materials for Supercritical CO2 Processing", Adv. Mater., in press.

Presentations

- IBM Self-assembly Workshop, Almaden, CA, Jan. 15, 2008. "Photopatternable Block Copolymers: Chemically Active BCP Resists", invited talk.
- International Symposium on Advanced Materials and Nano-materials with Precisely Designed Architectures, October 4th – 6th in Sapporo, Japan. "Studies in the biological-materials interface", invited talk.
- Conference on Nanomaterials for Defense Applications, San Diego, CA, April 24 – 26, 2007. Lithography and Biology: 2D and 3D Patterning for the Biology-Materials Interface, invited talk.

Recognitions/Awards

- 2007 Humboldt Research Prize for C.K. Ober
- Nelson Felix, ERC Simon Karecki Award, Feb 2007.

Environmentally Benign Vapor Phase and Supercritical CO_2 Processes for Patterned Low k Dielectrics

(Task Number: 425.017; Watkins sub-task)

PIs:

- **James J. Watkins, University of Massachusetts, Amherst**
- **Christopher K. Ober, Cornell University**
- **Karen K. Gleason, Massachusetts Institute of Technology**

Graduate Students:

- **Alvin Romang, UMass Chemical Engineering**
- **Sivakumar Nagarajan, UMass Polymer Science & Engineering**

Cost Share (other than core ERC funding):

- **NSF Center for Hierarchical Manufacturing, 40K**
- **NSF NIRT, 25K**

ULK Mesoporous Films Prepared in CO_2

First Generation Films Exhibit Excellent Performance

- k< 2.2 demonstrated
- Rapid process times, 1st generation survives CMP
- Low stress, high crack threshold
- Small pores are accessible via template blends

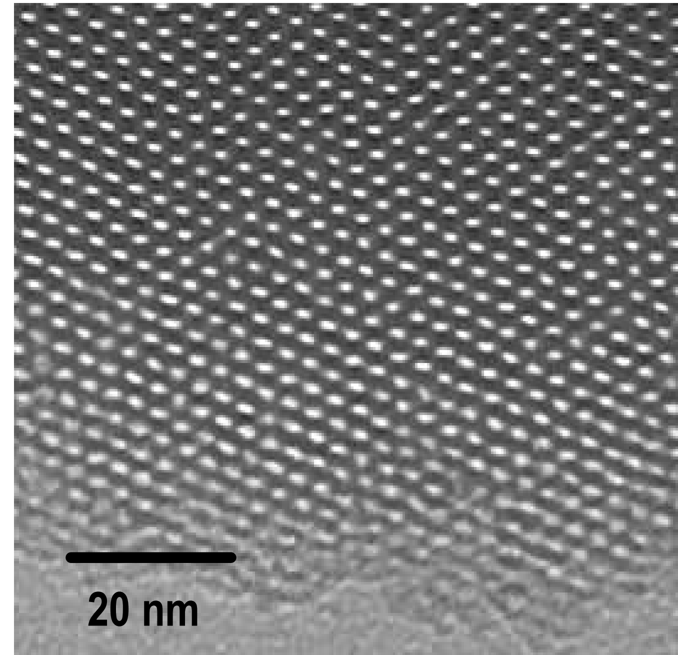

Program Objectives:

- **Improve Performance, Reduce ESH Burden**

- **Optimize Mechanical Properties**
  inclusion of novel POSS copolymer templates
  (see A. Romang poster)

- **Demonstrate Viable Direct Patterning Approach**
  simultaneous pattern generation of nanopores and device features
  eliminate/reduce traditional litho, etch, clean cycles
  process compression = cost savings + resource reduction
  fat lines now, subsequent entry point for ULK < 2.2

ESH Metrics and Impact of CO_2 as Solvent (Ober Talk)

	Usage Reduction			Emmision Reduction			
Goals/Possibilities	Energy	Water	Chemicals	PFCs	VOCs	HAPs	Other
Reduce organic solvents used in processing materials	No energy used to purify and treat water	Eliminate need for water usage	Up to 100% reduction of organic solvents used	N/A	Minimal use of organic solvents	Up to 100% reduction of HAPs	N/A
Reduce processing time / temperature	Reduce anneal process costs	N/A	N/A	N/A	N/A	N/A	N/A
Additive processing	N/A	N/A	Eliminate waste of costly material	N/A	Minimal use of organic solvents	N/A	N/A

Eliminates water usage in development --- Eliminates organic solvents --- Recyclable

Additional ESH Benefits of Direct Patterning (This Talk)

- Compression/Elimination of Multiple Solvent/Water/Waste Intensive Processes
- Eliminate traditional litho sequence
- Eliminate etch sequence
- Eliminate/reduce clean and repair sequences

Doping Templates with "Nanoparticle" Fillers to Improve Mechanical Properties

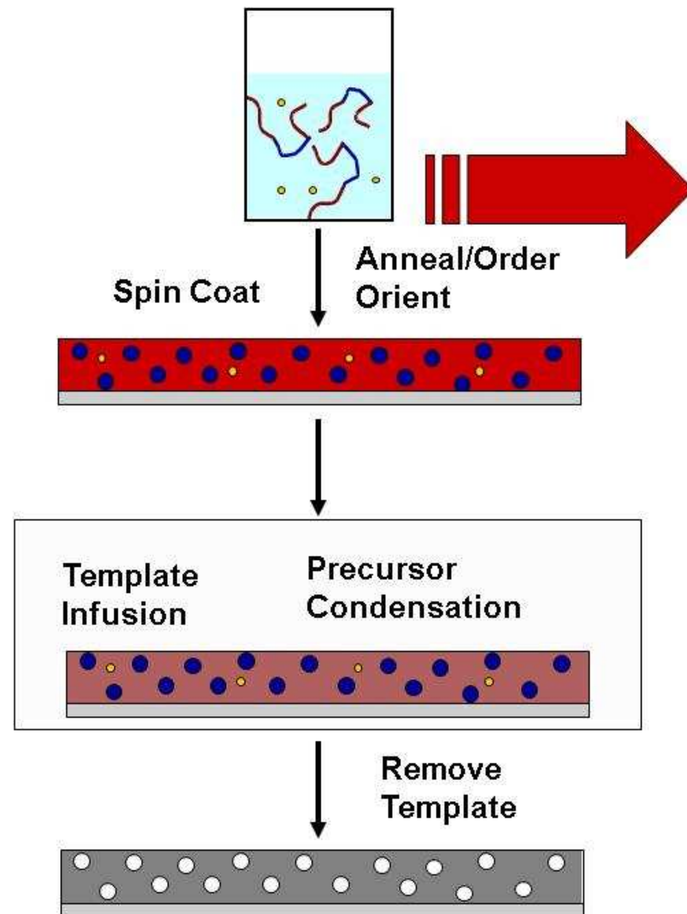

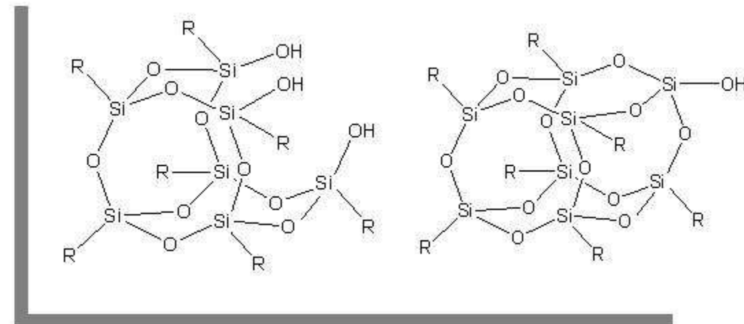

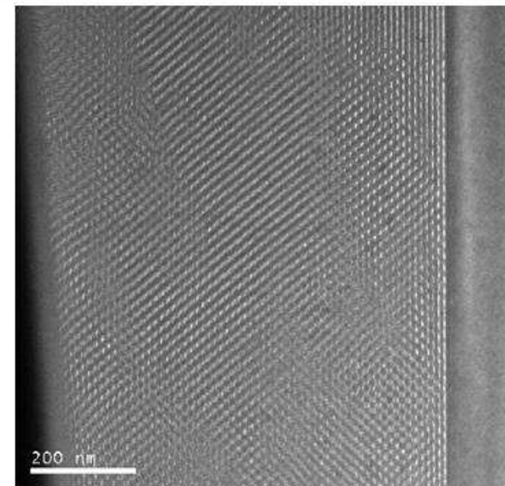

Image: Prof. Brian Gorman, UNT

Last year we reported promising feasibility results including improved modulus and hardness but film uniformity at the wafer scale was an issue

Copolymerization of Acryl isobutyl POSS with Acrylic Acid: Uniform template films, No POSS aggregation

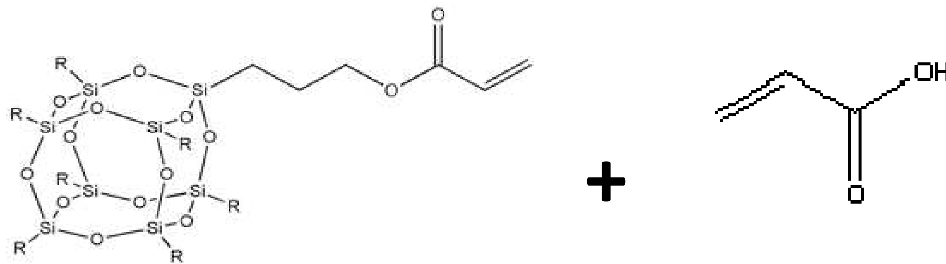

Free radical polymerization with 2 to 1 weight ratio of POSS to acrylic acid in THF

Smooth Silica/POSS Films upon Template Infusion

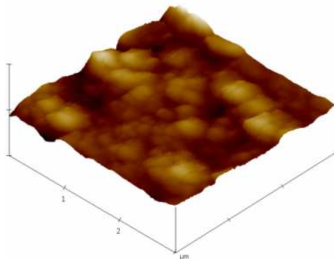

RMS Roughness: 5.7 nm
Z range: 49.7 nm
Z scale: 100 nm

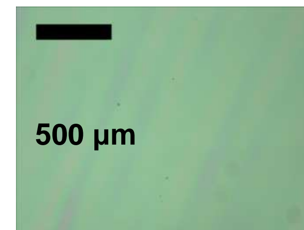

Optical micrograph showing long-range film smoothness

Addition of POSS Improves Mechanicals Significantly

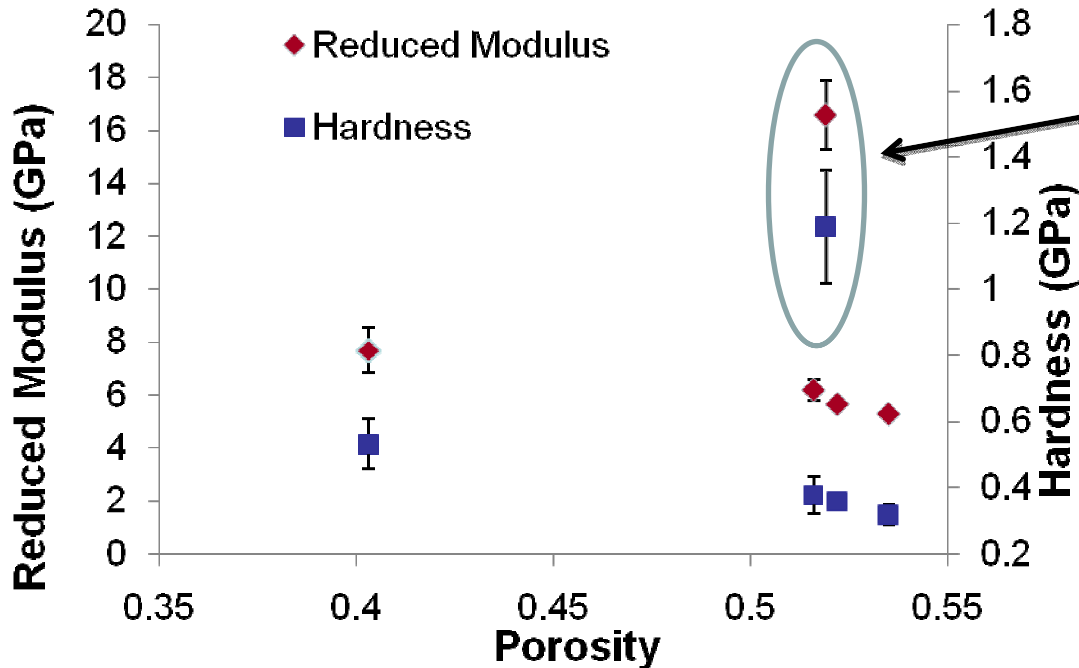

POSS Copolymer Template

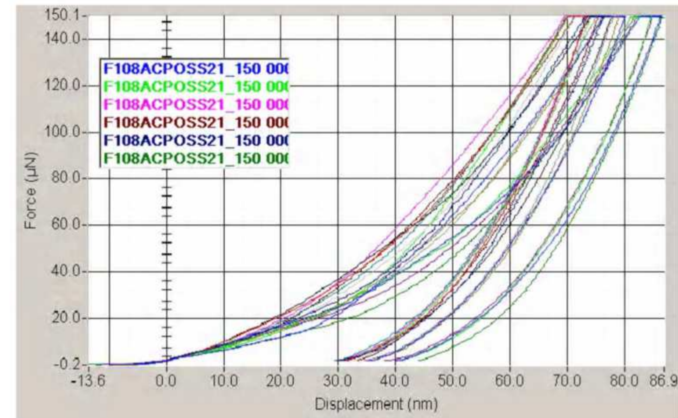

- **Significant increase in both modulus and hardness**
- **Good measurement replications**
- **Film templated from 2:1 POSS:AA blended with Pluronic F108 (3:7) (Circled)**
- **Bottom four films were synthesized with Pluronics (F108/PAA, F88/PAA, F68/PAA and F38/PAA)as templates**

Fabrication of Micro-patterned Mesoporous Silica Films

Domain (microscopic) and Device (nanoscopic) level control:

Controlling the presence of acid in two different length scales by using a photo acid generator (PAG) instead of normal acid (pTSA).

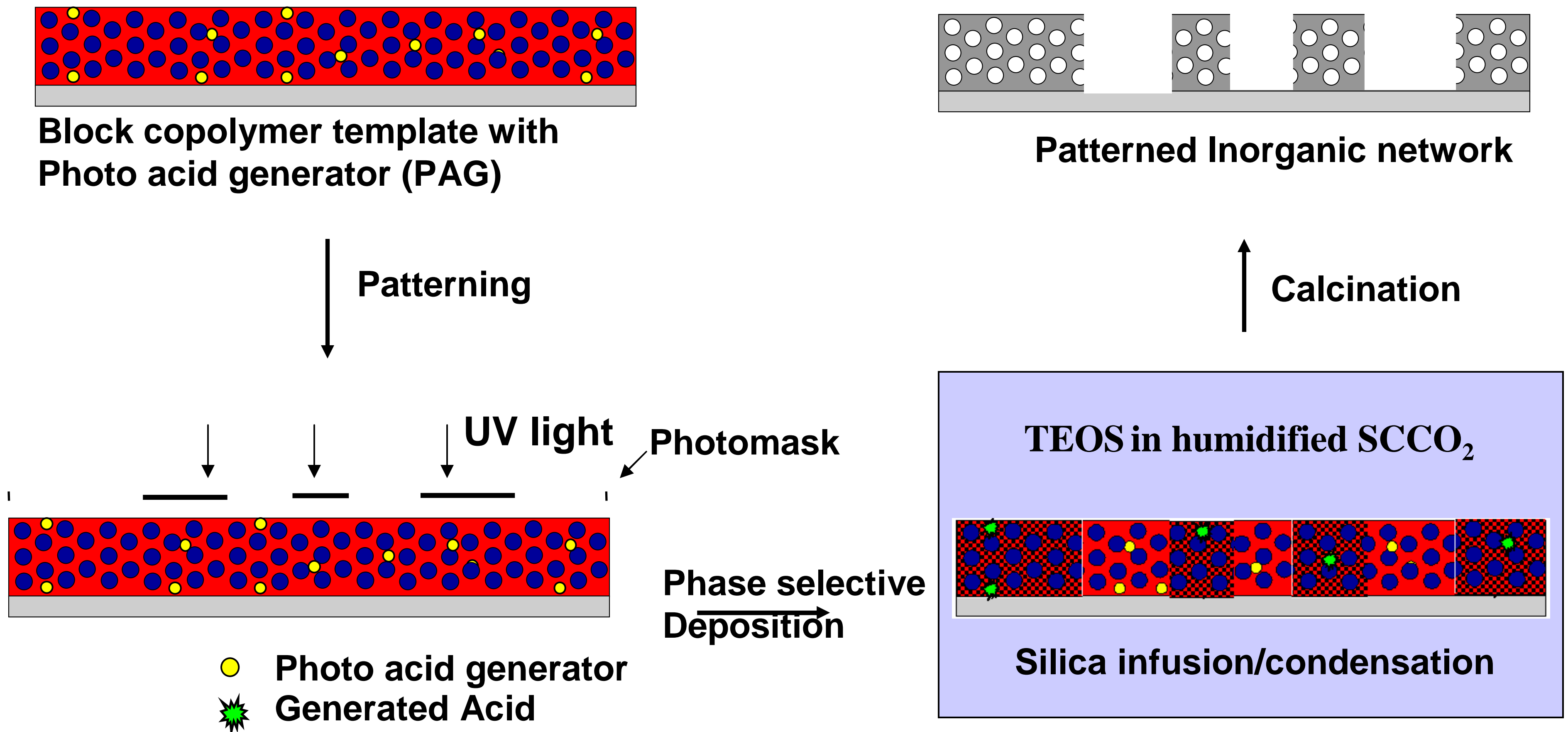

Summary of Process Steps

1. **Spin Coat Template Containing PAG**
   similar to photoresist spinning

2. **Expose Template Using Stepper**

3. **Infuse Template with CO_2 / Alkoxide Solution**
   infusion is rapid (minutes)
   low CO_2 volumes (2-3 vessel exchanges; purge, infuse, purge)

4. **Detemplate and Cap**
   in plasma using PECVD tool

Patterned Mesoporous silica films from PS-b-PtbocSt films

Collaboration with C. Ober

Domain (nanoscale) and Device (micron scale) level control

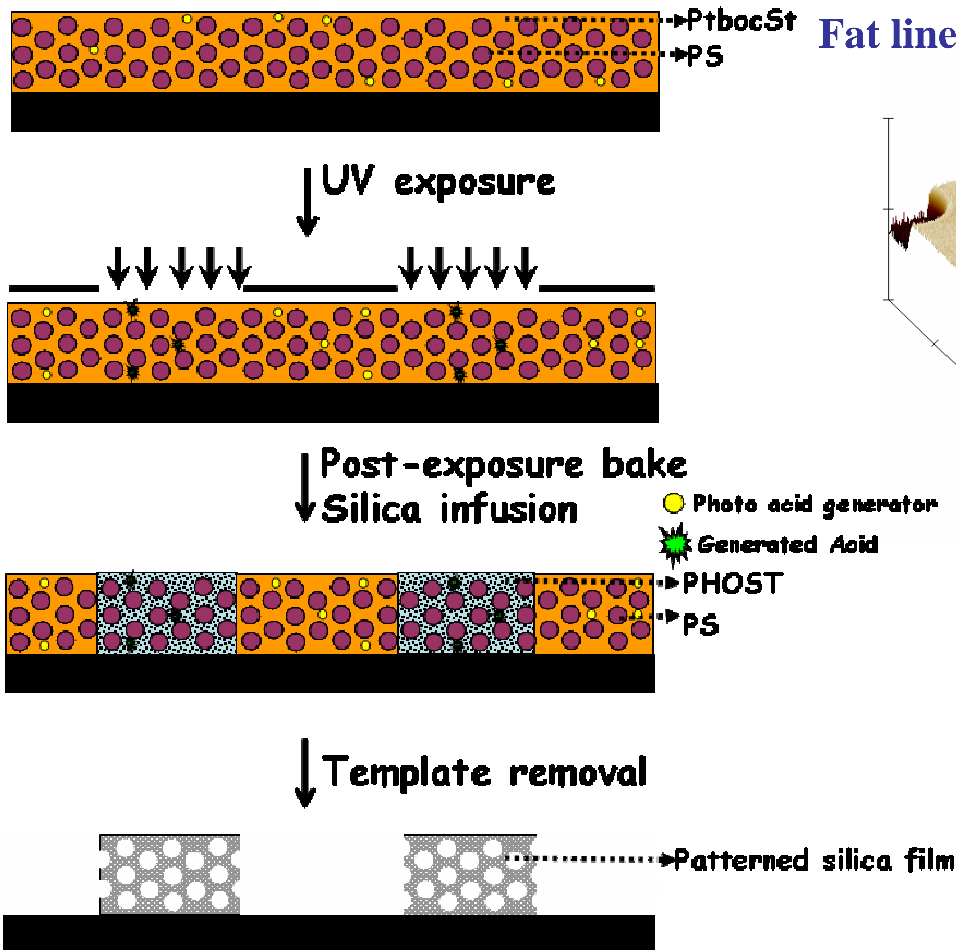

Feasibility Test – Crude Contact Mask

Fat lines are within reach. Extendible to sub 100 nm ?

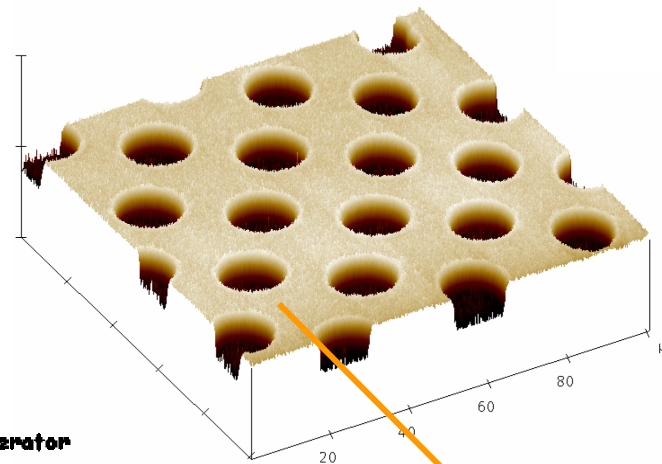

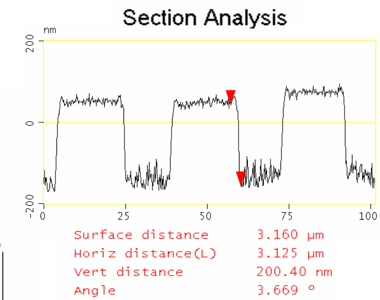

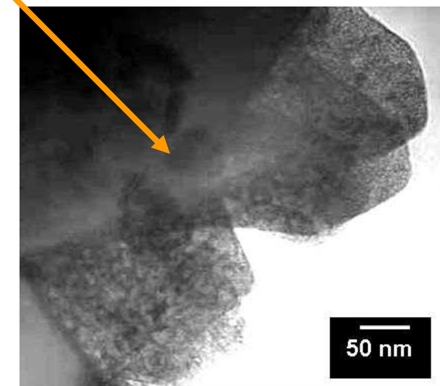

Last year we reported feasibility in 248 resists

This Year: Mesoporous silicate films from chemically amplified Poly(tertiary butyl methacrylate) copolymer templates

By using a PtbMA based block copolymers, micro-patterned mesoporous silicate films can be obtained via dual tone replications

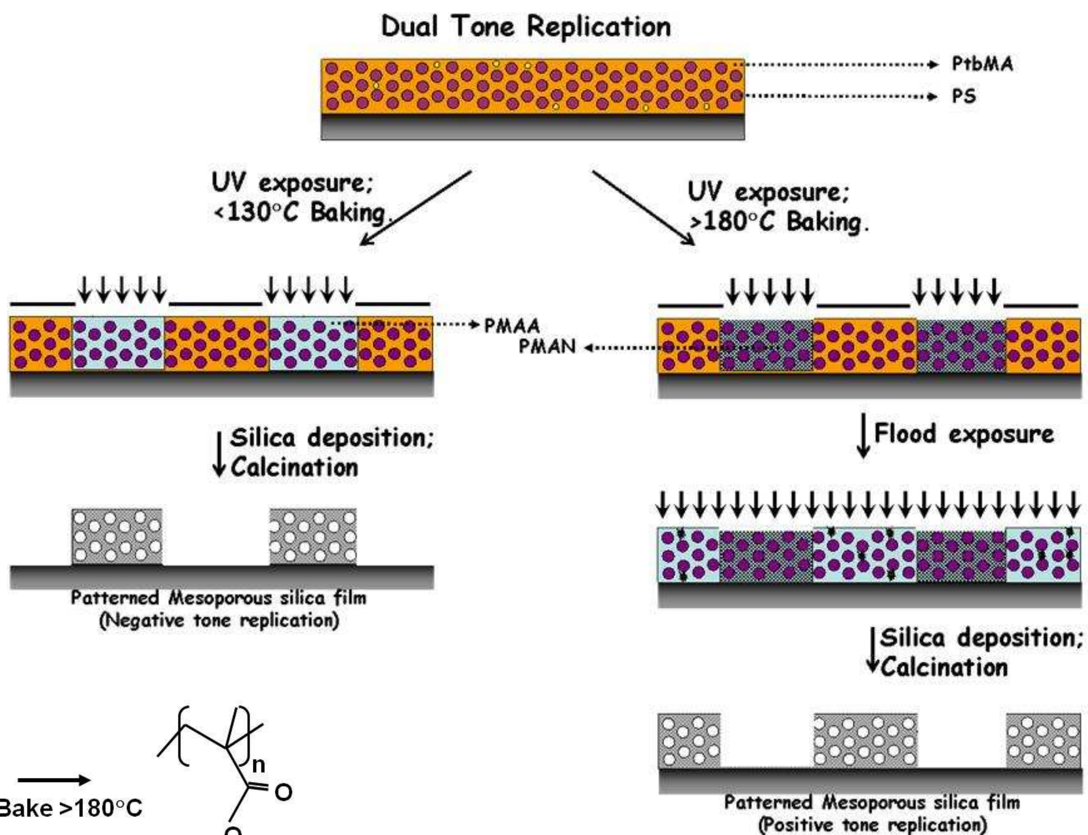

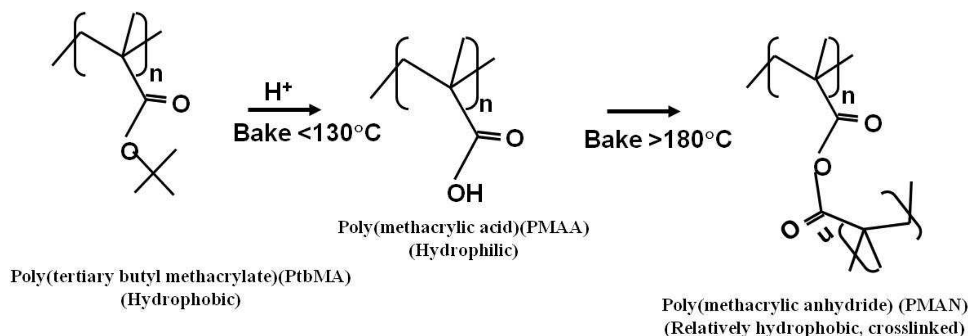

(Ito H et al., Macromolecules 1988)

Dual-tone Patterned Mesoporous Silica Films via SCF Processing:

Combining domain and device level replications

- Photolithography – done with crude contact mask

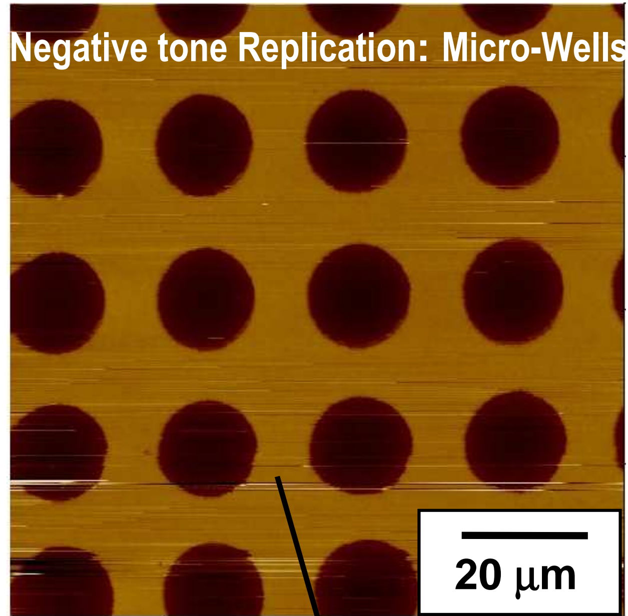

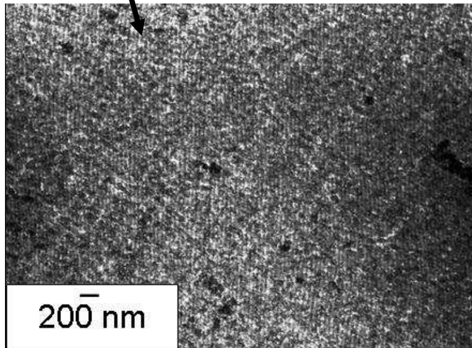

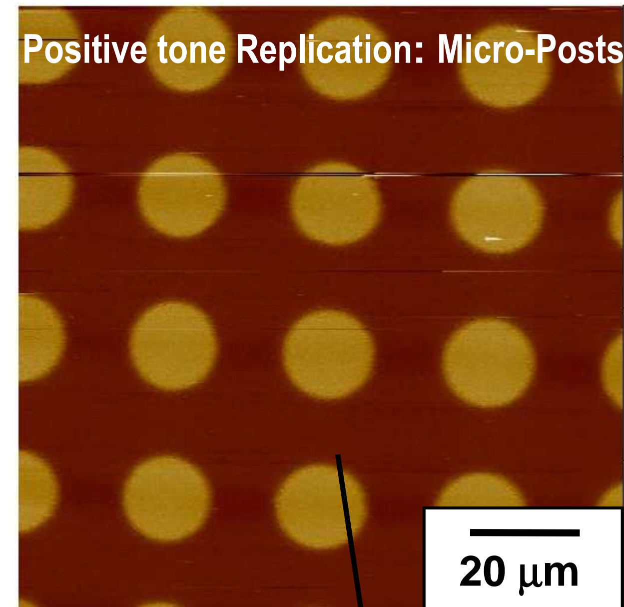

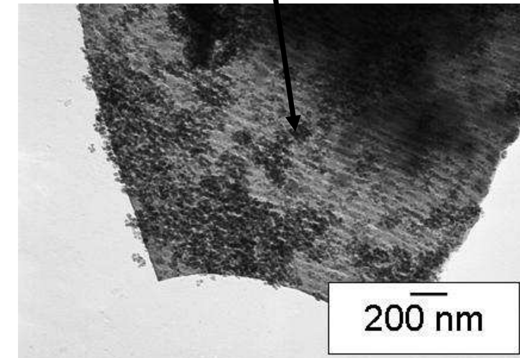

Negative tone replications using a crude contact mask: Patterns with various sizes of lines and spaces

Lines: ~ 4 μm ; Space: ~ 6μm

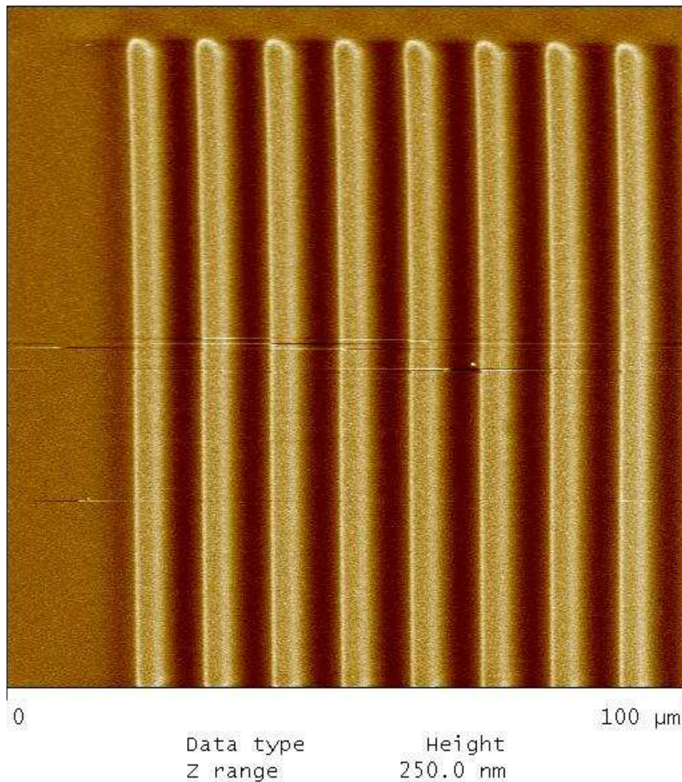

Lines: ~ 2.5 μm ; Space: ~ 6μm

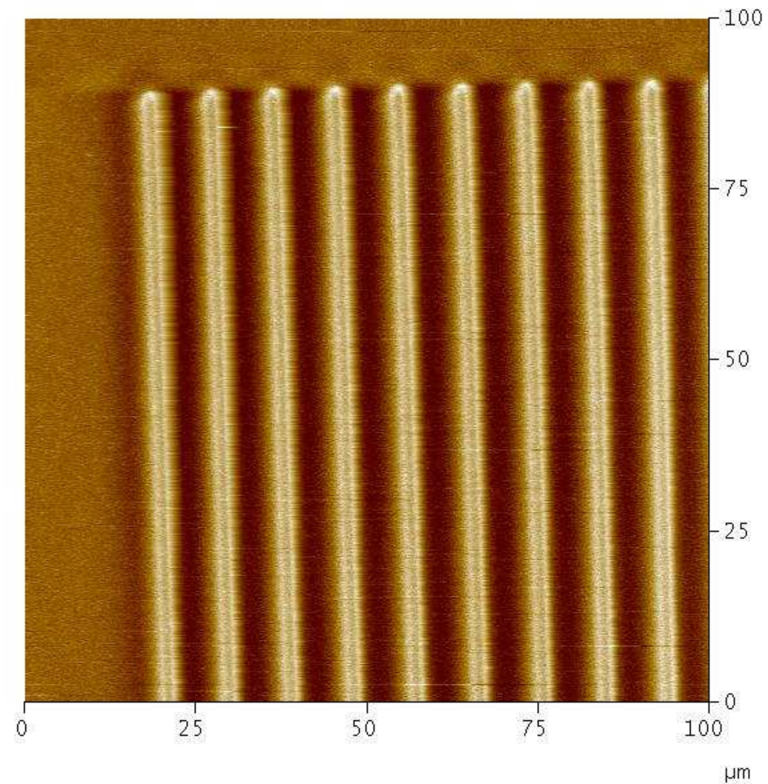

Directly Patterned Dielectric Films: Is High Resolution Possible?

- In collaboration with a partner, feasibility demonstration of direct patterning of sub -100 nm lines.
- First attempt, off-the-shelf resist, no optimization
- No etch!!

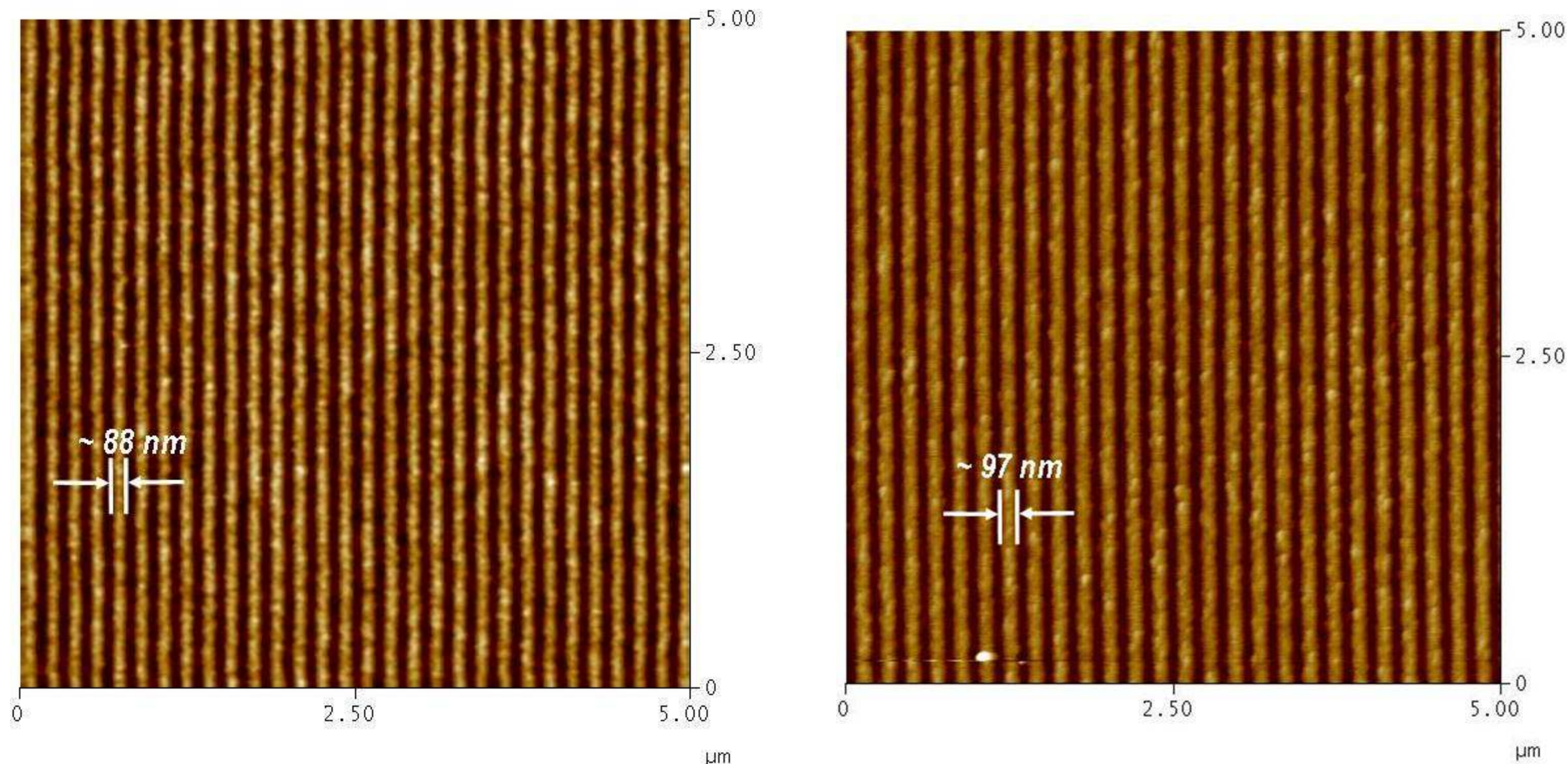

Impact: Potential for streamlined integration of ULKs, ESH benefits and, cost savings via process simplification

Conclusions

Use of POSS additives substantially improves mechanicals

- **this year we developed a POSS copolymer template that improves uniformity**
- **k measurements underway with Gleason**

Direct Patterning Shows Promise

- **last year feasibility at 248 using contacts masks demonstrated**
- **this year**
  - **extended to acrylate-based 193 nm resists**
  - **demonstrated domain level and device level replications**
  - **demonstrated feasibility of sub-100 nm resolution using un-optimized resists**

Process compression via direct patterning offers cost and ESH benefits

Recent acquisition of 200 mm tool will permit scale-up

Acknowledgments

Additional funding: UMass Center for Hierarchical Manufacturing and NSF NIRT

BOC Edwards 200 mm Tool Donation

Milestones and Future Work

- **Milestones**
  - **Substantial increase in film hardness**
    - POSS/acrylic acid copolymer blended with Pluronics offer increases in hardness and good uniformity
    - Hardness > 1.9 GPa, exceeds initial goals
  - **Directly patterned dielectrics**
    - Proof of concept achieved in 248 and 193 nm resists
    - Demonstrated good domain and device level replication
    - Demonstrated sub-100 nm patterning without etch
    - Significant co-funding from NSF CHM / NSF NIRT
- **Future Work**
  - **Optimize film and template chemistry**
    - optimize mechanical properties
    - develop families of films, establish k vs. hardness for doped materials
  - **Optimize resists and resolution for directly patterned dielectrics**
  - **Explore NIL of new monomers with Gleason**

Industrial Interactions and Technology Transfer

- Interactions with IBM Almaden Research Center
- Resist formulations from Rohm and Haas Microelectronics
- Interactions / collaboration on exposed resists with AMD
- Interactions with IMEC
- 200 mm tool donation from BOC
- SCF Clean Room Facility Operational at UMass

Publications, Presentations, and Recognitions/Awards

Publications

Nagarajan, S.: Joan K. Bosworth, J. K.; Ober, C.K.; Russell, T.P; Watkins, J. J. "Simple Fabrication of Micropatterned Mesoporous Silica Films Using Photoacid Generators in Block Copolymers" *Chemistry of Materials,* 2007, in press.

Tirumala, T. R.; Pai, R.A. Agarwal, S.; Bhatnagar, G. Romang A., Chandler C. Gorman, B. P. Jones, R. L.. Lin E. K. , Watkins, J.J. "Nanoporous Silica Films with Long-ranged Order Prepared from Block Copolymer/ Homopolymer Blend Templates" *Chemistry of Materials* 19(24); 5868-5874, 2007.

Presentations

Advanced Metallization Conference Short Course on Micro and Nano-Scale Interconnect Techniques , October 2007, invited

IUMRS-ICMAT-2007 Bangalore, India (October 2007), "Preparation of Device Nanostructures via Templating Techniques in Supercritical Fluids", invited

Materials Research Society 2007 Fall Meeting, Synthesis and Surface Engineering of 3D Nanostructures Symposium, Boston, MA (Nov 2007), invited.

ACS Division of Polymer Chemistry Workshop "Opportunities for Nanostructured Polymeric Materials for Device Fabrication, Lake Tahoe, NV (Nov. 2007), invited

Materials Research Society, 2007 Spring Meeting, Robust Ultra-Low K and Directly Patterned Interlayer Dielectrics via Templating Processes, San Francisco, (April 2007), invited

TechCon 2007 "Directly Patterned Dielectric Films Templated from Chemically Amplified Block Copolymers", Austin TX, presented by S. Nagarajan

Recognitions/Awards

UMass Chancellors Award for Excellence in Research to Jim Watkins

Destruction of Perfluoroalkyl Surfactants in Semiconductor Process Waters using Boron Doped Diamond Film Electrodes

(Task Number: 425.018; Subtask #1)

PIs:

- **James Farrell, Chemical and Environmental Engineering, UA**
- **Reyes Sierra, Chemical and Environmental Engineering, UA**

Graduate Students:

- **Kimberly Carter: PhD candidate, Chemical and Environmental Engineering, UA**

Other Researchers:

- **Zhaohui Liao, Postdoctoral Fellow, Chemical and Environmental Engineering, UA**

Cost Share (other than core ERC funding):

- **$100K from National Science Foundation, Small Grants for Exploratory Research**

Objectives

- **Determine the feasibility of electrochemical destruction of PFAS compounds in dilute aqueous waste streams.**
- **Determine the degree of electrolysis required to generate products that are readily biodegraded in municipal wastewater treatment plants.**
- **Develop an adsorptive method using activated carbon, hydrophobic zeolites, or anion exchange resins for concentrating PFAS compounds from dilute aqueous solutions.**
- **Test the proposed multistep treatment scheme on real semiconductor wastewaters containing PFAS compounds.**

ESH Metrics and Impact

1. Reduction in emission of ESH-problematic material to environment.

- 100% destruction of perfluoroalkyl surfactants in wastewaters
- technology can also be used for destruction of other ESH-problematic organic compounds

2. Reduction in the use of natural resources (water and energy).

- energy savings by avoiding costly reverse osmosis (RO) separation
- water savings by recovering all the treated wastewater (no RO retentate disposal)
- energy savings by avoiding combustion of PFAS compounds in RO retentate

3. Securing the critical use exemption status for PFAS and related compounds in the semiconductor industry.

Boron-Doped Diamond Film (BDD) Electrodes

- **Diamond film grown on p-silicon substrate using CVD**
- **Boron doping provides electrical conductivity**
- **Highly stable under anodic polarization**
- **No catalyst to foul or leach from electrode**
- **Emerging technology being adopted for water disinfection**

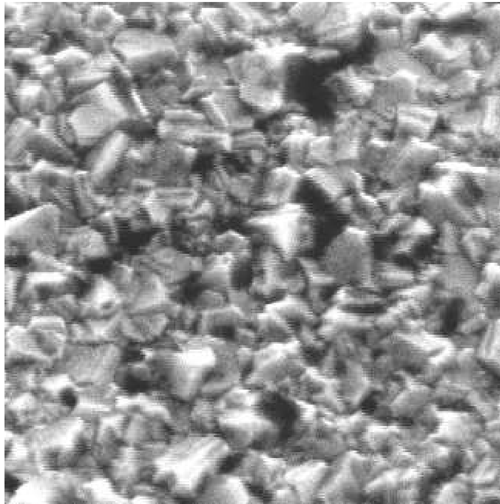

Scanning electron micrograph of BDD electrode. The individual diamond crystals are ~0.5 μm in size.

Proposed Treatment Scheme

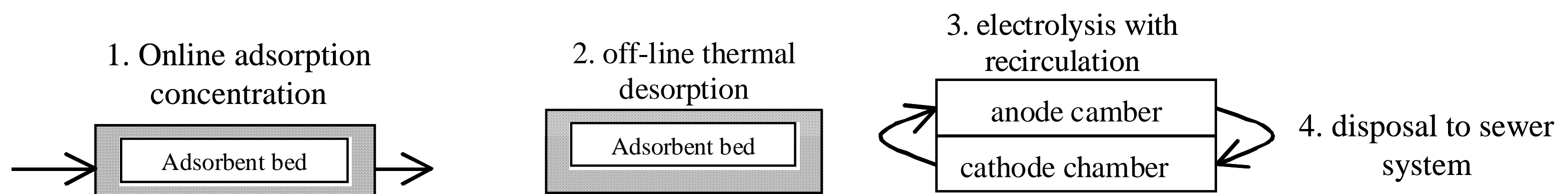

Multi-step treatment scheme:

1. **Concentrate PFAS from dilute aqueous solutions on an adsorbent.**

2. **Thermally desorb PFAS into a concentrated solution.**

3. **Recirculate concentrated PFAS solution through a BDD electrode reactor for electrolytic destruction.**

4. **Dispose of biodegradable electrolysis products to the sanitary sewer system.**

Experimental Systems

Rotating Disk Electrode (RDE) Reactor

- **no mass transfer limitations**
- **electrode surface area = 1 cm^2**
- **solution volume = 350 mL**
- **a_s = 0.00286 cm^2/mL**

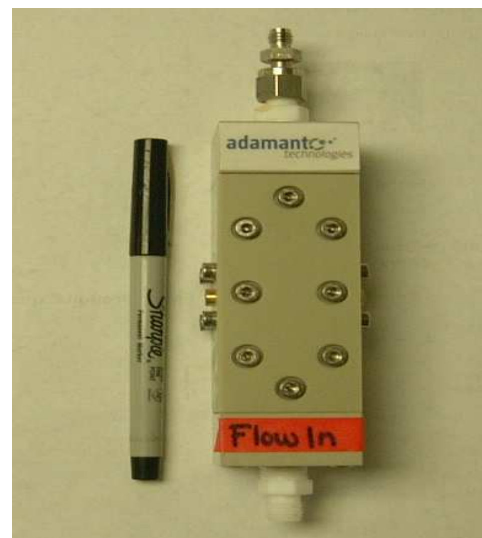

Parallel plate flow-cell

- **rates similar to real treatment process**
- **electrode surface area = 25 cm^2**
- **solution volume = 15 mL**
- **a_s = 1.67 cm^2/mL**

Experimental Results: Flow-Through Reactor

Perfluorooctane Sulfonate (PFOS)

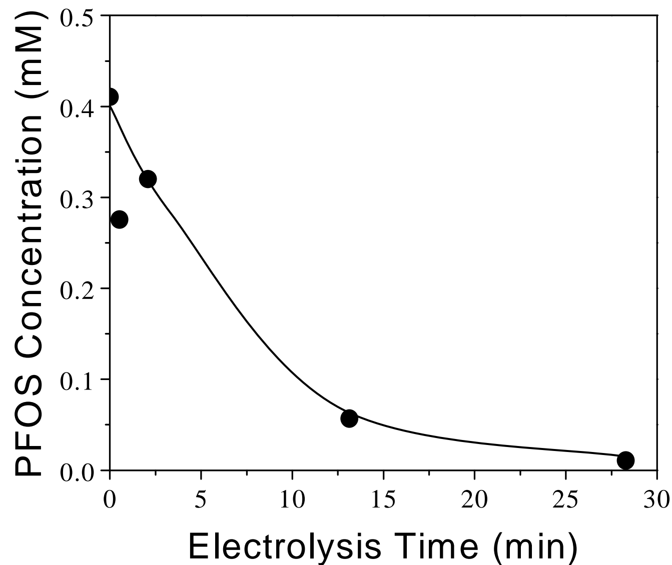

Perfluorobutane Sulfonate (PFBS)

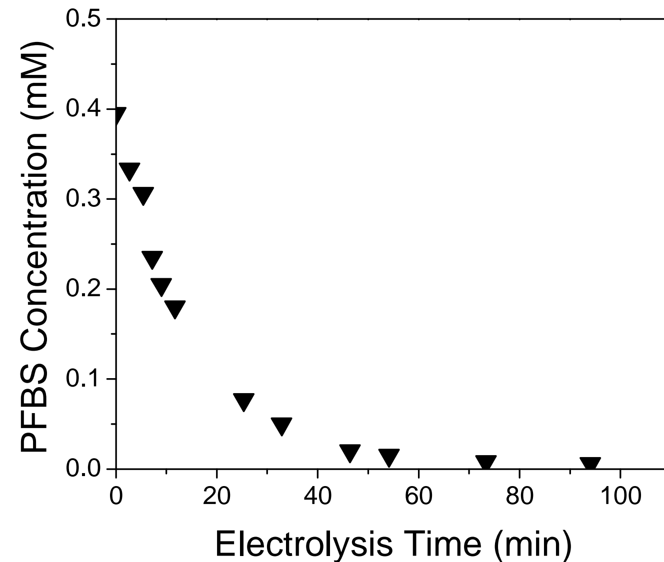

- **Both PFOS and PFBS can be readily removed from water.**
- **PFOS removal half-life: ~7 min; PFBS removal half-life: ~10 min.**
- **Reaction rates are first order in concentration.**

Experimental Results: RDE Reactor

PFOS

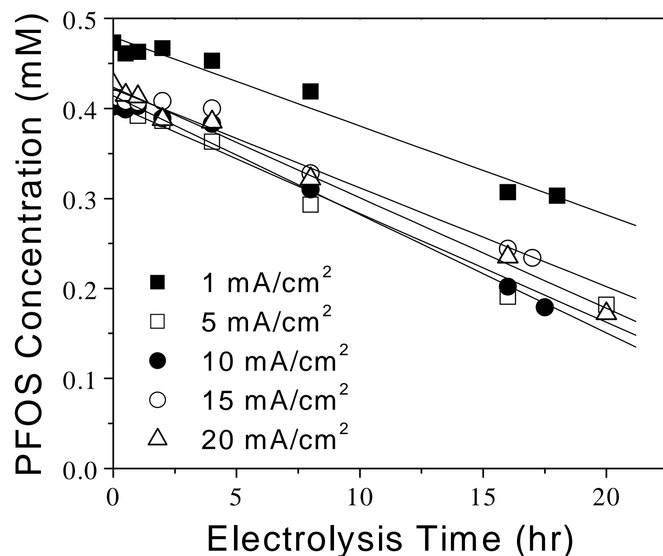

PFBS

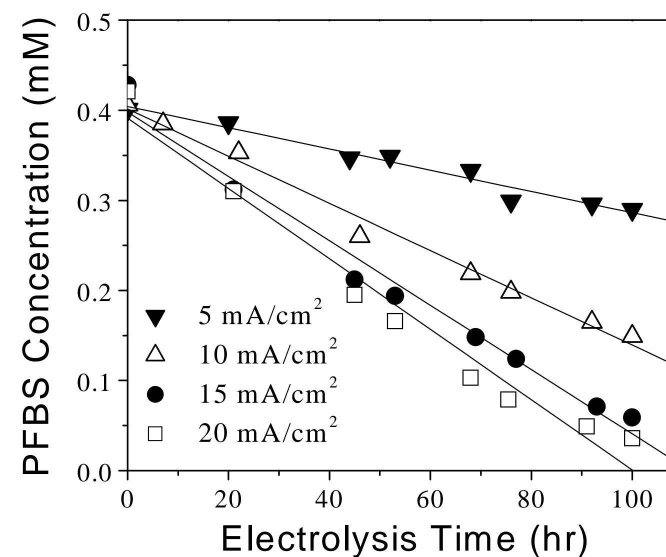

- **Both PFOS and PFBS reaction rates are 0th order in concentration.**
- **Reaction rates are limited by the available reaction sites.**

Reaction Products

PFBS in Flow-Through Reactor

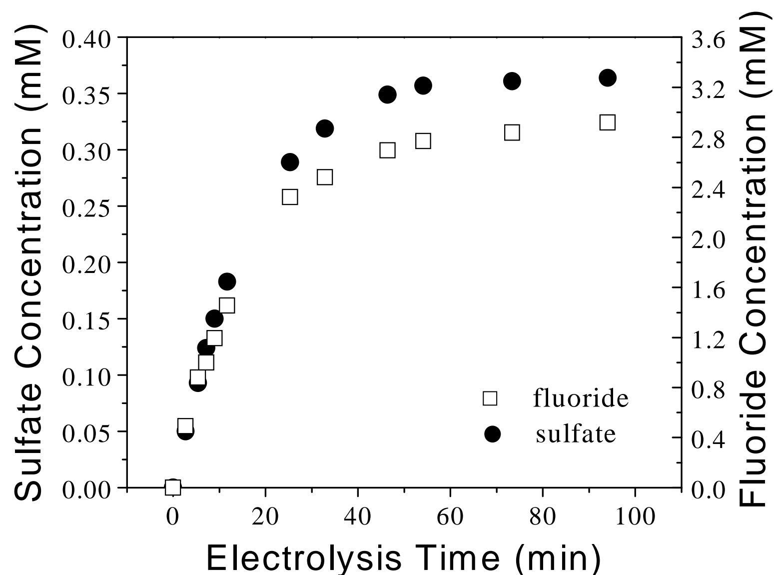

- **1 sulfate ion produced per PFBS or PFOS degraded.**
- **Fluoride ions recovery: 8.2 per PFBS degraded;**
  14 per PFOS degraded.
- **Trace amount of trifluoroacetic acid (TFA).**
- **Some fluoride loss via volatilization of HOF, HF and TFA.**

Arrhenius Plot

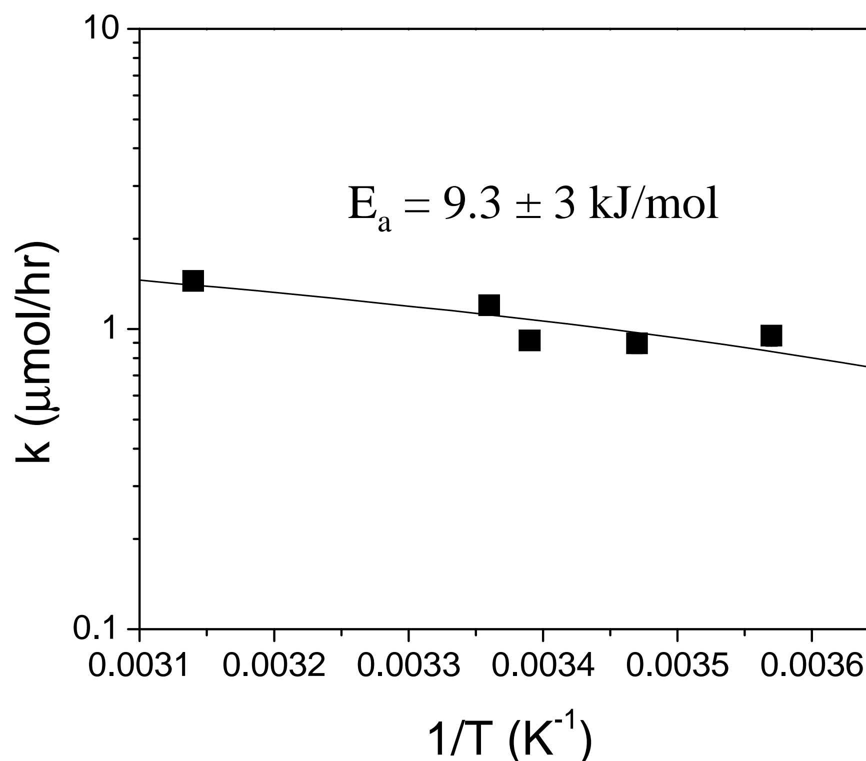

- **Apparent activation energy for PFBS oxidation: 9.3 kJ/mol.**
- **Apparent activation energy for PFBS oxidation: 4.2 kJ/mol.**

PFAS Oxidation Rate-limiting Mechanism

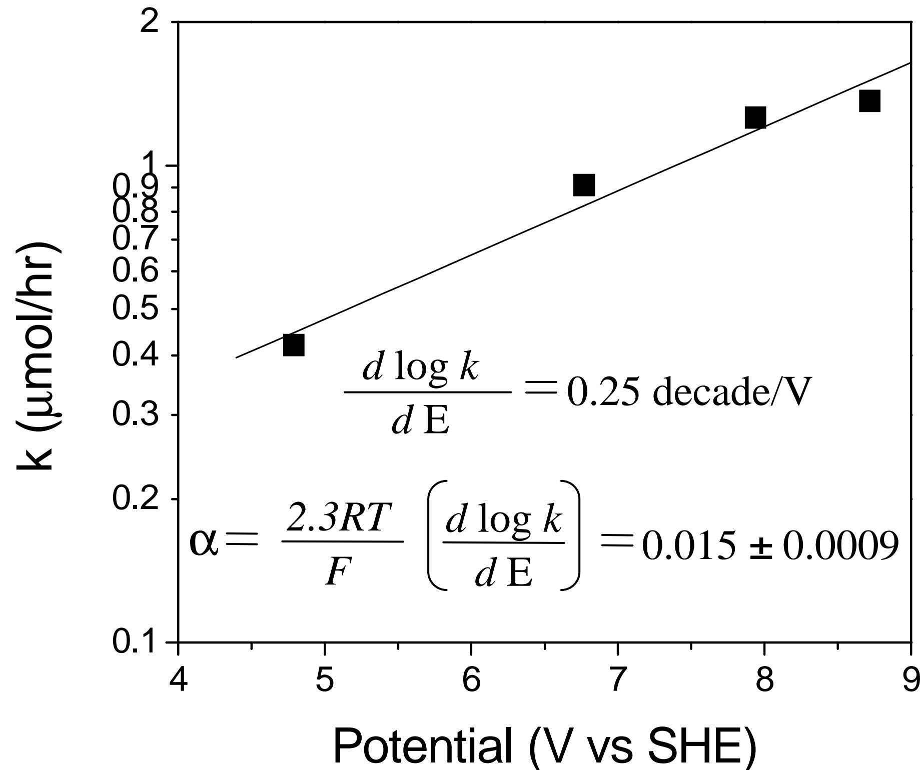

Direct Electron Transfer

$$rate = k[e^{\alpha F(E-E_{eq})/RT}]$$

Oxidation by HO•

Density functional theory (DFT) simulations used to distinguish between two possible RLMs.

Quantum Chemistry Modeling: Activation Energies for $HO^{\bullet}$ Attack

E_a= 123 kJ/mol

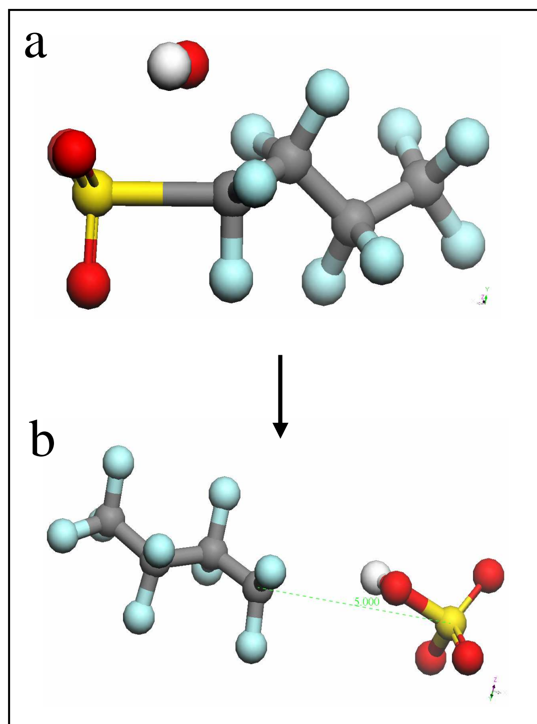

E_a= 172 kJ/mol

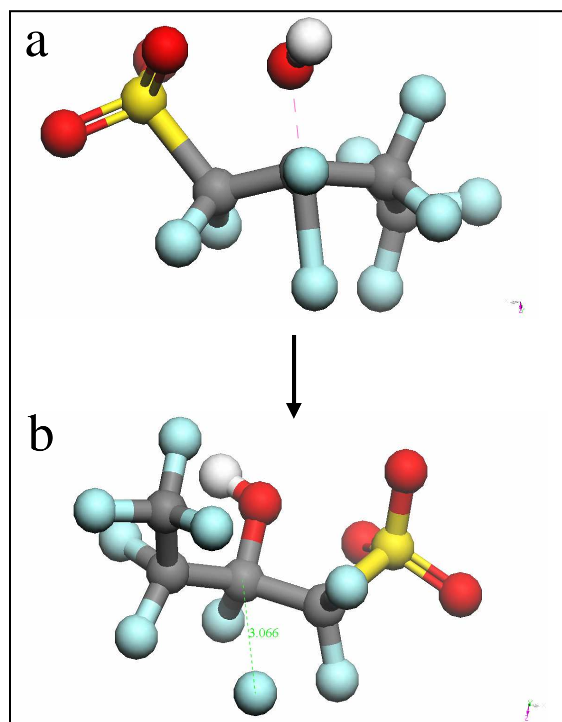

E_a= 288 kJ/mol

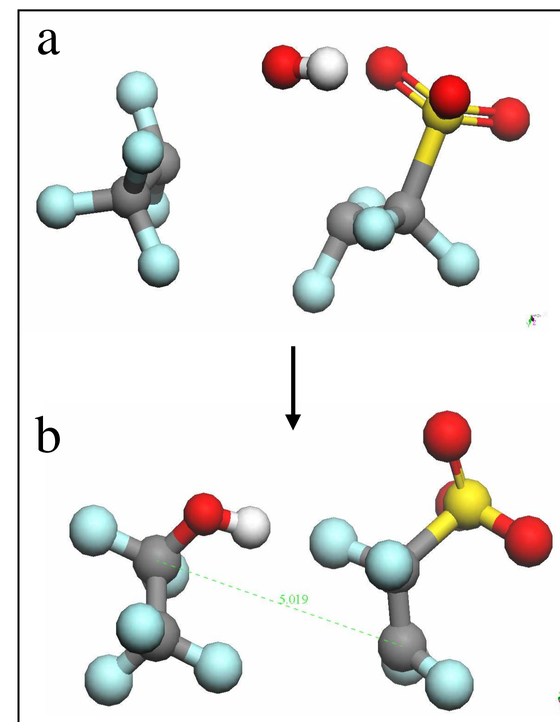

a: Transition State Structure; b: Final Product

Quantum Chemistry Modeling: E_a for Direct Electron Transfer

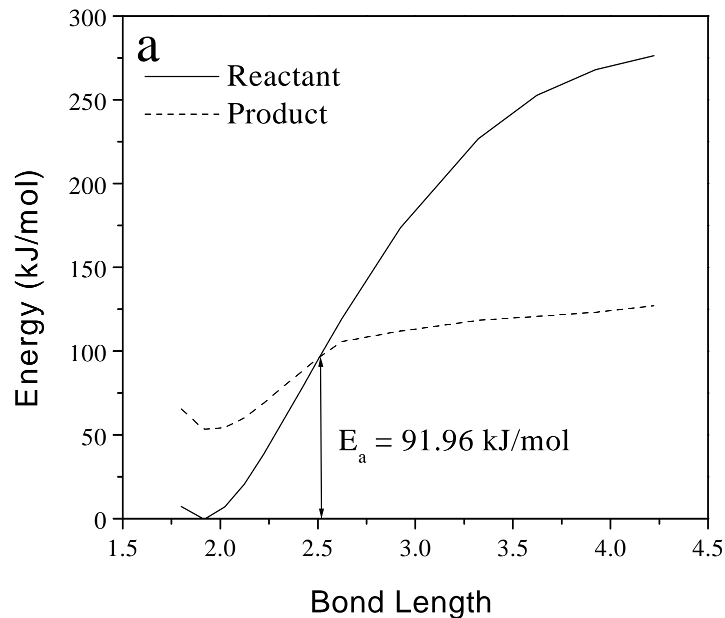

Energy profiles for reactant ($C_4F_9SO_3^-$) and products ($C_4F_9SO_3^{\cdot}$+ e^-) for vertical electron transfer as a function of the C-S bond length at an electrode potential of 2.5 V/SHE.

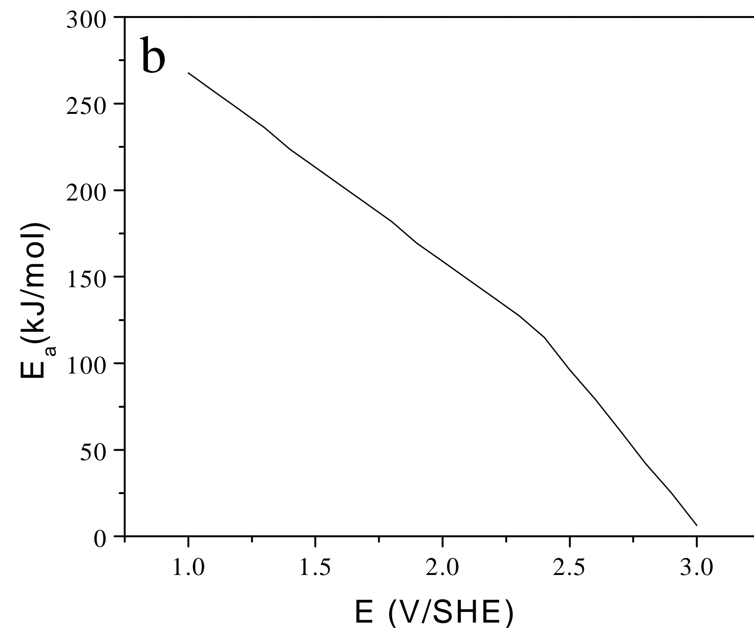

Activation energies as a function of electrode potential for a direct electron transfer reaction.

The rate limiting mechanism for PFAS oxidation appears to be direct electron transfer in the activationless overpotential region at E > 3.0 V/SHE.

Industrial Interactions and Technology Transfer

- Walter Worth, Sematech, Walter.Worth@ismi.sematech.org
- Tim Yeakley, Texas Instruments, t-yeakley@ti.com
- Thomas P. Diamond, IBM, tdiamond@us.ibm.com
- Jim Jewett, Intel, jim.jewett@intel.com
- Laura Mendicino, Freescale Semiconductor, Laura.Mendicino@freescale.com

Future Plans

Next Year Plans

- Bench testing of proposed treatment scheme using activated carbon and Amberlite® anion exchange media.

Long-Term Plans

- Pilot test treatment scheme on real process wastewaters.

Publications, Presentations, and Recognitions/Awards

- **K. E. Carter and J. Farrell, "Oxidative Destruction of Perfluorooctane Sulfonate using Boron Doped Diamond Film Electrodes" *Environ. Sci. Technol.*, Submitted.**

- **Z. Liao and J. Farrell, "Electrochemical Oxidation of Perfluorobutane Sulfonate using Boron Doped Diamond Film Electrodes" *J. Phys. Chem.* A, Submitted.**

- **J. Farrell, "Electrochemical Water Purification using Boron Doped Diamond (BDD) Film Electrodes" invited oral presentation at University of California at Los Angeles (UCLA).**

Destruction of Perfluoroalkyl Surfactants in Semiconductor Process Waters using Boron Doped Diamond Film Electrodes

(*Task Number: 425.018; Subtask #2*)

PIs:

- **Jim A Farrell / Reyes Sierra, Chemical and Environmental Engineering, UA**

Graduate Students:

- **Valeria Ochoa, PhD candidate, Chemical and Environmental Engineering, UA**

Undergraduate Students: ---

Other Researchers:

- **Sandra Hernandez, PhD candidate, University Autonomous of Coahuila, Mexico**

Cost Share (other than core ERC funding):

CONACyT grant (to S. Hernandez)

Objectives

- Determine the degree of electrolysis required for PFOS and PFBS to generate products that are readily biodegraded in municipal wastewater treatment plants.
- Determine the impact of electrolysis on the microbial toxicity of the degradation products from PFOS and PFBS.
- Develop an adsorptive method using hydrophobic zeolites and/or anion exchange resins for concentrating PFAS compounds from dilute aqueous solutions.

ESH Metrics and Impact

1. *Reduction in emission of ESH-problematic materials to environment: ≈ 100% removal of PFOS and other PFAS from aqueous waste streams.*

2. *Reduction in the use of natural resources involved in alternative treatment methods (energy, chemicals):*

   - Aid chemicals are not required.
   - Considerable reduction in energy consumption compared to alternative treatment methods such as reverse osmosis, ultrasonic treatment, etc.

3. *Securing the critical use exemption status for PFAS and related compounds in the semiconductor industry*

Method of Approach

Electrochemical treatment:

PFOS (0.52 mM) underwent electrolysis in a batch reactor (V= 350 ml, anode surface= 1 cm^2, current= 10 mA) for 0-24 h. PFBS (0.4 mM) was electrolyzed in a flow-through reactor (100 ml/min, current density of 2.5 mA/cm^2). Samples were obtained after 0, 1, 2, 3, 4 d. Exogenous electrolyte was not added.

Microbial Toxicity:

Inhibition of methanogenic microorganisms in anaerobic wastewater treatment sludge was tested in batch assays at 30ºC utilizing H_2 as substrate.

Microbial degradation:

The anaerobic biodegradability of solutions containing (partly) electrolyzed PFOS products were determined in batch bioassays supplied with H_2 as as the electron donor. F^- was determined using an ion selective electrode and fluorinated compounds by HPLC.

Method of Approach

Adsorption isotherms with activated carbon and zeolites:

Adsorption isotherms were determined at constant ionic strength in a pH 7.2 phosphate buffer at 30°C. The adsorptive capacity of the various activated carbons over a range of different concentrations was determined by fitting the experimental data to Langmuir and Freundlich models.

Results:

Time course of PFAS electrolysis

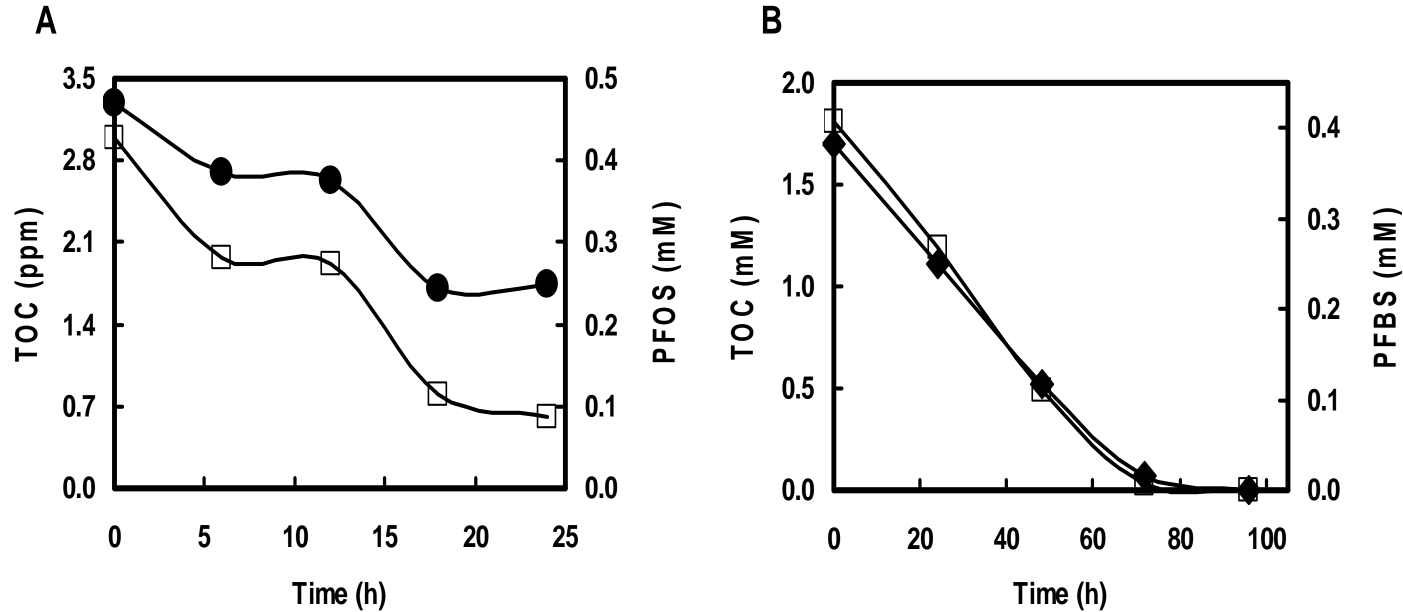

Concentration of PFAS and total organic carbon (TOC) as a function of time in the electrolysis experiments. Samples for evaluation of microbial toxicity and biodegradability were collected after 6. 12, 18 and 24 h. Legend: A) PFOS (●) and B) PFBS (■) and TOC (□).

- ❖ PFOS and PFBS are completely removed by electrochemical treatment.
- ❖ PFBS does undergo electrochemical attack at considerably lower rates than PFOS.

Results:

Chemical composition of PFAS electrolysis products

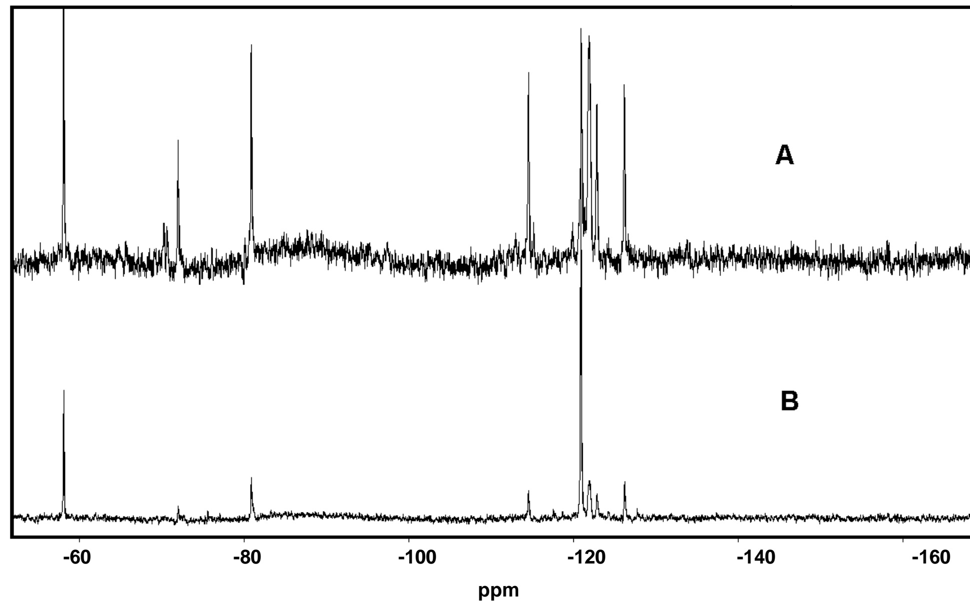

*^{19}F-NMR spectra of (**A**) PFOS and (**B**) PFOS subjected to electrochemical attack for 18 h in a BDD batch reactor operated at a current of 10 mA.*

- No fluorinated compounds detected after 18 h of PFOS electrolysis.
- Fluoride (shift -122 ppm) only F-compound detected.

Results:

Microbial Inhibition by Products of PFAS Electrolysis

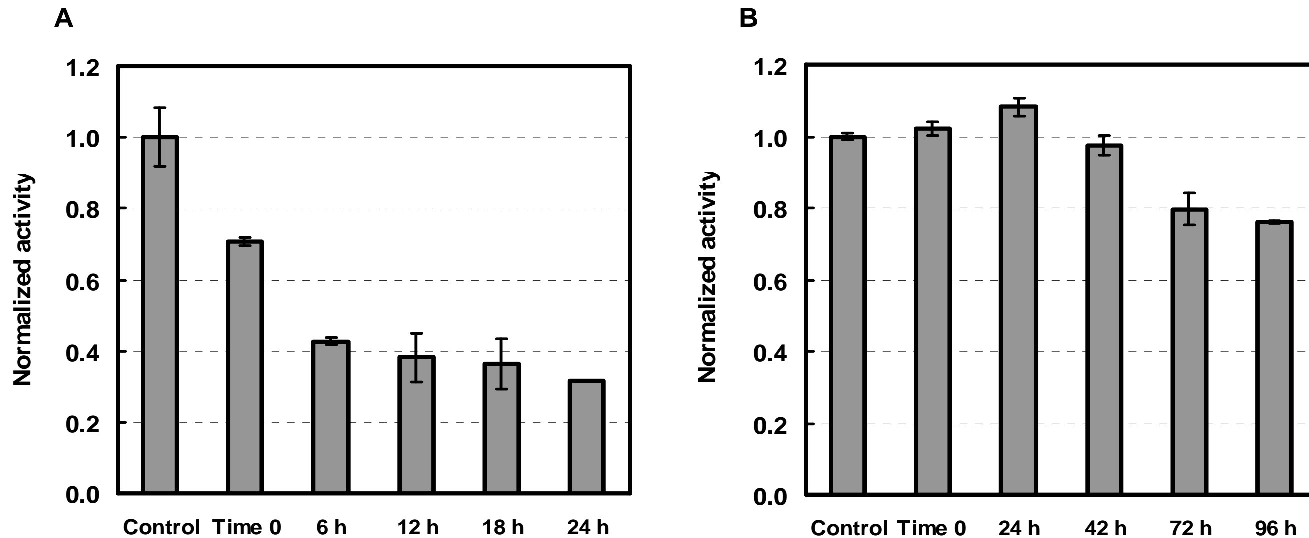

Methanogenic activity of PFAS solutions subjected to electrochemical treatment for different time periods. Legend: A) PFOS and B) PFBS solutions.

- PFOS/PFBS electrolysis products caused microbial inhibition.
- Inhibition likely due to increasing levels of toxic F^- ions and other unidentified degradation products.

Results:

Microbial Degradation of PFAS Electrolysis Products

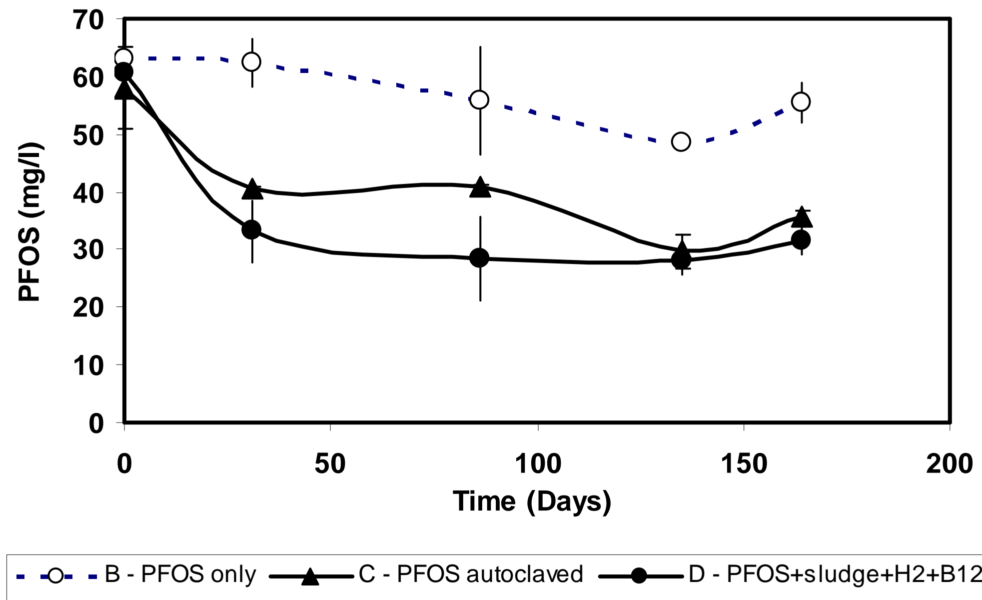

Time course of the anaerobic degradation of PFOS electrolyzed for 24 h. Abiotic control(■), killed sludge control (▲) and full treatment (●).

- FPOS electrolysis products not biodegraded after extended incubation.
- PFOS partly adsorbed by microbial sludge.

Results:

Adsorption of PFOS and other PFAS by Activated Carbon

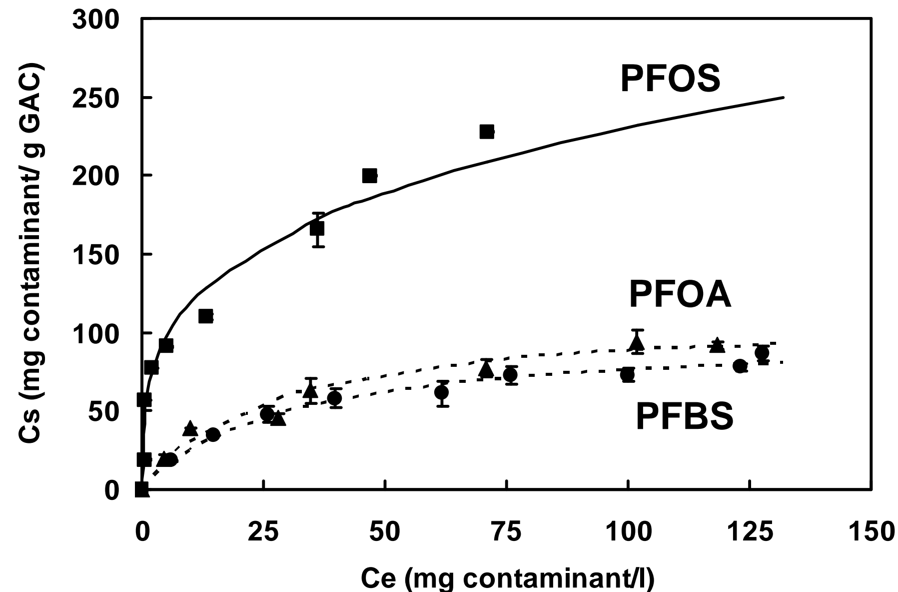

- PFAS in aqueous solutions are adsorbed onto activated carbon.
- Substitution of sulfonic- by carboxylic group and decreasing fluorocarbon chain leads to weaker compound adsorption.
- The affinity of activated carbon for PFOS is moderate when compared to chemical compounds traditionally considered suitable for carbon treatment.

Results:

Adsorption of PFOS and other PFAS by Zeolites

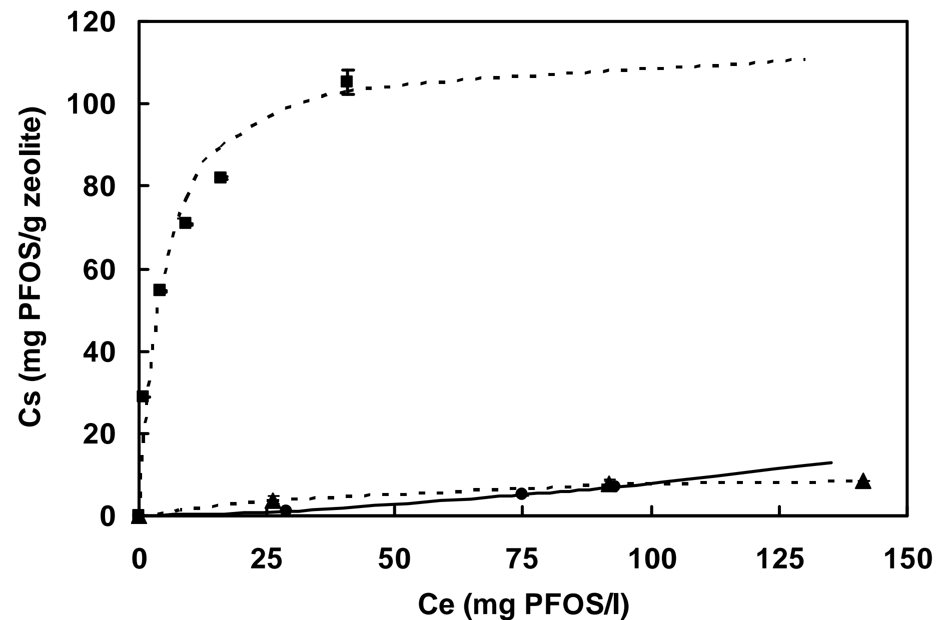

NaY80 (Si/Al 80) (■); NaY (Si/Al 5.5) (●), and 13X (Si/Al 2.8).

Hydrophobic zeolites with high silica content (eg. zeolite NaY80, Si/Al = 80) adsorb PFOS, but low silica zeolites (Si/Al < 5.5) show very poor sorption capacity.

Conclusions

- No evidence for the microbial degradation of products of PFOS electrolysis.
- Electrolysis increased the microbial toxicity of PFOS, likely due to the release of F^- and possibly other degradation products.
- PFOS/PFAS can be removed from dilute solutions by adsorption onto activated carbon.
- PFOS is readily adsorbed by hydrophobic zeolites with a high silica content (eg. NaY80, Si/Al = 80).

Industrial Interactions and Technology Transfer

Industrial liaisons:

- Walter Worth, Sematech, Walter. Worth@ismi.sematech.org
- Tim Yeakley, Texas Instruments, t-yeakley@ti.com
- Thomas P. Diamond, IBM, tdiamond@us.ibm.com
- Jim Jewett, Intel, jim.jewett@intel.com
- Laura Mendicino, Freescale Semiconductor, Laura.Mendicino@freescale.com

Future Plans

Next Year Plans

- Investigate the microbial degradation of products from the incomplete electrolysis of PFBS.

- Evaluate the microbial degradation of partially fluorinated compounds to microbial degradation.

- Perform column breakthrough experiments with activated carbon to determine the mass transfer characteristics for the best performing PFAS adsorbents.

Long-Term Plans

- Build and evaluate a prototype treatment system and test it on real PFAS containing wastewaters generated during semiconductor manufacturing.

Publications, Presentations, and Recognitions/Awards

- **Publications**

  Ochoa-Herrera et al. "Removal of perfluorinated surfactants by sorption onto granular activated carbon, zeolite and sludge". (Submitted).

  Ochoa-Herrera et al. "Impact of electrochemical treatment on the microbial degradation of perfluorinated surfactants" (In preparation).

- **Awards**

  Ochoa-Herrera, V. Outstanding teaching assistant of the Department of Chemical and Environmental Engineering, academic year 2006/2007.

Low Environmental Impact Processing of Sub-50 nm Interconnect Structures

(*Task Number: 425.019*)

PIs:

- **Karen K. Gleason, Department of Chemical Engineering, MIT**

Graduate Students:

- **Chia-Hua Lee: PhD Candidate, Department of Material Science and Engineering, MIT**
- **Wyatt Tenhaeff, Ph.D Candidate, Department of Chemical Engineering, MIT (NSF Fellow)**

Cost Share (other than core ERC funding):

- **$70k (NSF Fellowship for Wyatt Tenhaeff)**

Objectives

- **Develop new methods to deposit patterns at resolution of 50 nm and below without conventional lithography**
  - **Using Dip-Pen Nanolithography (DPN) and microcontact stamping to create surface quantum dot patterns on the polymer substrate.**
  - **Using carbon nanotubes (CNTs) as the etching masks to create high resolution functional polymer patterns.**
- **Use EHS focused design approach to minimize process steps in the novel patterning processes**
- **Use low energy iCVD method as the process platform technology.**
- **Develop integration methods for quantum dots (QDs), allowing integration of high performance devices onto flexible substrates, relying on the naturally small dimensions of the QDs to achieve high resolution.**

ESH Metrics and Impact

1. *Resist-free lithography would eliminate use of photoresist. Approximately 25,000 liters of photoresist materials is used annually in typical semiconductor foundries, at a cost of about $1,600 per liter. Through spin-on process approximately 95% of resist is wasted and disposed as toxic material [1] .*
2. *Typical iCVD process requires between .02-.12 W/cm^2 [3] for polymer deposition compared to conventional PECVD which uses 0.4-2.1 W/cm^2[4,5] . No plasma etch eliminates additional >7.1 W/cm^2[6] power requirement.*

[1] Percin et al., IEEE Transactions on Semiconductor Manufacturing (2003) 16 (3)
[2] Lee et al., J. Micromech. Microeng. (2005) 15
[3] Martin et al.Surf. Coating Tech. (2007) 201
[4]Castex et al. Microelec. Eng. (2005) 82
[5]Wong et al. Thin Sol. Films 462–463 (2004)
[6]Berruyer et al. J. Vac. Sci. Technol. A. 16.3 (1998)

Initiated CVD of Functionalizable Polymers

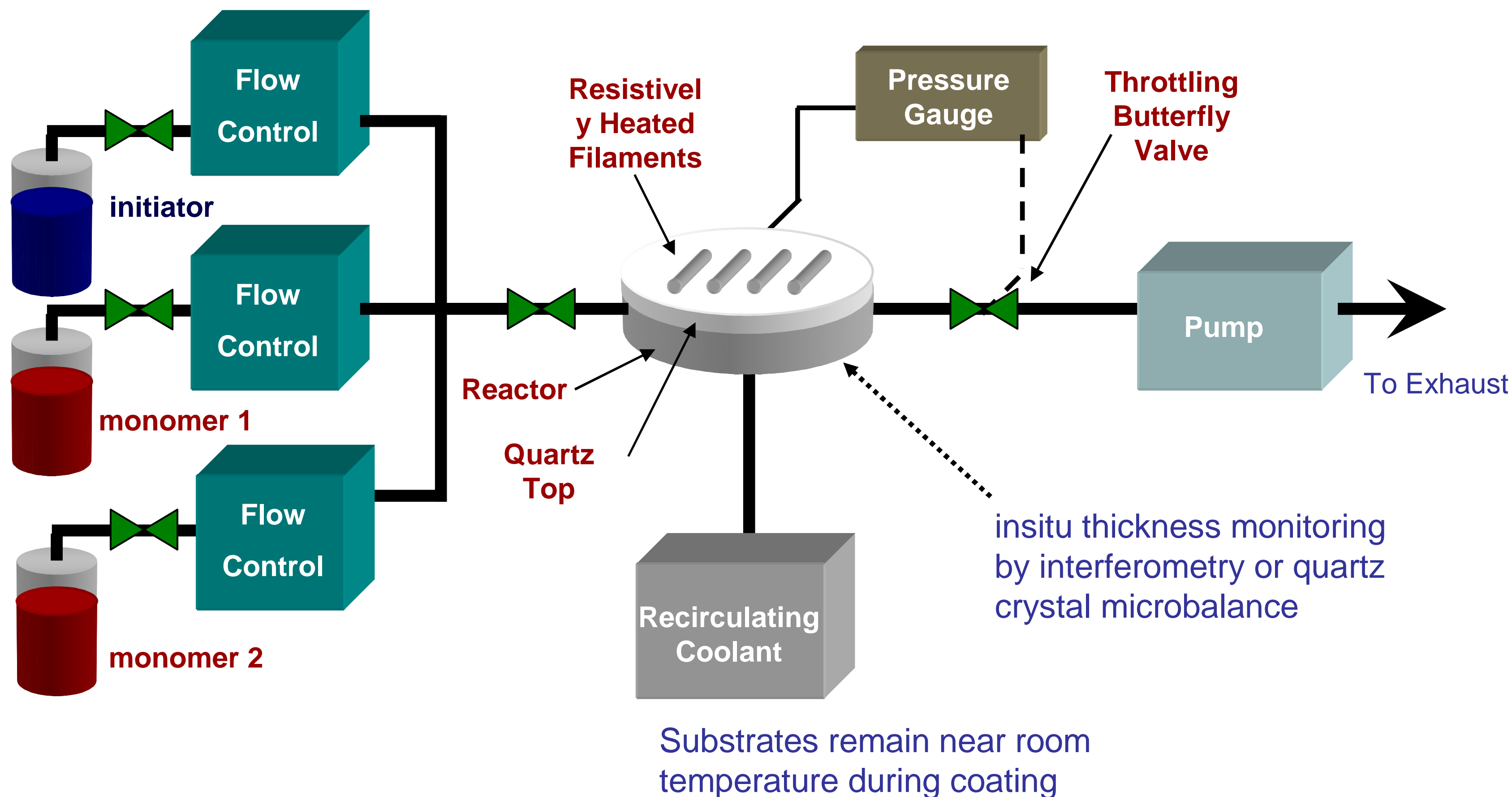

Functional groups in iCVD films can be used to covalently tether nanoparticles

iCVD poly(styrene-alt-maleic anhydride)

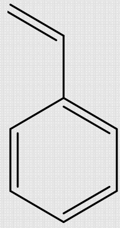

Styrene

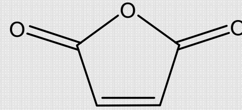

Maleic Anhydride

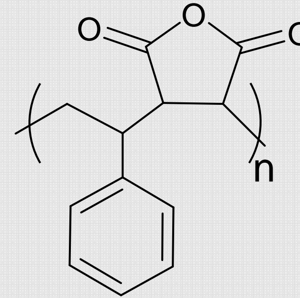

Poly(styrene-alt-maleic anhydride) (PSMa)

12 C: 3 O per unit (80% carbon)

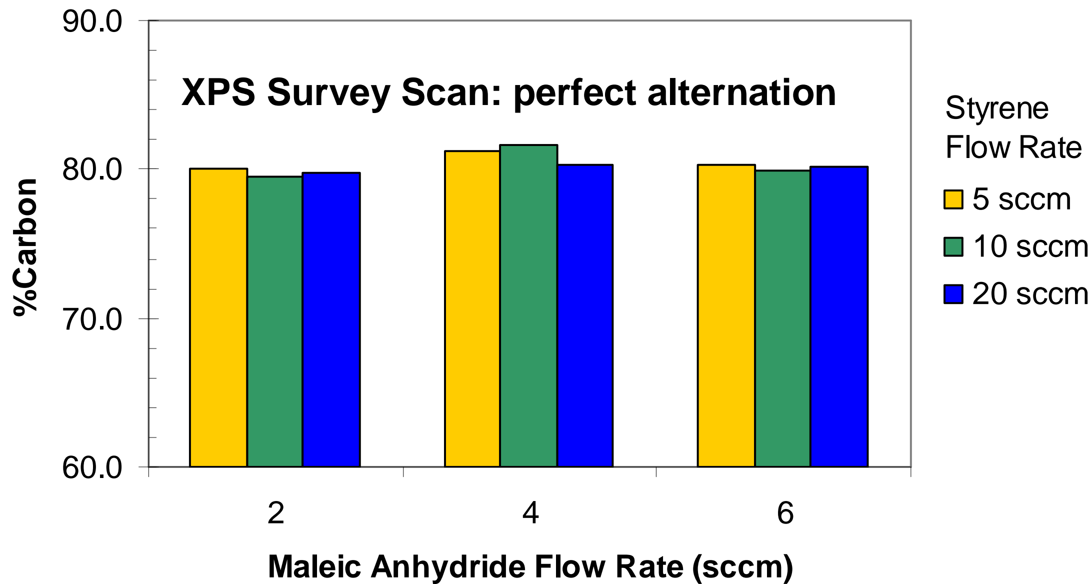

^{13}C NMR :

Only alternating triads: M-S-M

No M-S-S or S-S-S detected

W.E. Tenhaeff and K.K. Gleason
Langmuir 23, 6624 (2007).

Direct writing with QD ink on iCVD PSMa

Microcontact stamping

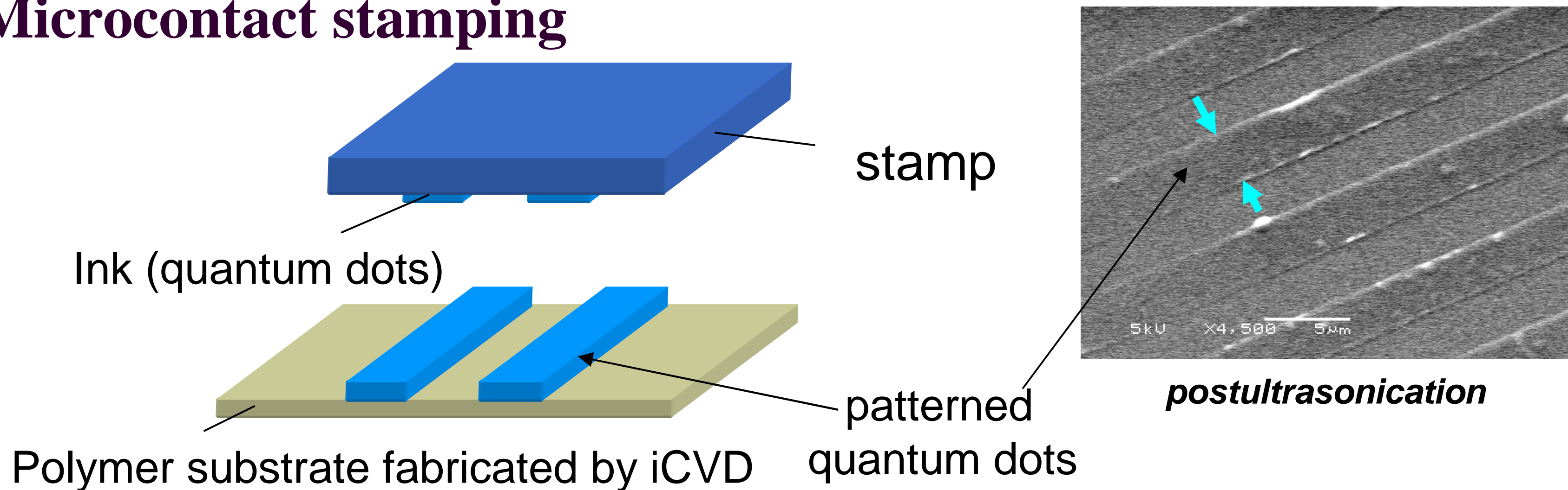

DPN

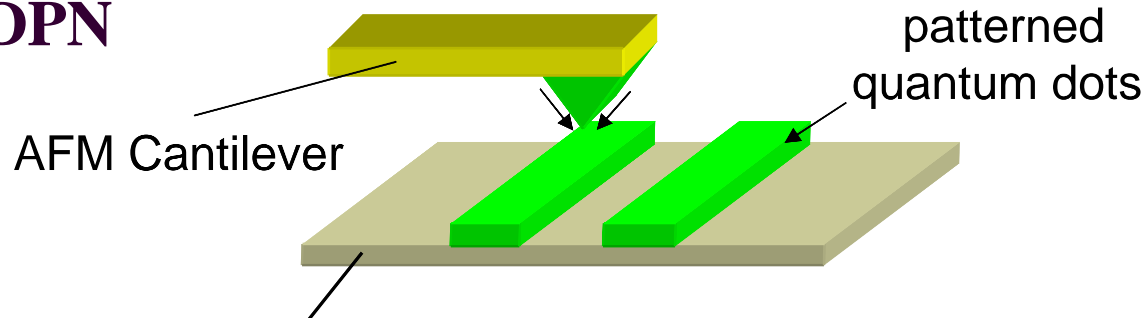

Writing speed can be increased by using multiple cantilevers in parallel

Covalent attachment of QDs to iCVD PSMaß

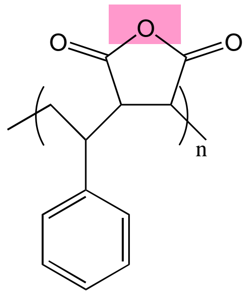

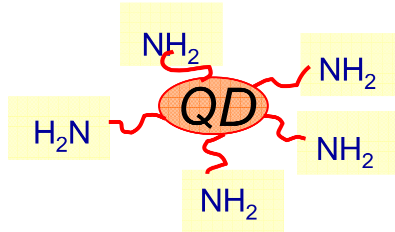

- **Poly(styrene-alt-maleic anhydride) (PSMa)**
- **CdSe quantum dots (QD)**

  capped bifunctional ligands $-NH_2$

QD Size ~ 5 nm

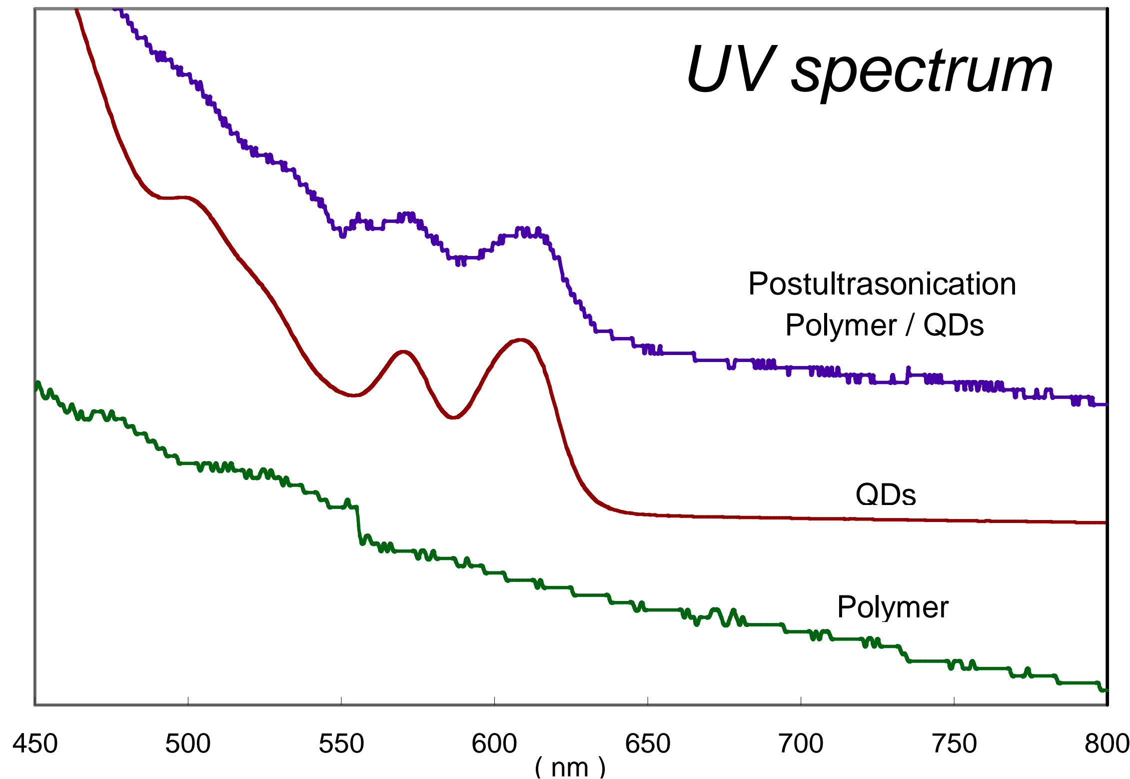

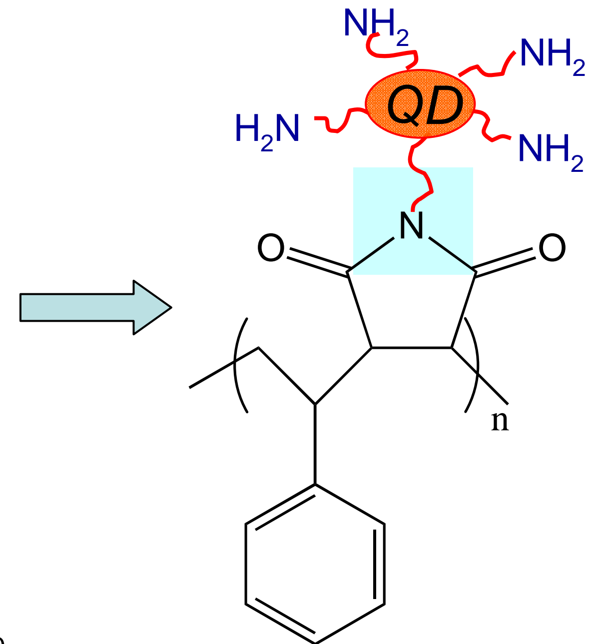

CNT masks for patterning iCVD PSMa

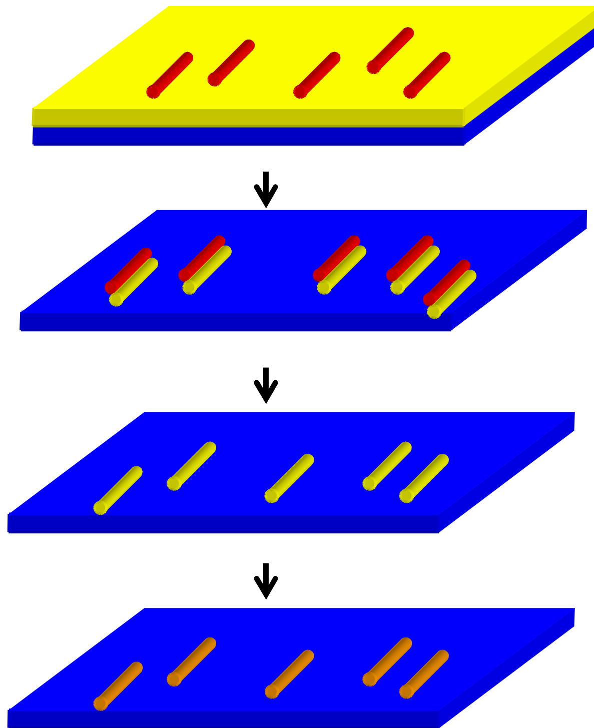

Spin casting of CNT masks on the iCVD PSMa polymer thin film

Oxygen plasma etching

Removal of CNT masks

Quantum dots incorporation

Use of semiconducting QDs removes the need for substrates to be high quality substrates.

Inexpensive, lightweight flexible substrates possible. Avoids energy intensive fabrication of high purity silicon wafers.

Carbon Nanotube (CNT) masking results

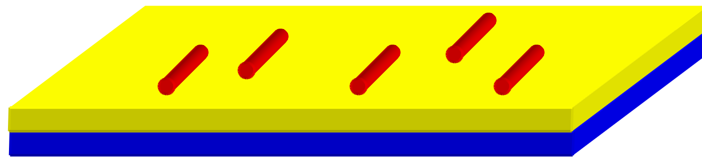

After spin-casting of CNTs

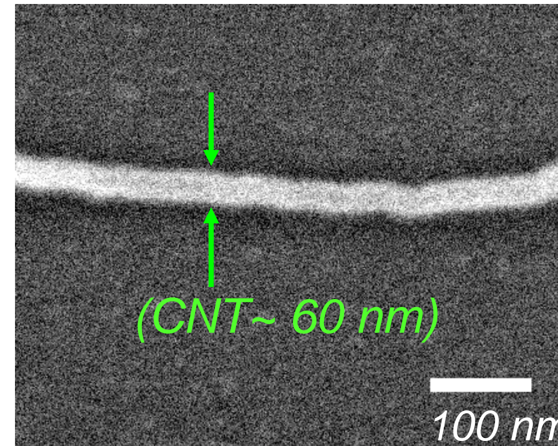

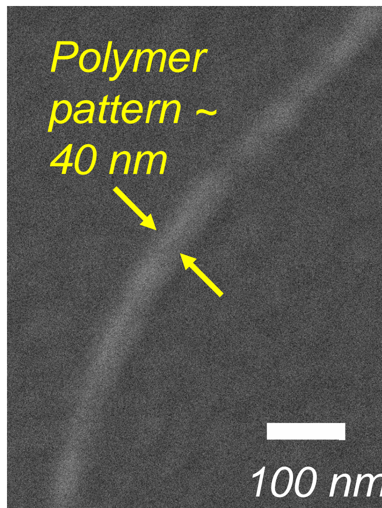

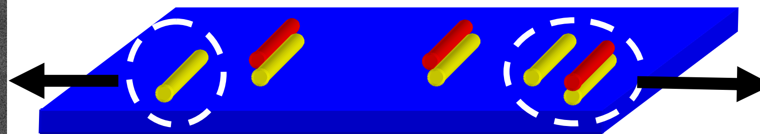

After etching and partial removal of the CNTs

Pattern in polymer is smaller than CNT diameter

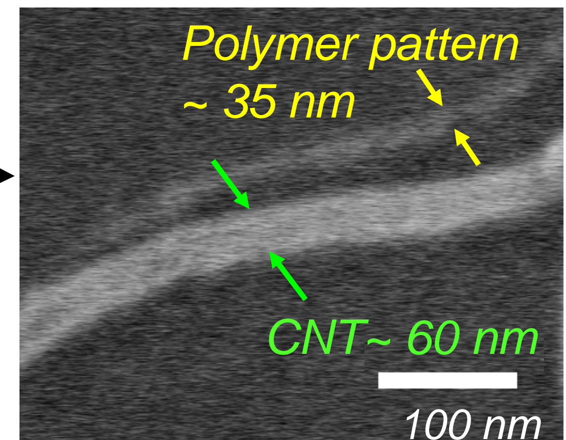

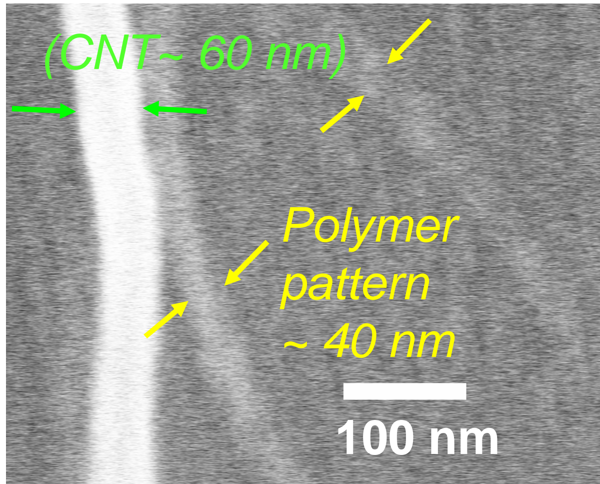

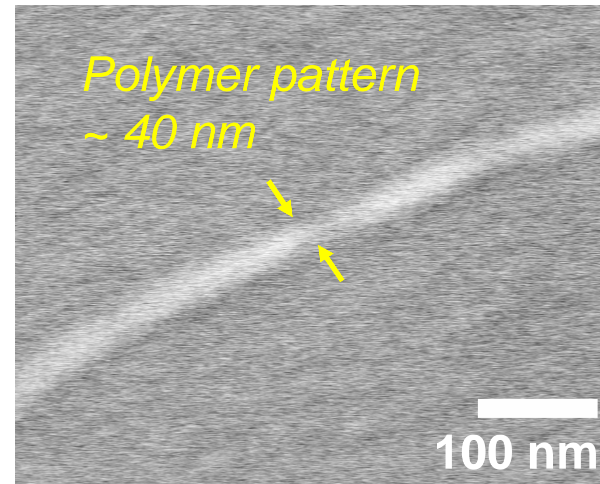

Pattern sizes depend on the etching time

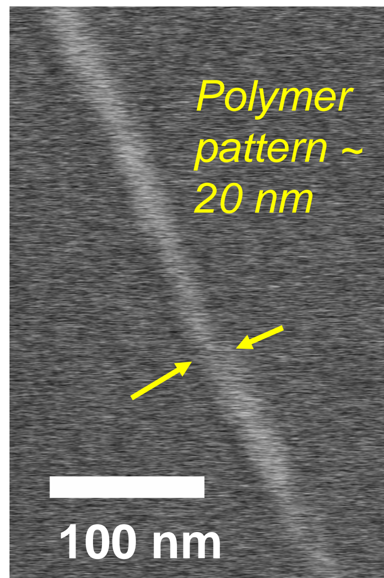

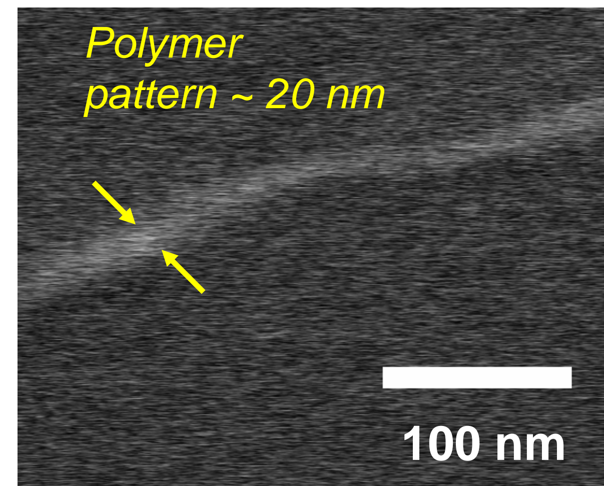

Future Plans

Next Year Plans

- **Optimize the incorporation of the monodisperse and functionalized quantum dots in collaboration with Prof. Muscat's group**
- **Use functional iCVD polymers to align the carbon nanotubes**
- **Fabricate simple quantum dot devices using the novel patterning strategies**

Long-Term Plans

- **Demonstrate the performance of high resolution devices on flexible, low cost, light weight substrates.**

Publications, Presentations, and Recognitions/Awards

PUBLICATIONS

- W.E. Tenhaeff, K.K. Gleason, Initiated Chemical Vapor Deposition of Alternating Copolymers of Styrene and Maleic Anhydride, Langmuir 23(12), 6624-6630 (2007).
- Wyatt E. Tenhaeff and Karen K. Gleason, Initiated chemical vapor deposition of perfectly alternating poly(styrene-alt-maleic anhydride),Surface And Coatings Technology 201,9417-9421 (2007)

PRESENTATIONS

- K.K. Gleason, Polymeric Nanocoatings by Chemical Vapor Deposition, Pall Corporation, 2/6/2007
- K.K. Gleason, Design of CVD processes for low k dielectrics and air gap formation, 2007 MRS Spring Meeting:Symp. B, San Francisco, CA 4/11/2007 (invited)
- K.K. Gleason, Initiated chemical vapor deposition (iCVD) of polymeric nanocoatings, 16th European Conference on Chemical Vapor Deposition, Den Haag, Netherlands, 9/20/2007 (invited).
- W. Tenhaeff and K.K. Gleason, Initiated chemical vapor deposition of perfectly alternating Poly(styrene-alt-maleic anhydride), 16th European Conference on Chemical Vapor Deposition, Den Haag, Netherlands, 9/20/2007
- K.K. Gleason, Chemical Vapor Deposition of Polymeric Nanocoatings, U. Calgary, Dept. Chemical Engineering, 10/5/2007 (invited).
- K.K. Gleason, Conformal Polymeric Thin Films via Initiated Chemical Vapor Deposition, AVS Seattle, WA, 10/15/2007 (invited)
- K.K. Gleason, Engineering Polymeric Nanocoatings by Vapor Deposition 31th Annual Symposium of the Macromolecular Science and Engineering Program at the University of Michigan., Ann Arbor, MI, 10/25/2007 (invited).
- W.E. Tenhaeff and K.K. Gleason, Initiated Chemical Vapor Deposition of Functional Thin Hydrogel Films to Incorporate Quantum Dots, MRS Fall Conference, Boston, MA, 11/30/2007

Low Environmental Impact Processing of sub-50 nm Interconnect Structures

(*Task Number: 425.019*)

PIs:

- **Anthony Muscat, Chemical and Environmental Engineering, UA**
- **Masud Mansuripur, College of Optical Sciences, UA (added 2008)**

Other Researchers:

- **Zhengtao Deng, Postdoctoral Fellow, ChEE & Optical Sciences, UA**

Cost Share (other than core ERC funding):

- **$85k from Arizona TRIF**

Objectives

- **Reduce the power required for switching and to transmit signals on a chip and between chips by using light**
- **Reduce the water, energy, and materials required to fabricate interconnect wiring**
- **Use clusters of crystalline semiconductors (quantum dots) to build interconnect structures**
  - **Inherently small 1-5 nm q-dots $\Rightarrow$ scaling**
  - **Tunable band gap and photosensitivity $\Rightarrow$ optical switching or signal transmission**
- **Develop processes to**
  - **(1) grow crystalline quantum dots in water and in a gas phase**
  - **(2) pattern quantum dots on surfaces and thin films with alternative lithographic processes**
  - **(3) use materials that have low ESH impact**

ESH Metrics and Impact

Risk category	Material Selection Criteria
Environment	No toxicity to aquatic and non-aquatic systems
Safety	Flash point > 55˚C
Health	No toxic solvents No carcinogens/mutagens or reproductive toxins

Sustainability metrics			
Process	Water l/bit/masking layer	Energy J/bit/masking layer	Materials g/bit/masking layer
Subtractive 32 nm*	3.3×10^{-10}	1.5×10^{-12} EUV	2.9×10^{-16}
Additive	3.6×10^{-13}	9.2×10^{-17}	1.8×10^{-19}

*D. Herr, Extending Charge-based Technology to its Ultimate Limits: Selected Research Challenges for Novel Materials and Assembly Methods. Presentation at the NSF/SRC EBSM Engineering Research Center Review Meeting: February 24, 2006.

Methods and Approach

- **Develop fast, simple, reproducible, cost-efficient, and environmentally friendly routes to fabricate highly luminescent quantum dots with tunable photoluminescence (PL) peaks**

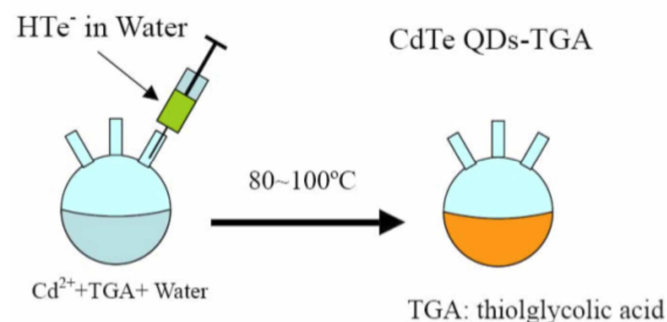

- **Water based and gas phase synthesis routes that are scaleable to commercial applications**
- **Deposit on Si and dielectric surfaces by tuning ligand**
  - **Thiol ligands with different chain lengths and chemistries**
- **Validate properties of quantum dots in solution and on surfaces**
  - **Bleaching**
  - **Fluorescence intensity intermittency (blinking) and frequency shift**

Fabricated Quantum Dots in Water

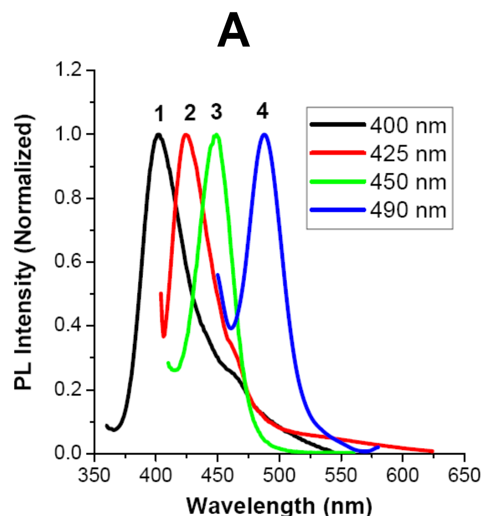

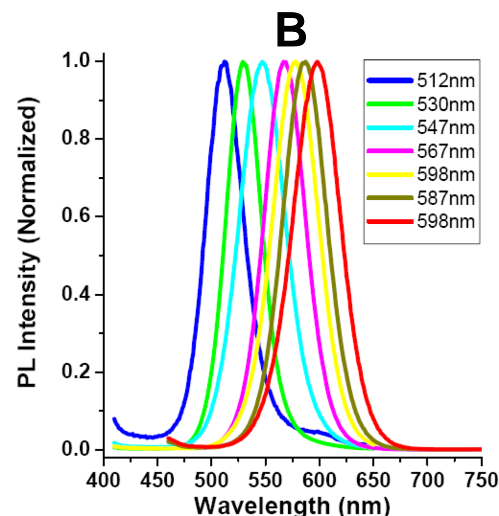

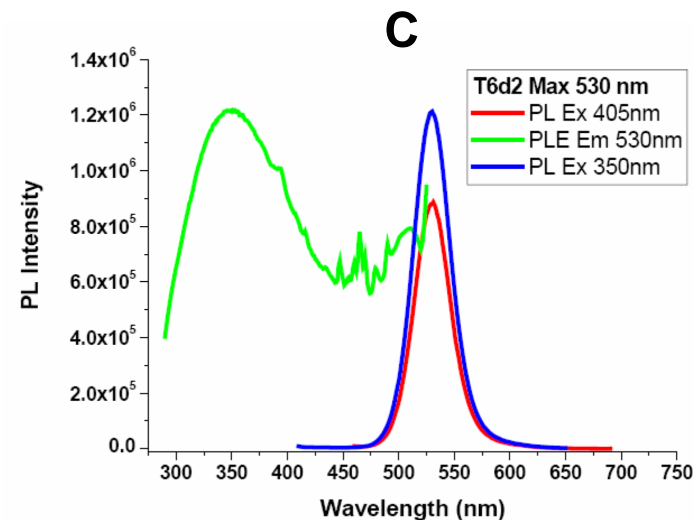

A photoluminescence (PL) spectra of a series of thiolglycolic acid capped $Zn_xCd_{1-x}Se$ QD samples
B PL spectra of a series of thiolglycolic acid capped CdTe QD samples
C PL and PLE spectra of one typical thiolglycolic acid capped CdTe QD samples

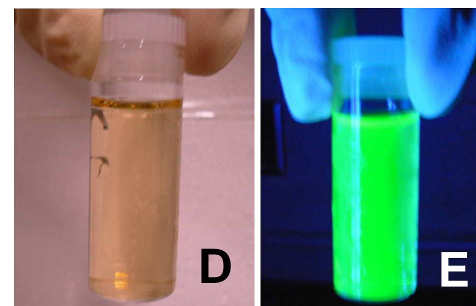

Pictures of typical TGA-capped CdTe QDs samples under
D room light
E 365 nm UV light

AFM of QDs Deposited on Si Surface

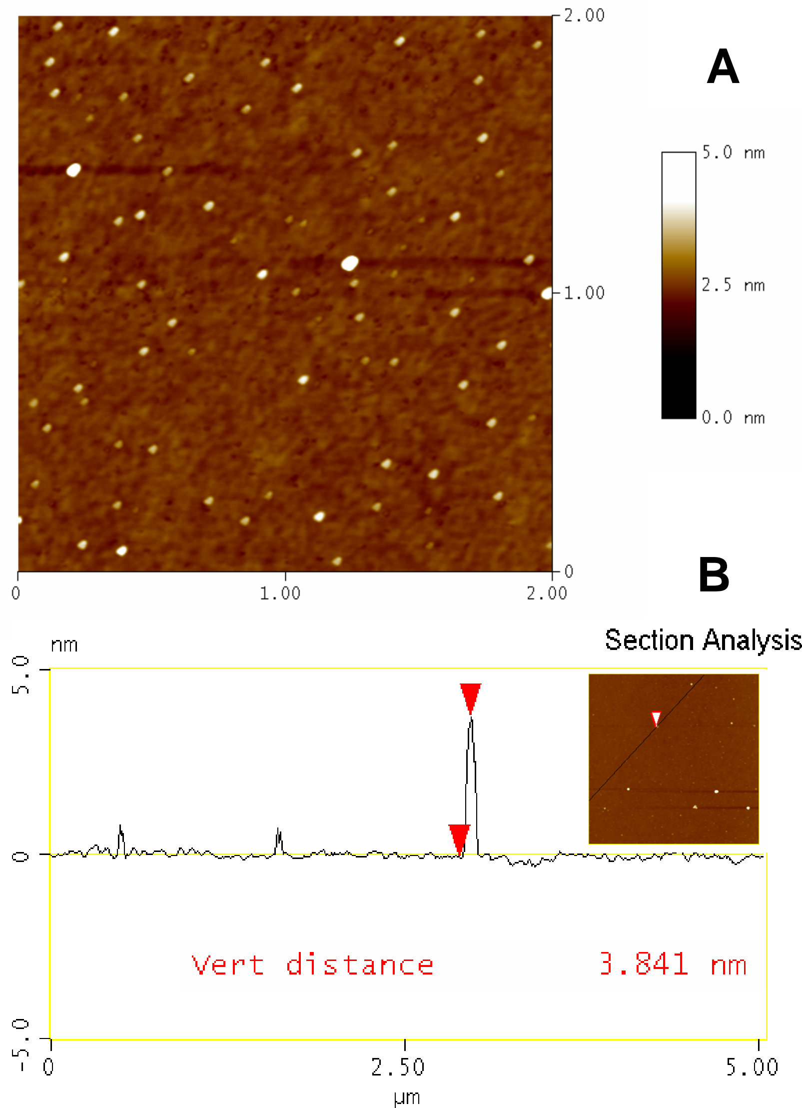

A AFM topography image of TGA-capped quantum dots with maximum emission at 590 nm on hydrophilic silicon wafer substrate

B Height profile of AFM line scan in the image shown in the inset. Red arrows define dimensions of one typical quantum dot with a diameter close to 3.8 nm.

TEM of QDs

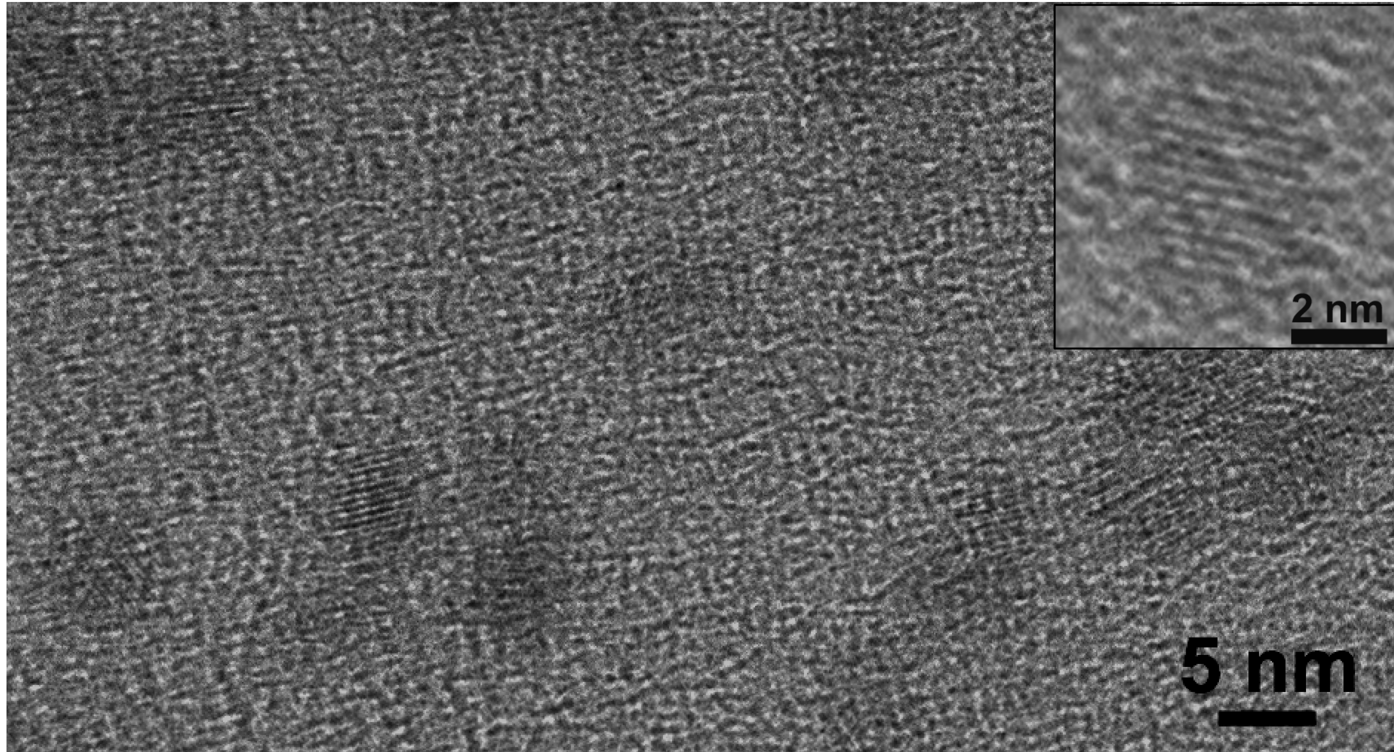

Transmission electron microscopy image of thiolglycolic acid capped CdTe quantum dots deposited on TEM grid

Band Gap of QD Clusters Computed by Molecular Modeling

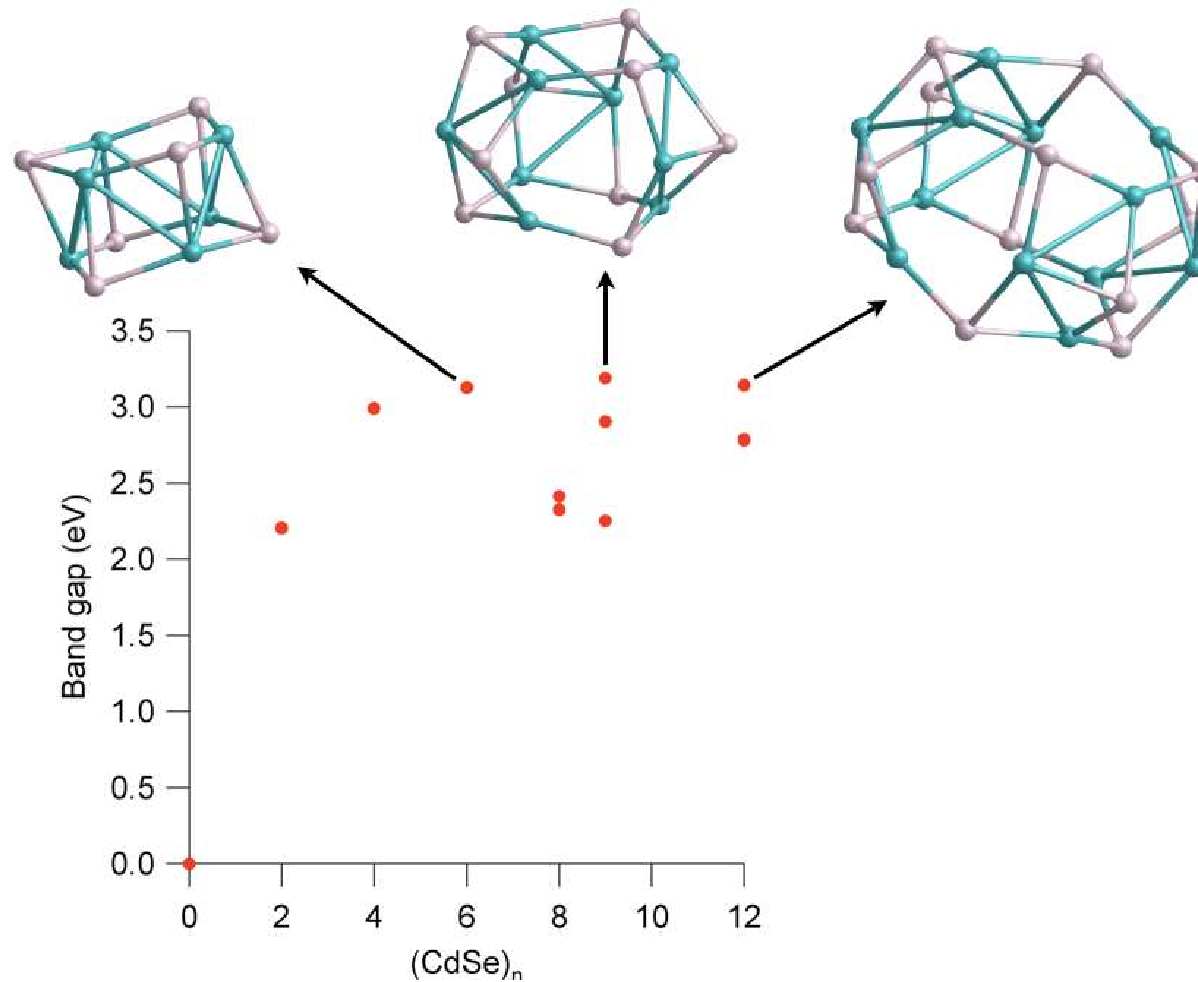

Density Functional Theory
B3LYP exchange-correlation functional
LANLD2Z effective core potential/basis set
Gamess code: http://www.msg.chem.iastate.edu/GAMESS/GAMESS.html

Industrial Interactions and Technology Transfer

- **Will work with companies to develop a model to assesses whether the new processing technology is cost-effective and manufacturing-worthy**

Future Plans

Next Year Plans

- Investigate replacing the reproductive toxin Cd with Cu or Mn
- Model q-dot structure and properties with computational chemistry
- Deposit q-dots on semiconductor and dielectric surfaces by varying ligand chemistry
- Define prototype devices
- Assess costs of introducing new processing technology

Long-Term Plans

- Work with Prof. Karen Gleason's group at MIT to selectively deposit q-dots on surfaces patterned using iCVD
- Build a prototype device based on q-dots

Publications, Presentations, and Recognitions/Awards

- **Z. Deng, et al., "*A Simple Open-to-Air Water-Based Route to Ligand-Selective Synthesis of ZnSe and $Zn_xCd_{1-x}Se$ Quantum Dots with Finely Tunable UVA to Blue Photoluminescence*," under consideration by the Journal of Physical Chemistry**

An Integrated, Multi-Scale Framework for Designing Environmentally Benign Copper, Tantalum and Ruthenium Planarization Processes

(*Task Number: 425.020*)

Subtask 1: Wear Phenomena and Their Effect on Process Performance

PI:

- Ara Philipossian, Chemical and Environmental Engineering, UA

Graduate Students:

- Xiaomin Wei: Ph. D. candidate, Chemical and Environmental Engineering, UA
- Ting Sun: Ph. D. candidate, Chemical and Environmental Engineering, UA
- Anand Meled: Ph. D. candidate, Chemical and Environmental Engineering, UA

Undergraduate Students:

- Geoff Steward, Chemical and Environmental Engineering, UA
- Roy Dittler, Chemical and Environmental Engineering, UA

An Integrated, Multi-Scale Framework for Designing Environmentally Benign Copper, Tantalum and Ruthenium Planarization Processes

(*Task Number: 425.020*)

Subtask 1: Wear Phenomena and Their Effect on Process Performance

Other Researchers:

- **Yun Zhuang, Research Associate, Chemical and Environmental Engineering, UA**
- **Jiang Cheng, Visiting Scholar, Chemical and Environmental Engineering, UA**

Cost Share (other than core ERC funding):

- **In-kind donation (pads and slurries) from Cabot Microelectronics Corporation**
- **In-kind donation (diamond discs) from Mitsubishi Materials Corporation**
- **In-kind donation (retaining rings) from Entegris, Inc.**
- **In-kind support from Araca, Inc.**

Objectives

- **Investigate diamond and diamond disc substrate wear during copper CMP process.**
- **Investigate the effect of conditioning on pad topography.**
- **Investigate the effect of pad conditioning on slurry film thickness in pad-wafer interface area through dual emission UV enhanced fluorescence (DEUVEF) technique.**
- **Investigate the effect of materials of construction and design on retaining ring wear.**
- **Investigate the effect of retaining ring design on slurry flow.**

ESH Metrics and Impact

1. *Reduce diamond disc consumption by 20%*

2. *Reduce pad consumption by 33%*

3. *Reduce slurry consumption by 20%*

4. *Extend retaining ring life and reduce retaining ring consumption by 33%*

Identify Active Diamond - Short Draw Test

Conditioner is pulled
only about quarter-inch

Scratch origins are marked

• Faint scratches
• Partial scratches

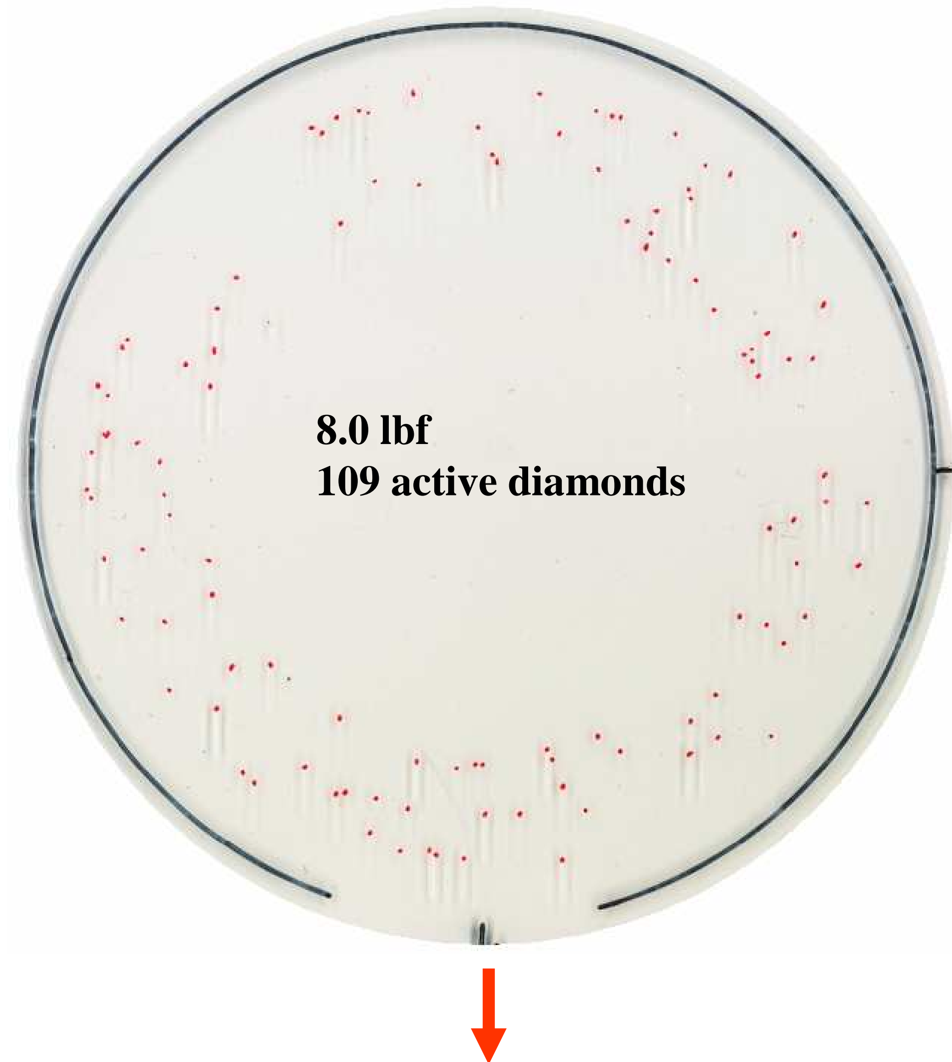

Identify Aggressive Diamond - Long Draw Test

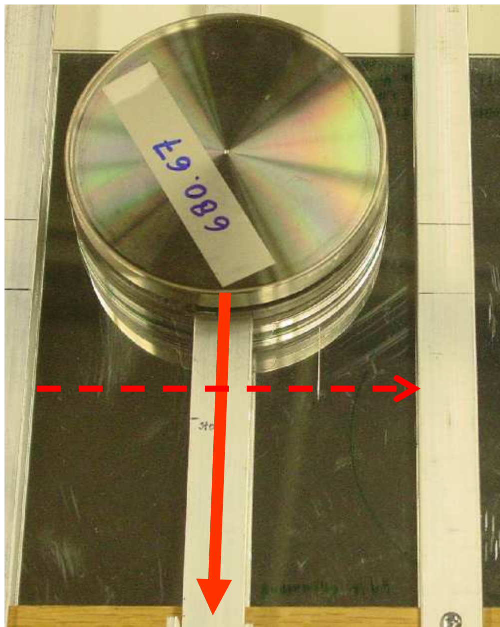

Conditioner is pulled more than one diameter of the disc.

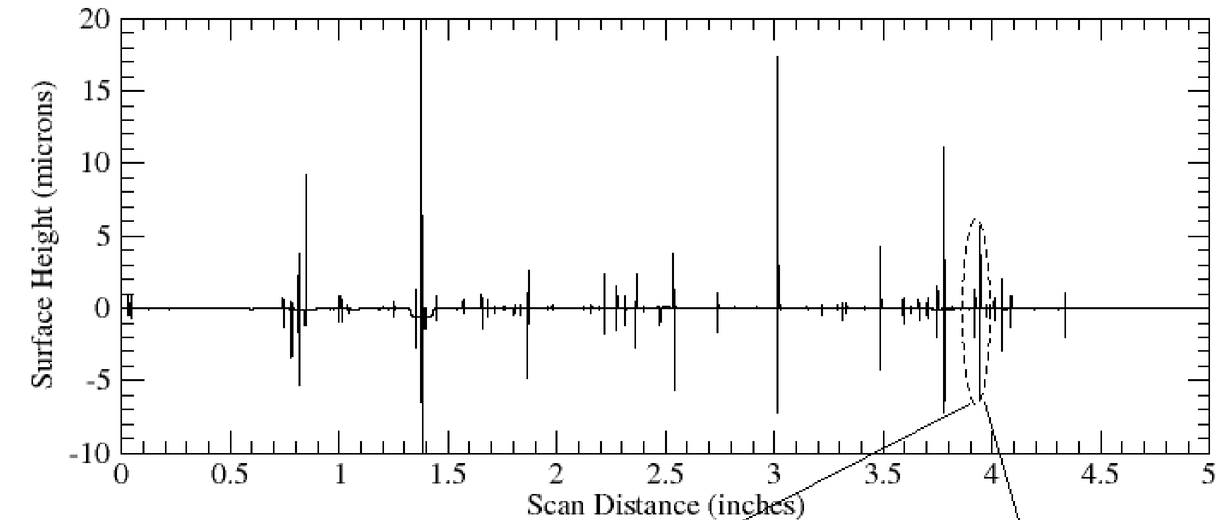

Polycarbonate surface is profiled

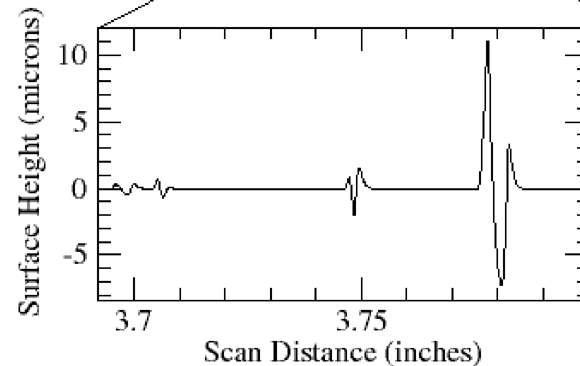

Locating Aggressive Diamonds

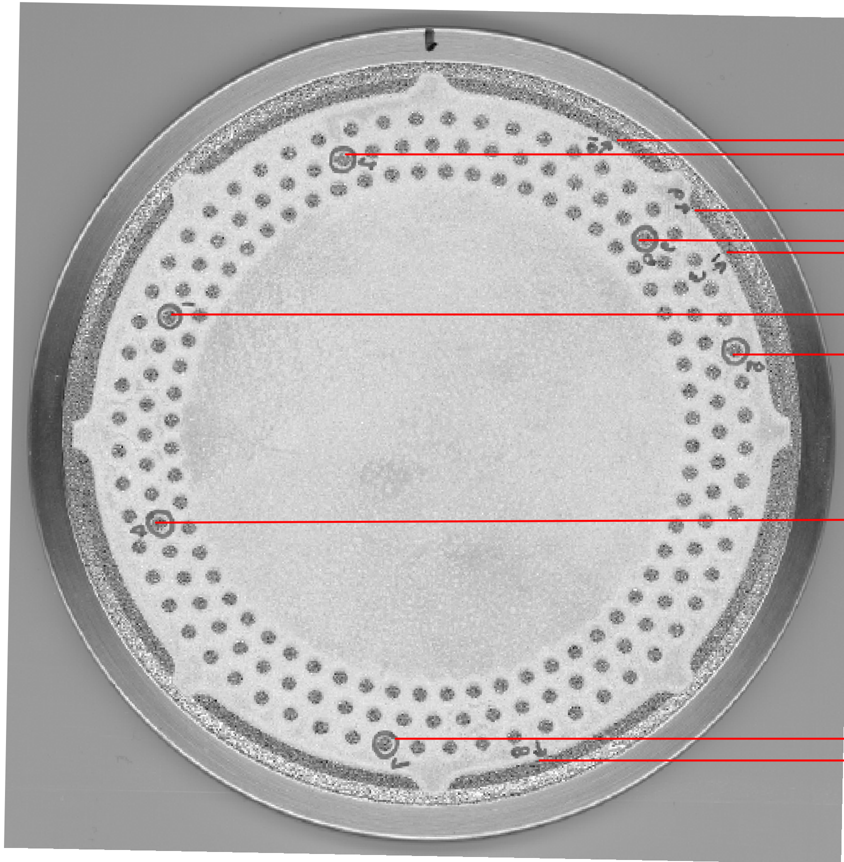

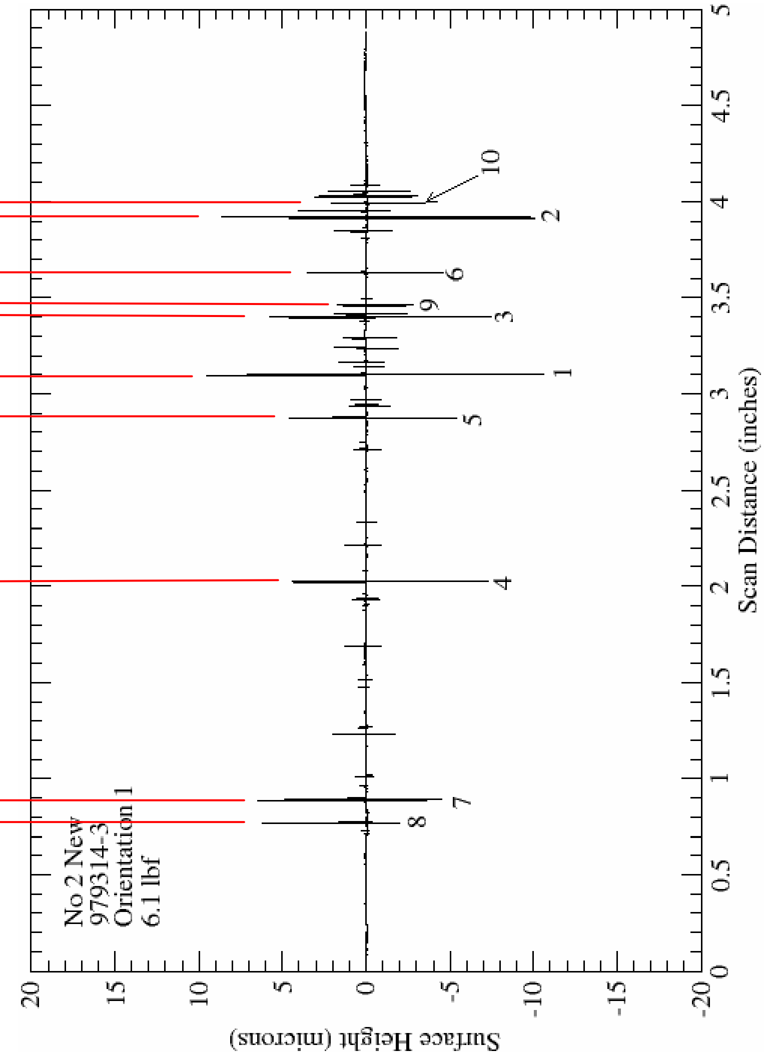

Diamond Wear

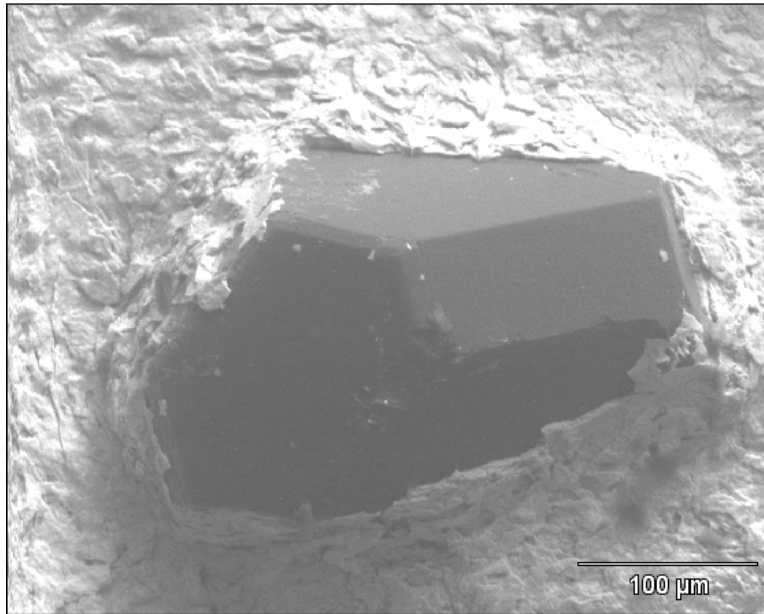

New aggressive diamond

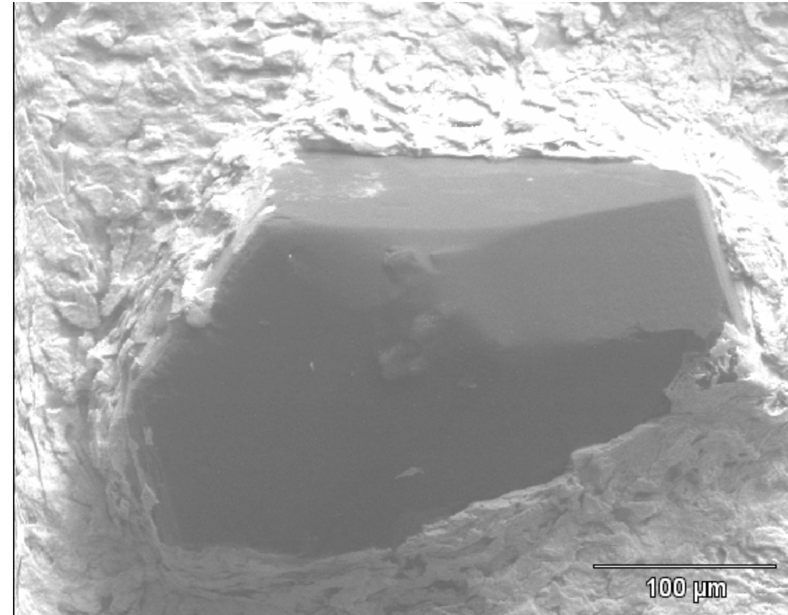

Same diamond after wear test

Normally there is no bulk wear on the diamond and micro wear occurs on the cutting edges of the diamond.

Relevance of Pad Surface Abruptness (λ)

Profilometry analysis: surface roughness (top pad asperities to pad valleys), no consistent correlation with material removal rates.

White light interferometry and incremental loading analysis: surface abruptness (top 20 - 30 μm pad asperities), closely correlated with material removal rates.

Two-step modified Langmuir-Hinshelwood removal rate model:

Removal rate $RR = \frac{M_w}{\rho} \frac{k_2 k_1}{k_2 + k_1}$

Chemical rate constant $k_1 = A \cdot e^{-E/k\bar{T}}$

Mechanical rate constant $k_2 = c_p \mu_k pV$

Wafer surface reaction temperature $\bar{T} = \bar{T}_p + \frac{\beta_1 \kappa_s^{3/4} \lambda^{-1/4} \eta_s^{-1/2}}{V^{1/2+e}} \mu_k pV$

COF $\mu_k = \mu_{pa} + \mu_{visc}^1 \kappa_s^{0.19} \lambda^{-0.17}$

Effect of Conditioning on Pad Surface Abruptness

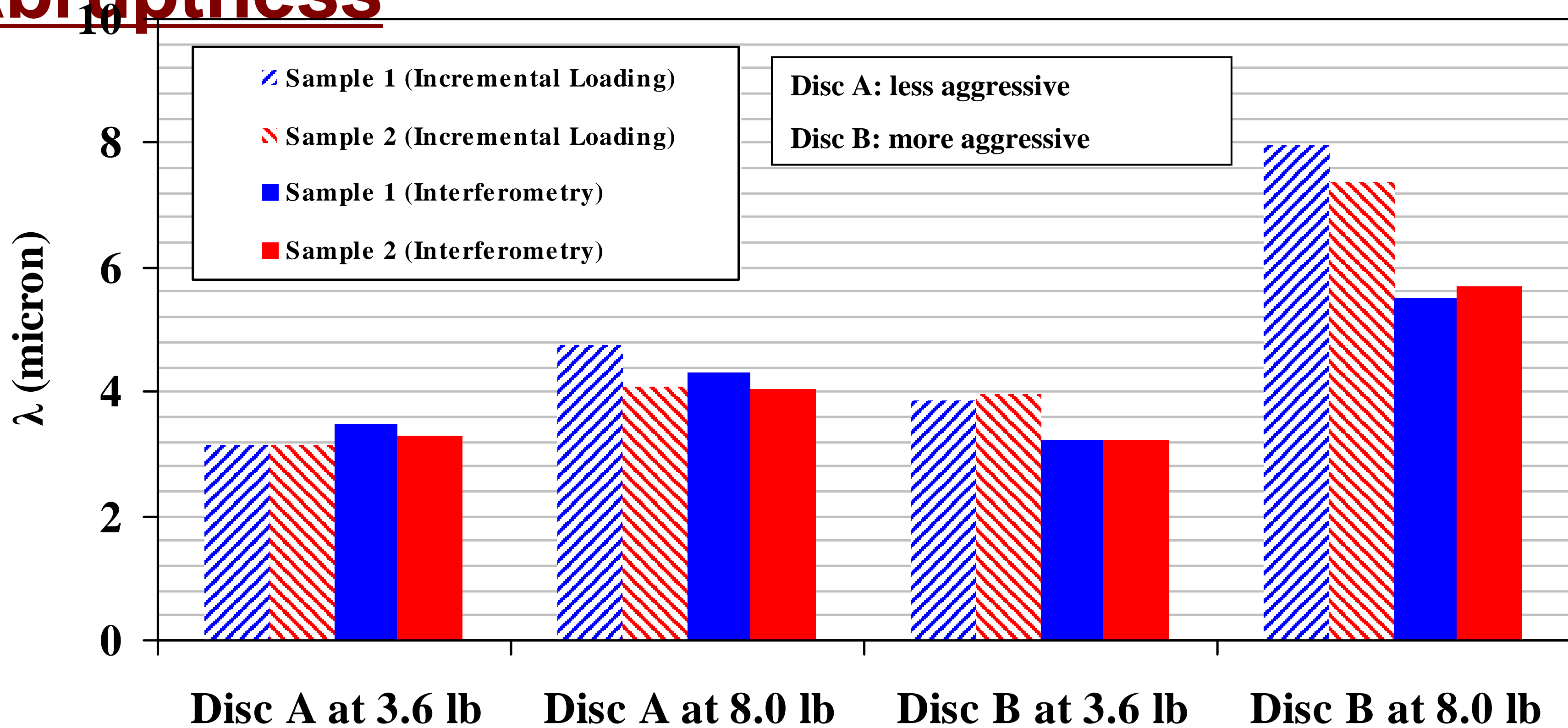

The surface abruptness extracted from the incremental loading analysis and interferometry is consistent. A more aggressive diamond disc generates a more abrupt pad surface under a higher conditioning force.

Effect of Conditioning on COF, Pad Temperature, and Oxide Removal Rate

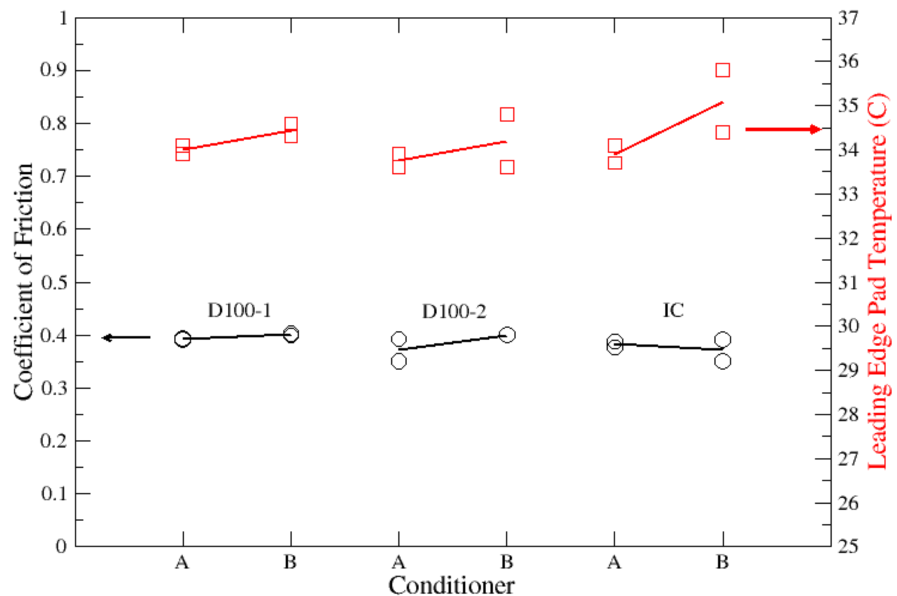

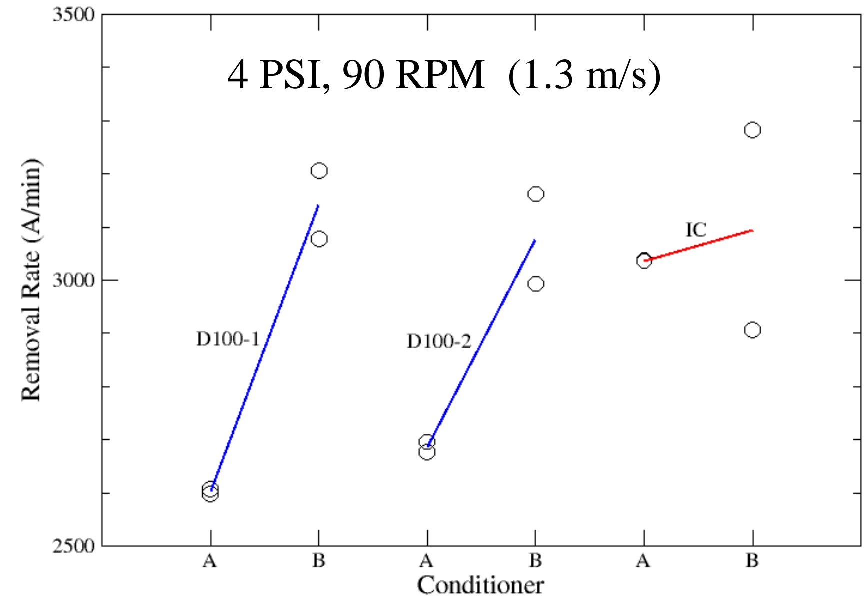

A more aggressive diamond disc generates a higher pad temperature and higher oxide removal rate.

Pad Surface Contact Area Analysis

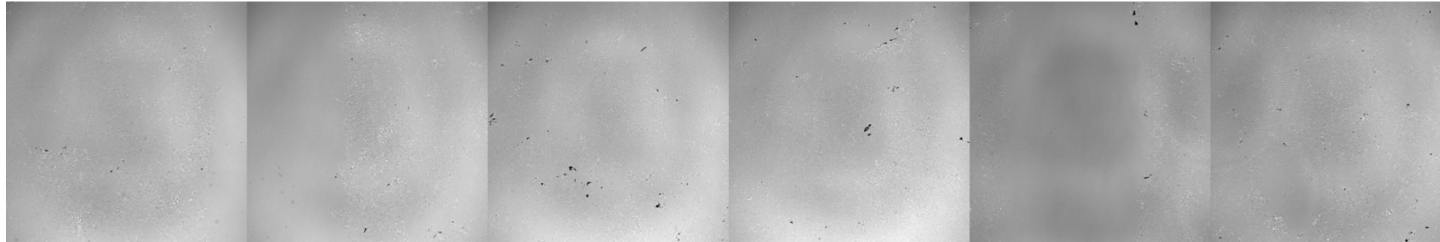

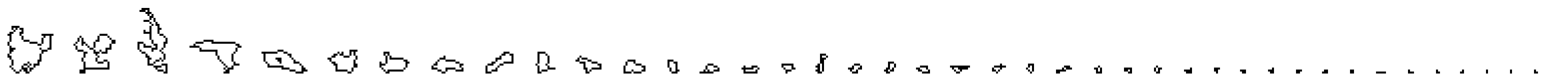

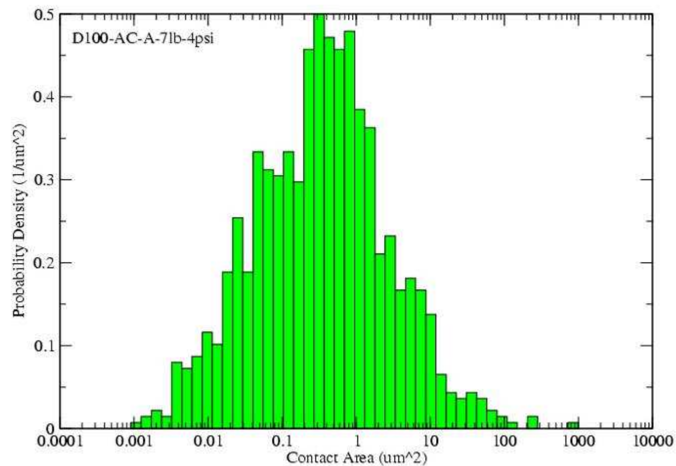

Pad contact area histogram

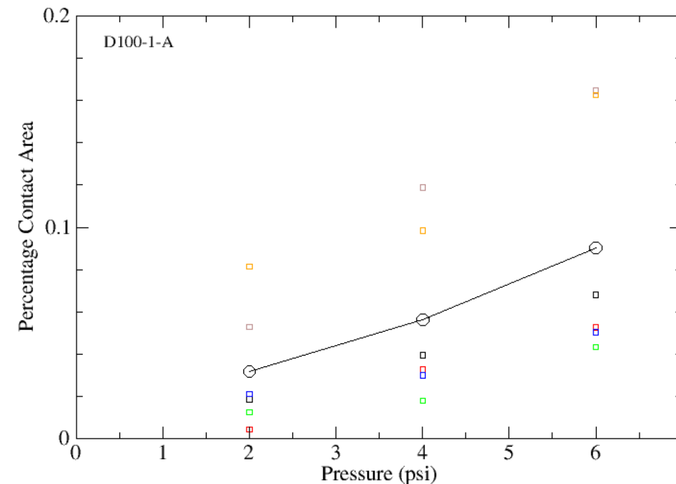

Pad contact area vs. Pressure

Effect of Conditioning on Contact Area

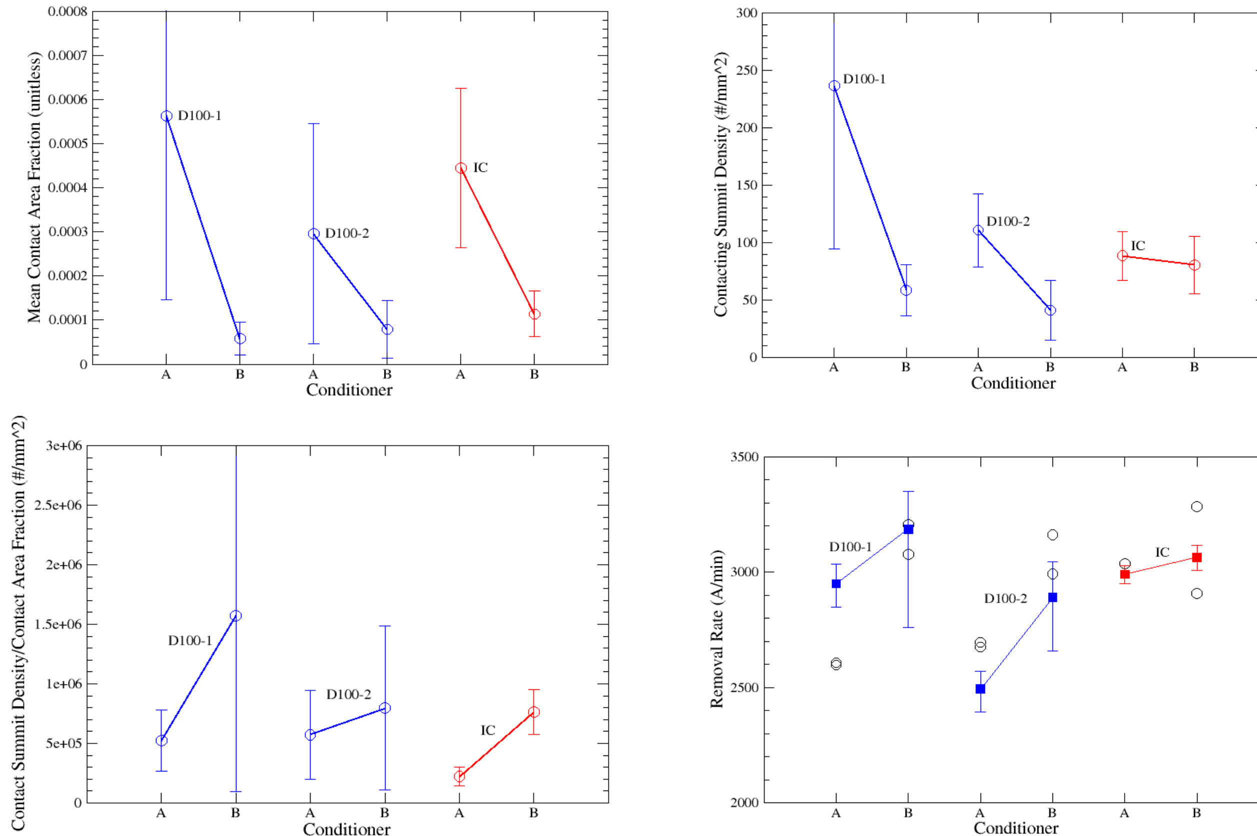

The ratio of the contacting summit density to the contact area fraction is more important than either measured separately since the ratio determines the mean real contact pressure.

Removal rate simulation indicates that the conditioning effect arises from the influence of the mean real contact pressure on the chemical rate of the polishing process.

Effect of Conditioning on Slurry Film Thickness

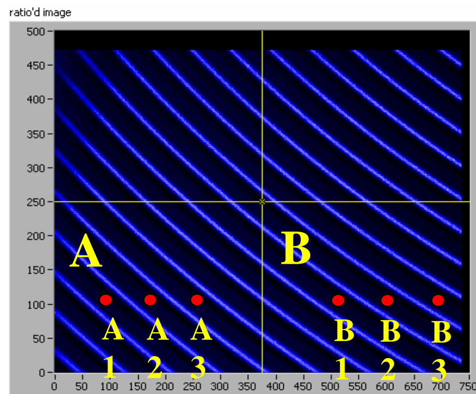

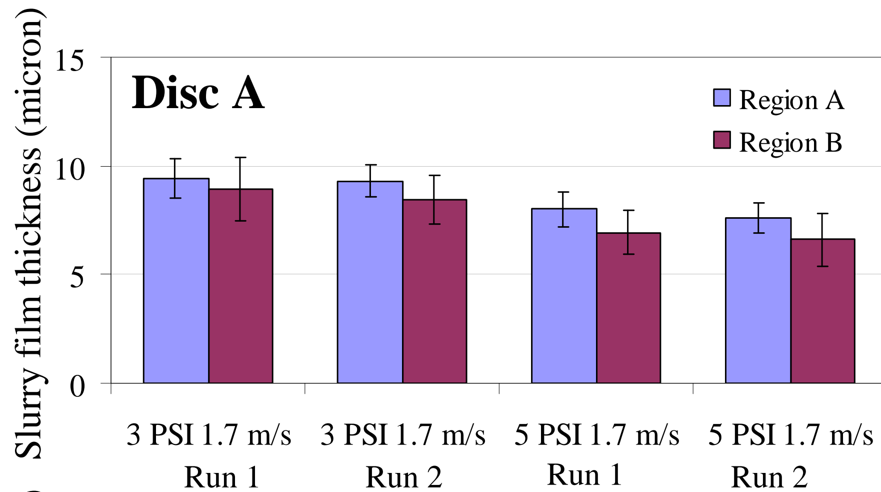

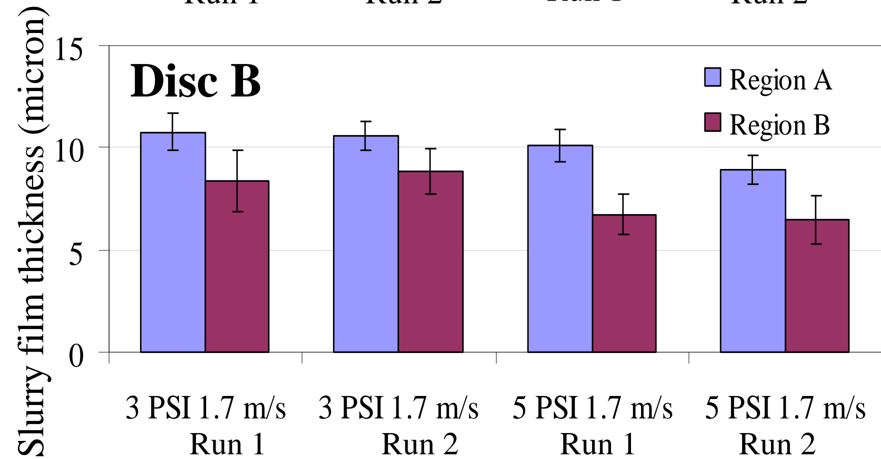

A more aggressive disc generates a more abrupt pad surface, leading to a thicker slurry film in the pad-wafer interface area.

Retaining Ring Material and Design

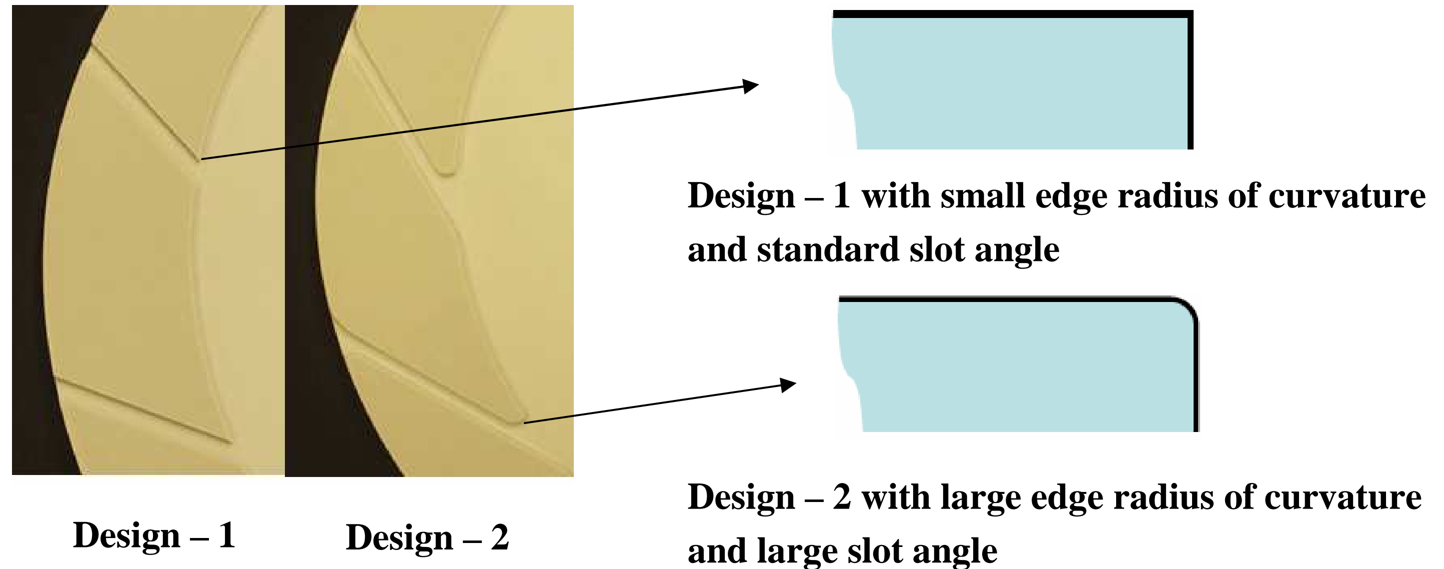

Three retaining rings were investigated:

- **PPS – 1: made of PPS (polyphenylene sulfide) with Design – 1**
- **PEEK – 1: made of PEEK (polyetherenterketone) with Design – 1**
- **PEEK – 2: made of PEEK (polyetherenterketone) with Design – 2**

Retaining Ring Wear Rate

Pre and post interferometry results from the micro-machined trenches indicate the following wear rates:

- **PPS - 1 ring: 28.2 µm/hour**
- **PEEK - 1 ring: 24.0 µm/hour**
- **PEEK - 2 ring: 23.5 µm/hour**

This indicates that the retaining ring material, not design, is the main factor influencing the wear rate.

Micrometry results (taken from areas adjacent to the micro-machined trenches) indicate a difference of ± 13 percent compared to interferometry results.

COF and Pad Temperature

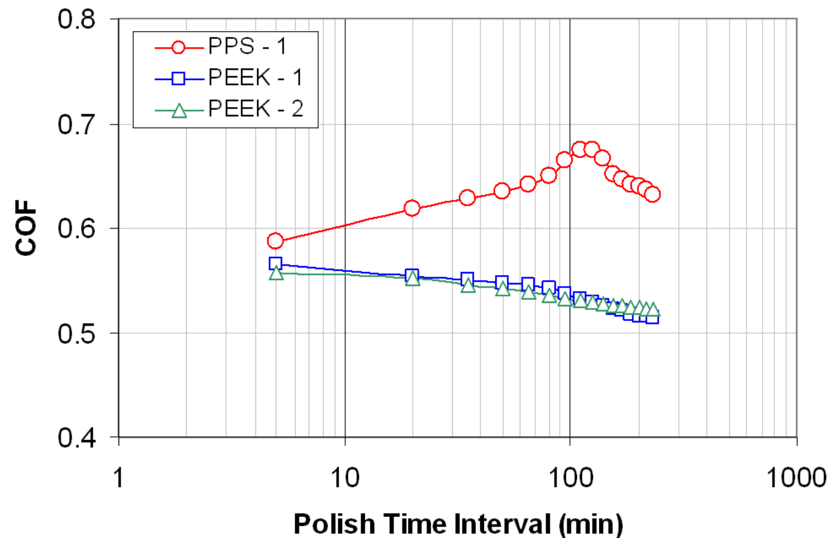

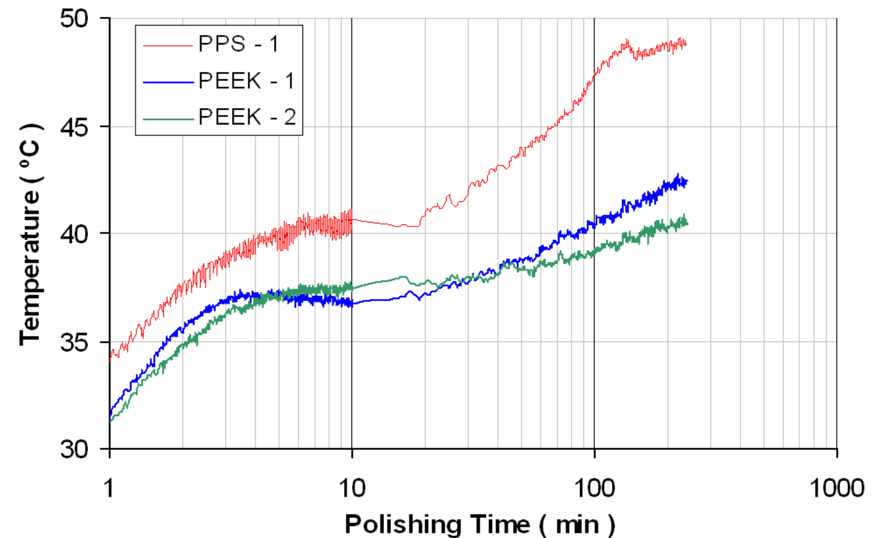

The PEEK rings achieve better lubricity and COF stability than the PPS ring.

Higher temperatures associated with the PPS ring can cause higher material removal rates, thus indicating that thermal effects need to be taken into account when qualifying rings made of new materials.

Pad Surface Interferometry Analysis

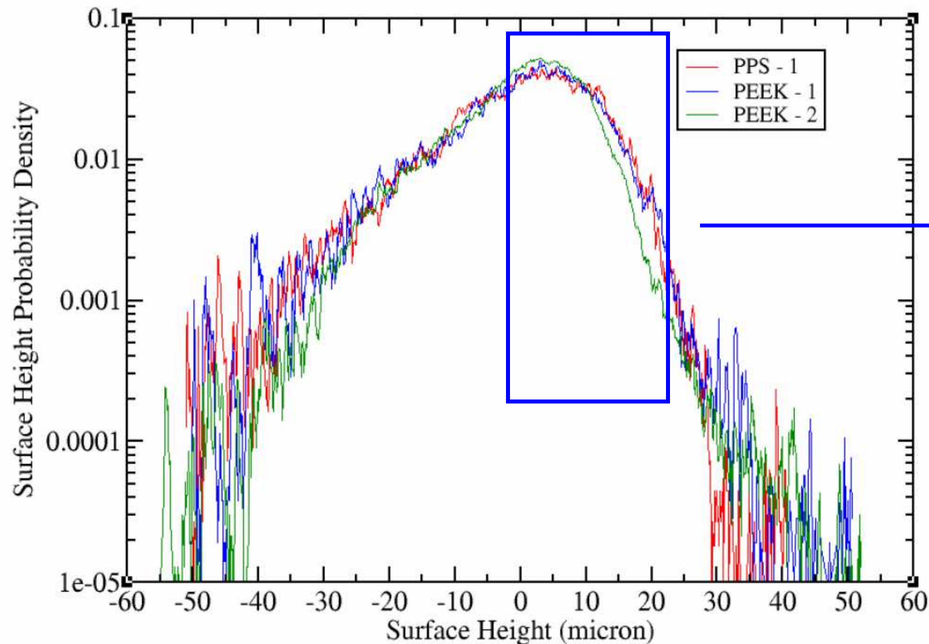

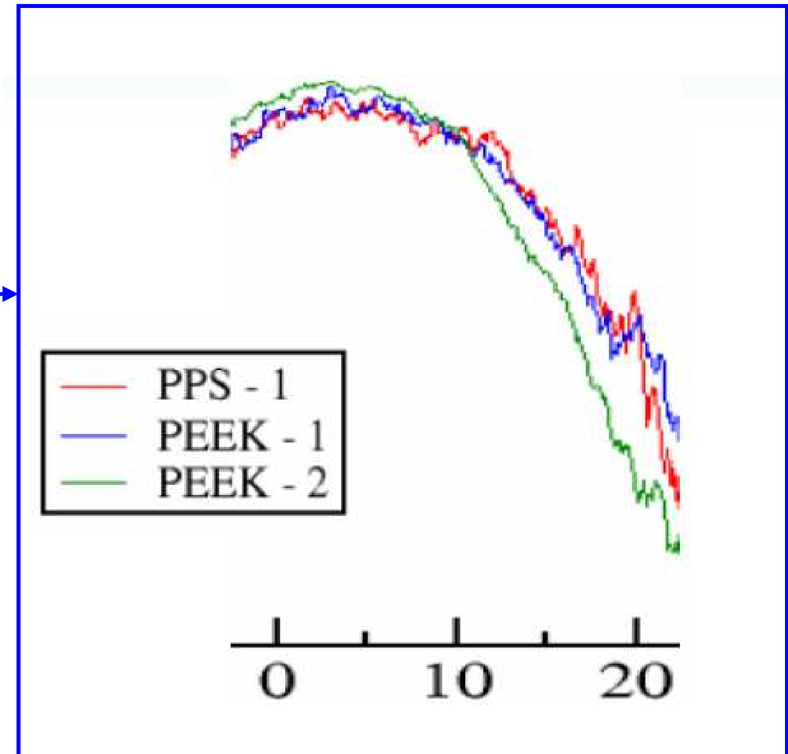

The PEEK – 2 ring achieves a narrower pad surface height distribution than the PPS – 1 and PEEK – 1 rings, suggesting that the slot design and the edge rounding plays significant roles in shaping the pad micro texture.

Slurry Mean Residence Time

PEEK - 1

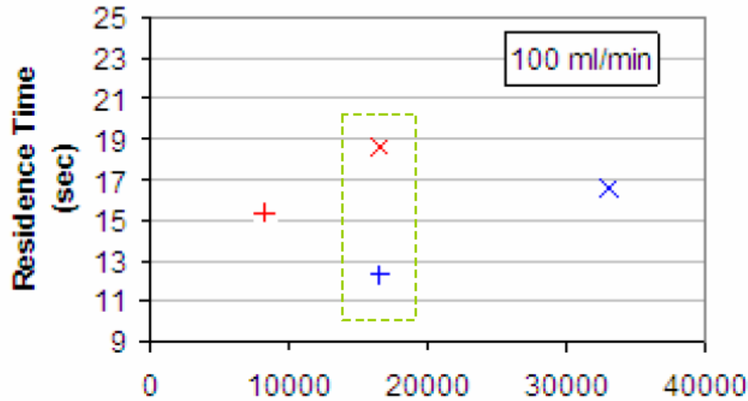

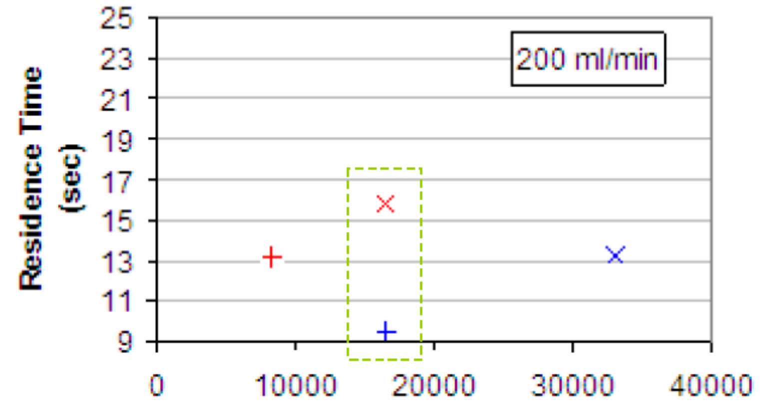

PEEK - 2

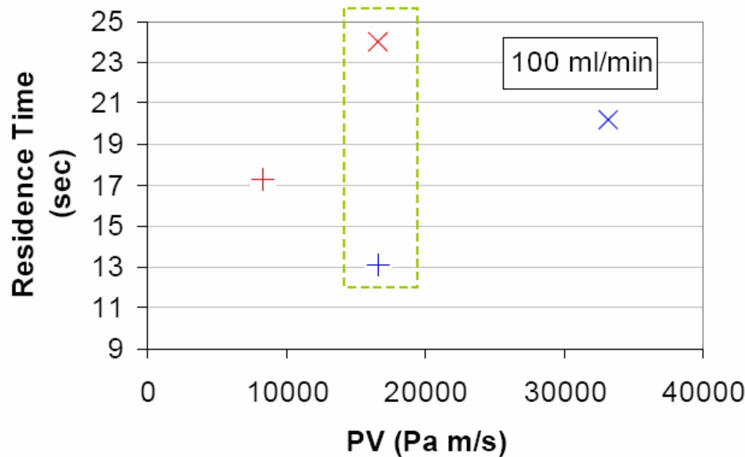

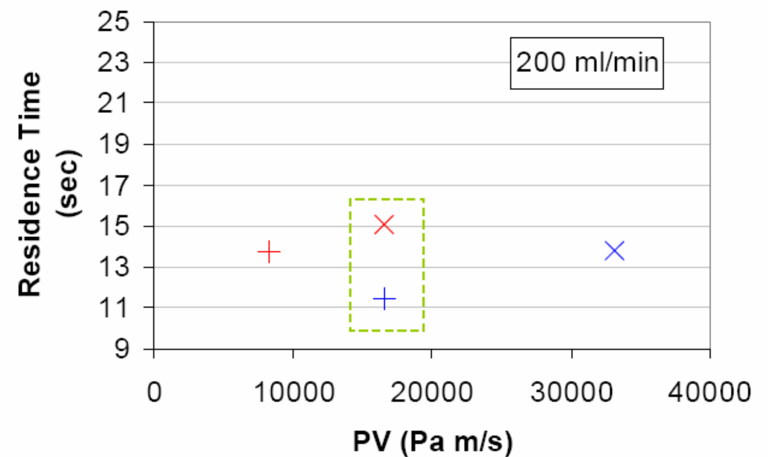

Design – 1 is 10 – 20 percent more efficient in getting slurry in and out the wafer-pad interface.

Industrial Interactions and Technology Transfer

Industrial Mentors / Contacts:

- **Sriram Anjur (Cabot Microelectronics Corporation)**
- **Abaneshwar Prasad (Cabot Microelectronics Corporation)**
- **Ananth Naman (Cabot Microelectronics Corporation)**
- **Cliff Spiro (Cabot Microelectronics Corporation)**
- **Naoki Rikita (Mitsubishi Materials Corporation)**
- **Christopher Wargo (Entegris, Inc.)**
- **Leonard Borucki (Araca, Inc.)**

Future Plans

Next Year Plans

- Perform static etch tests and wear tests on diamond discs and quantify the extent of diamond micro-wear and diamond disc substrate wear.
- Investigate the effect of conditioning on pad topography for metal CMP processes.
- Perform DEUVEF (dual emission UV enhanced fluorescence) tests to investigate the effect of retaining ring design on slurry film thickness in the pad-wafer interface.

Long-Term Plans

- Obtain fundamental understanding of diamond and diamond disc substrate wear mechanism and extend diamond disc life.
- Achieve fundamental understanding of the effect of conditioning on pad topography and polishing performance for CMP processes.
- Improve retaining ring design to achieve better slurry utilization efficiency and extend retaining ring life .

Publications

- **Diamond Conditioner Wear Characterization for a Copper CMP Process. L. Borucki, Y. Zhuang, A. Philipossian, R. Kikuma, R. Rikita, T. Yamashita, K. Nagasawa, H. Lee, T. Sun, D. Rosales-Yeomans and T. Stout. Transactions on Electrical and Electronic Materials, 8(1), 15-20 (2007).**

- **Investigation of Diamond Effect on Pad Topography, Friction Force and Removal Rate during ILD CMP Process. Y. Zhuang, L. Borucki, N. Rikita, F. Sudargho, Y. Sampurno, X. Wei, G. Steward and A. Philipossian. 12th International Conference on Chemical-Mechanical Polish (CMP) Planarization for ULSI Multilevel Interconnection Proceedings, 277-282 (2007).**

- **CMP Active Diamond Characterization and Conditioner Wear. L. Borucki, R. Zhuang, Y. Zhuang, A. Philipossian and N. Rikita. Materials Research Society Symposium Proceedings, Vol. 991, C01-01 (2007).**

- **Investigation of Diamond Grit Size and Conditioning Force Effect on CMP Pads Topography. T. Sun, L. Borucki, Y. Zhuang and A. Philipossian. Materials Research Society Symposium Proceedings, Vol. 991, C01-07 (2007).**

- **Tribological, Kinetic, Thermal and Flow Characteristics of PPS and PEEK Retaining Rings. A. Philipossian, X. Wei, Y. Sampurno, F. Sudargho, Y. Zhuang, C. Wargo and L. Borucki. International Conference on Planarization/CMP Technology Proceedings, 31-35 (2007).**

Presentations

- Investigation of Diamond Effect on Pad Topography, Friction Force and Removal Rate during ILD CMP Process. Y. Zhuang, L. Borucki, N. Rikita, F. Sudargho, Y. Sampurno, X. Wei, G. Steward and A. Philipossian. 12th International Conference on Chemical-Mechanical Polish (CMP) Planarization for ULSI Multilevel Interconnection, Fremont, California, March 5-8 (2007).

- CMP Active Diamond Characterization and Conditioner Wear. L. Borucki, R. Zhuang, Y. Zhuang, A. Philipossian and N. Rikita. 2007 Materials Research Society Spring Meeting, San Francisco, California, April 9-13 (2007).

- The Effect of Conditioning on Pad Topography and Shear-Induced Flow Resistance during CMP. T. Sun, L. Borucki, R. Zhuang, Y. Zhuang and A. Philipossian. 2007 Materials Research Society Spring Meeting, San Francisco, California, April 9-13 (2007).

- On the Relationship between Contact Area Data and Polishing. L. Borucki, T. Sun, Y. Sampurno, F. Sudargho, X. Wei, Y. Zhuang, S. Anjur and A. Philipossian. 12th International Symposium on Chemical-Mechanical Planarization, Lake Placid, New York, August 12-15 (2007).

- Tribological, Kinetic, Thermal and Flow Characteristics of PPS and PEEK Retaining Rings. A. Philipossian, X. Wei, Y. Sampurno, F. Sudargho, Y. Zhuang, C. Wargo and L. Borucki. International Conference on Planarization/CMP Technology, Dresen, Germany, October 25-27 (2007).

An Integrated, Multi-Scale Framework for Designing Environmentally Benign Copper, Tantalum and Ruthenium Planarization Processes

(*Task Number: 425.020*)

Subtask 2: Real-Time Detection and Modeling of Pattern Evolution

PIs:

- Ara Philipossian, Chemical and Environmental Engineering, UA
- Duane Boning, Electrical Engineering and Computer Science, MIT
- Chris B. Rogers, Mechanical Engineering, Tufts University
- Vincent P. Manno, Mechanical Engineering, Tufts University
- Robert D. White, Mechanical Engineering, Tufts University

Graduate Students:

- Yasa Sampurno, Ph. D. candidate, Chemical and Environmental Engineering, UA
- Caprice Gray: Ph. D. candidate, Mechanical Engineering, Tufts University
- James Vlahakis: Ph. D. candidate, Mechanical Engineering, Tufts University

An Integrated, Multi-Scale Framework for Designing Environmentally Benign Copper, Tantalum and Ruthenium Planarization Processes

(*Task Number: 425.020*)

Subtask 2: Real-Time Detection and Modeling of Pattern Evolution

Graduate Students (continue):

- **Douglas Gauthier: M.S. candidate, Mechanical Engineering, Tufts University**
- **Nicole Braun: M.S. candidate, Mechanical Engineering, Tufts University**
- **Andrew Mueller: Mechanical Engineering, Tufts University, graduated with M.S. degree in August 2007**
- **Hong Cai, Materials Science, MIT, graduated with Ph. D. degree in June 2007**
- **Xiaolin Xie, Physics, MIT, graduated with Ph. D. degree in June 2007**
- **Wei Fan, Ph. D. candidate, Electrical Engineering and Computer Science, MIT**

Undergraduate Student:

- **Zhipeng Li, Electrical Engineering and Computer Science, MIT**

An Integrated, Multi-Scale Framework for Designing Environmentally Benign Copper, Tantalum and Ruthenium Planarization Processes

(*Task Number: 425.020*)

Subtask 2: Real-Time Detection and Modeling of Pattern Evolution

Other Researchers:

- **Yun Zhuang, Research Associate, Chemical and Environmental Engineering, UA**
- **Fransisca Sudargho, Research Technician, Chemical and Environmental Engineering, UA**
- **Siannie Theng, Research Technician, Chemical and Mechanical Engineering, UA**
- **Ed Paul, Visiting Professor, Stockton College**

An Integrated, Multi-Scale Framework for Designing Environmentally Benign Copper, Tantalum and Ruthenium Planarization Processes

(*Task Number: 425.020*)

Subtask 2: Real-Time Detection and Modeling of Pattern Evolution

Cost Share (other than core ERC funding):

- $50,000 from Intel Corporation
- $50,000 from Cabot Microelectronics Corporation
- In-kind donation (slurries) from Hitachi Chemical Co., Ltd.
- In-kind donation (pads) from Neopad Technologies Corporation
- In-kind support from JSR Micro, Inc.
- In-kind support from Araca, Inc.

Objectives

- Determine whether shear force and down force spectral analysis can generate unique spectral fingerprints before, during, and after transition from oxide to Si_3N_4 layer during STI patterned wafer polishing.
- Explore shear force spectral fingerprints to understand the effect of break-in time and in-situ pad conditioning duty cycle during copper CMP.
- Use Dual Emission Laser Induced Fluorescence (DELIF) to obtain in-situ images of the slurry layer thickness during CMP and quantify wafer-pad contact during polishing.
- Investigate the feasibility of using particle image velocimetry (PIV) to quantitatively measure particle-slurry flow in-situ.
- Use custom micro-machined sensors to measure local (100-micron scale), high sample rate (0.1 ms) asperity scale forces at the pad-wafer interface during CMP.
- Investigate chip- and feature-scale performance of CMP processes by connecting with physical investigations, metrology, and wafer level for control.
- Understand how pad bulk and surface properties relate to the planarization capability of CMP processes
- Optimize pad properties to achieve processes with reduced time, consumables, and waste, as well as reduced dishing, erosion, and within die non-uniformity.

ESH Metrics and Impact

1. *Reduce slurry consumption by 25%*
2. *Reduce pad consumption by 25%*
3. *Reduce diamond disc consumption by 25%*
4. *Improve yield (multiplication over all inputs/outputs) by 1-2%*

APD – 500 Polisher & Tribometer

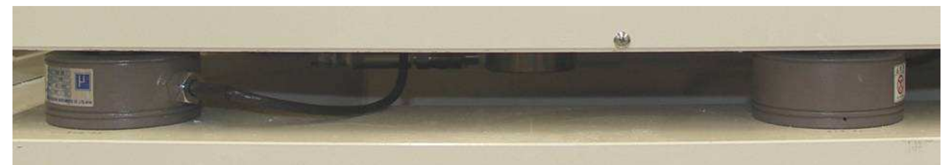

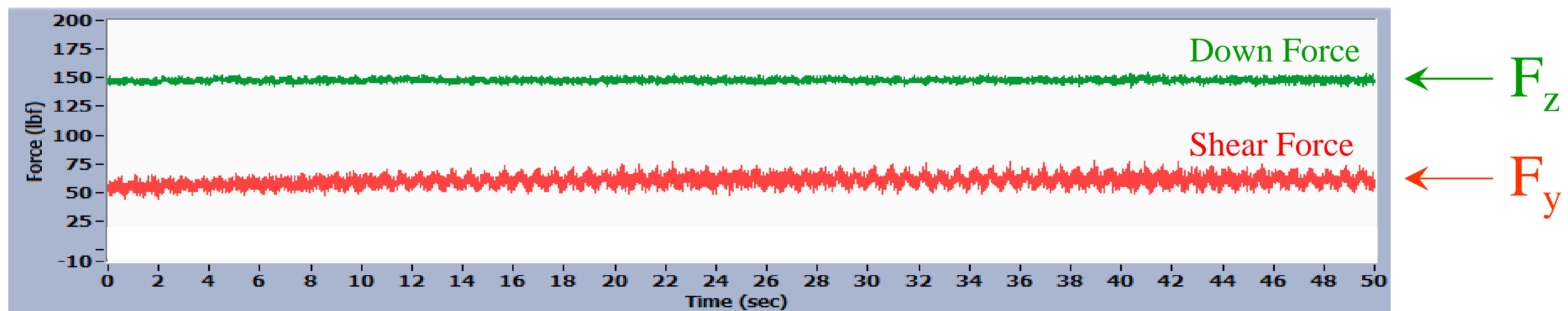

← F_z

← F_y

SRC/SEMATECH Engineering Research Center for Environmentally Benign Semiconductor Manufacturing

Shear Force and Down Force Measurement

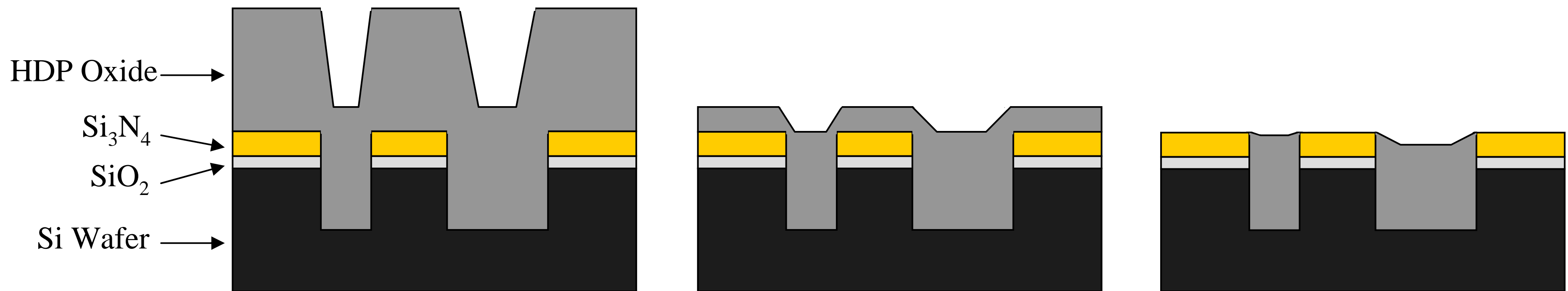

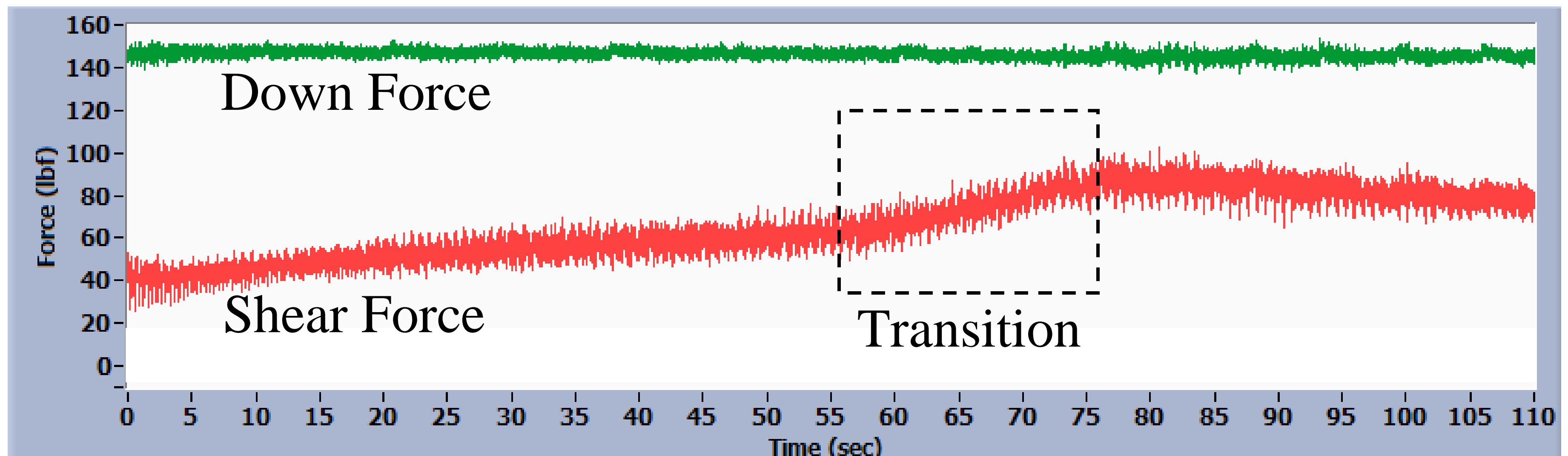

COF Transients

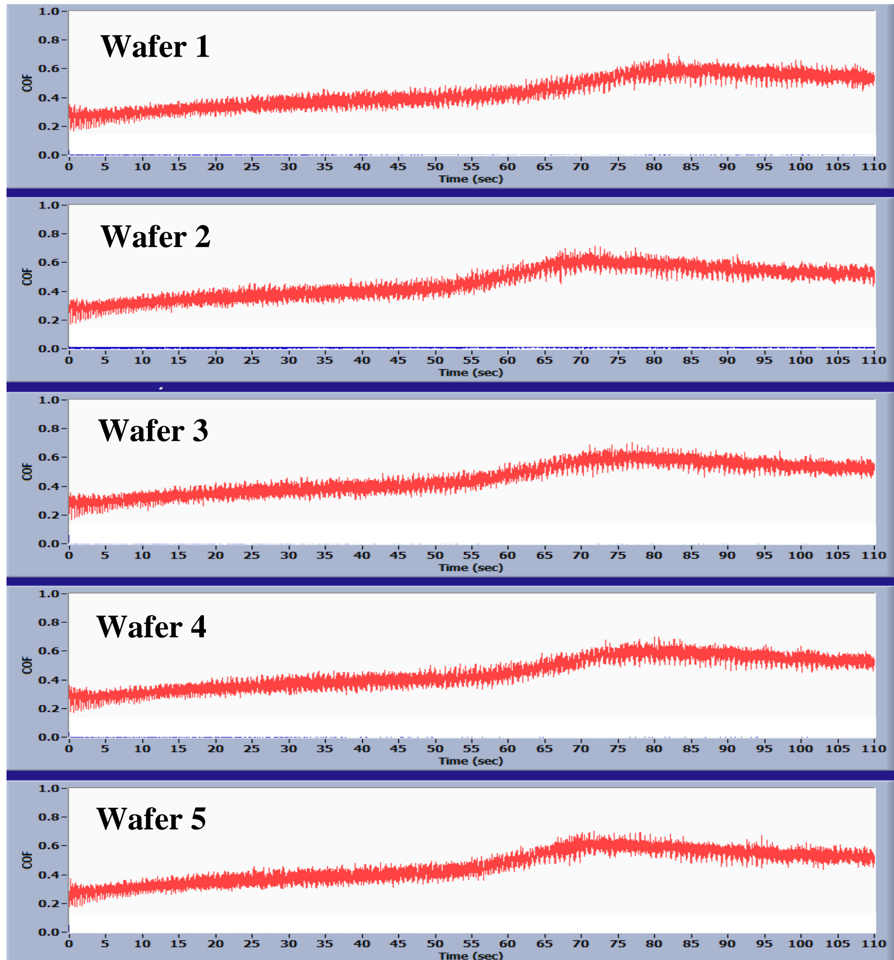

Polish Time

	Transition Start (s)	Transition End (s)
Average	56.4	71.4
SD	3.4	4.5
RSD	6.1%	6.3%

Coefficient of Friction

	Before Transition	During Transition	After Transition
Average	0.361	0.510	0.566
SD	0.004	0.006	0.008
RSD	0.1%	0.3%	0.5%

The COF shows consistent transition during STI patterned wafer polishing.

Force Transients

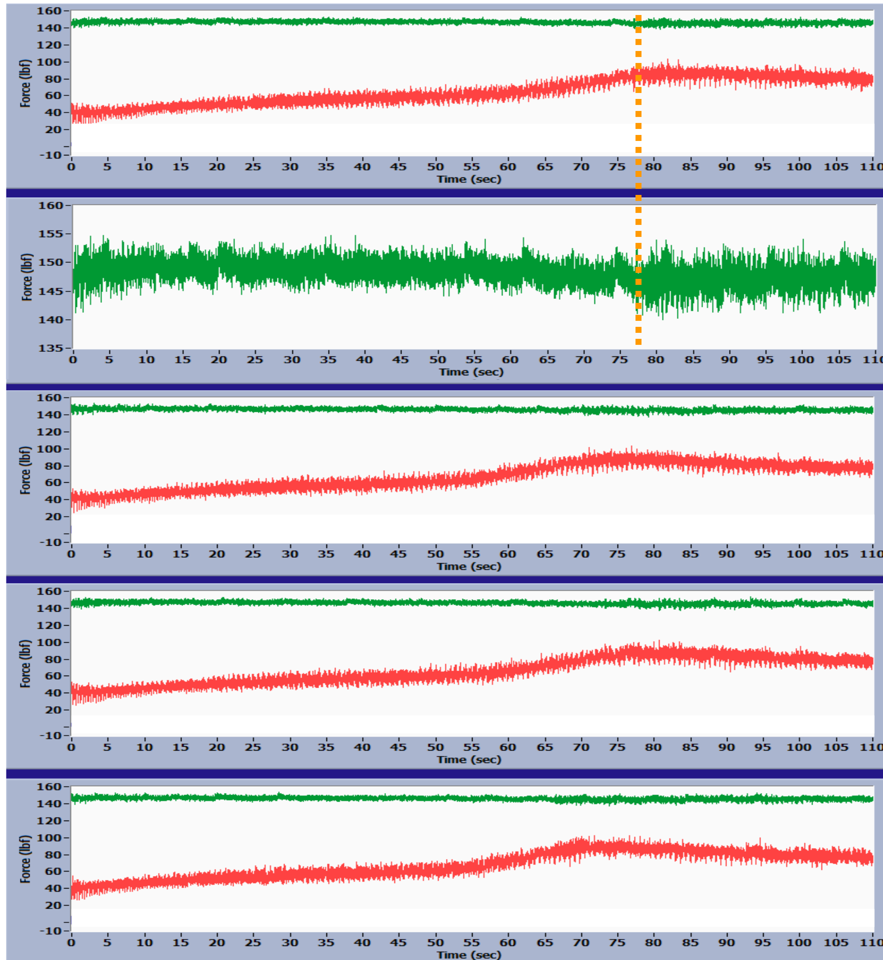

Polish Time

	Transition Start (s)	Transition End (s)
Average	56.4	71.4
SD	3.4	4.5
RSD	6.1%	6.3%

Variance of Shear Force (σ^2)

	Before Transition (lb_f^2)	During Transition (lb_f^2)	After Transition (lb_f^2)
Average	58.7	57.8	33.6
SD	2.8	7.7	9.2
RSD	4.7%	13.3%	27.4%

Variance of Down Force (σ^2)

	Before Transition (lb_f^2)	During Transition (lb_f^2)	After Transition (lb_f^2)
Average	2.3	2.2	3.4
SD	0.03	0.22	0.19
RSD	1.3%	10%	5.5%

The variances of shear force and down force show consistent transition during STI patterned wafer polishing.

Shear Force Spectral Analysis

Wafer #1

Raw Shear Force Data **Shear Force Spectral Analysis**

Before Transition

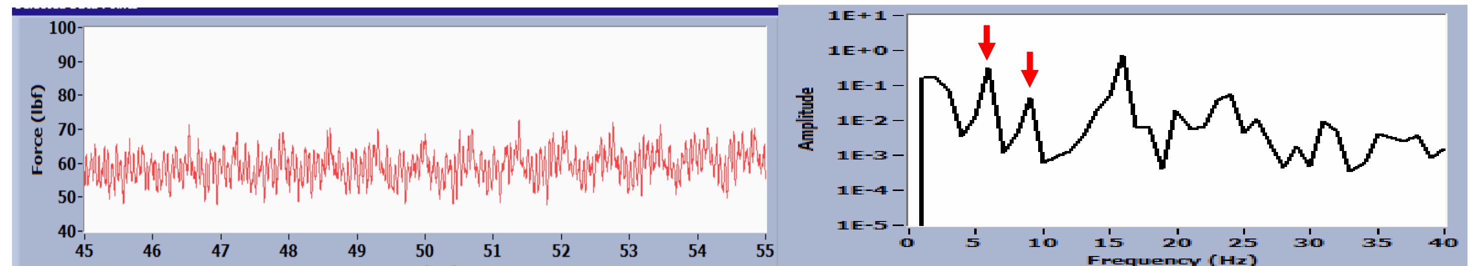

During Transition

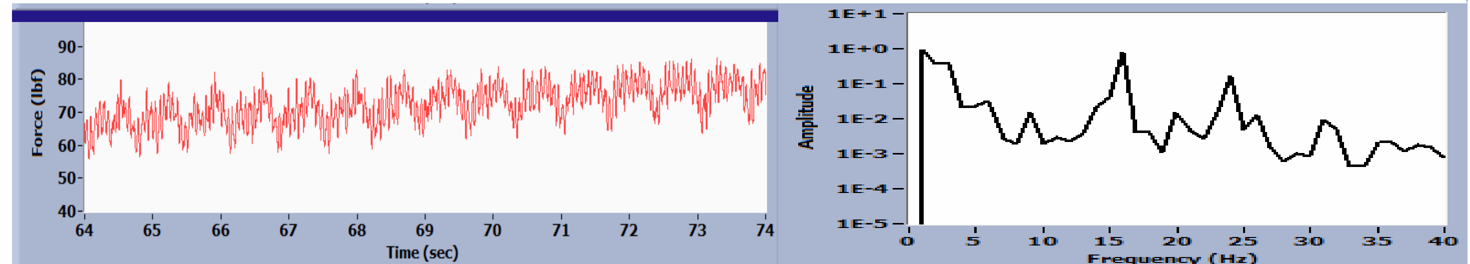

After Transition

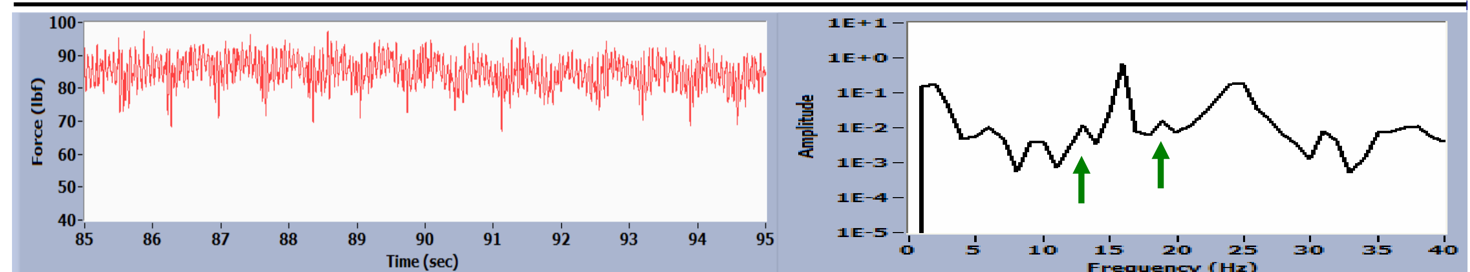

Shear Force Spectral Analysis

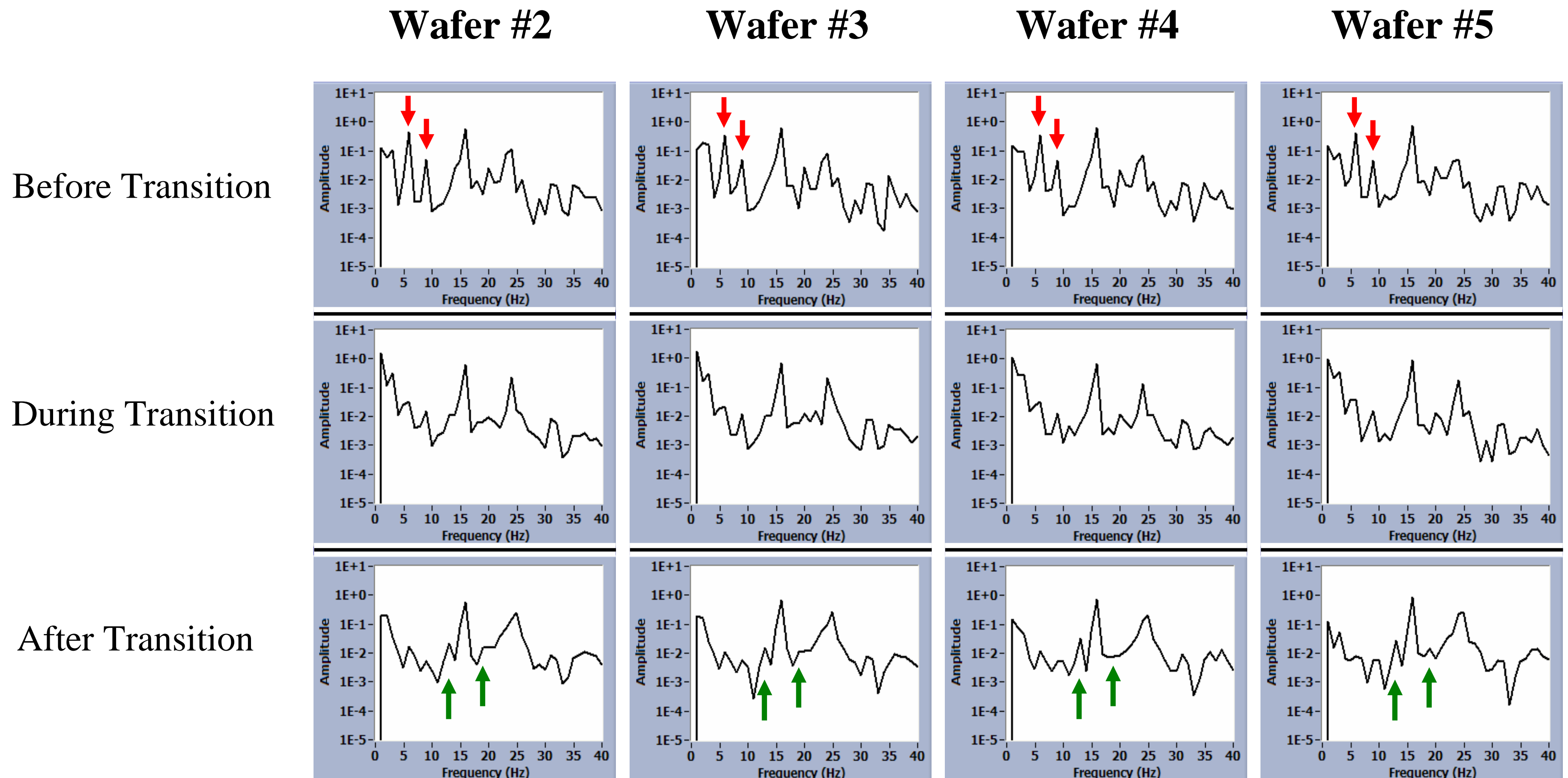

The shear force spectral analysis shows consistent spectral transition during STI patterned wafer polishing.

Down Force Spectral Analysis

Wafer #1

Raw Down Force Data | **Down Force Spectral Analysis**

Before Transition

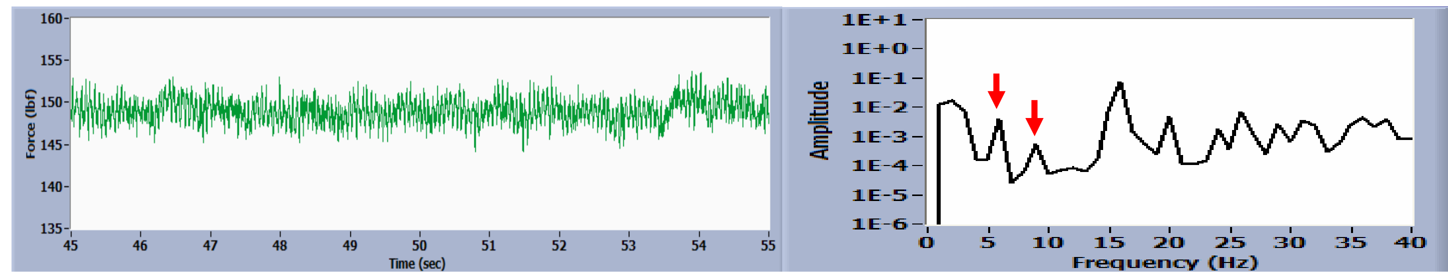

During Transition

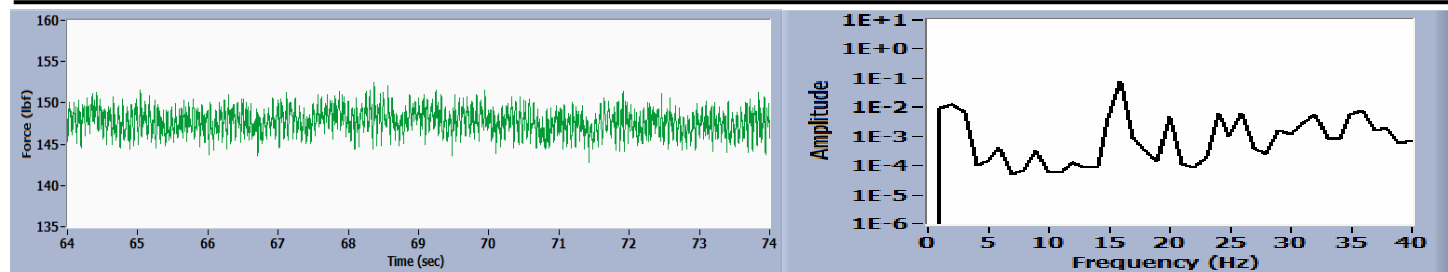

After Transition

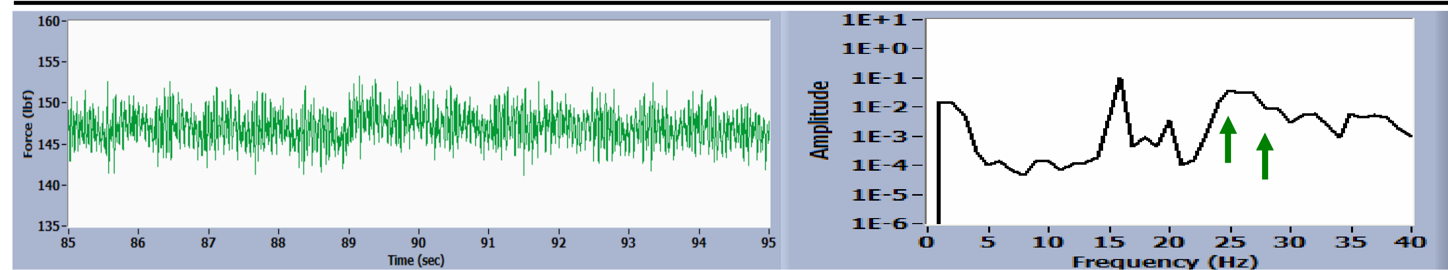

Down Force Spectral Analysis

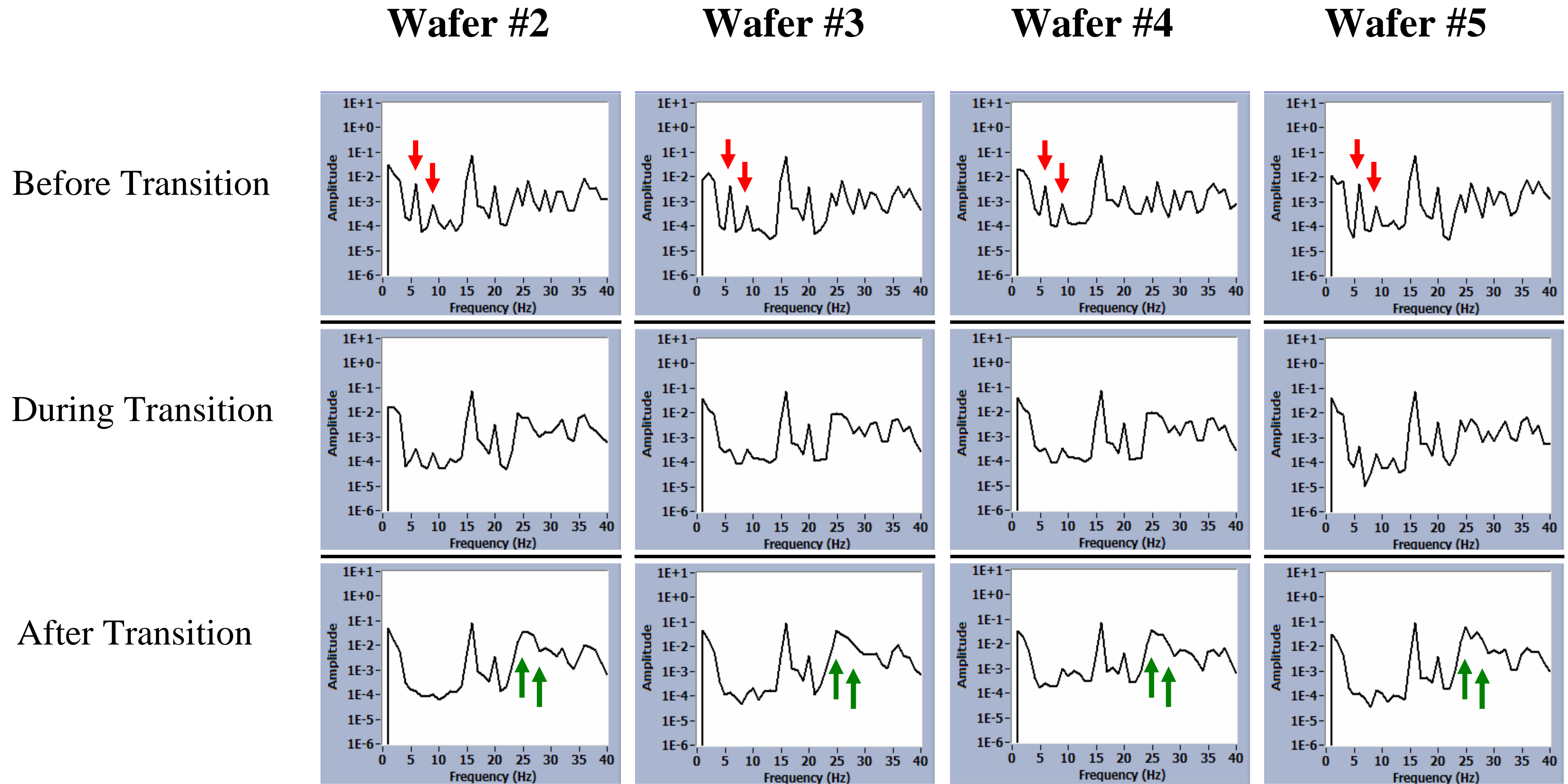

The down force spectral analysis shows consistent spectral transition during STI patterned wafer polishing.

Pad Break-In Time Study

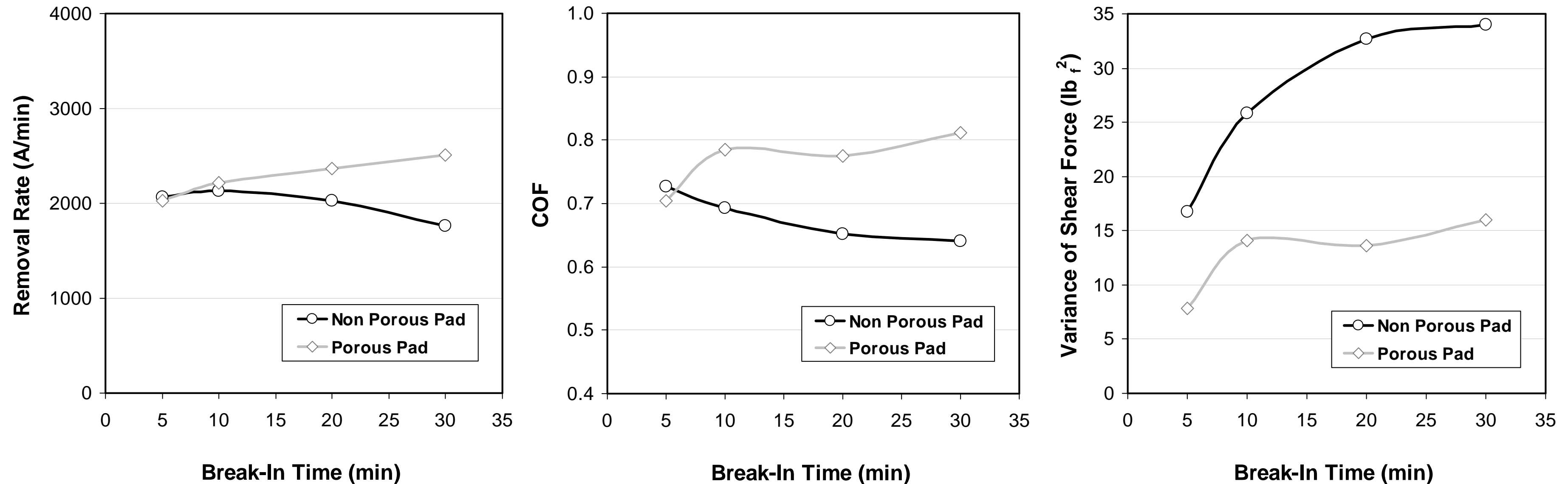

Pad break-in time has opposite effects on removal rate and COF for porous and non-porous pads.

The variance of shear force initially increases with the pad break-in time and then reaches a plateau for both porous and non-porous pads.

Spectral Analysis

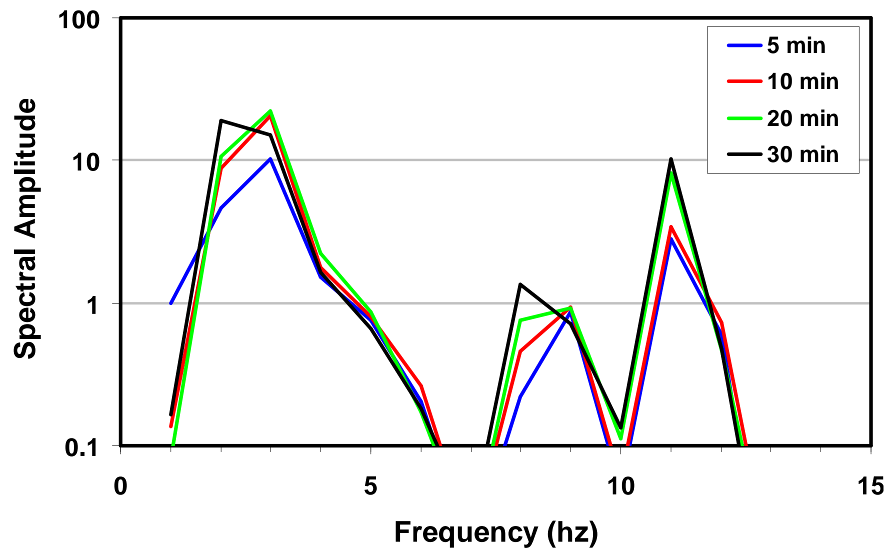

Non-porous pad

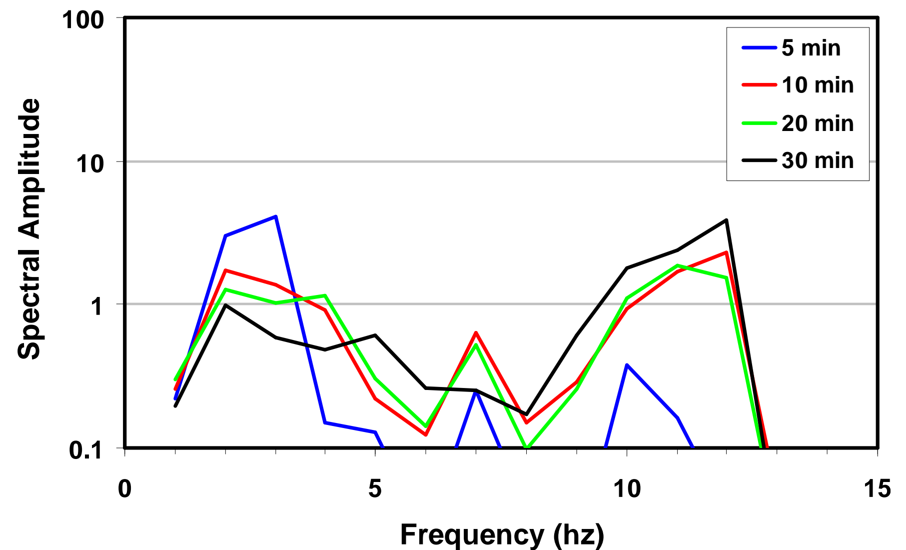

Porous pad

The non-porous pad shows consistent spectra under different pad break-in time.

In-Situ Conditioning Duty Cycle Study

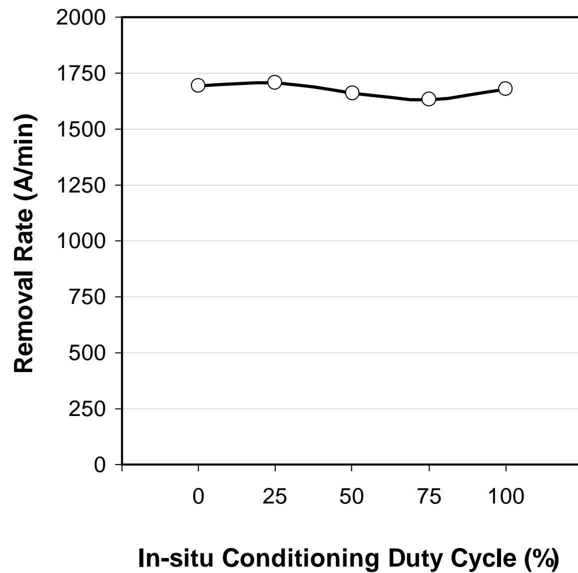

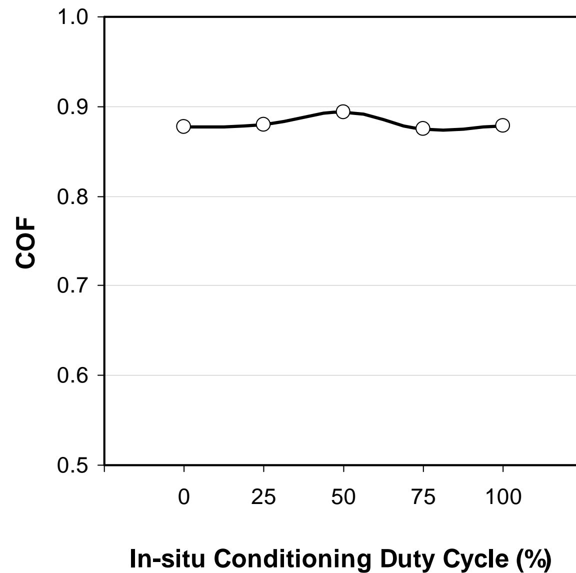

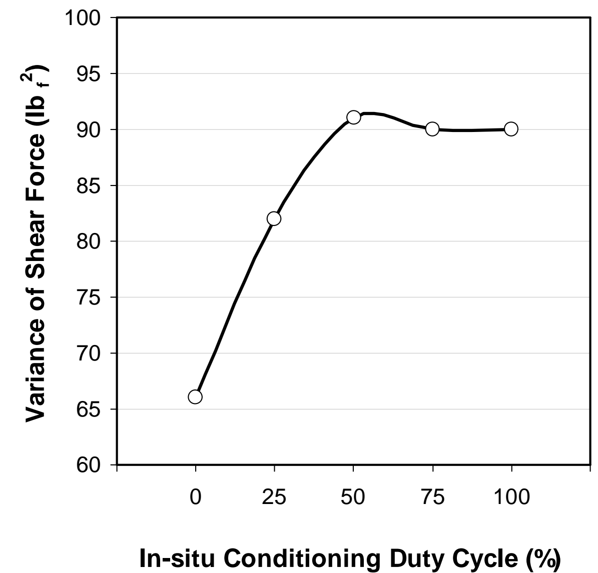

Removal rate and COF are not affected by the conditioning duty cycle.

The variance of shear force initially increases with the conditioning duty cycle and then reaches a plateau.

Shear Force Spectral Analysis

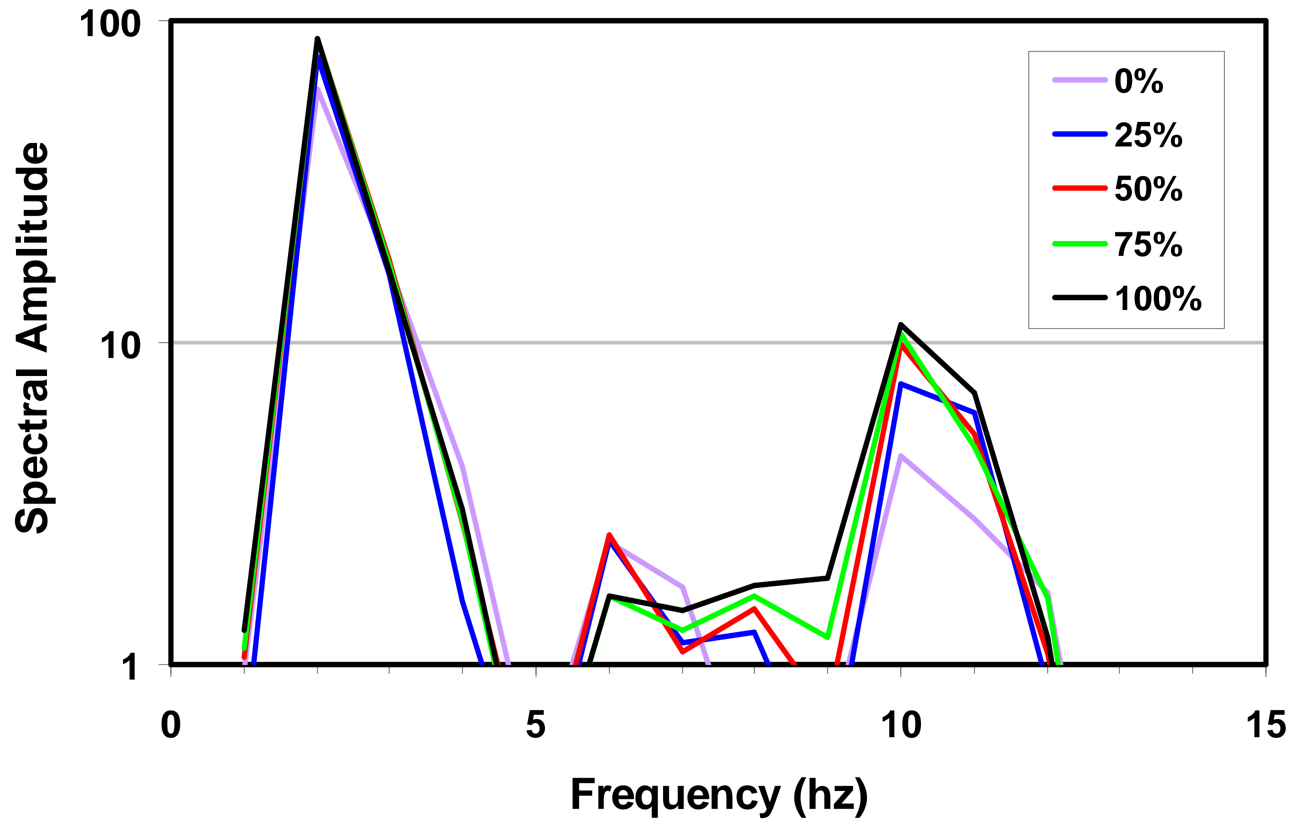

High duty cycles result in similar spectral amplitude distributions.

Mean Furrow Density Under Wafer

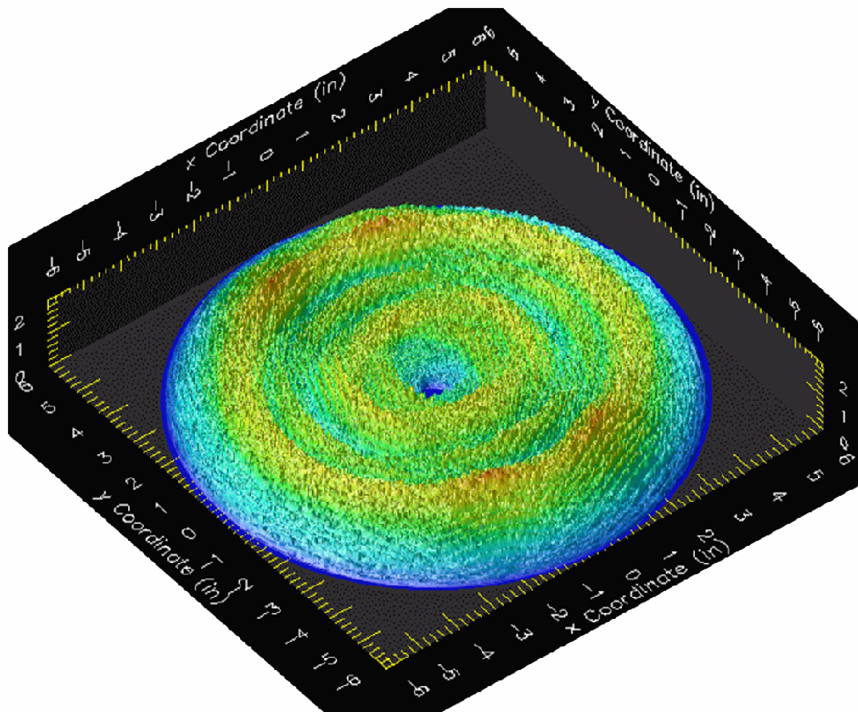

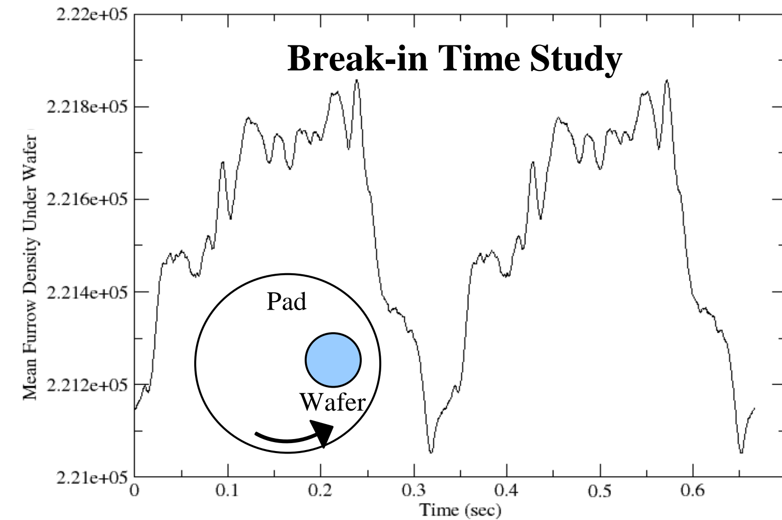

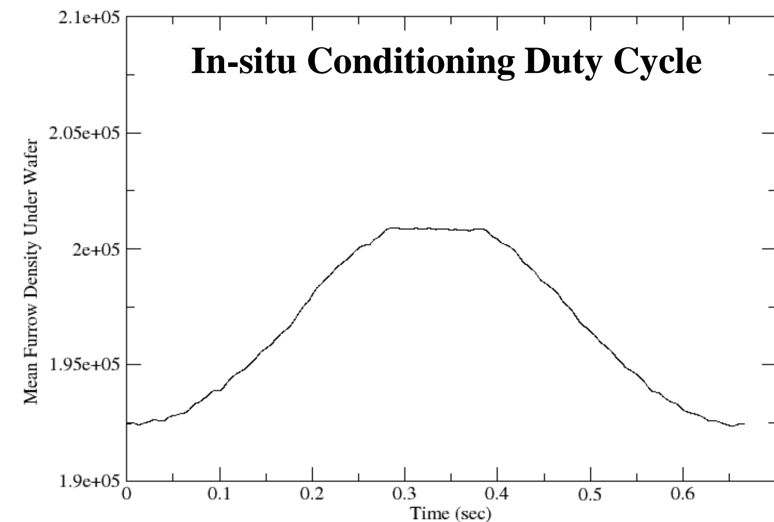

Monte Carlo simulation of pad topography with the microscopic furrows generated by the pad conditioner.

Spectral Analysis of Furrow Density Under Wafer

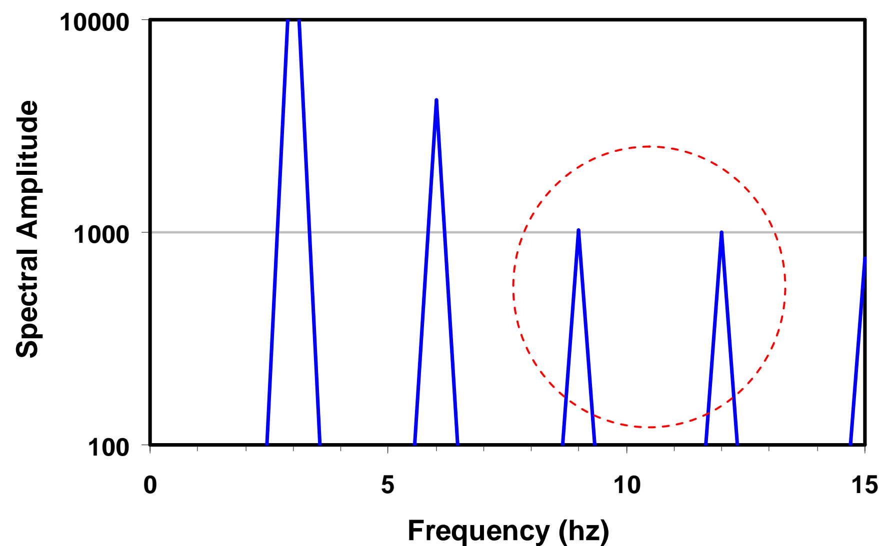

Pad Break-in Time Study

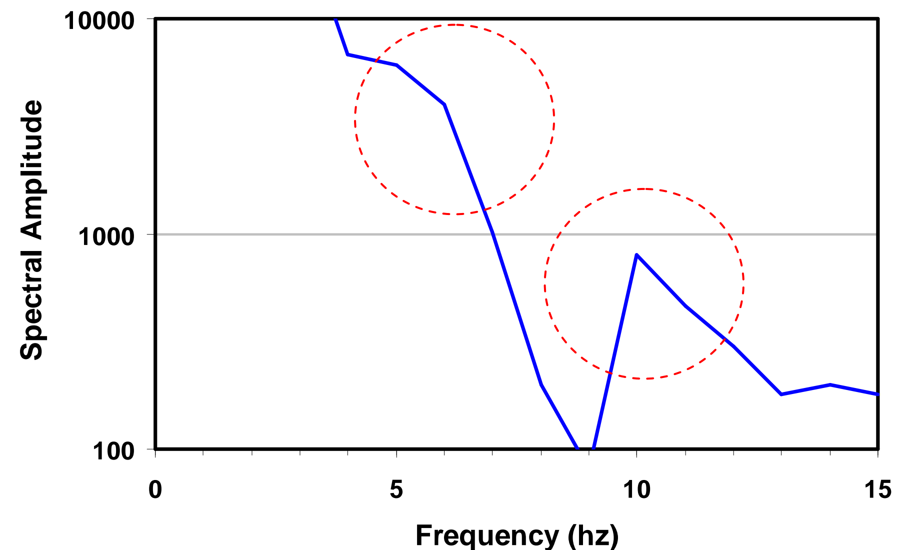

In-situ Conditioning Duty Cycle Study

The simulated furrow density spectrums show similar spectral distributions to the shear force spectrums, suggesting some specific peaks are associated with pad conditioning.

Dual Emission Laser Induced Fluorescence

Dual Emission Laser Induced Fluorescence (DELIF)

- **In-situ contact images**
- **6 ns time integration, 2 images/sec**
- **~3 micron/pixel to resolve asperity sized features**
- **Pads (all polyurethane based): CMC D100, CMC D200, Fruedenburg FX9, IC1000**

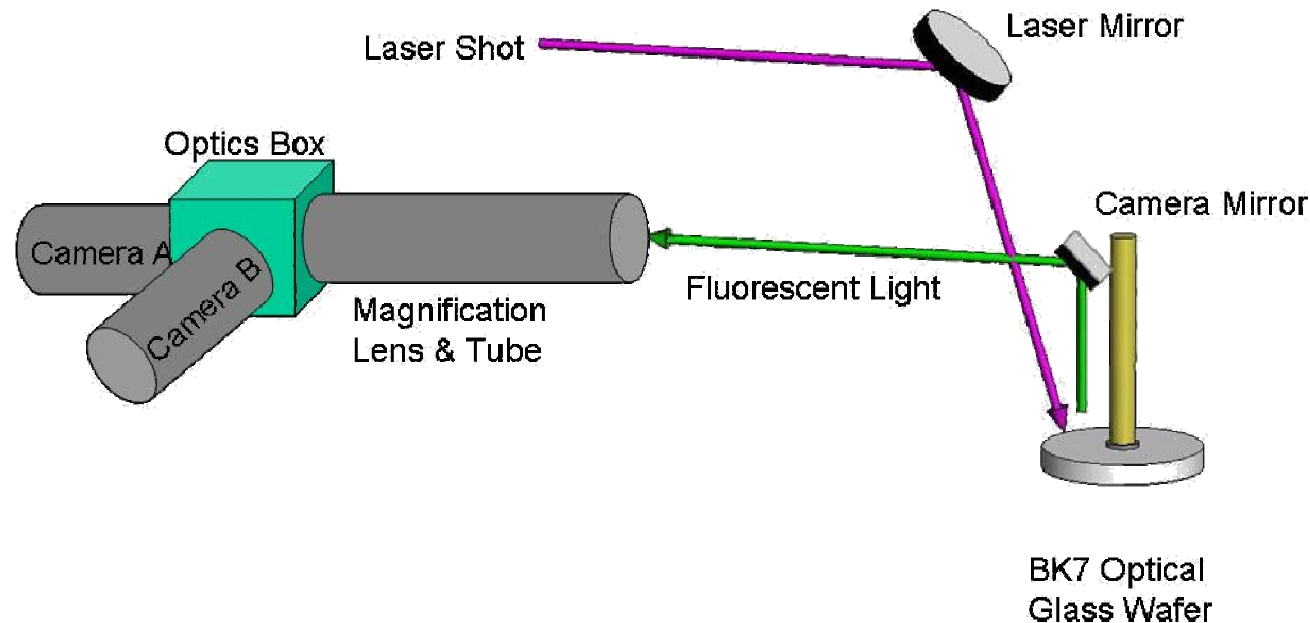

DELIF: Film Thickness

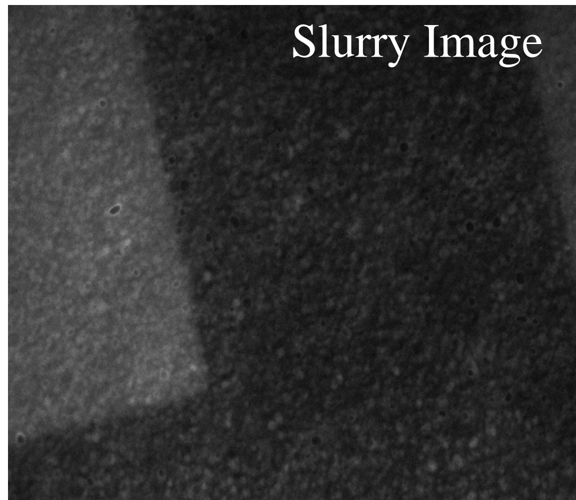

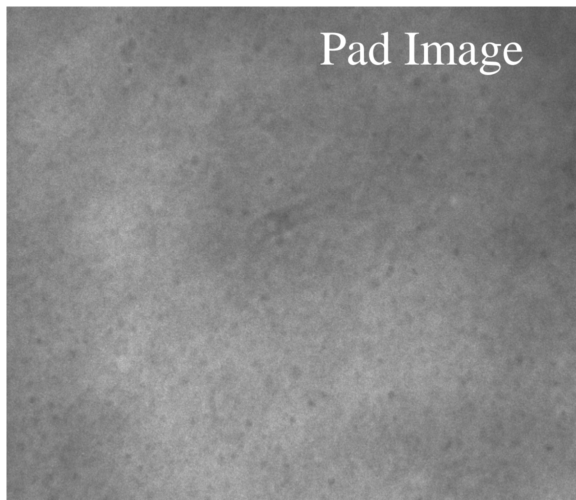

Two cameras:

(1) wavelength of slurry dye

(2) wavelength of pad fluorescence

Image ratio cancels source intensity variation

=

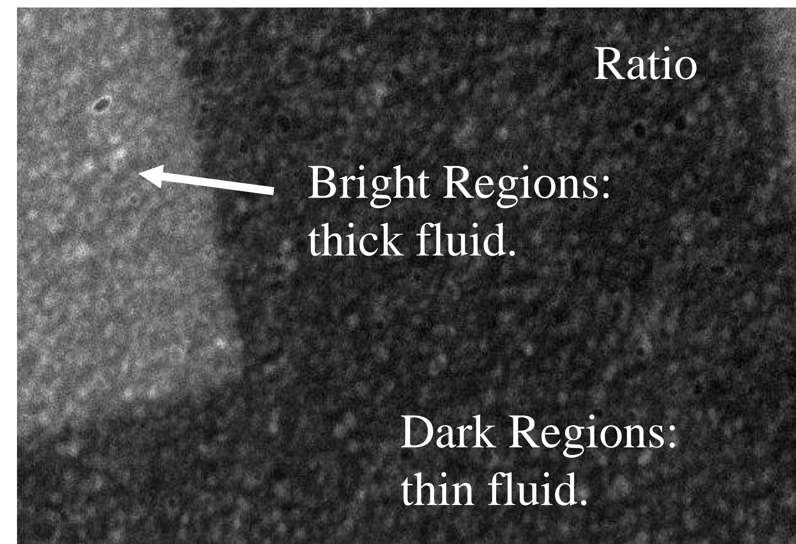

Brighter regions are thicker fluid layers.

DELIF: Static Contact

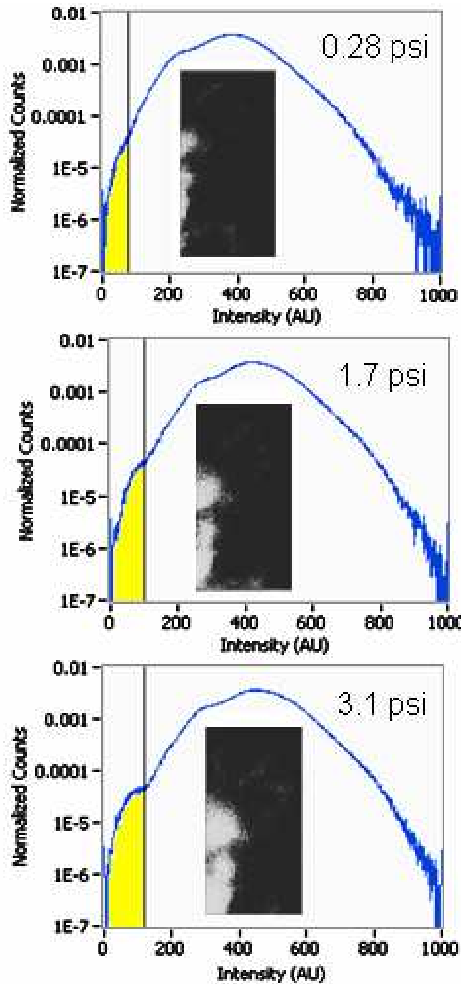

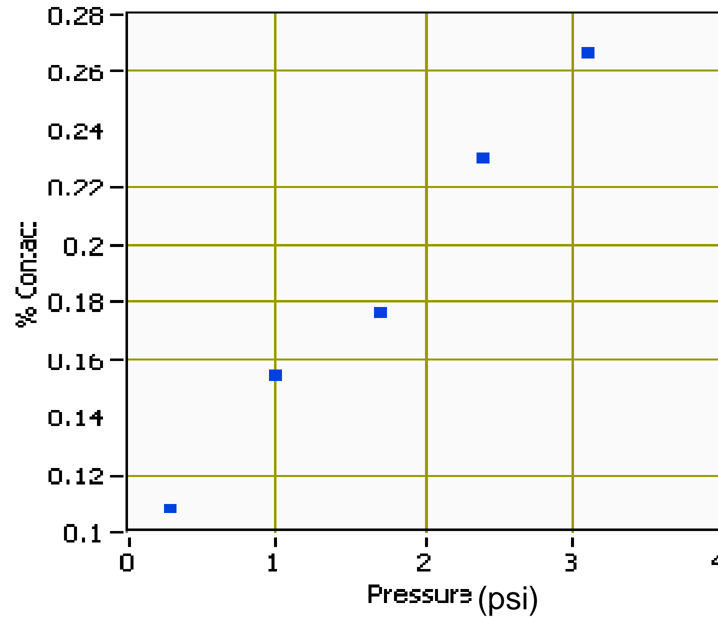

CMC D100 pad

BK7 glass wafer

9:1 Cab-o-sperse SC1 slurry (fumed silica, 3 wt% at this dilution)

Static contact area is linearly pressure dependent.

Static contact percent is on the order of 0.2%.

Gray, C., Rogers, C. Manno, V., White, R., Moinpour, M., Anjur S.."*Determining Pad-Wafer Contact using Dual Emission Laser Induced Fluorescence*", Proceedings of the Material Research Society, Vol. 991, Symposium C, Advances and Challenges in Chemical Mechanical Planarization (0991-C01-04), 2007.

DELIF: Dynamic Contact

Contact appears to be higher near groove edges *for this pad*.

Contact is on the order of 0.2%.

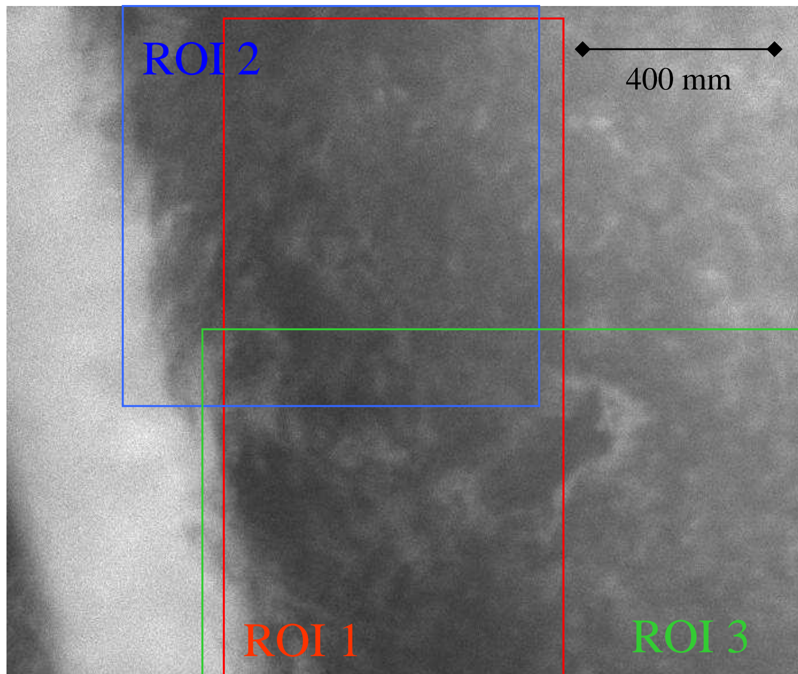

CMC D100 pad, AC grooves, 9:1 Cab-o-Sperse SC1 (3 wt%), 30 RPM, 1 PSI

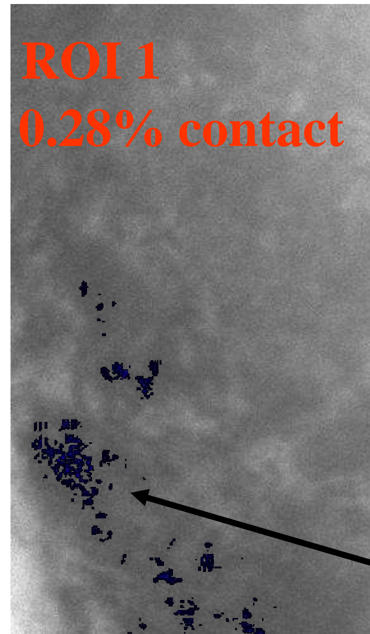

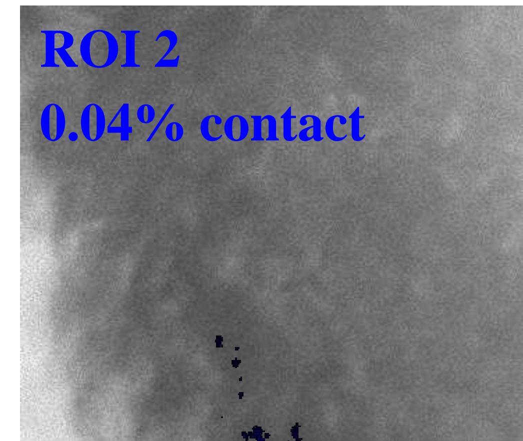

Black regions indicate contact.

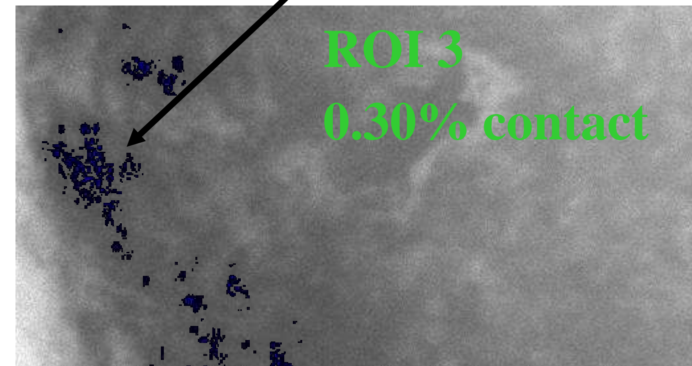

Flow Visualization

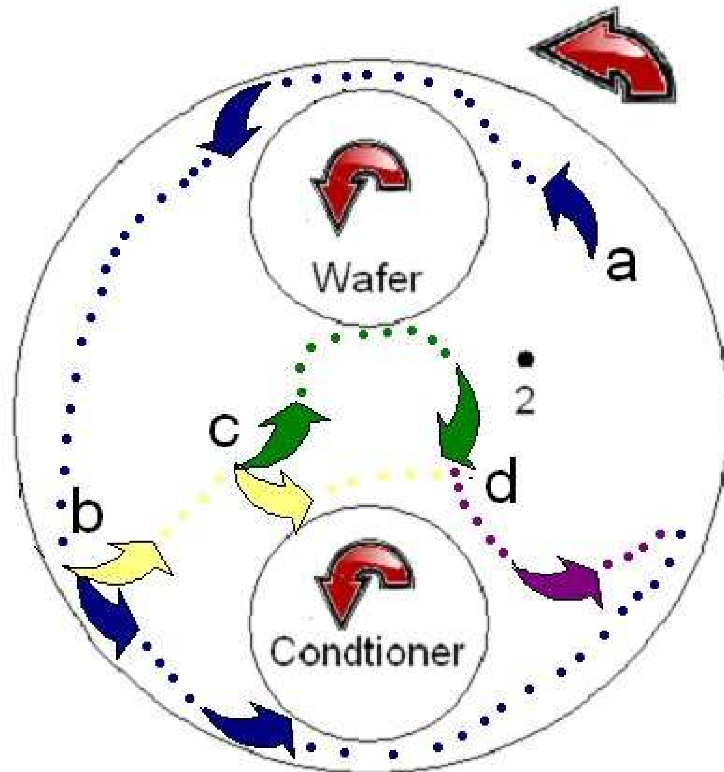

Flow visualization using particle tracers allows determination of:

1. Presence of vorticity
2. Presence of bow waves
3. Slurry path
4. Slurry residence

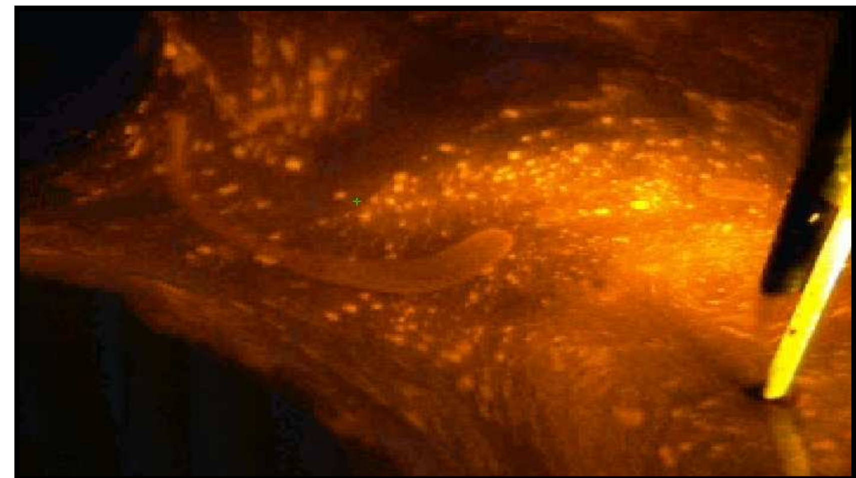

Variables of interest:

1. **Slurry injection point**
2. **Wafer speed**
3. **Down force**

Data is available at:
http://docs.google.com/Doc?id=dc9dhhdb_13fphfz7dp

PIV: Quantifying Flow

- **PIV is difficult in the CMP environment because tracer particles become embedded in the pad.**
- **Pad grooving exacerbates this problem.**
- **Quantification of induced errors is ongoing.**
- **PIV data will be available for most pads for short times.**

PIV takes movies of particle motion and turns them into velocity fields.

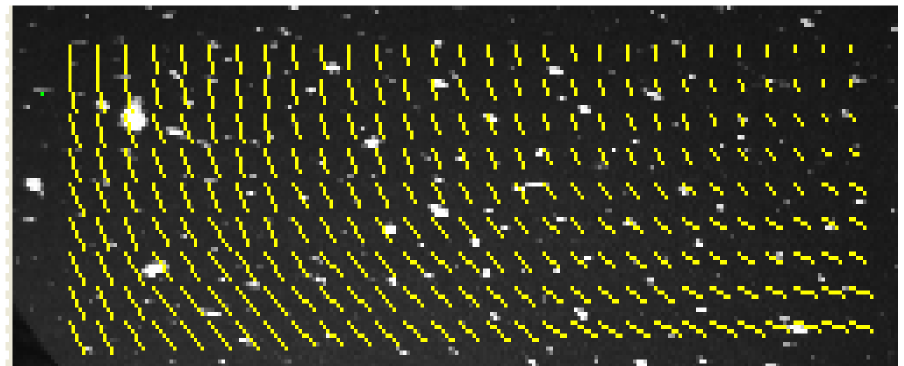

In-Plane Force Spectra

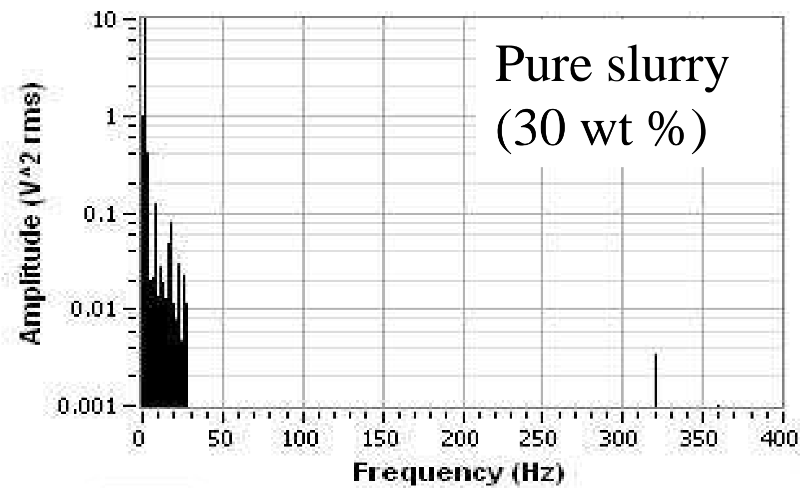

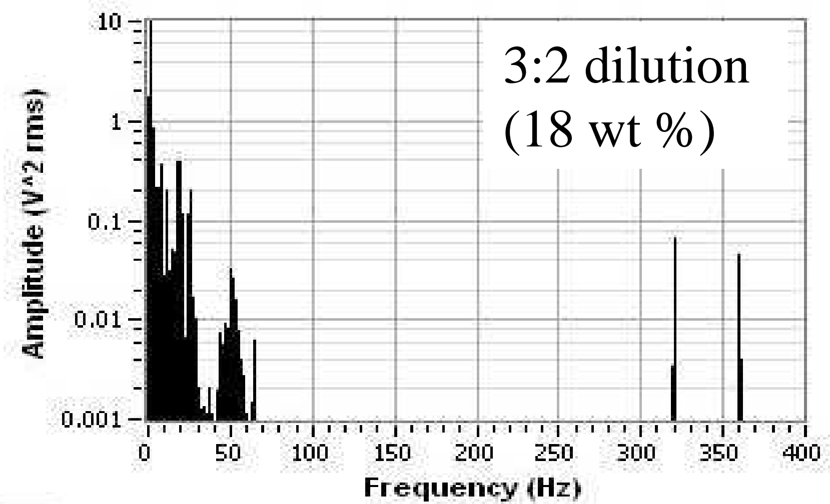

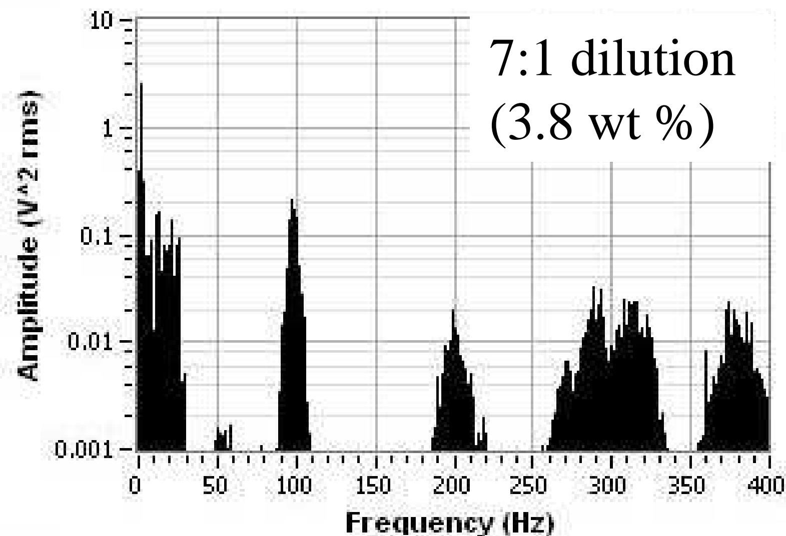

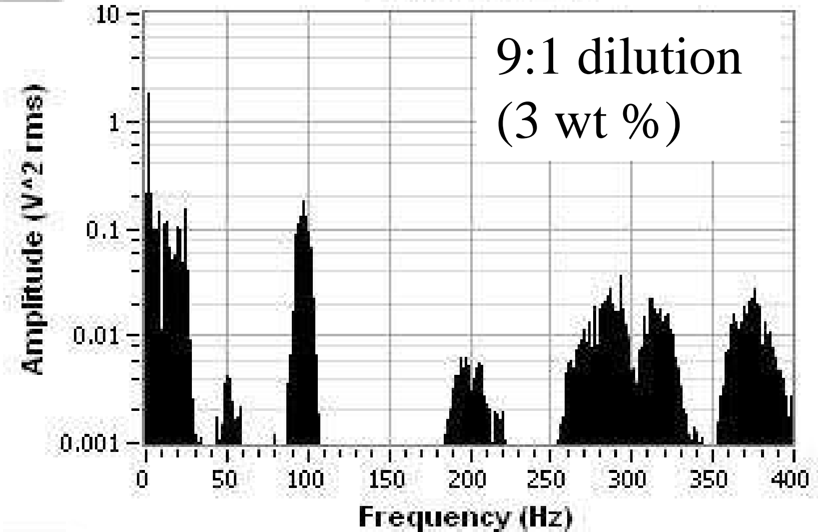

Spectral signatures vary with slurry concentration. 30 wt % slurry (fumed silica slurry) exhibits the least high frequency force content.

MEMS Force Sensors

- **Cylindrical PDMS posts:**
  - **100 micron tall, 30-100 micron diameter.**
  - **Deflect due to shear force.**
  - **Recessed in wells.**
- **Calibrated sensitivity is linear:**
  - **200 nm/mN for 100 micron diameter**

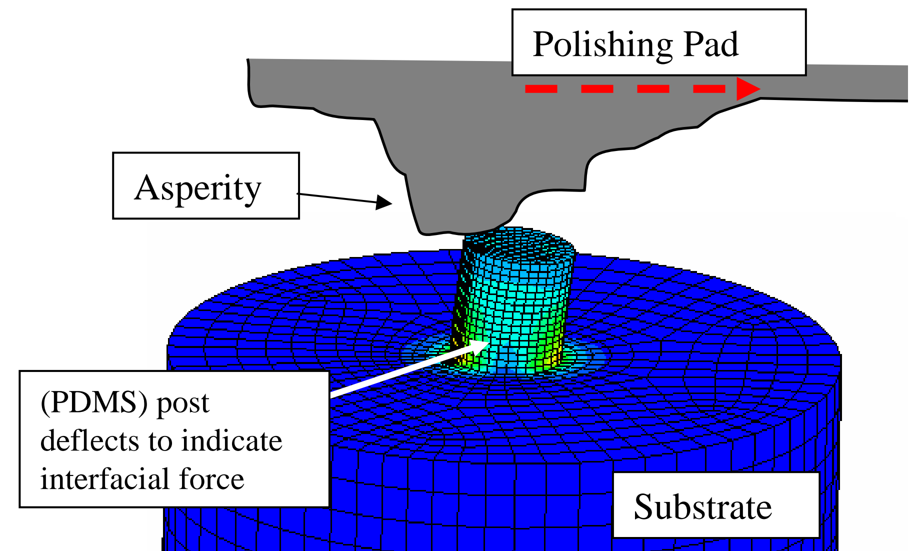

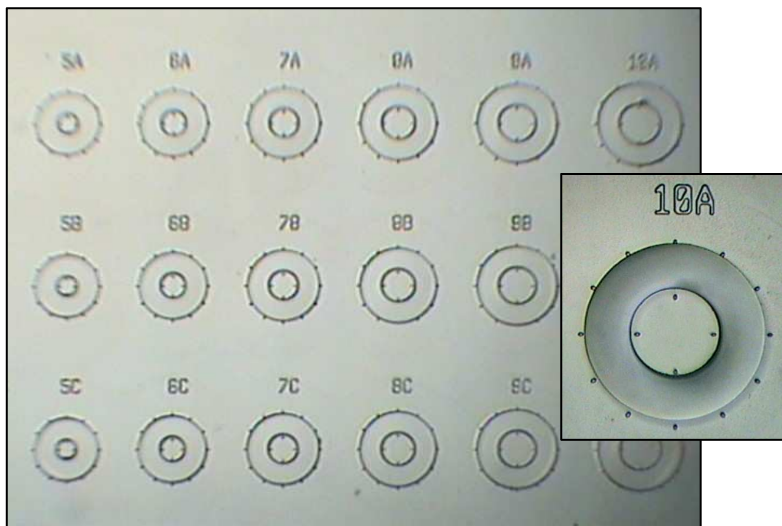

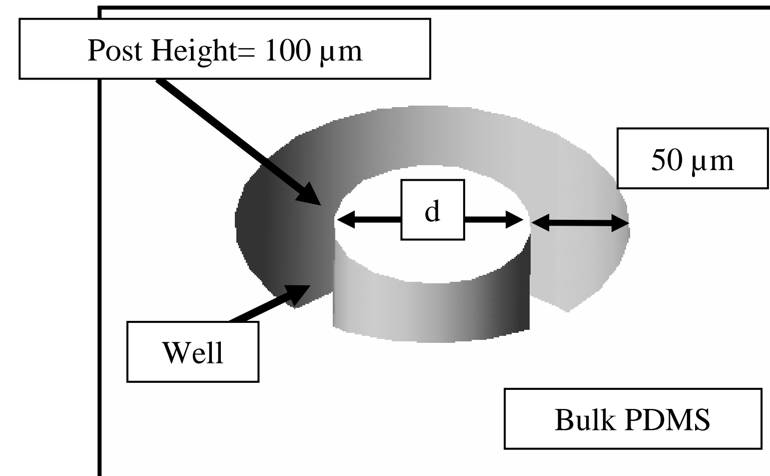

Asperity Level Forces

Image processing extracts motion of the post from high-speed (10,000 fps) video.

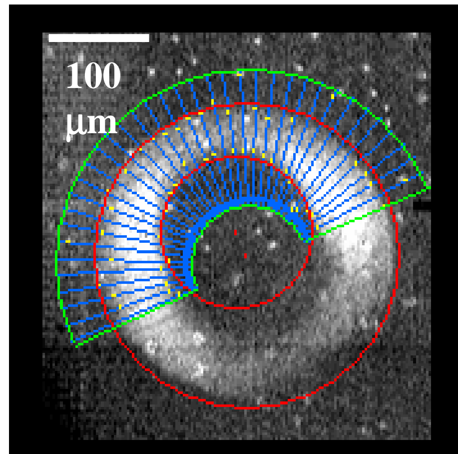

Deflected

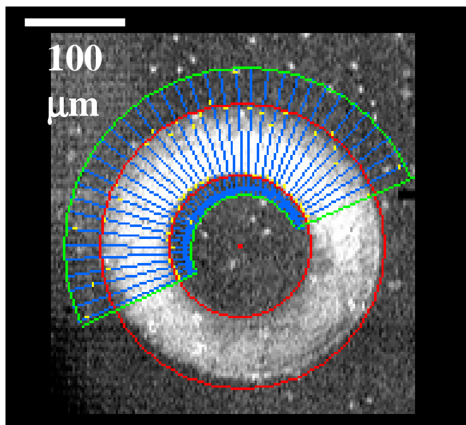

Not deflected

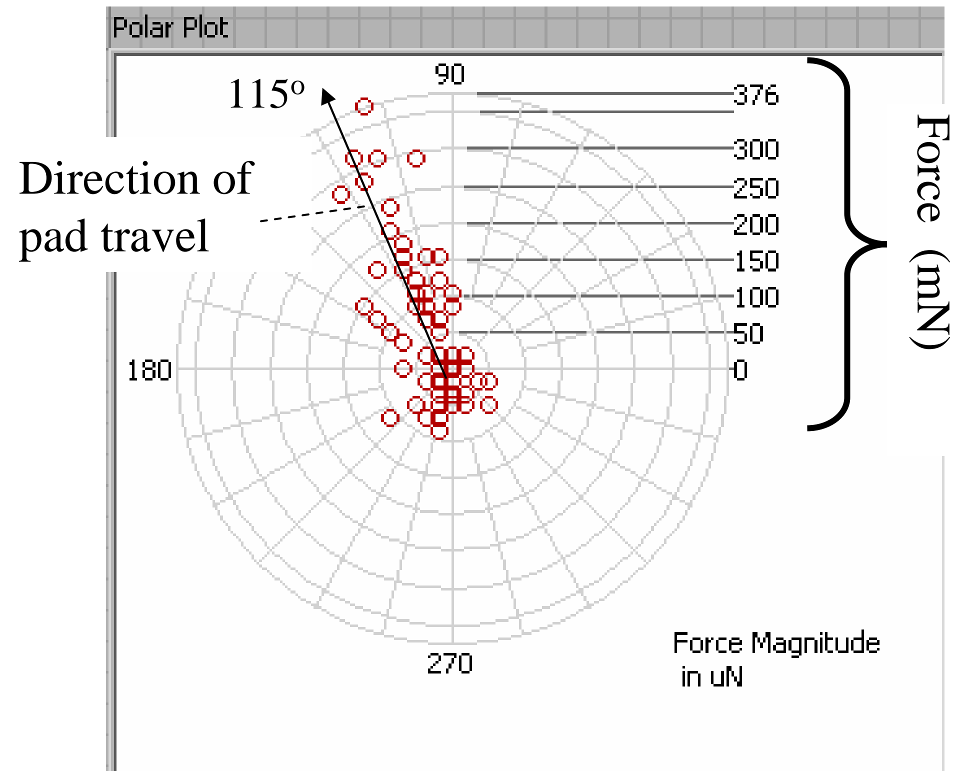

Each point corresponds to the force (direction and magnitude) measured at each 100 microsecond time step. The average force direction aligns with the direction of pad travel.

Asperity Level Forces

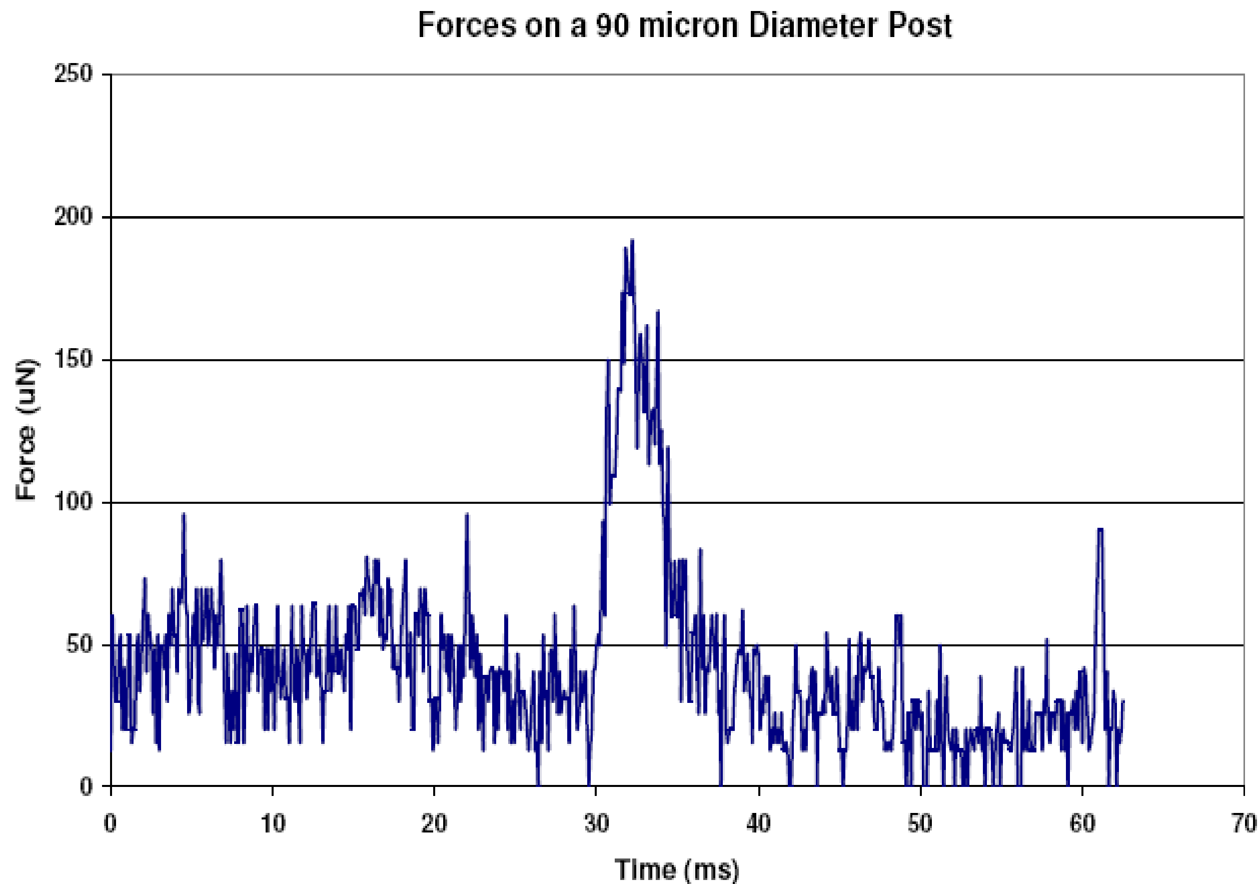

Example force trace for ***PDMS polishing*** with ***no wafer rotation*** and ***no conditioning***.

Large force events (> 100 mN) occur less than 10% of the time and last 0.5-5 ms.

Lateral force vs. time on a 90 micron post. 30 RPM, 1 PSI, 9:1 slurry.

Asperity Level Forces

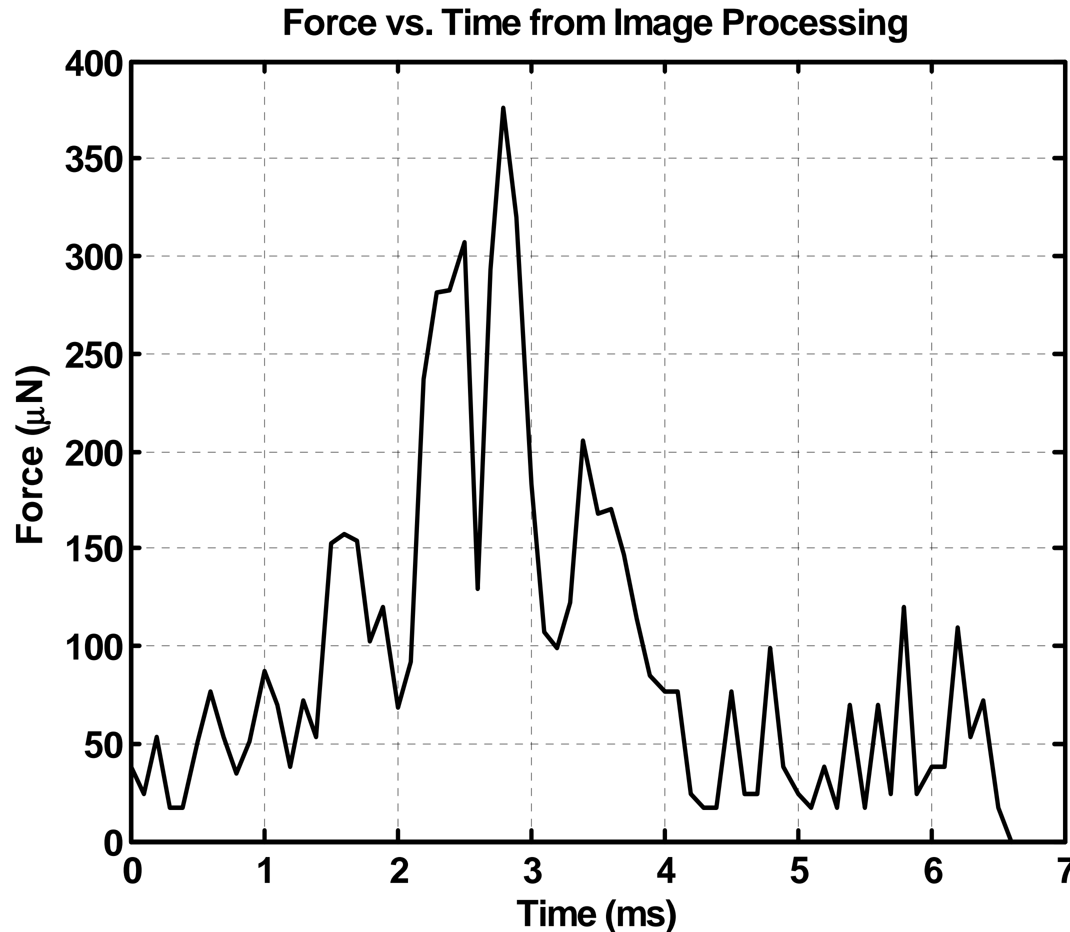

Large force events appear to come in "clusters" with individual event durations on the order of 0.5 ms and cluster durations on the order of 3 ms. 0.5 ms is approximately the time for a point on the pad to pass over the structure.

Lateral force vs. time, 100 micron post. 30 RPM, 1 PSI, 9:1 slurry.

Asperity Level Forces: Trends

- Increase **in pad rotation leads to a** decrease **in local shear force.**
- Increase **in structure size leads to an** increase **in local shear force.**
- Increase **in down force leads to an** increase **in local shear force only at lower speeds.**
- **Maximum shear forces for 100 micron structures are approximately 300 mN.**

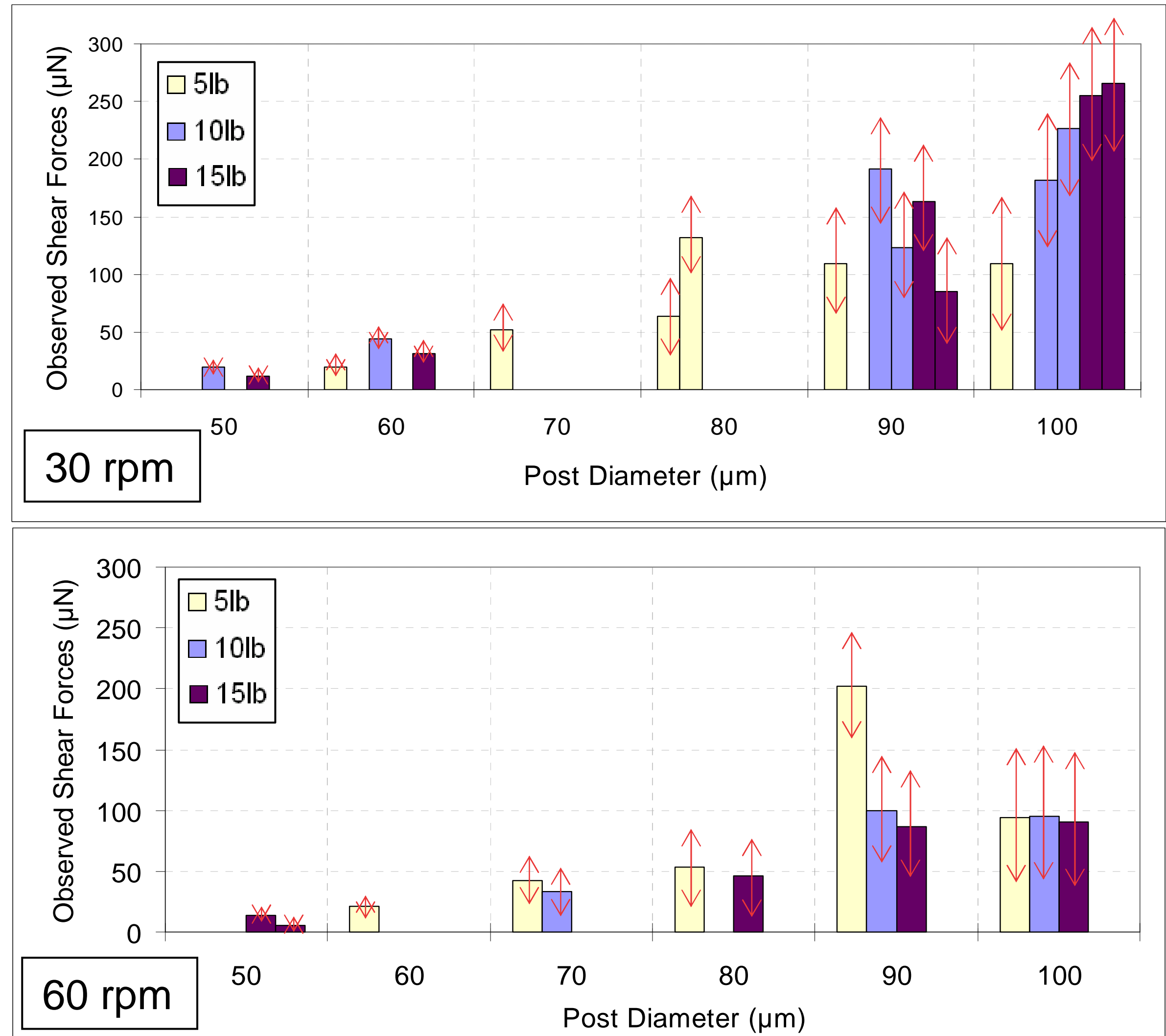

Plots show peak shear forces for maximum force events.

Parameters of Physical CMP Chip-Scale Model

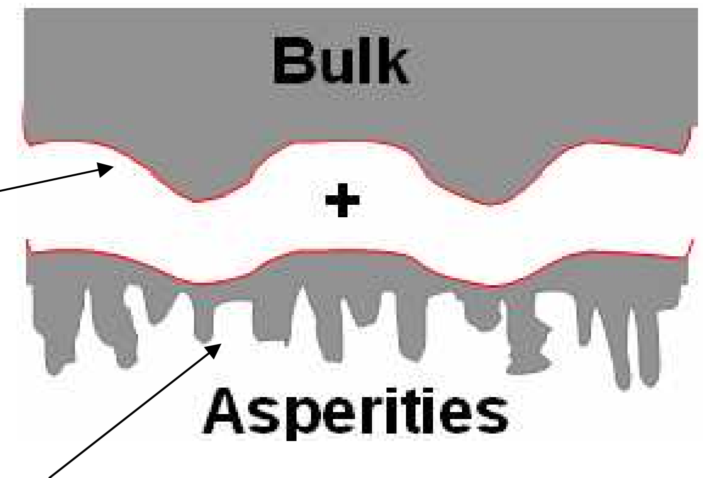

- *E* Effective Young's Modulus

(Property of pad bulk)

- λ Characteristic Asperity Height

(Property of pad asperities)

- *K* Blanket Removal Rate at reference pressure

(Scaling factor of the system)

Pad Bulk: Contact Mechanics

Contact Mechanics describes the relationship between pad displacement w(x,y) and pad pressure P(x,y)

- Point pressure, w(r) ~ 1/r
- Linear superposition

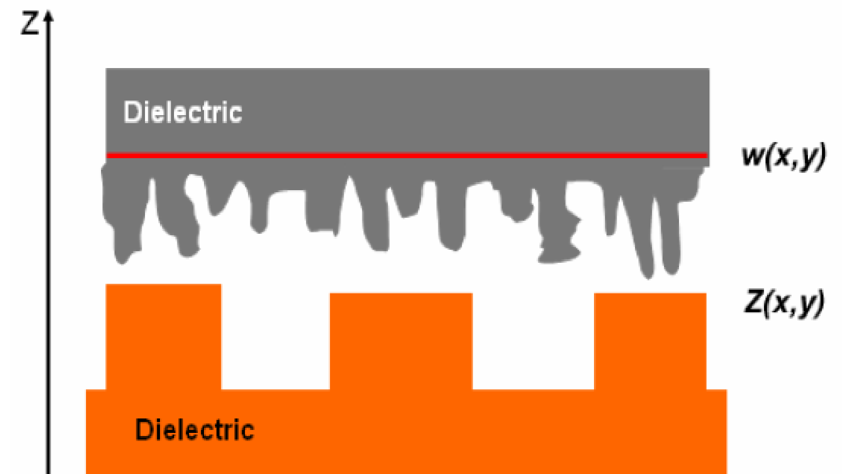

$$w(x,y) - w_0 = \frac{1-\nu^2}{\pi E_p} \int d\xi \int d\eta \frac{P(\xi,\eta)}{\sqrt{(x-\xi)^2 + (y-\eta)^2}}$$

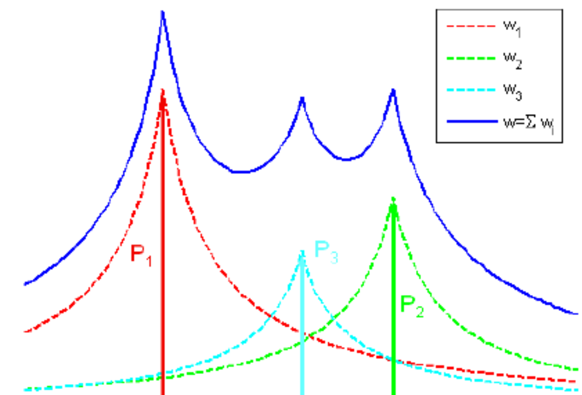

Pad Asperities

Assumptions:

1. **Negligible width**
2. **Exponential distribution of height, mean λ**
3. **Hooke's law: force proportional to compressed amount**

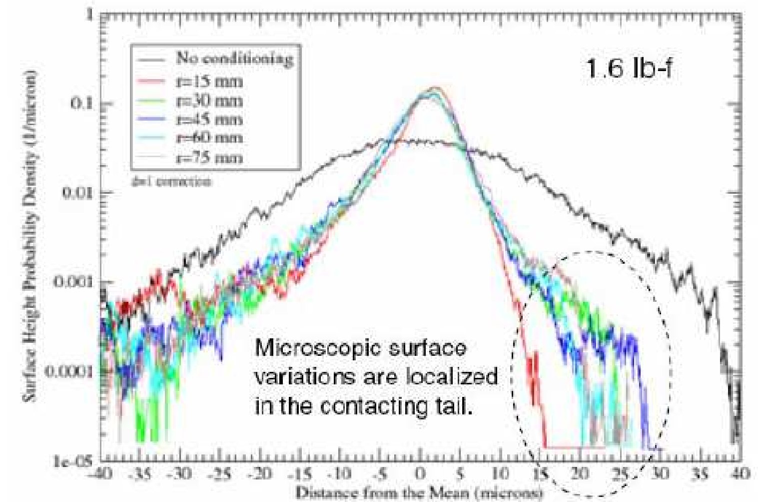

Surface Height Distribution
L. Borucki, 2006, ICPT

$$\begin{cases} P_d = \dfrac{1}{1+\rho(e^{h/\lambda}-1)}P \\ P_u = \dfrac{e^{h/\lambda}}{1+\rho(e^{h/\lambda}-1)}P \end{cases} \Rightarrow \begin{cases} K_d = \dfrac{1}{1+\rho(e^{h/\lambda}-1)}K \\ K_u = \dfrac{e^{h/\lambda}}{1+\rho(e^{h/\lambda}-1)}K \end{cases}$$

Interpreting Pattern-Density / Step-Height Parameters

- **Planarization length L_P**
  z_u (across chip)
  - **increases with E**
  - **insensitive to asperity height distribution**

- **Characteristic step-height h^***
  step height evolution
  - **Depends strongly on asperity height distribution**
  - **insensitive to E**

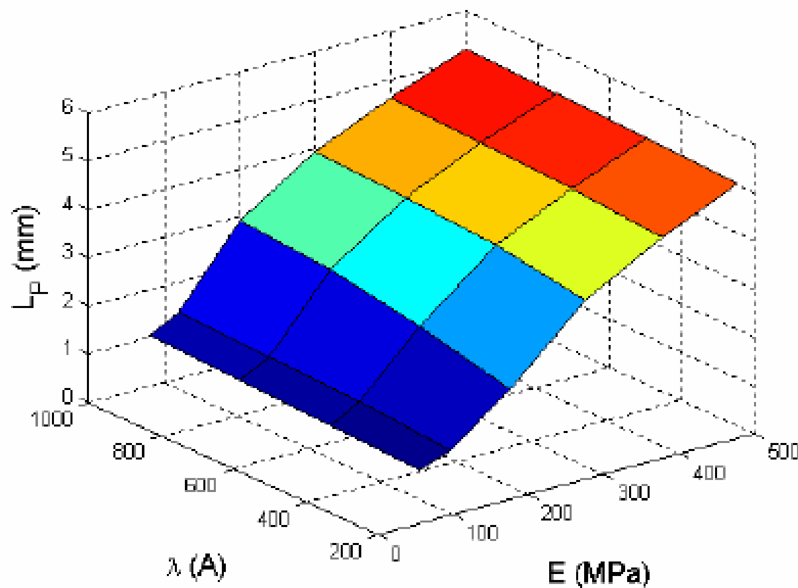

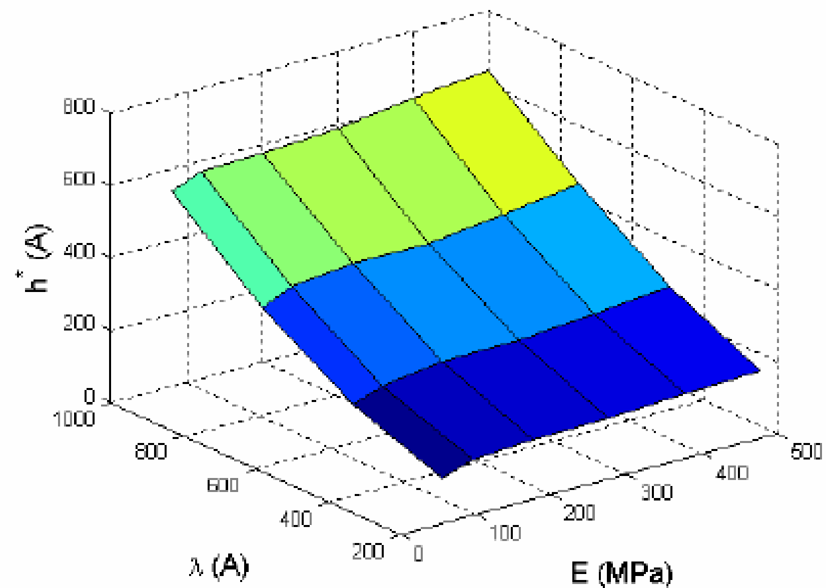

Physically-Based Model Results

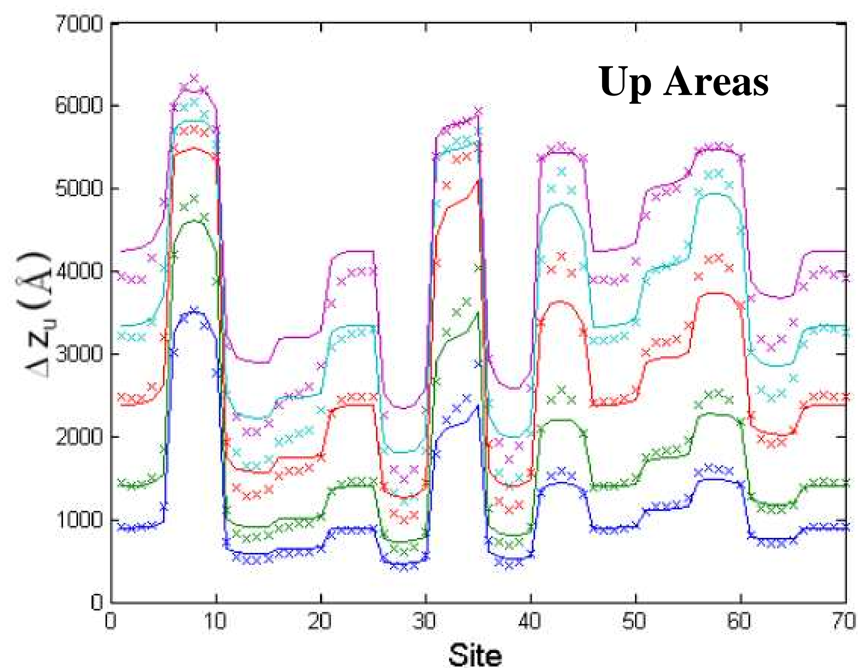

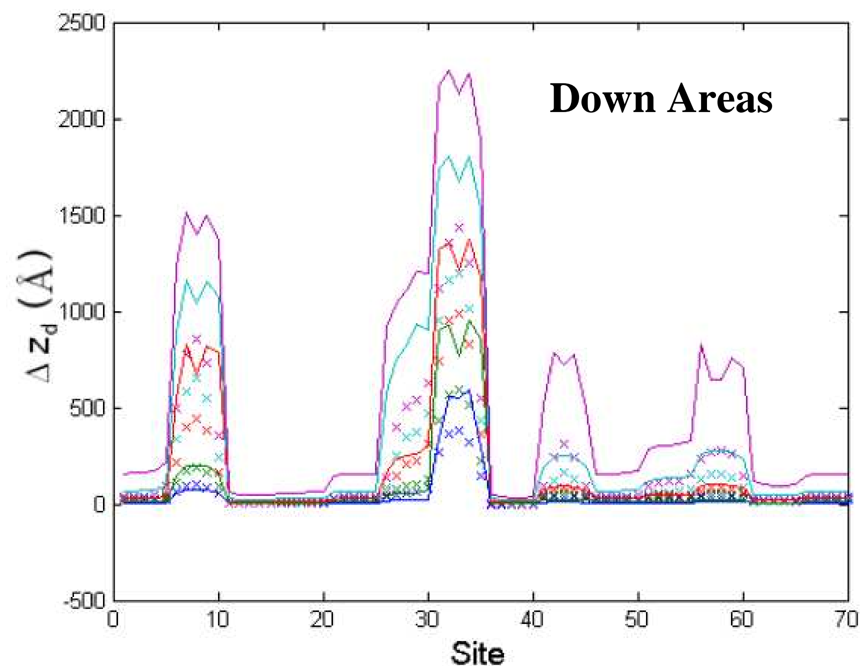

- **Fitting errors:**
  Δz_u is 251 Å
  Δz_d is 262 Å

Model Application: Study of Pad/Planarization Dependencies

- **Pad with water soluble particles (WSP's)**
  - Keeps pad bulk rigid (increased bulk stiffness)
  - Pores aid in slurry transport
  - Modifies/controls pad surface/asperity structure

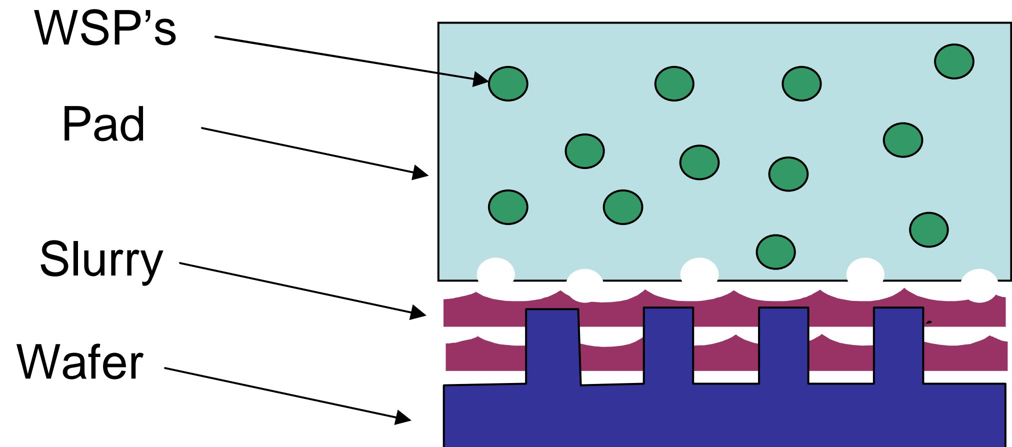

- **Goal of study**
  - Extract chip-scale model parameters for different WSP pad designs
  - Understand chip-scale performance as function of pad parameters

- **Experiments**
  1. Vary WSP size (fixed concentration)
  2. Vary WSP concentration (fixed size)

Performance Metrics

Up-Area Range (Max-Min) Across Chip

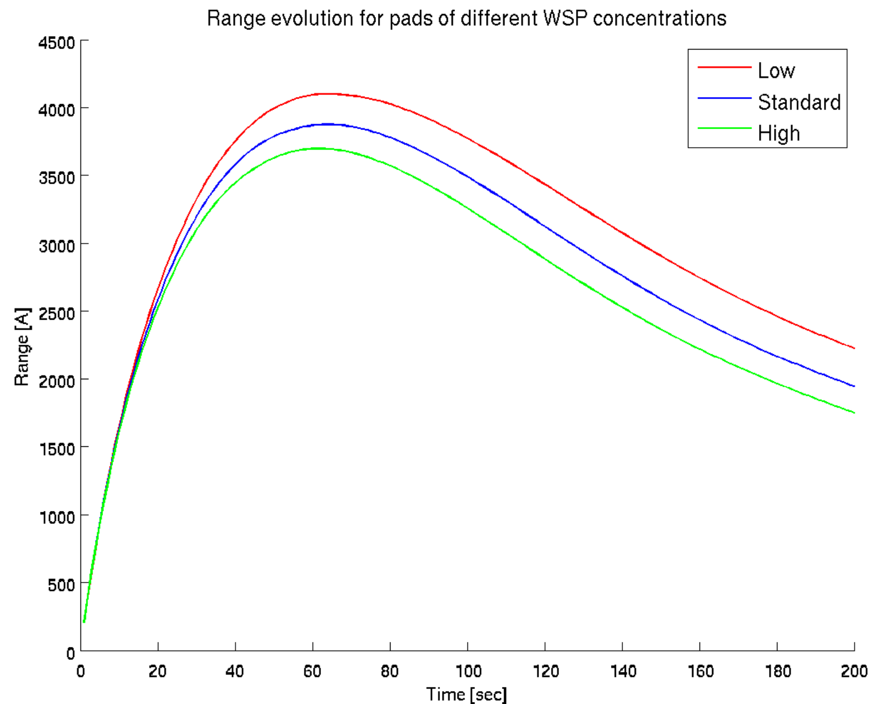

Planarization Efficiency

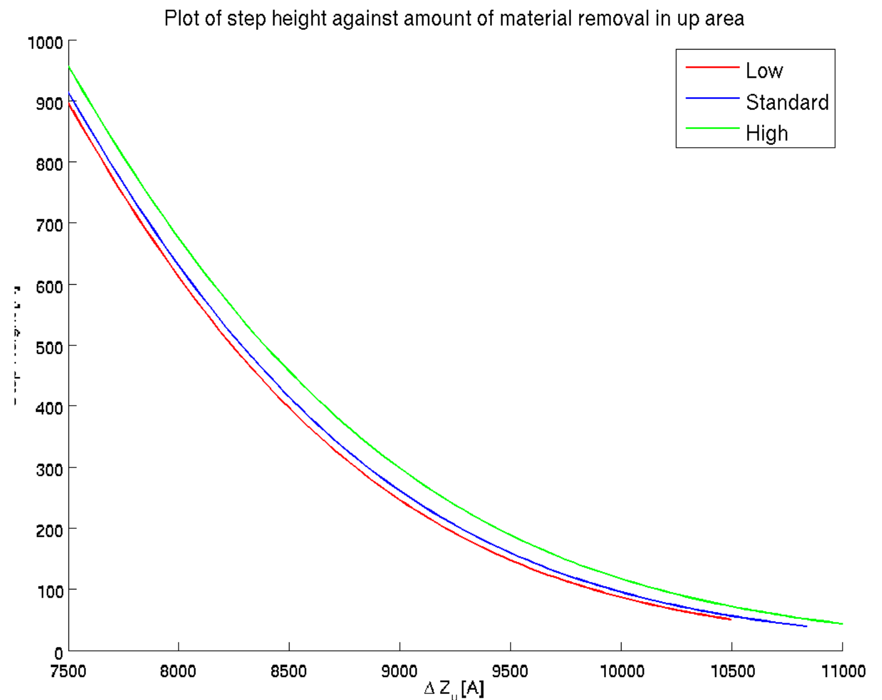

- **Enables exploration of trade-off or joint optimization between**
  - **Chip-scale (within-die) uniformity**
  - **Feature-scale planarization (dishing)**

Modulus: Physical Measurement vs. Model Parameter

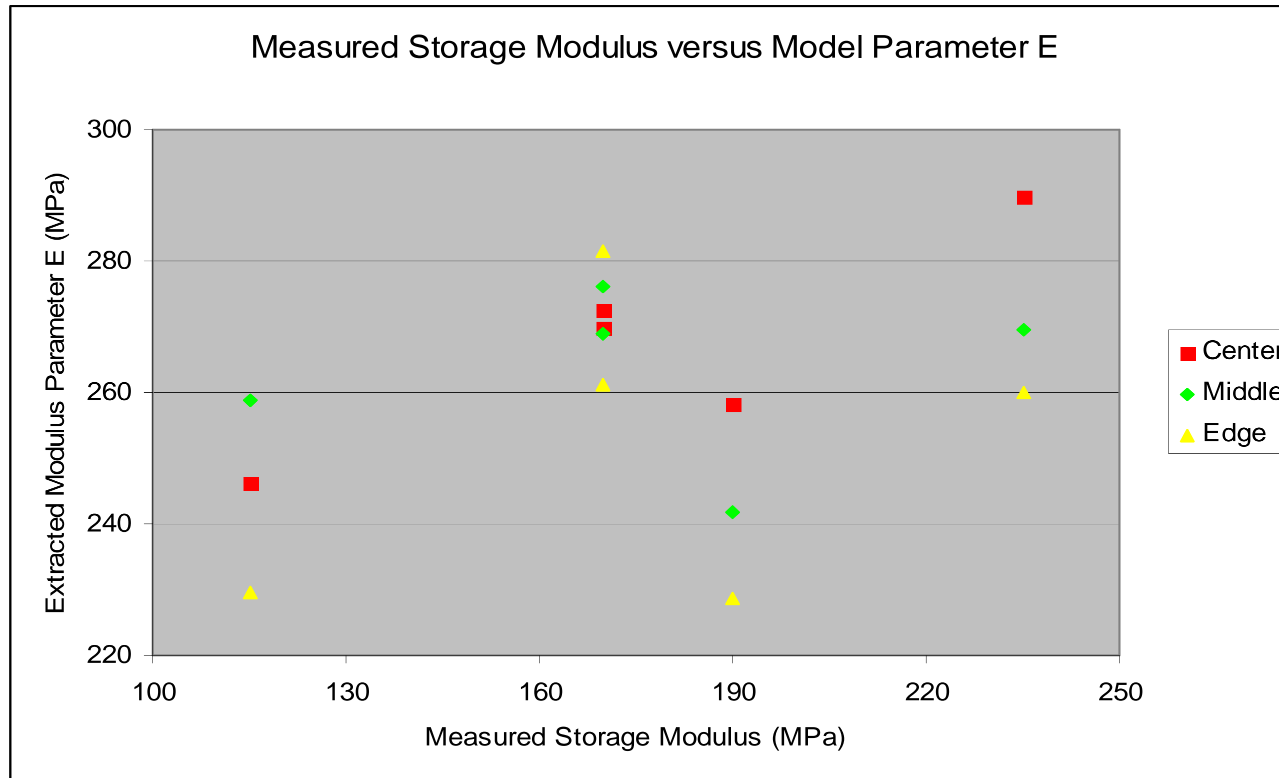

- **Need to understand difference**
  - **"Effective" bulk Young's modulus?**
  - **Experimental measurement of bulk vs. asperity mechanical properties**

Industrial Interactions and Technology Transfer

Industrial Mentors / Contacts:

- Mansour Moinpour (Intel Corporation)
- Sriram Anjur (Cabot Microelectronics Corporation)
- Toranosuke Ashizawa (Hitachi Chemical Co., Ltd.)
- Hiroyuki Morishima (Hitachi Chemical Co., Ltd.)
- Sudhanshu Misra (Neopad Technologies Corporation)
- Karey Holland (Neopad Technologies Corporation)
- Leonard Borucki (Araca, Inc.)

Future Plans

Next Year Plans

- **Investigate the shear force and down force transition during early evolution of wafer topography for STI CMP.**
- **Continue pad-wafer contact and slurry thickness measurement through DELIF.**
- **Continue wafer-scale characterization of CMP mechanics and particle image velocimetry for CMP slurry flow.**
- **Continue to develop MEMS for asperity scale force measurement in CMP.**

Long-Term Plans

- **Investigate the shear force and down force transition during evolution of wafer topography for metal CMP.**
- **Deploy the newly demonstrated *in situ* measurement technologies (DELIF, wafer attitude, PIV, MEMS force sensing) to a 200-mm polisher.**
- **Integrate feature, chip and wafer-scale CMP model with sensor models to identify stage of planarization, dishing, and erosion across chip and wafer.**

Publications

- Simulated Effects of Measurement Noise on Contact Measurements between Rough and Smooth Surfaces. C. Gray, R.D. White, V.P. Manno and C. B. Rogers. Tribology Letters, In Press.
- Determining Pad-Wafer Contact using Dual Emission Laser Induced Fluorescence. C. Gray, C. Rogers, V. Manno, R. White, M. Moinpour, S. Anjur. Materials Research Society Symposium Proceedings, Vol. 991, C01-04 (2007).
- Micromachined Shear Stress Sensors for Characterization of Surface Forces During Chemical Mechanical Polishing. A. Mueller, R. White, V. Manno, C. Rogers, C. Barns, S. Anjur, M. Moinpour. Materials Research Society Symposium Proceedings, Vol. 991, C06-03 (2007).
- Wafer Level Modeling of Electrochemical-Mechanical Polishing (ECMP). D. Truque, X. Xie, D. Boning. Materials Research Society Symposium Proceedings, Vol. 991, C11-04 (2007).
- In-Situ Investigation of Wafer-Slurry-Pad Interactions during CMP. N. Braun, C. Gray, A. Mueller, J. Vlahakis, D. Gauthier, V.P. Manno, C. Rogers, R. White, S. Anjur, M. Moinpour. International Conference on Planarization/CMP Technology Proceedings, 37-42 (2007).
- Applications of Shear Force Spectral Analysis in STI CMP. Y. Sampurno, F. Sudargho, Y. Zhuang, T. Ashizawa, H. Morishima and A. Philipossian. International Conference on Planarization/CMP Technology Proceedings, 129-133 (2007).

Presentations

- Determining Pad-Wafer Contact using Dual Emission Laser Induced Fluorescence. C. Gray, C. Rogers, V. Manno, R. White, M. Moinpour, S. Anjur. 2007 Materials Research Society Spring Meeting, San Francisco, California, April 9-13 (2007).
- Micromachined Shear Stress Sensors for Characterization of Surface Forces During Chemical Mechanical Polishing. A. Mueller, R. White, V. Manno, C. Rogers, C. Barns, S. Anjur, M. Moinpour. 2007 Materials Research Society Spring Meeting, San Francisco, California, April 9-13 (2007).
- Wafer Level Modeling of Electrochemical-Mechanical Polishing (ECMP). D. Truque, X. Xie, D. Boning. 2007 Materials Research Society Spring Meeting, San Francisco, California, April 9-13 (2007).
- Physical-based Die-level CMP Model. X. Xie and D. Boning. 2007 Materials Research Society Spring Meeting, San Francisco, California, April 9-13 (2007).
- Chip-Scale Modeling of CMP and Plating Processes. D. Boning. Fourth International Copper Interconnect Technology Symposium, Fudan University, Shanghai, China, May (2007). Also at Tsinghua University, Beijing, China, May (2007).
- Modeling of Chip-Scale Pattern Dependencies in Interconnect Fabrication Processes. D. Boning. Advanced Metallization Conference, Albany, New York, October (2007).
- In-Situ Investigation of Wafer-Slurry-Pad Interactions during CMP. N. Braun, C. Gray, A. Mueller, J. Vlahakis, D. Gauthier, V.P. Manno, C. Rogers, R. White, S. Anjur, M. Moinpour. International Conference on Planarization/CMP Technology, Dresen, Germany, October 25-27 (2007).
- Applications of Shear Force Spectral Analysis in STI CMP. Y. Sampurno, F. Sudargho, Y. Zhuang, T. Ashizawa, H. Morishima and A. Philipossian. International Conference on Planarization/CMP Technology, Dredsen, Germany, October 25-27 (2007).
- Green Fab and Manufacturing. D. Boning. International Solid-State Circuits Conferences, San Francisco, California, February (2008).

Low-Water and Low-Energy Rinsing and Drying of Patterned Wafers, Nano-Structures, and New Materials Surfaces

(Task Number: 425.021)

PIs:

- Farhang Shadman, Chemical Engineering, UA
- Bert Vermeire, Electrical Engineering, ASU

Other Researchers:

- Jun Yan, Postdoctoral Fellow, Chemical Engineering, UA
- Omid Mahdavi, Micro/Nano Fabrication Center, UA

Graduate Students:

- Kedar Dhane, PhD candidate, Chemical Engineering, UA
- Nijad Anabtawi, PhD, Electrical Engineering, ASU
- Xu Zhang, PhD, Electrical Engineering, ASU

Cost Share (other than core ERC funding):

- NSF, Freescale, Samsung, EMC

Objective and Approach

Objective:

- **Investigate the fundamentals of the cleaning, rinsing, and drying of micro- and nano-structures; develop new technologies (hardware, process models, and process recipes) to reduce water, chemicals, and energy usage during these processes.**

Method of Approach:

- **Develop and apply metrology method for in-situ and real-time monitoring of the dynamics of impurity transport inside micro- and nano-structures.**
- **Apply both novel metrology methods as well as process modeling to understand the controlling steps (bottlenecks) in the cleaning, rinsing, and drying of small structures.**

ESH Metrics and Impact

Goal and impact:

- Water: water use reduction of 40% (cold rinse)
- Energy: hot water use reduction by 50%
- Decrease in the use of monitor wafers
- Decrease in the usage of chemicals in cleaning applications
- Decrease in the use of purge gas and energy in drying applications
- Increase in throughput; minimizing delays due to external metrology

Metrology Requirements:

- Low ppt sensitivity
- On-line, real time, in-situ
- Compatible with cleaning chemicals, and rinse/dry conditions

Novel Electro-Chemical Residue Sensor (ECRS)

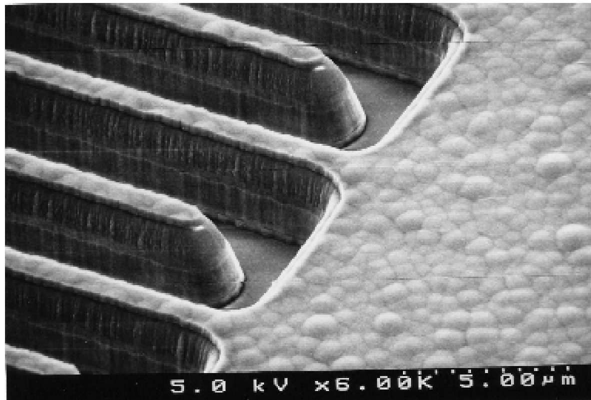

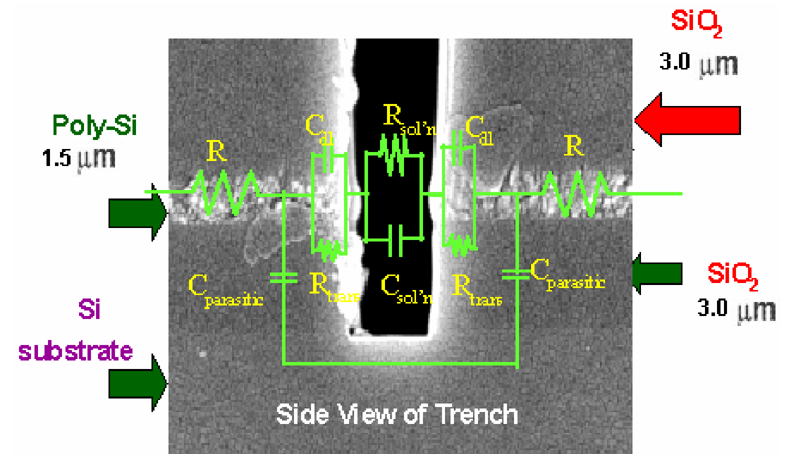

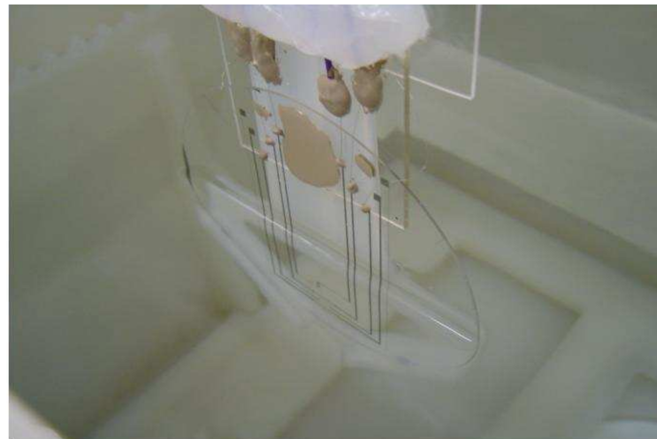

Effect of Feature Size on Rinse Time and Water Usage

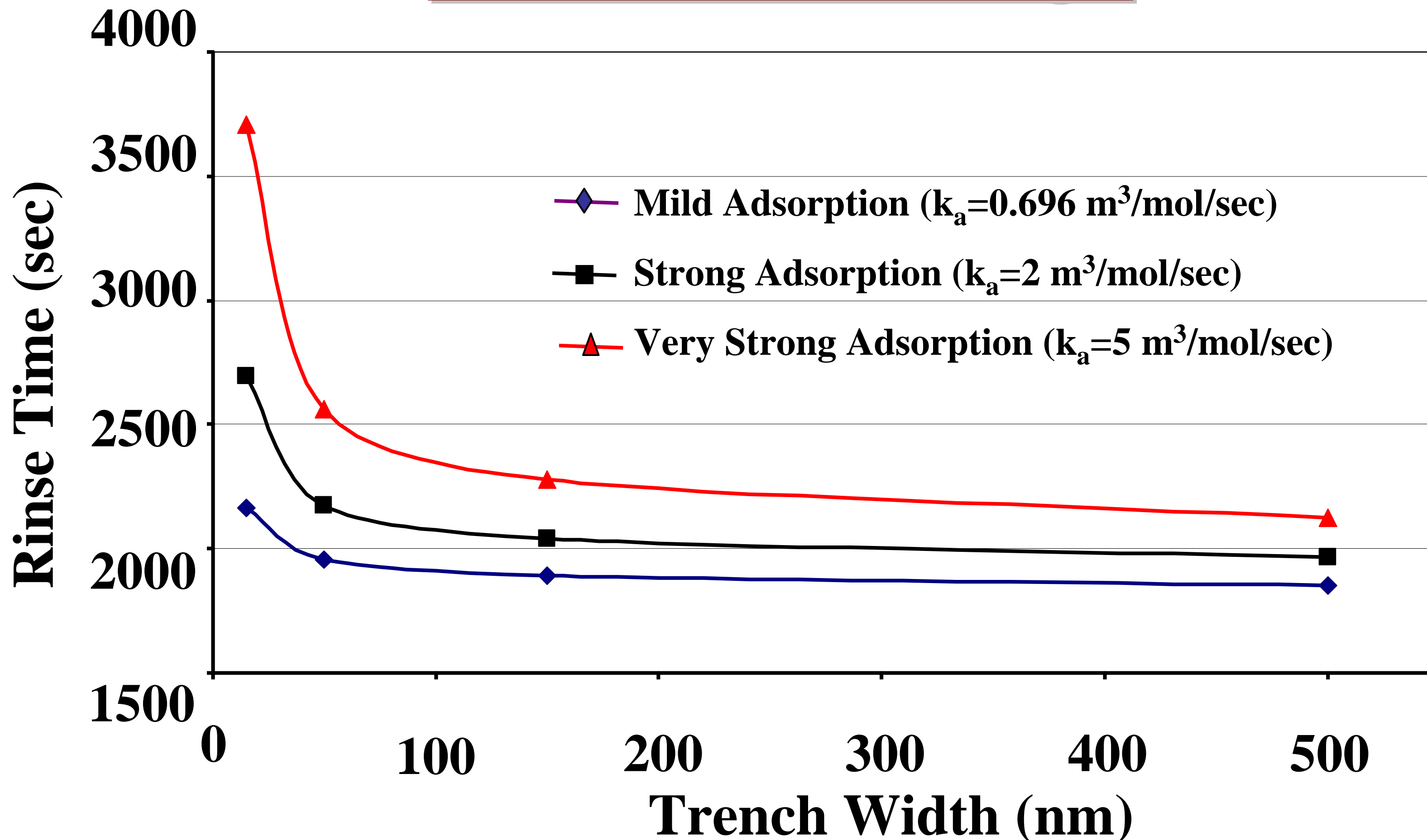

Rinse time to reach 10^{12} ions/cm^2 on the surface of the trench.

Dynamics of Drying

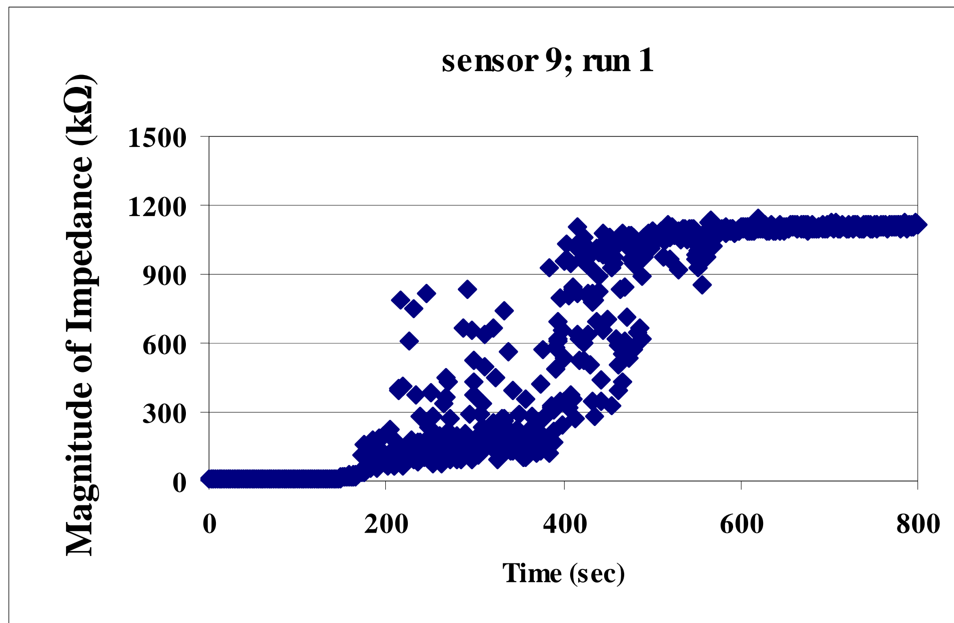

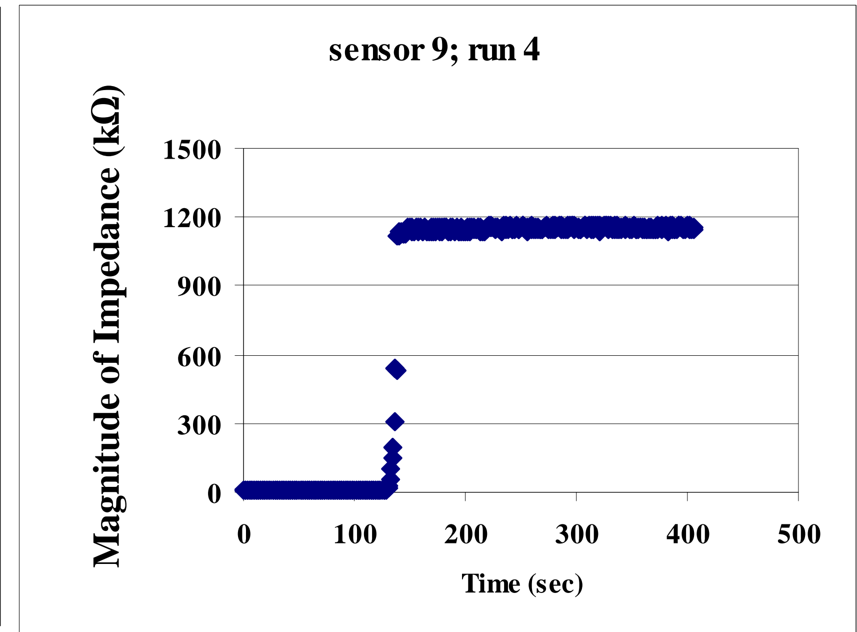

Hydrophilic **Hydrophobic**

- Time required for drying depends on the surface condition.
- ECRS detects complex mechanism for drying, particularly for hydrophilic surfaces.

Mechanism of Drying of Small Structures

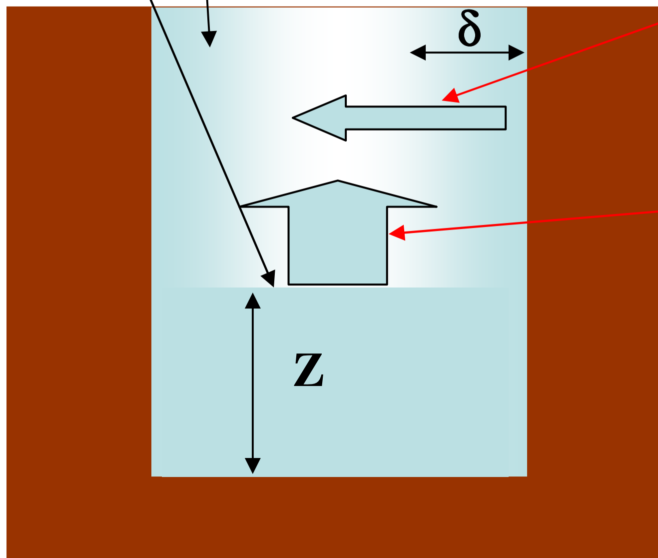

Removal rate from adsorbed layer:

$$R_d = k_d C_s - k_a C_g$$

Removal rate from bulk liquid:

$$R_e = k^{'} (P_s^{'} - P_{bulk})$$

Total removal rate from pore:

$$R = R_e + R_d$$

Two simultaneous processes:

- **Conventional evaporation of liquid-like molecules (mild feature size effect)**
- **Adsorption and desorption in a multi-layer (both chemisorbed and physisorbed; strong feature size dependence)**

Dynamics of Drying of Nano-Structures

Feature Size Dependence

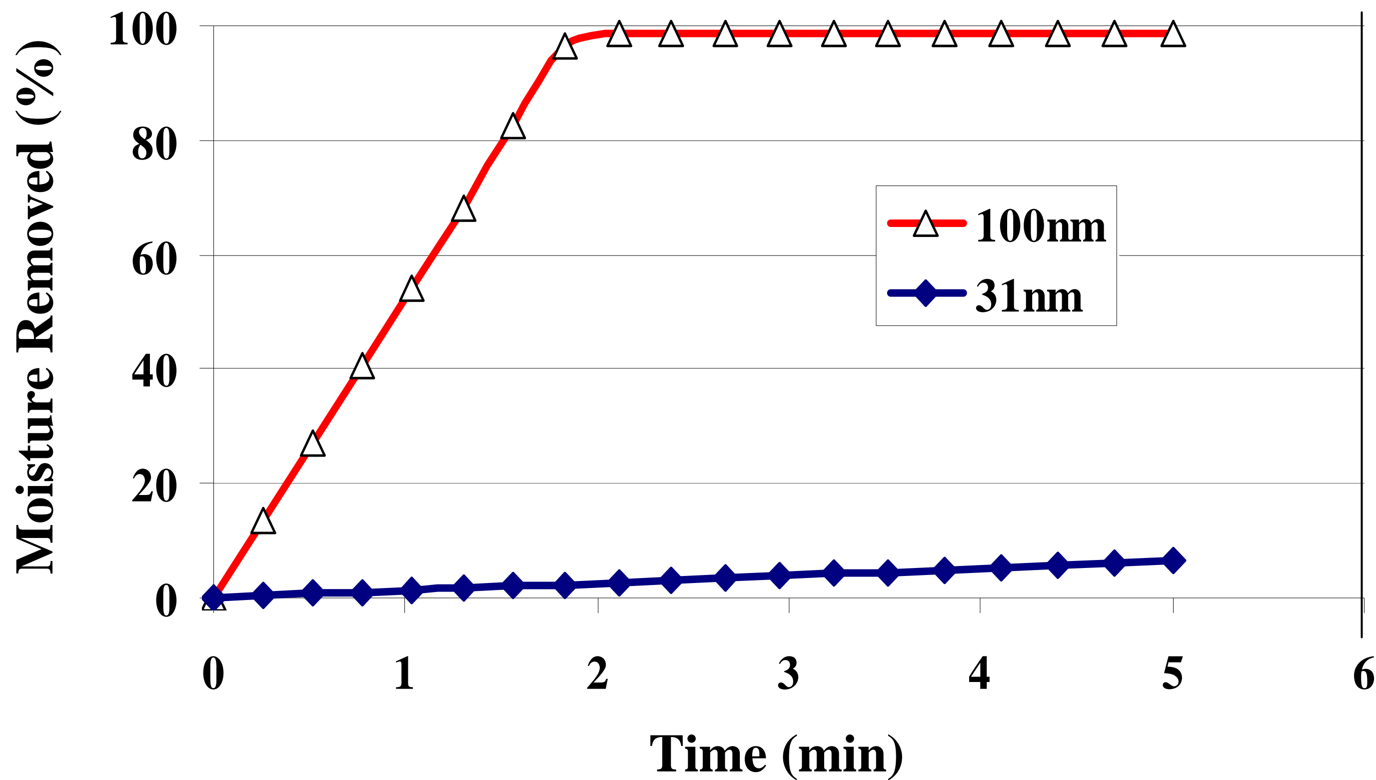

Dynamics of Drying of Nano-Structures

Feature Size Dependence

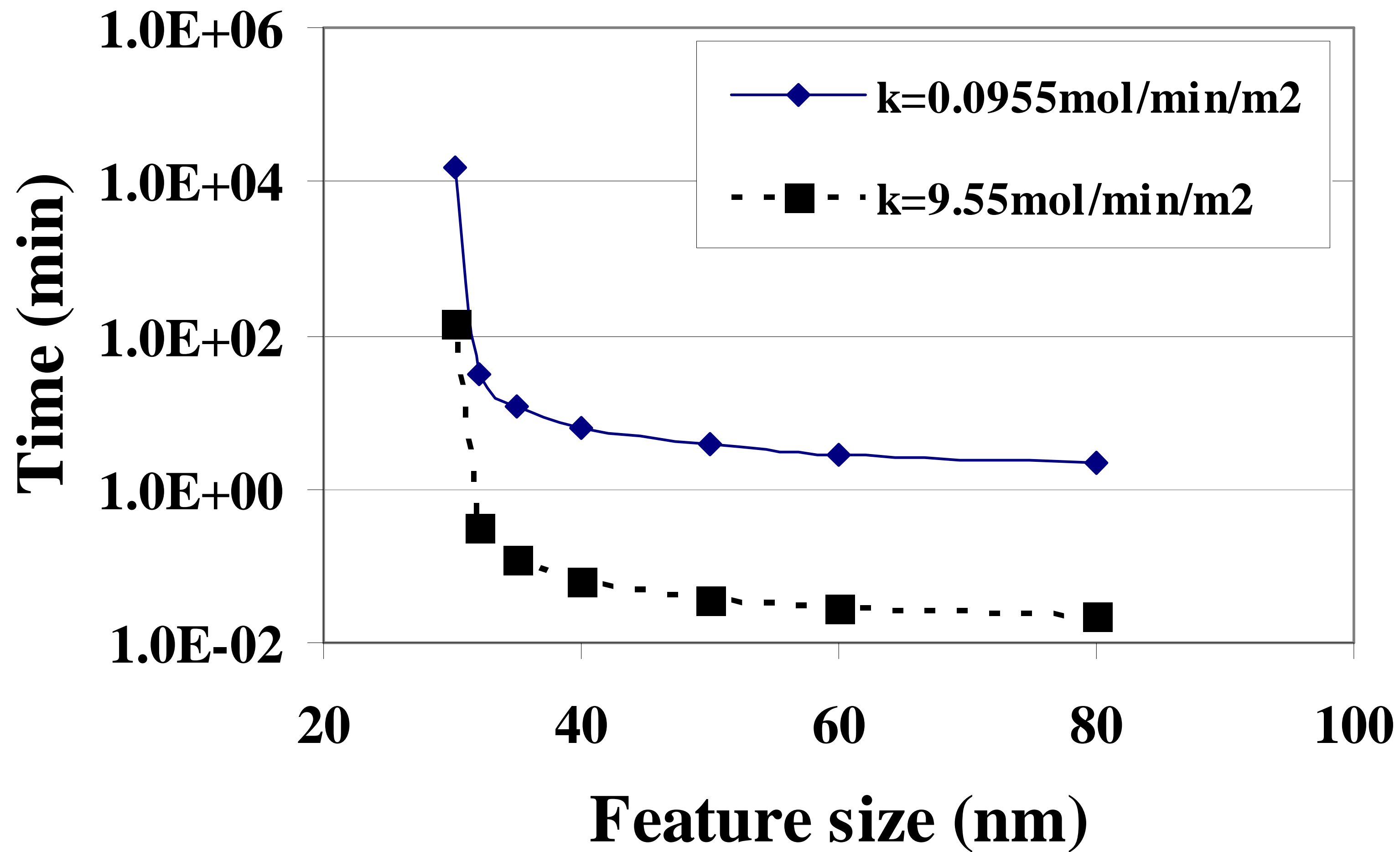

Cleaning of Micro- and Nano-Structures

- **Etching creates residues on the sidewalls of the trenches and vias.**
- **Side wall cleaning becomes more complex, more difficult, and more resource intensive as we move further into manufacturing of high-aspect-ratio nano-features**
- **No in-situ sensor is available for on-line monitoring of residues; ECRS would result in significant reduction is use of cleaning chemicals.**

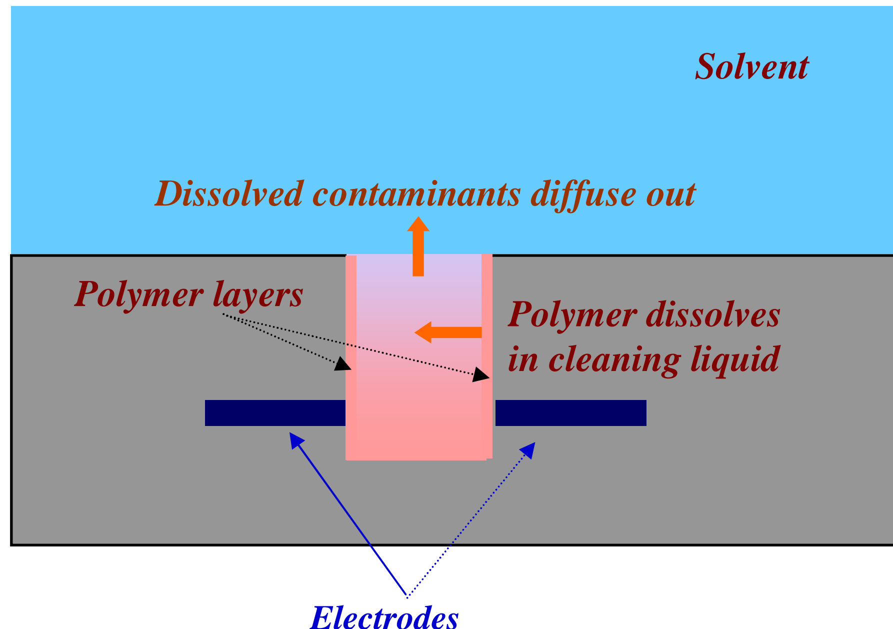

Cleaning of Micro- and Nano-Structures

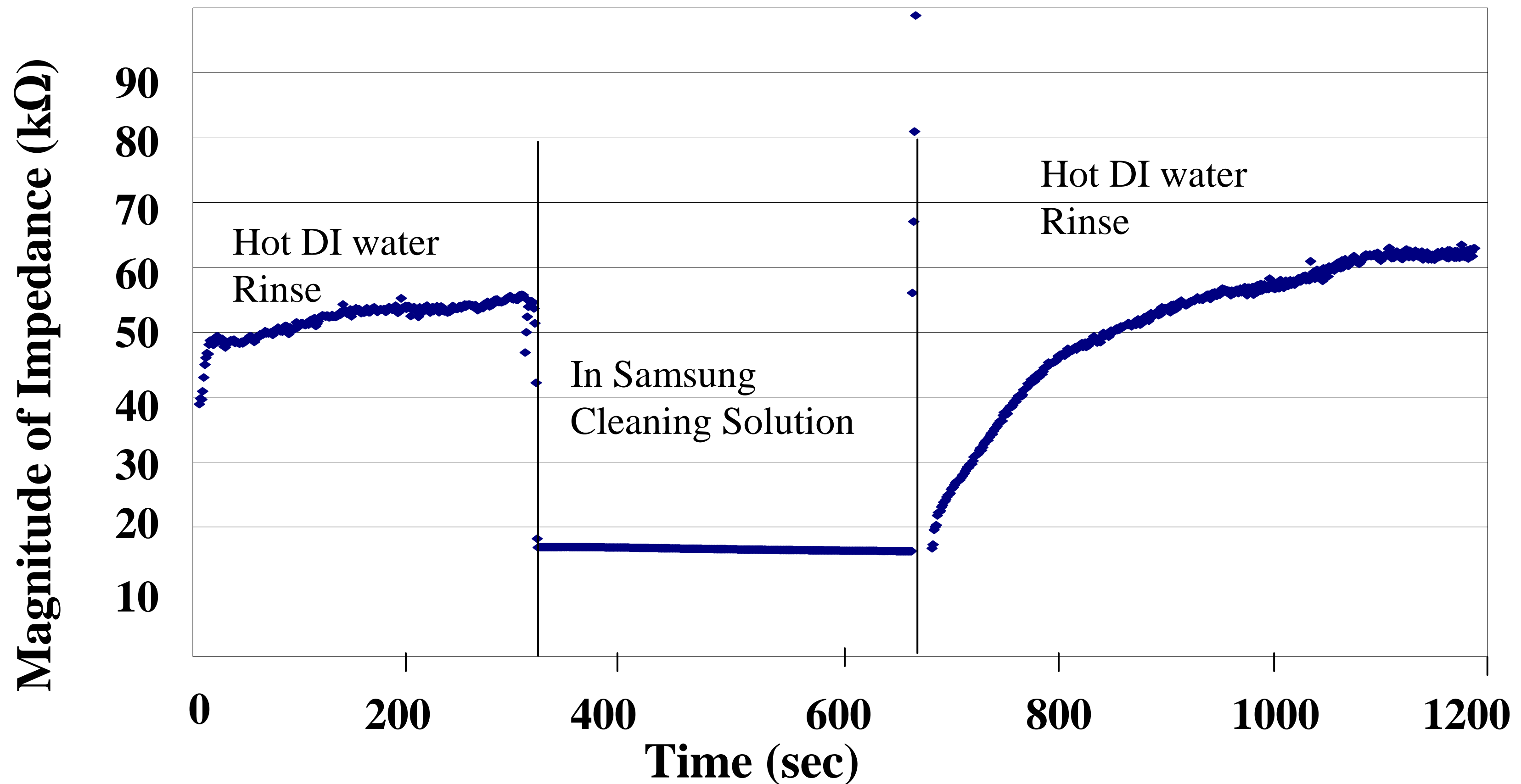

ECRS can monitor cleaning of the polymer residue inside trench

Cleaning of Micro- and Nano-Structures

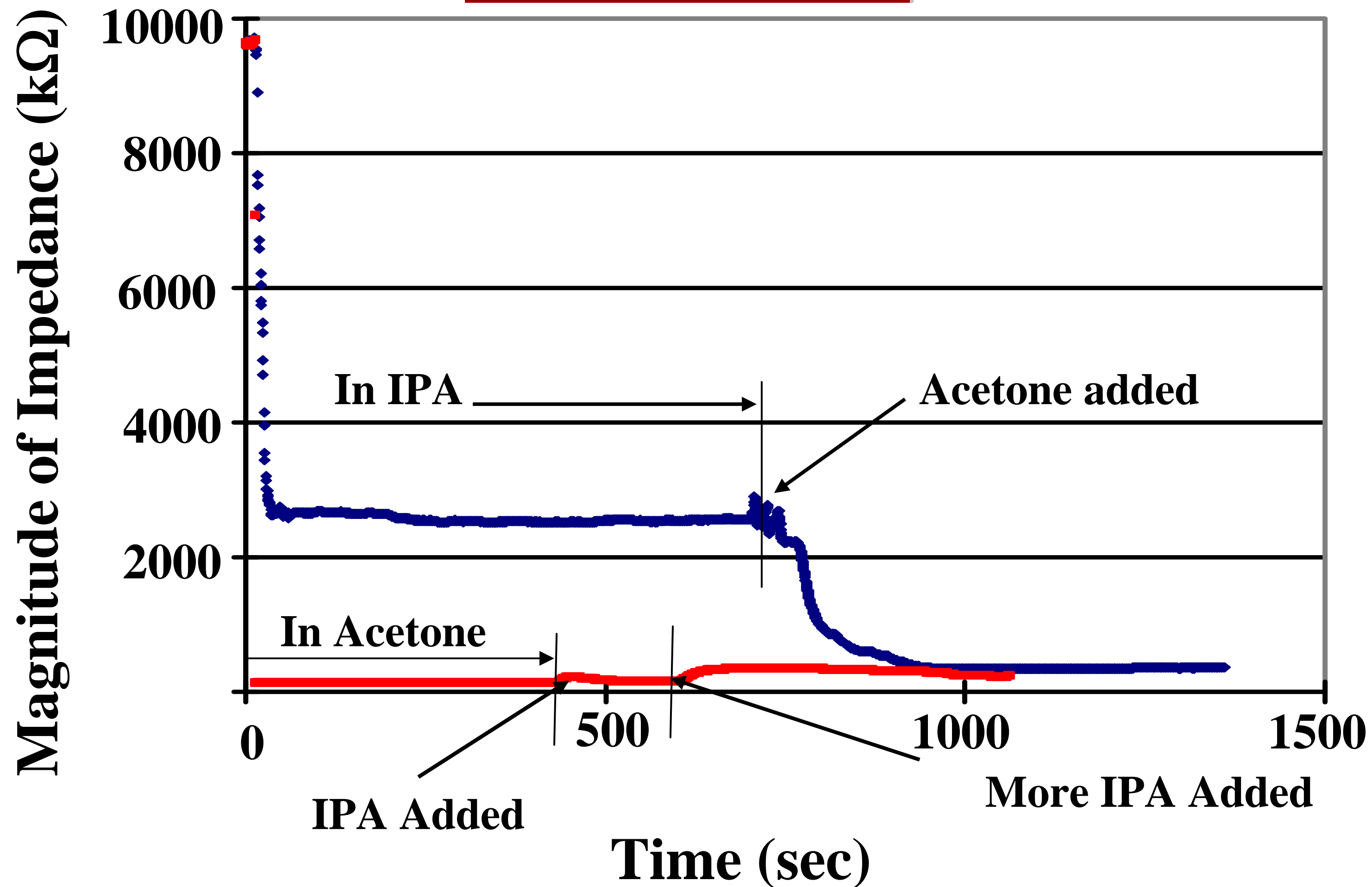

Future Plans and Industrial Interactions

- **Continue work on development of methods for monitoring the process of cleaning of nano-structures and lowering the chemical usage (joint work with EMC and Samsung).**
- **Continue work on development of low-water rinse methods using in-situ process metrology/control (joint work with EMC, Freescale, and Samsung).**
- **Fundamental work on a novel wireless metrology version of ECRS**

Presentations, Awards

- **Dhane, K., Yan, J., Vermeire, B., Shadman, F., "*In-Situ and Real Time Metrology during Cleaning, Rinsing and Drying of Micro- and Nano Structures*", TECHCON, September 2007**

❖ **Selected as the Best Paper in Session, TECHCON, September 2007**

Environmentally-Friendly Cleaning of New Materials and Structures for Future Micro- and Nano-Electronics Manufacturing

(*Task Number: 425.022*)

Subtask: Post Etch Residue Removal in Copper Damascene Structures

PI:

- **Srini Raghavan, Materials Science and Engineering, University of Arizona**

Graduate Student:

- **Nandini Venkataraman, PhD candidate, Materials Science and Engineering, University of Arizona**

Objectives

- **Evaluate and optimize chemical systems having low solvent and fluoride content, for the selective removal of copper oxides (CuO_X) over copper and dielectric**
- **Understand the mechanism of removal of copper oxide films on copper using electrochemical impedance spectroscopy**

ESH Metrics and Impact

- *ESH objective:* Reduction of solvent content in semi aqueous fluoride (SAF) based solutions for removal of post etch residue

Solution components	Weight % in typical formulations	Weight % in best formulation in this study	% Reduction
Solvent Water Fluoride	> 60% < 40% ~ 1-2%	29% 71% 1%	> 50% - 35% (increase) 0 – 50%

- The project will ultimately lead to the development of all aqueous chemical systems

Experimental Approach

- **Samples**
  - CuO_X films of controlled thicknesses formed by thermal oxidation of copper blanket wafers at 300^0C
- **Selection of Chemical Systems**
  - Semi aqueous solutions containing Dimethyl Sulfoxide (DMSO), NH_4F and water, buffered with oxalic acid in the pH range of 4-6
  - Variables studied for optimization: pH (Natural pH, 5, 6), DMSO content (0% to 69%)
- **Determination of Removal Rates**
  - CuO_X and Cu removal rates determined by solution analysis using Atomic Absorption Spectrophotometry
  - Removal Rate of TEOS determined by Ellipsometry
- **Electrochemical Impedance Spectroscopy**
  - Impedance measurements of CuO_X films and patterned wafer structures in various cleaning formulations performed by multi- sine technique using PARSTAT 2273 potentiostat/impedance analyzer
  - Equivalent circuit fitting performed using ZView software (Version 2.b)

Removal Rates of Copper Oxides

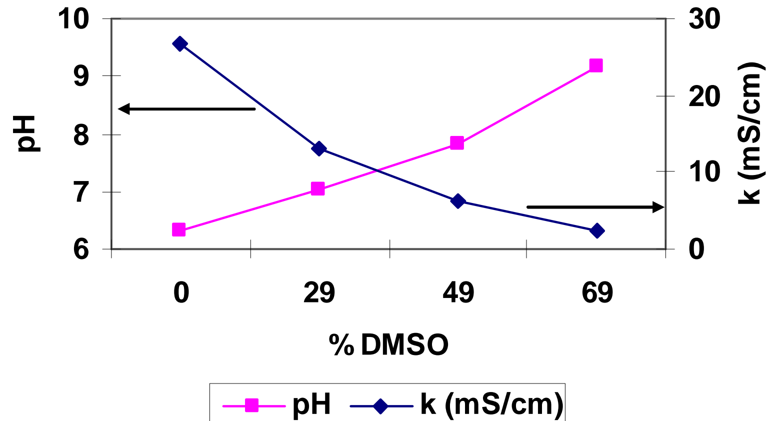

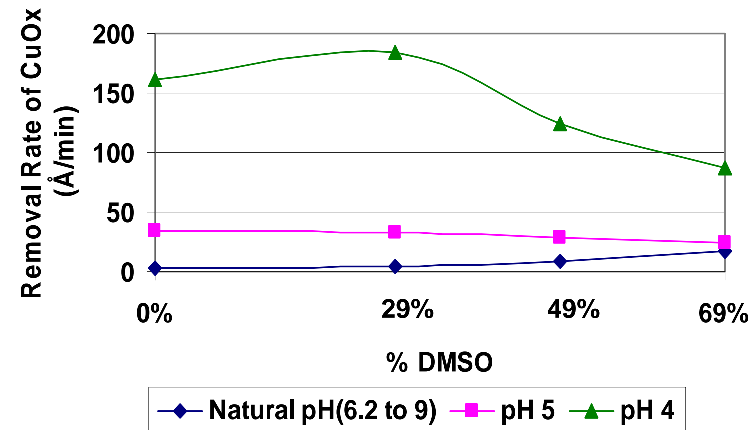

- **Effect of pH**
  - Removal rate is a strong function of pH
  - Increase in removal rate with decrease in pH
- **Effect of DMSO concentration**
  - Above 29% DMSO, removal rate decreases

•1 wt% NH_4F in all formulations

• pH increases and conductivity decreases with increase in DMSO concentration

•At pH 4, removal rate ~ 160 Å/min for DMSO concentration ≤ 29%

Selective Removal of CuO_X over Cu and TEOS

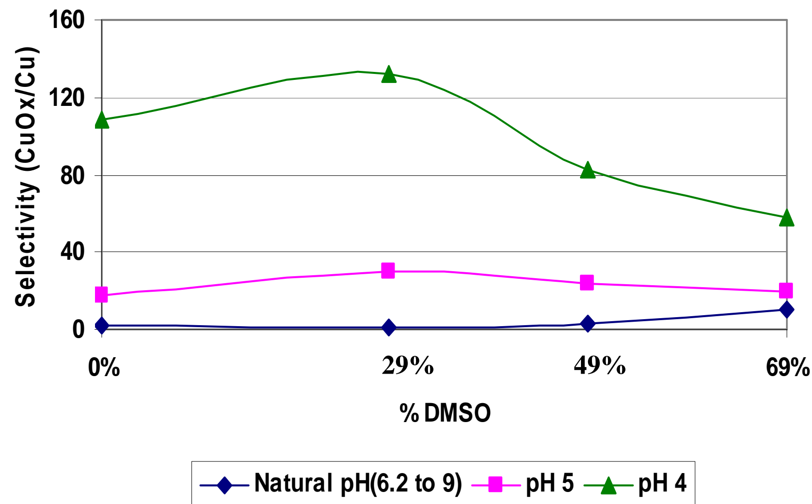

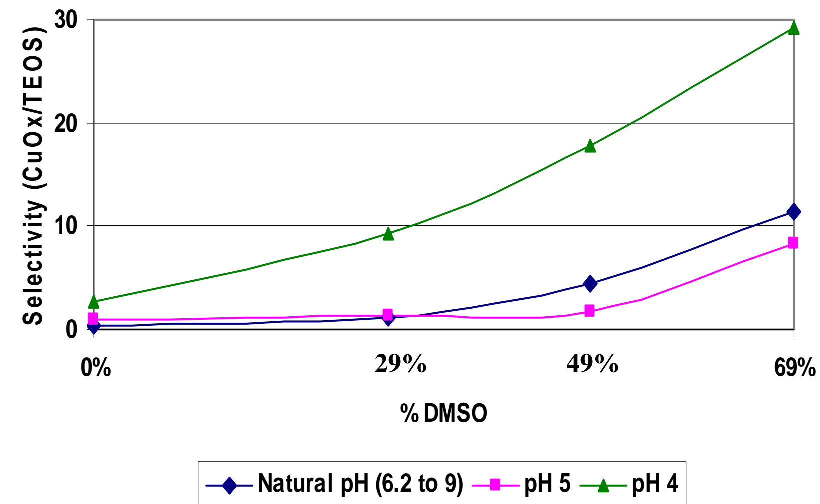

CuO_X/Cu selectivity:

- Removal rate of Cu < 3Å/min in most cases
- **pH:** Decrease in pH increases CuO_X/Cu selectivity
- **DMSO content**: Better selectivity for DMSO concentration ≤ 29%
- Highest selectivity of ~ 130:1 in solutions containing 29% DMSO at pH 4

CuO_X/TEOS selectivity:

- **DMSO:** Decrease in selectivity with increase in DMSO content
- **pH:** Reducing pH increases TEOS and CuO_X removal rate
- CuO_X removal is a stronger function of pH than TEOS removal
- Highest selectivity of ~ 30:1 obtained in solutions containing 69% DMSO at pH 4

Solution containing 29% DMSO and 1% NH_4F at pH 4 provides CuO_X removal rate of 180 Å/min with CuO_X/Cu selectivity of ~ 130:1 and CuO_X/TEOS selectivity of ~ 10:1

Electrochemical Impedance Spectroscopy

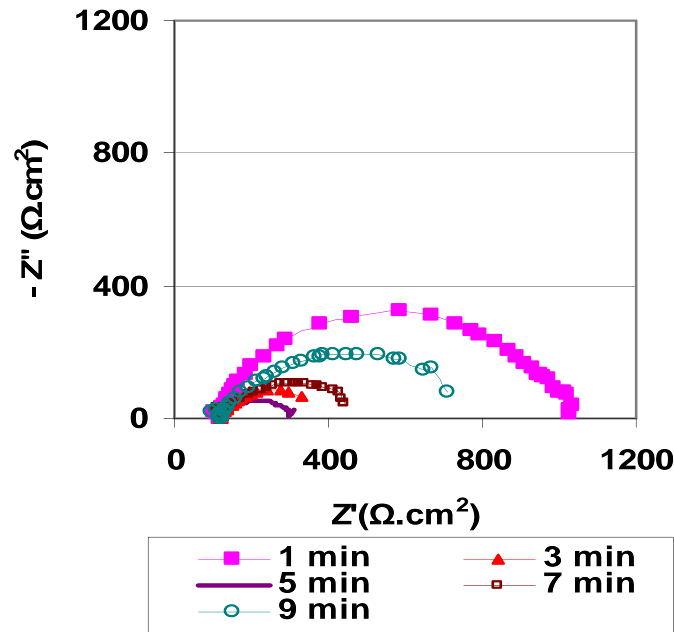

Impedance Spectra of CuO_X film as a function of time in solution containing 49% DMSO, 1% NH_4F and 50% H_2O (pH 4)

Ω

- **Sample:** CuO_X film of thickness ~55 nm
- **Electrochemical Setup**
  - Working Electrode – CuO_X film
  - Reference Electrode – Pt wire (quasi reference)
  - Counter Electrode – Pt foil
- Amplitude of AC signal: 5 mV rms
- Measurement frequency range – 10^5 Hz to 0.1 Hz
- Impedance spectra consists of a single depressed semicircle
- Semicircle diameter decreases first and then increases after a certain duration

Equivalent Circuit Modeling

Uniform Dissolution Model

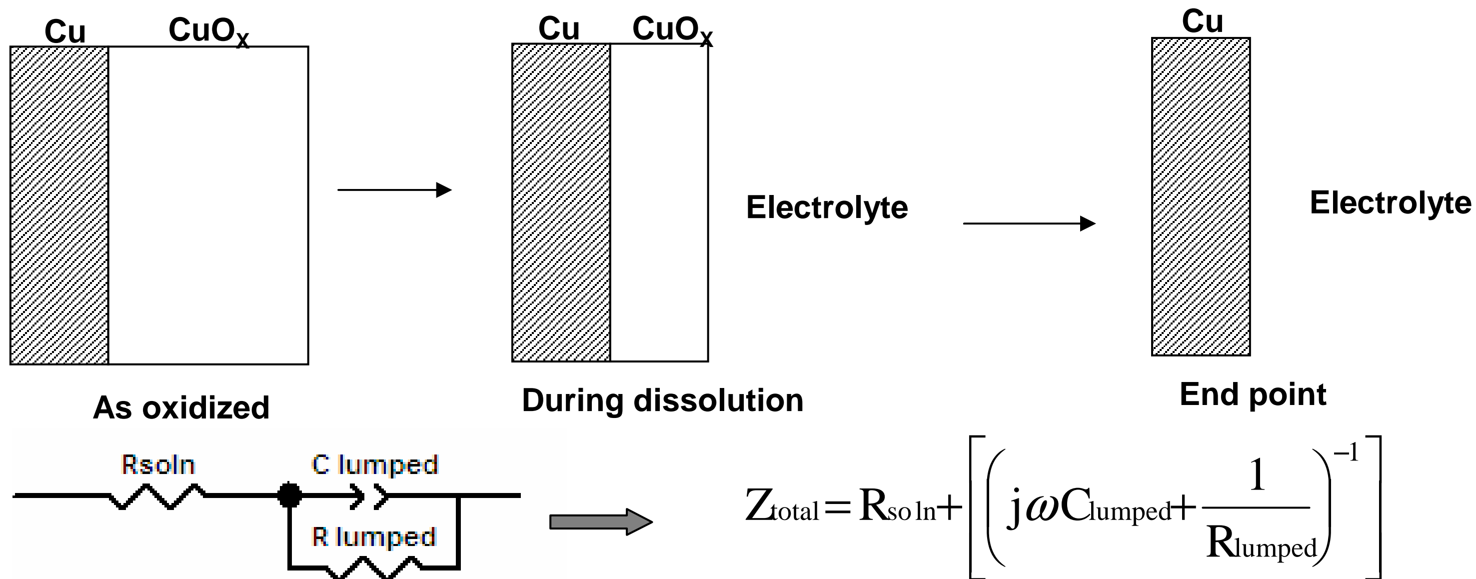

$$Z_{total} = R_{soln} + \left[\left(j\omega C_{lumped} + \frac{1}{R_{lumped}} \right)^{-1} \right]$$

- Lumped parameter model; exhibits excellent fit to the impedance data
- Major contributions to C_{lumped}: Double layer capacitance at CuO_X/electrolyte interface (C_{dl}) and film capacitance (C_{oxide})
- Major contributions to R_{lumped}: Charge transfer resistance at interface (R_{ct}) and film resistance (R_{oxide})
- C_{dl} and R_{ct} expected to be nearly constant during dissolution; Typical values of $C_{dl} \approx$ 10-50 $\mu F/cm^2$
- C_{oxide} and R_{oxide} depend on thickness of the film
- $C_{oxide} = \varepsilon\varepsilon_0 A/d$; $R_{oxide} = \rho d/A$

Uniform Dissolution Model

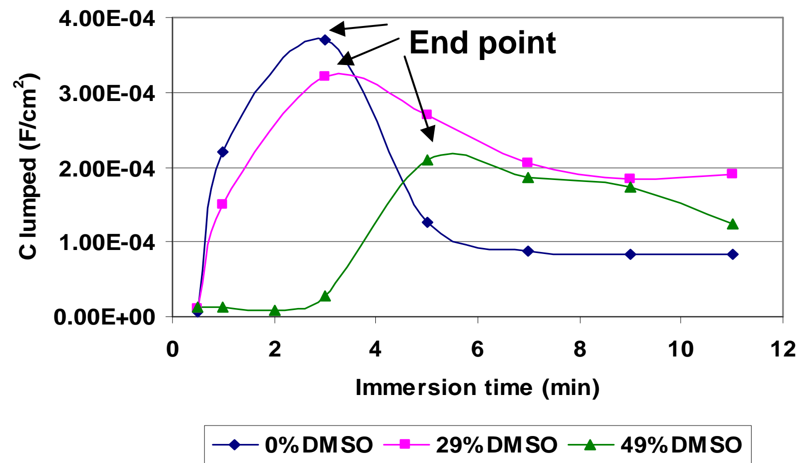

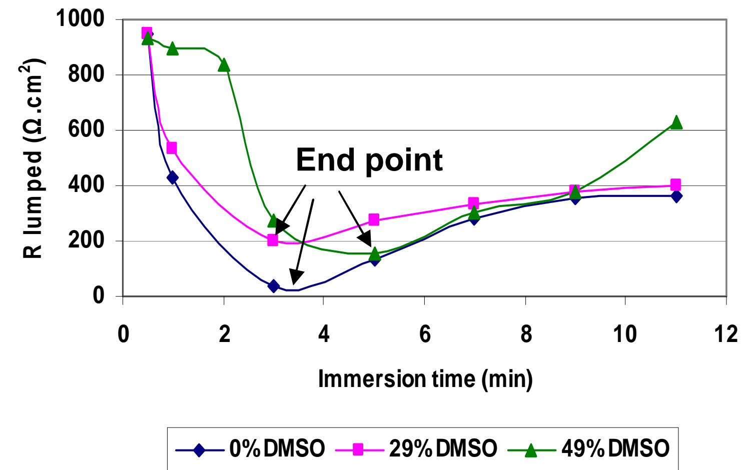

- Formulations contain 1% NH_4F and maintained at pH ~ 4
- During dissolution
  - Increase in C_{lumped} attributed to decrease in film thickness (increase in C_{oxide} contribution)
  - Decrease in R_{lumped} attributed to decrease in R_{oxide}
- At end point
  - C_{lumped} mainly due to C_{dl} at Cu/electrolyte interface
  - R_{lumped} mainly due to R_{ct} at Cu/electrolyte interface
- Beyond end point
  - Decrease in C_{lumped} and increase in R_{lumped} attributed to adsorption/repassivation of the surface (possibly reoxidation)

Porous Film Model

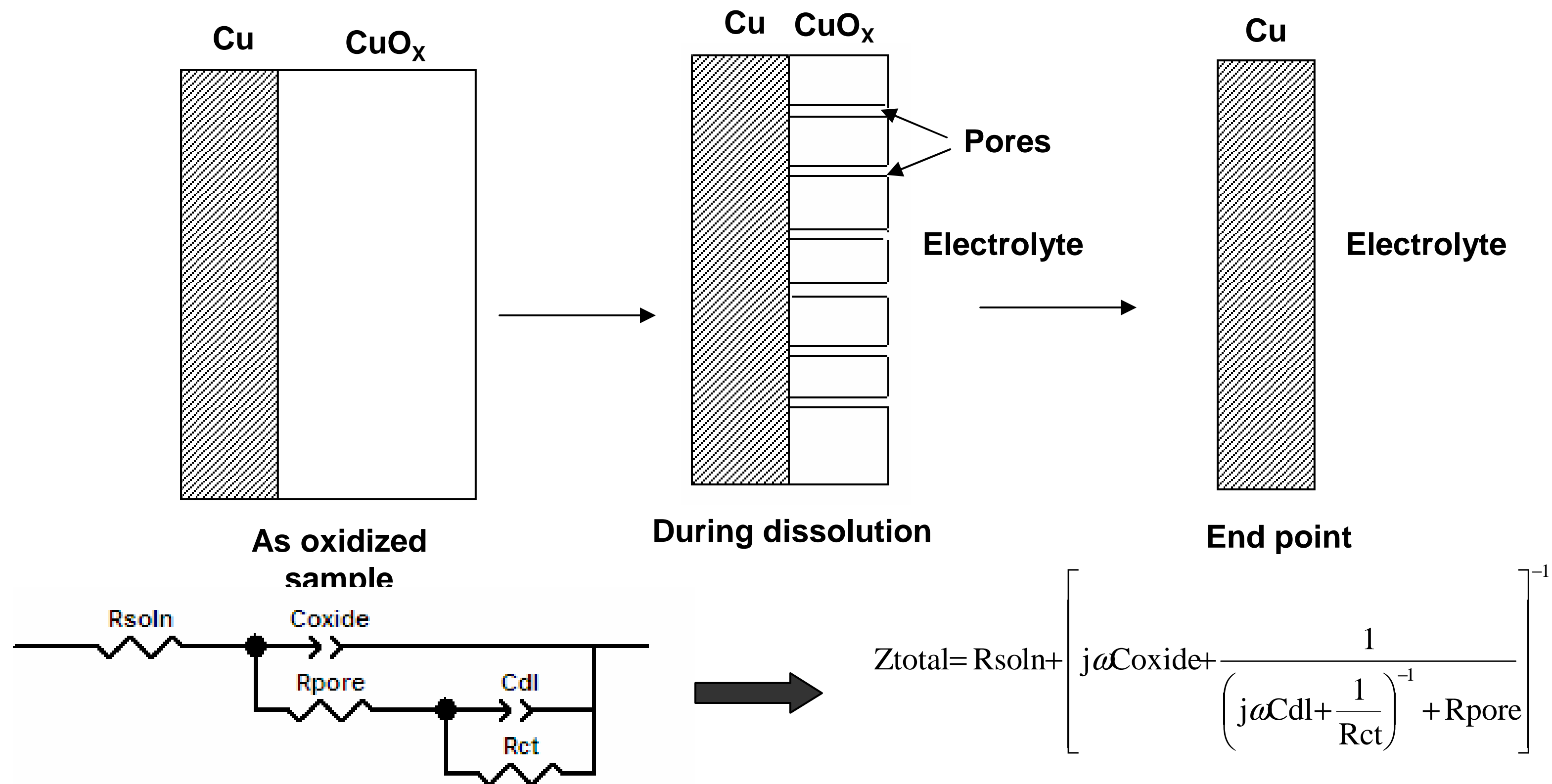

$$Ztotal = Rsoln + \left[j\omega Coxide + \frac{1}{\left(j\omega Cdl + \frac{1}{Rct} \right)^{-1} + Rpore} \right]^{-1}$$

- Also provides excellent fit to acquired data
- **Model Features:**
  - Pores develop in passive CuO_X film during dissolution; underlying copper exposed to solution
  - Charge transfer at Cu/electrolyte interface
  - Porosity of the film increases as dissolution occurs

Porous Film Model

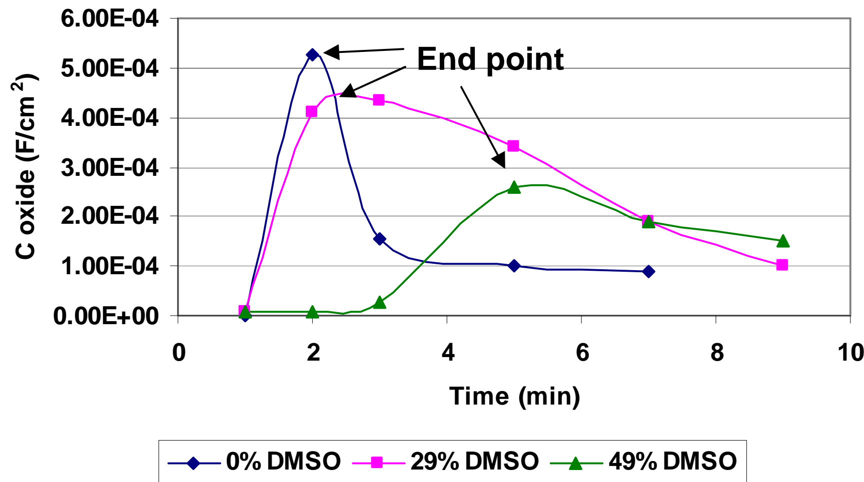

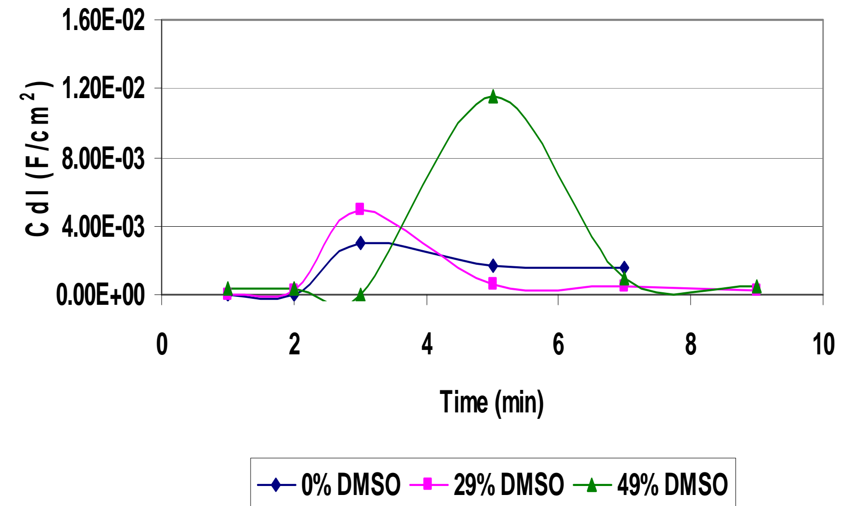

- Increase in C_{oxide} during dissolution due to loss of oxide
- After end point, decrease in C_{oxide} due to repassivation
- Increase in C_{dl} during dissolution, due to increase in exposed Cu area (increase in porosity)
- Values of C_{dl} abnormally high to represent double layer capacitance – reasons are being investigated

Patterned Test Structure

(Developed at Intel D2 fab, Santa Clara)

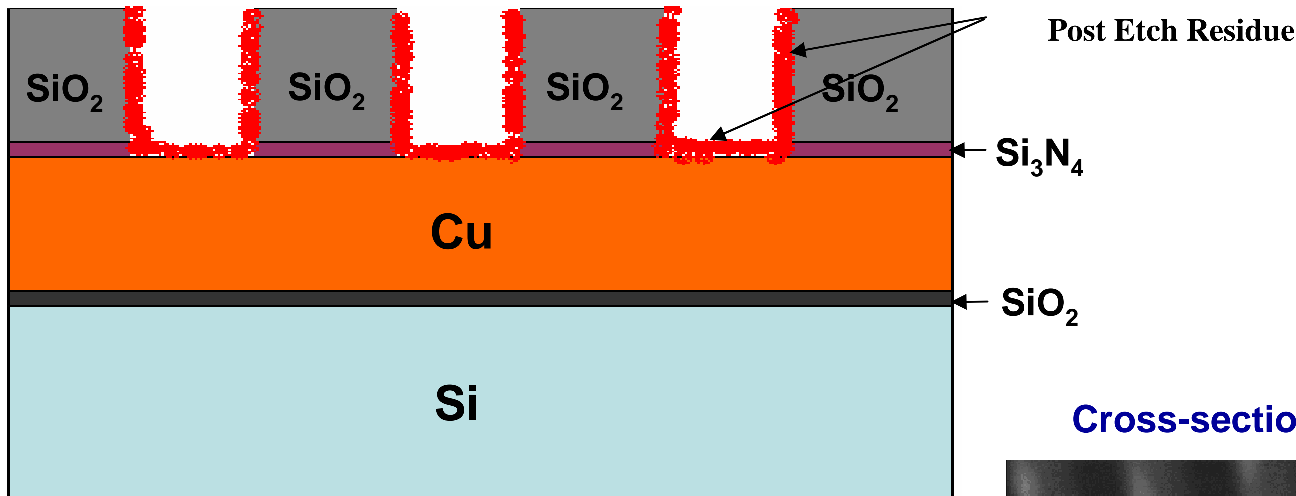

Cross-sectional SEM of test structure

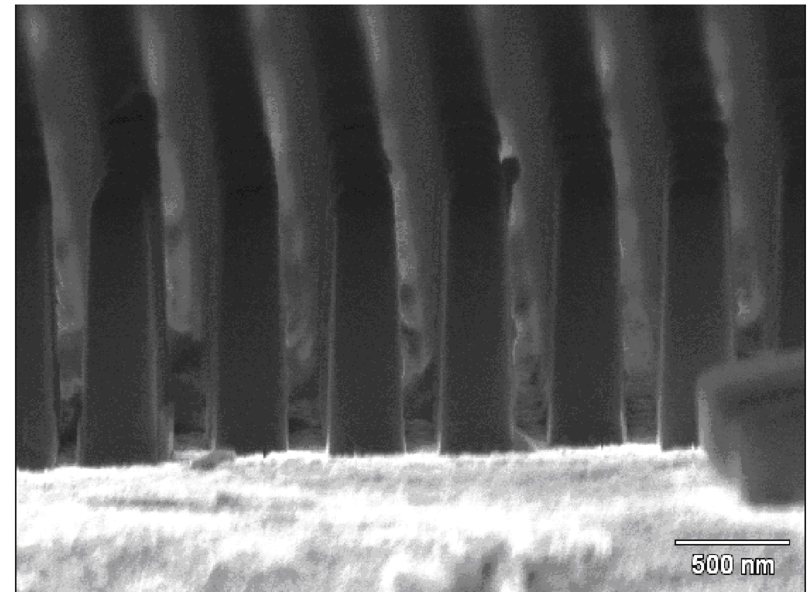

- Patterned test structures contain vias plasma etched in SiO_2
- Width of vias ~ 180 nm
- Aspect ratio ~ 4:1
- Ongoing work
  - End point detection in patterned structures by Electrochemical Impedance Spectroscopy
  - Impedance data is being acquired and various models are under investigation

Summary

• Selective removal of CuO_X over copper and dielectric in buffered DMSO, NH_4F based chemical systems has been systematically investigated

• CuO_X removal rate of ~180 Å/min with CuO_X/Cu selectivity of ~ 130:1 and CuO_X/TEOS selectivity of ~ 10:1 has been obtained in 1% NH_4F solutions containing 29% solvent at pH 4.

• Reasonable selectivity over TEOS requires some amount of DMSO

• Electrochemical Impedance spectroscopy and equivalent circuit modeling has been used to detect end point of copper oxide removal in DMSO, NH_4F based chemical systems

Industrial Interactions

- Patterned test structures were developed at Intel Corp., Santa Clara with the assistance of Dr. Liming Zhang, Dr. Zhen Guo and Dr. Michael Ru
- Telephone discussions with Dr. Liming Zhang, Dr. Zhen Guo and Dr. Michael Ru, Intel Corp., Santa Clara
- Discussions with Dr. Robert Small, R.S. Associates, Tucson

Future Plans

Next Year Plans

- Improve selectivity towards TEOS in solutions with very low or no solvent content
- Perform detailed Electrochemical Impedance Spectroscopy investigations on the patterned test structures
- Study rinsing processes

Long-Term Plans

- Identify and investigate novel aqueous chemical systems, compatible with low k materials, for post etch residue removal

Publications, Presentations, and Recognitions/Awards

Publications

- N. Venkataraman, A. Muthukumaran, S. Raghavan, "Evaluation of Copper Oxide to Copper Selectivity of Chemical Systems for BEOL Cleaning Through Electrochemical Investigations", **Mater. Res. Soc. Symp. Proc.** Volume 990, Paper # 0990-B08-25, 2007

Awards

- **AMAT Graduate Fellowship** awarded to Nandini Venkataraman by Applied Materials, Santa Clara, for 2007-2008

Environmentally-Friendly Cleaning of New Materials and Structures for Future Micro- and Nano-Electronics Manufacturing

(*Task Number: 425.022*)

Subtask: Cleaning and Drying of Dielectrics

PI:

- **Farhang Shadman, Chemical and Environmental Engineering, UA**

Graduate Students:

- **Harpreet Juneja: PhD candidate, Chem & Env Eng, UA**
- **Junpin Yao: PhD candidate, Chem & Env Eng, UA**
- **Asad Iqbal: PhD, Chem Eng, UA, graduated 2007 (currently with Intel)**

Undergraduate Students:

- **Paul Swift: Chem & Env Eng, UA**

Cost Sharing:

- **Sematech (samples)**
- **TI (samples; joint work with Dr. Tsui)**

Objectives

- Determine the fundamentals of the dynamics of moisture uptake and removal in both blanket and processed dielectric films. This will assist in the selection and integration of these dielectrics in semiconductor processing.
- Develop experimental techniques and process models for minimizing both chemical and energy usage during the cleaning and outgassing of low-k films.

ESH Metrics and Impact

Illustration of significant impact on reducing cost and usage of purge gas, chemicals, and energy by applying the project results

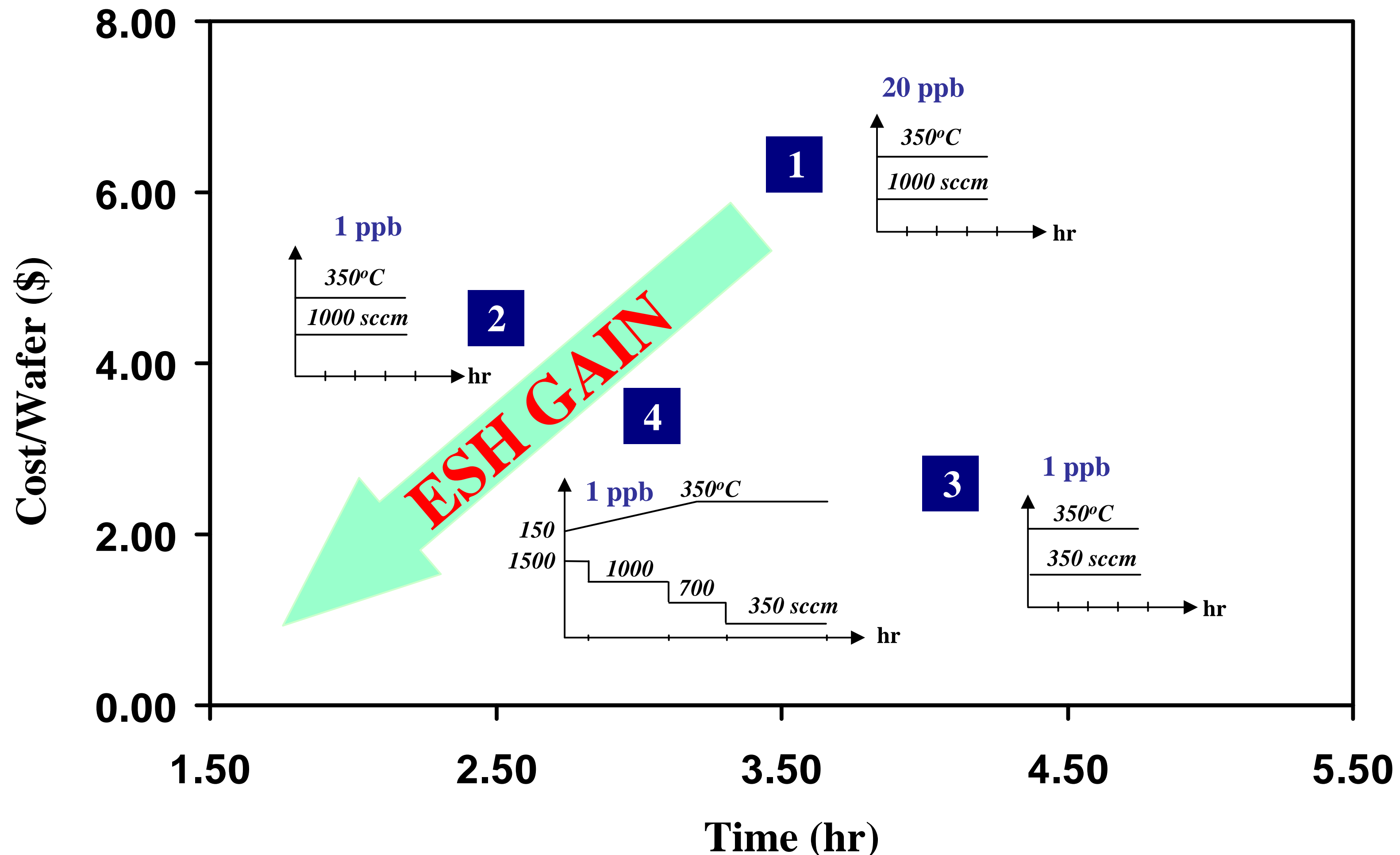

Experimental Setup

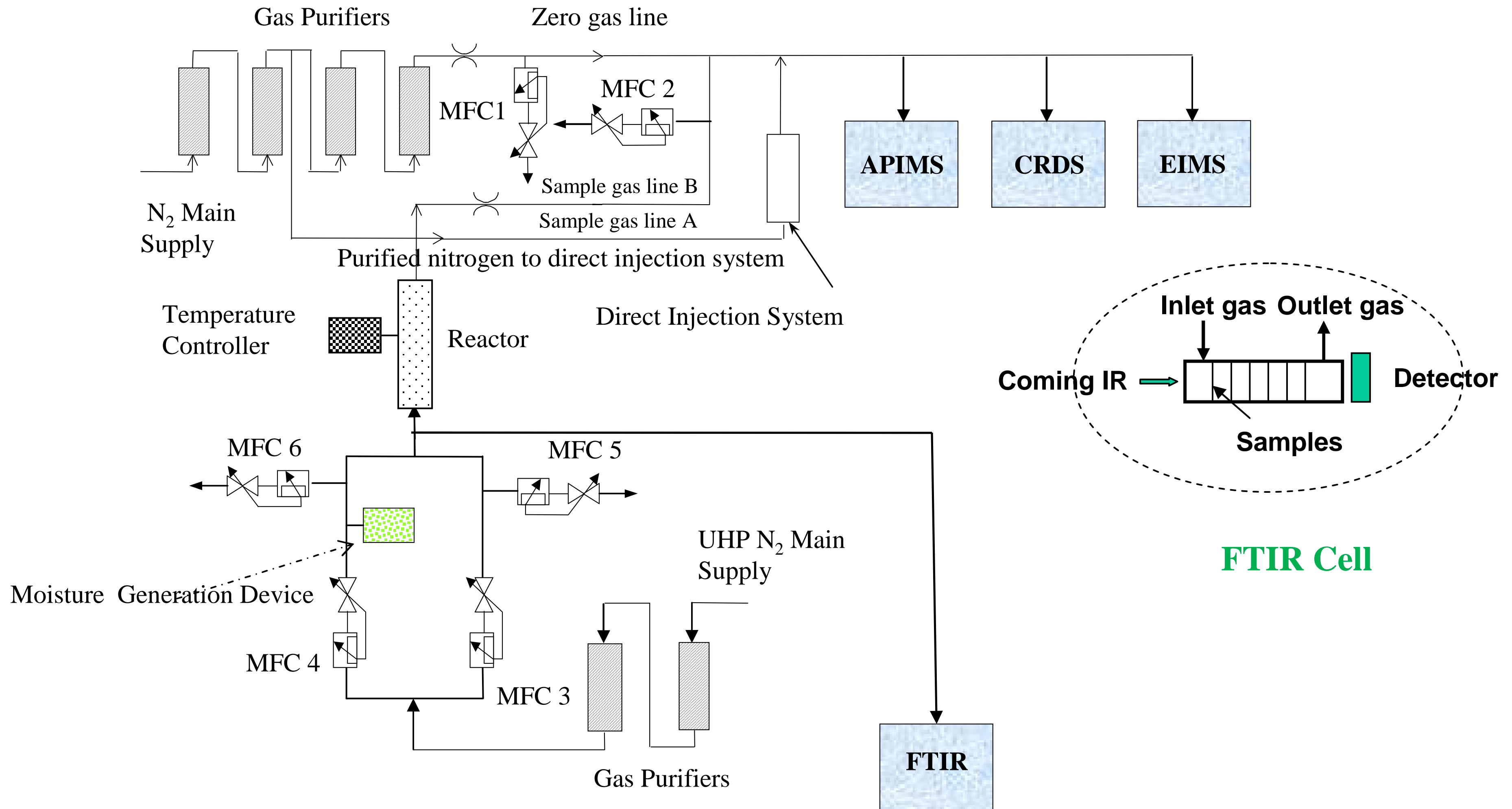

Experimental Procedure

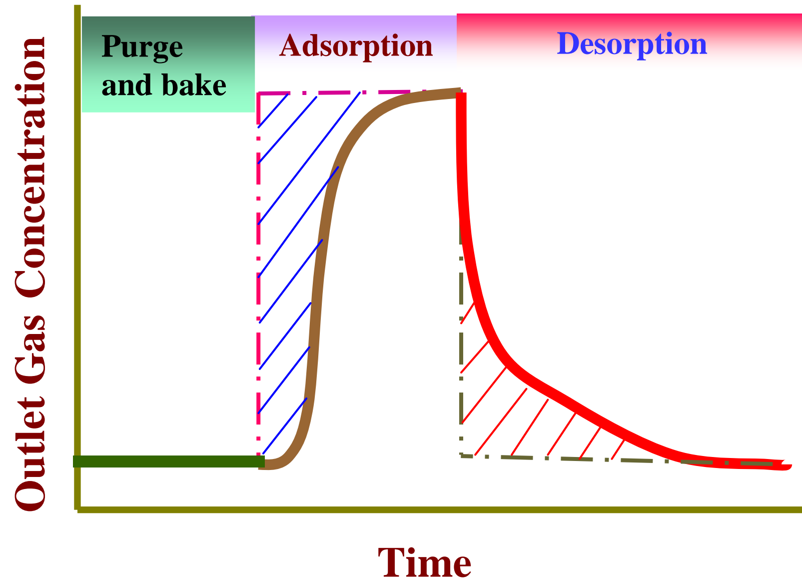

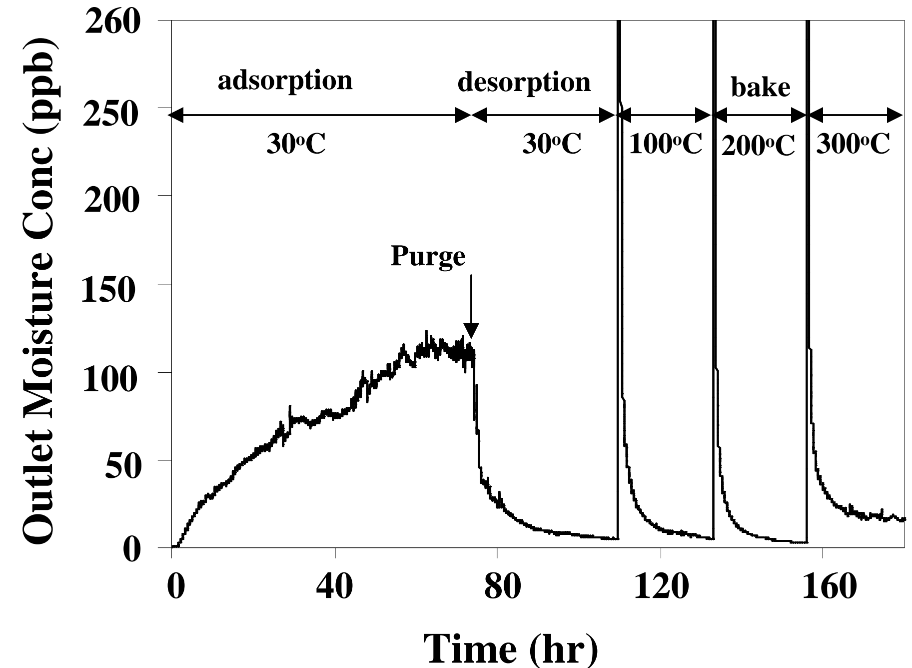

Experimental procedure

Adsorption at 30°C; then desorption at 30°C; followed by bake-out at 100, 200 & 300°C

Temporal profile

Exposure to 110 ppb moisture; followed by temperature-programmed desorption

Contamination with Low-k Materials

Potential issues associated with moisture contamination of low-k materials:

- **Increase in k values, create adhesion problems, and cause reliability issues.**
- **Signal propagation delays and cross-talk between interconnects.**

*k value and Si-OH**

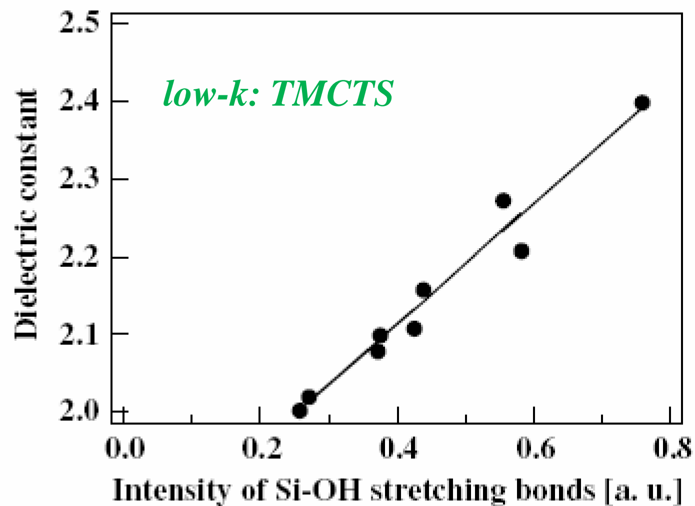

*Y. Uchida et al. / Microelectronic Eng. 83(2006)

O-H stretching Bonds include:

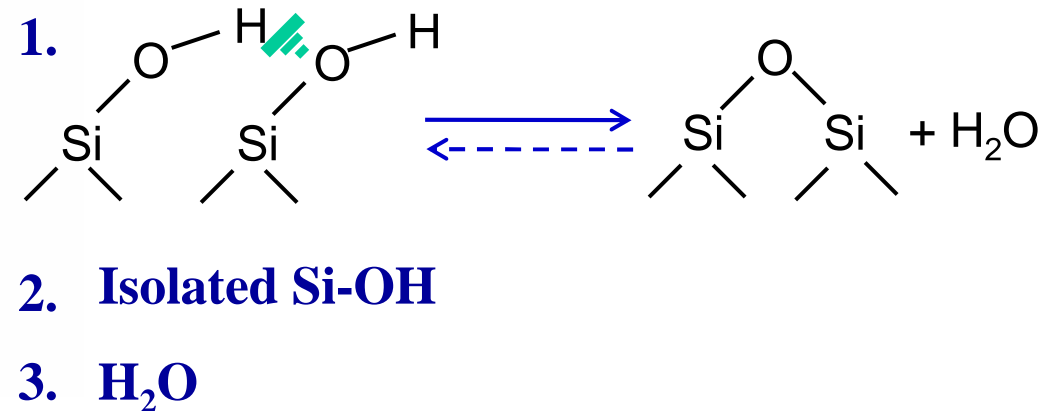

2. **Isolated Si-OH**
3. **H_2O**

Purge Performance of FTIR Cell

Peak signature: CH_3 stretches, 2950 – 3000 cm^{-1}

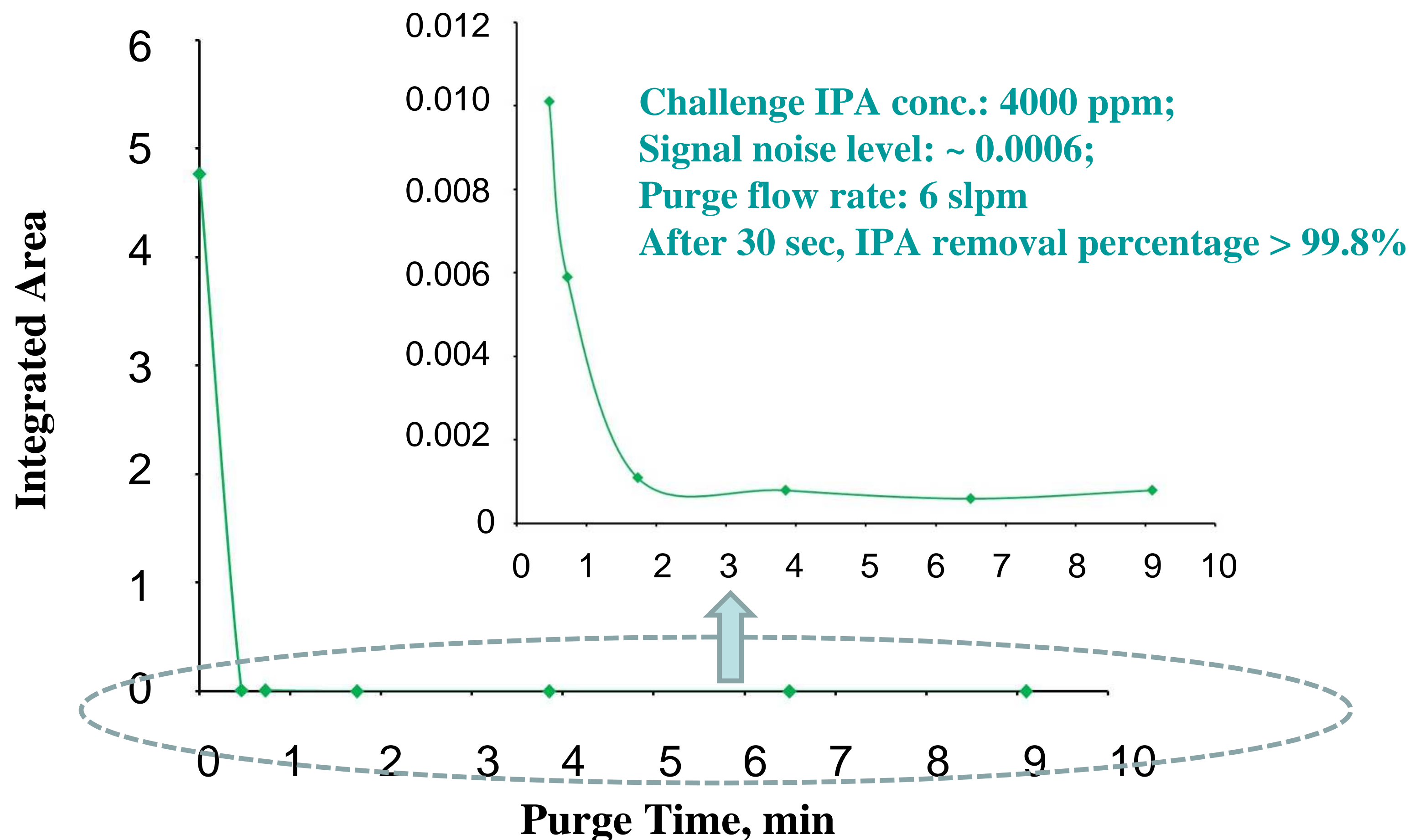

The cell is well purged, no accumulation of gas phase IPA in the cell

Dynamics of IPA Outgassing

Initially films were saturated with liquid IPA;

Peak signature: CH_3 stretches, 2950 – 3000 cm^{-1}

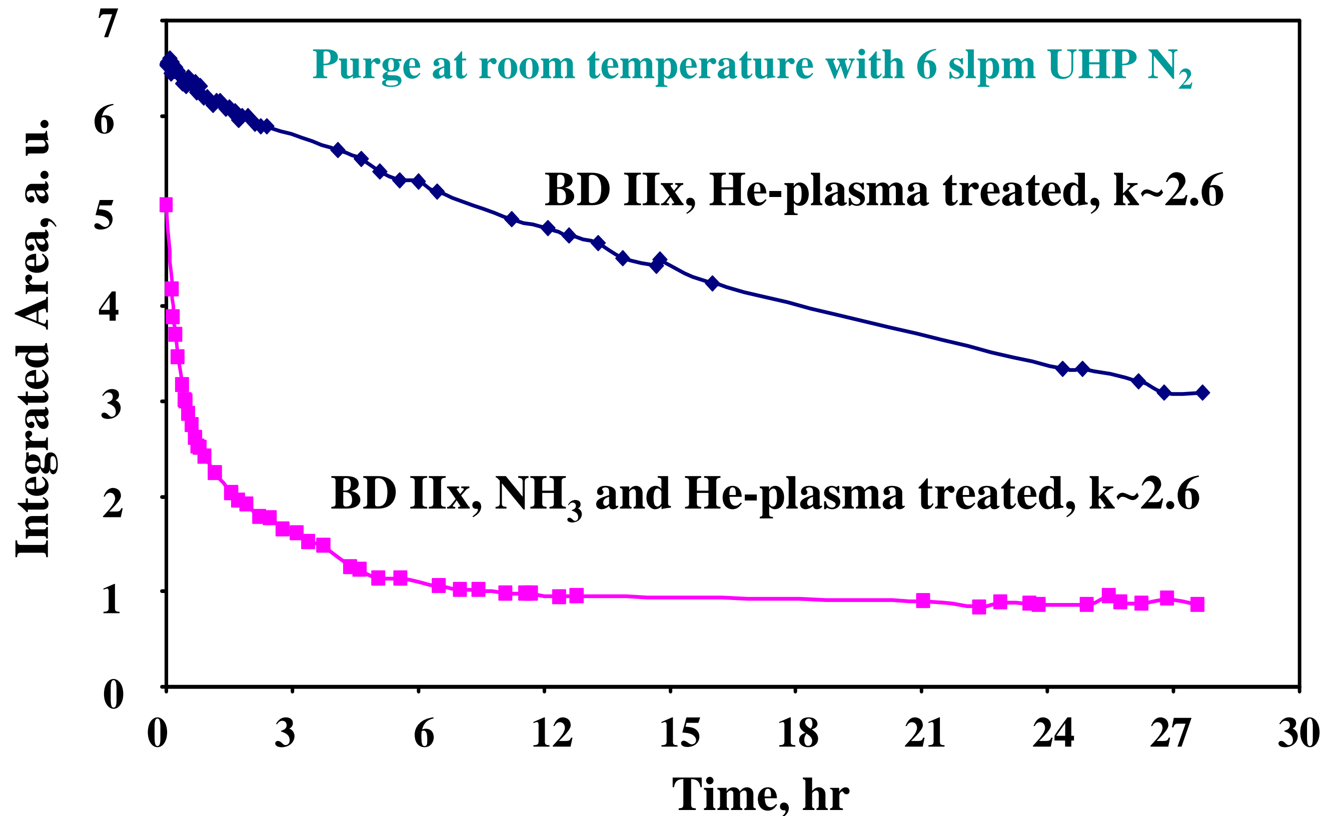

IPA removal is a slow process; plasma treatment changes film outgassing.

Purging/Cleaning of Low-k Films

Low-k: BD IIx, blanket and cured; p-MSQ, blanket and cured

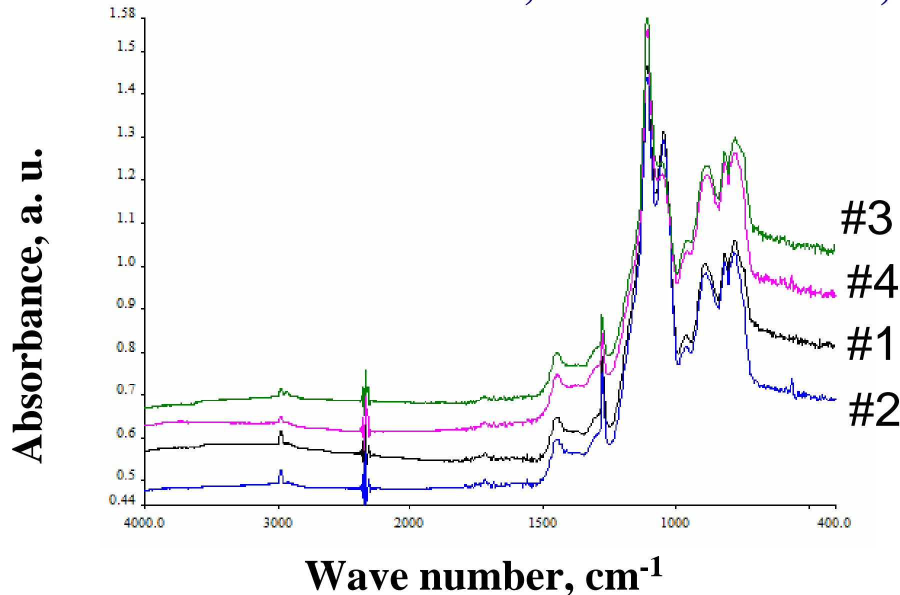

Cleaning: UHP N_2 at 200 °C for 10 hrs

O-H stretches: 3200-3700 cm^{-1}

CH_3 Stretches: 2950-3000 cm^{-1}

Area below the peaks	BD IIx		p-MSQ	
	As-received, #1	Cleaned, #2	As-received, #3	Cleaned, #4
O-H stretches	0.9428	0.2118	1.1320	0.0226
CH_3 Stretches	0.5979	0.5640	0.2912	0.2797

-OH intensity in the film decreases significantly after outgassing

Dynamics of Moisture Outgassing

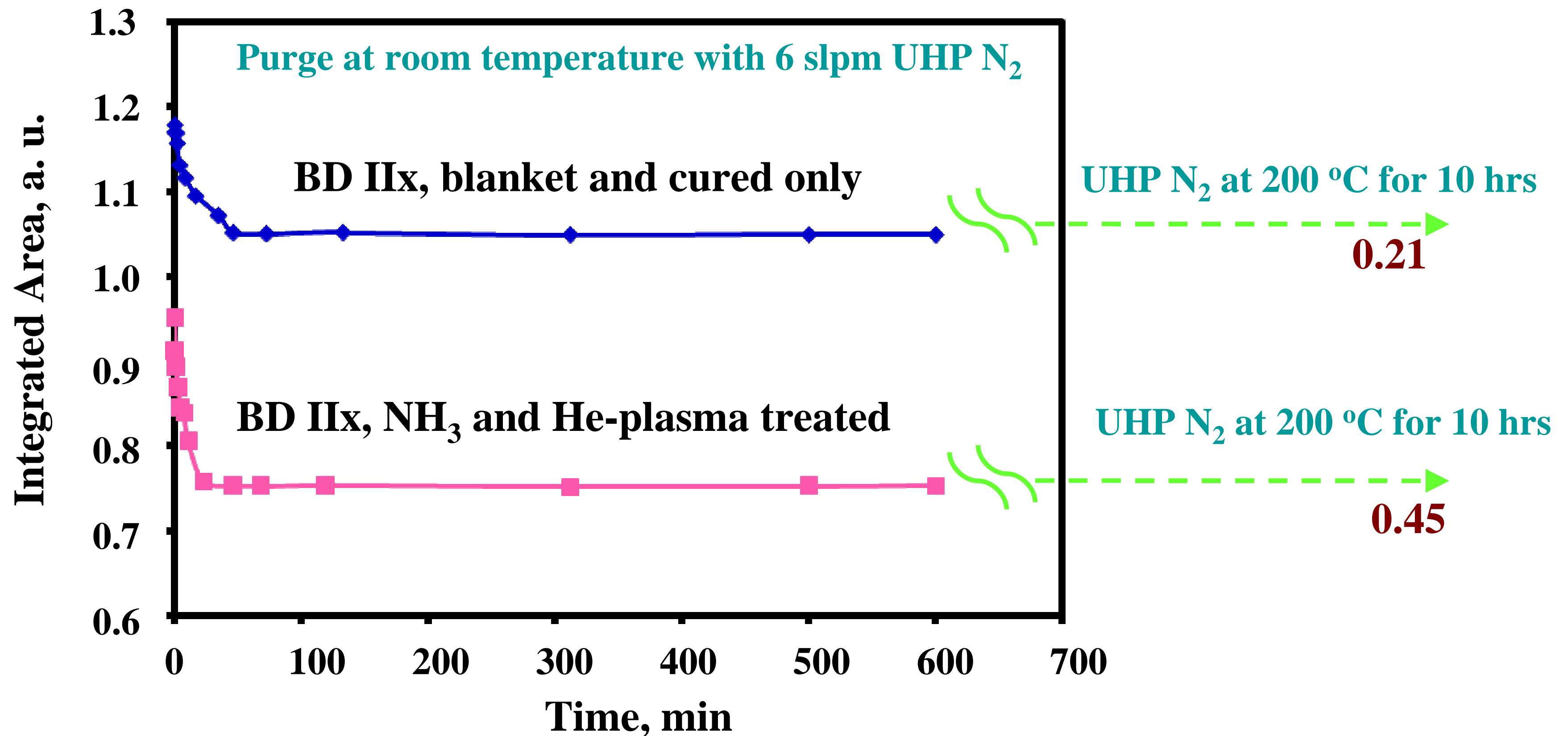

Moisture removal is a slow and activated process

Removal of Moisture and Organic Contaminants

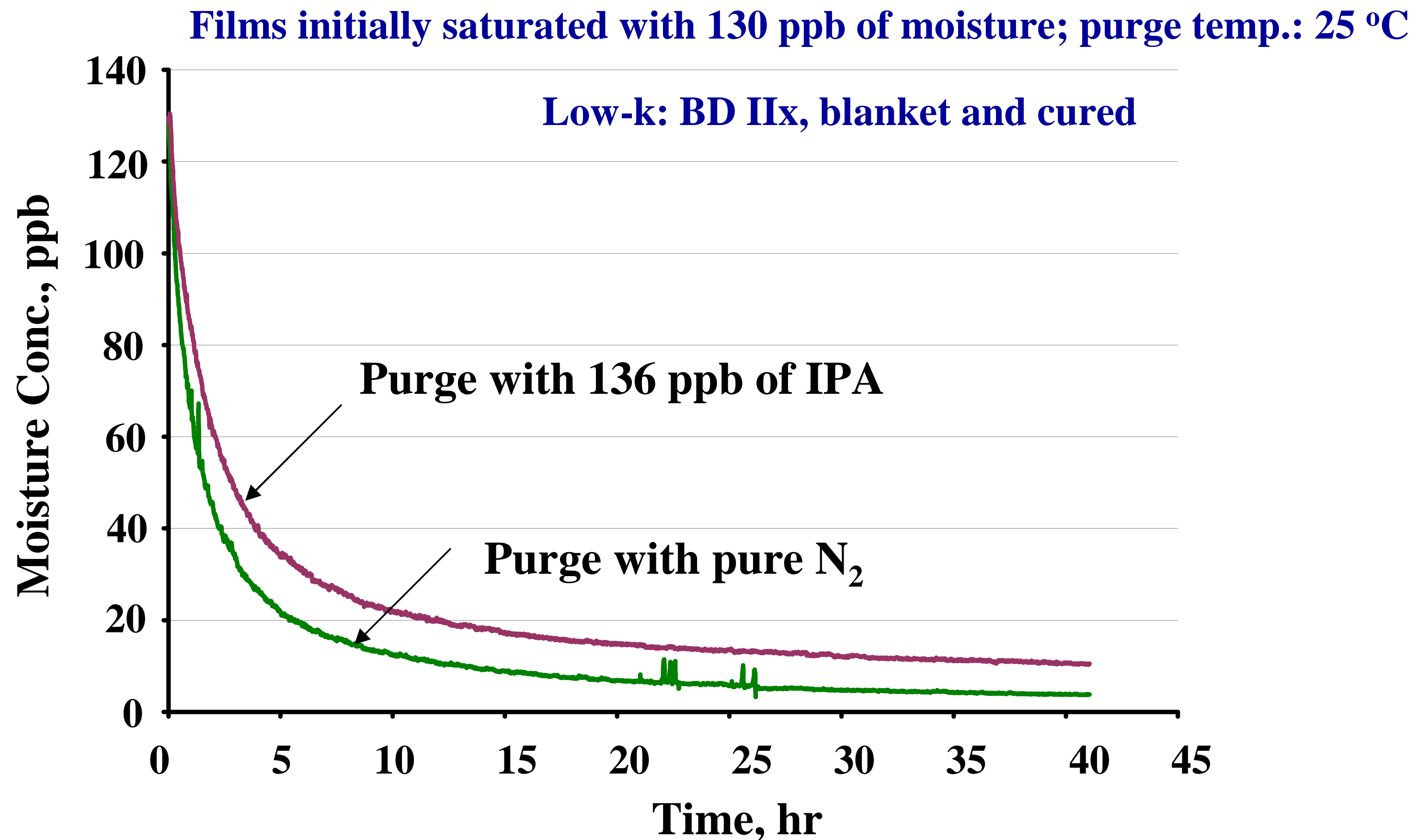

IPA enhances moisture removal in low-k film

Conclusions, Future Plans, and Interactions

- A methodology is developed for optimizing the procedure for outgassing and drying of porous low-k films; applying this methodology will result in significant reduction in purge gas and energy usage.
- The work will continue on applying the combined experimental and processes modeling approach to drying and cleaning of other nano-structures and nano particles.
- Work was in collaboration with Sematech and Texas Instruments; in particular, preparation of samples and consultation on process application are acknowledged.
- Software package for application will be made available to members.

Publications and Presentations

- **H. Juneja, J. Yao, A. Iqbal, Ting Tsui, F. Shadman, "Dynamics of Moisture Uptake and Removal in Porous Low-k Dielectric Films", Poster Presentation, *MRS Spring Meeting*, 2007.**
- **A. Iqbal, J. Yao, H. Juneja, R. Sperline, F. Shadman, "In-Situ Characterization of Dynamics of Impurity Absorption and Outgassing in Porous Low-k Dielectric Thin Films", *AIChE Annual Meeting*, November 2007.**
- **J. Yao, A. Iqbal, H. Juneja, F. Shadman, " Moisture Uptake and Outgassing in Patterned and Capped Porous Low-k Dielectric Films, *Journal of the Electrochemical Society*, 154(10) G199-206 (2007).**
- **J. Yao, A. Iqbal, H. Juneja, F. Shadman, and Ting Y. Tsui, "Moisture Uptake and Removal in Porous MSQ and Black Diamond Low-k Dielectric Films", *Techcon 2007*, September, 2007**

ESH Assessment: Materials, Structures and Processes for Nano-Scale MOSFETs with High-Mobility Channel

(*Task Number: 425.023*)

PIs:

- **Paul C. McIntyre, Materials Science and Engineering, Stanford**
- **Krishna C. Saraswat, Electrical Engineering, Stanford**

Graduate Students:

- **Eunji Kim: PhD candidate, Materials Science and Engineering, Stanford**

Undergraduate Students:

Other Researchers:

- **Byungha Shin, Postdoctoral Fellow, Materials Science and Engineering, Stanford**

Cost Share (other than core ERC funding):

- **$50K (gift) from Intel Corp.**
- **$150K from SRC Non-Classical CMOS research center**

Objectives

- III-V based MOSFETs are of great interest for their high effective carrier mobilities and low supply voltage.
- Achieving a native oxide-free semiconductor surface prior to high-k dielectric deposition is the key for fabrication of high-performance III-V-based MOSFETs.
- A chemically-stable passivation of the III-V substrate surface allows wafers to be queued during manufacturing and reduces the need for subsequent surface cleans, which holds advantages of reducing As-containing effluents from III-V surface cleans.
- As a way of improving interfacial properties, post-deposition anneals may result in “self-cleaning” of the III-V surface by the high-k film, avoiding cleaning steps prior to high-k deposition. This has the potential to save on water usage and reduce chemical usage and hazardous effluents resulting from wet cleaning of the III-V surface.

ESH Metrics and Impact

Native oxide removal process

HCl-etching

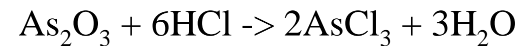
$As_2O_3 + 6HCl \rightarrow 2AsCl_3 + 3H_2O$

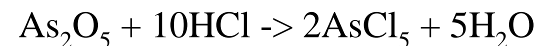
$As_2O_5 + 10HCl \rightarrow 2AsCl_5 + 5H_2O$

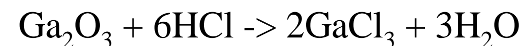
$Ga_2O_3 + 6HCl \rightarrow 2GaCl_3 + 3H_2O$

Toxic or harmful effluents :

$AsCl_3$, $AsCl_5$, $GaCl_3$

S-passivation

$(NH_4)_2S$ solution

Hardly produce any As-containing effluents

Disposal as hazardous waste

- **S-passivation reduces emission of As-containing effluents by reduceing the need for subsequent surface cleans**

HfO_2 deposition

Atomic layer deposition

TDEAH, water, 150 °C

- **Low thermal budget**
- **Relatively lower vacuum**

➢ **Lower energy cost compared to other deposition methods (e.g. MBE)**

Post-deposition anneal

Rapid thermal anneal

N_2, 650 °C

- **High temperature process**
- **No need of chemical cleans**

➢ **Reduction in emission of ESH-problematic effluents and in the use of chemicals**

S-Passivation and Anneal Studies: Methods

S-passivation

Epitaxial Be-doped GaAs ($1\sim5*10^{17}cm^{-3}$)

Sonication in acetone for 5 min

Short DI water dip

18% HCl etching for 3min (2% HF etching for 3 min)

Short DI water dip

5% $(NH_4)_2S$ for 15 min

Short DI water dip

Atomic Layer Deposition of HfO_2

TDEAH, water, 150 ^oC

XPS

High Temp. Anneal

Epitaxial Be-doped GaAs ($1\sim5*10^{17}cm^{-3}$)

Atomic Layer Deposition of HfO_2

TDEAH, water, 150 ^oC

Post Deposition Anneal

N_2, 650 ^oC, 3 min

SIMS, XPS

Highlight of Results: S-passivation

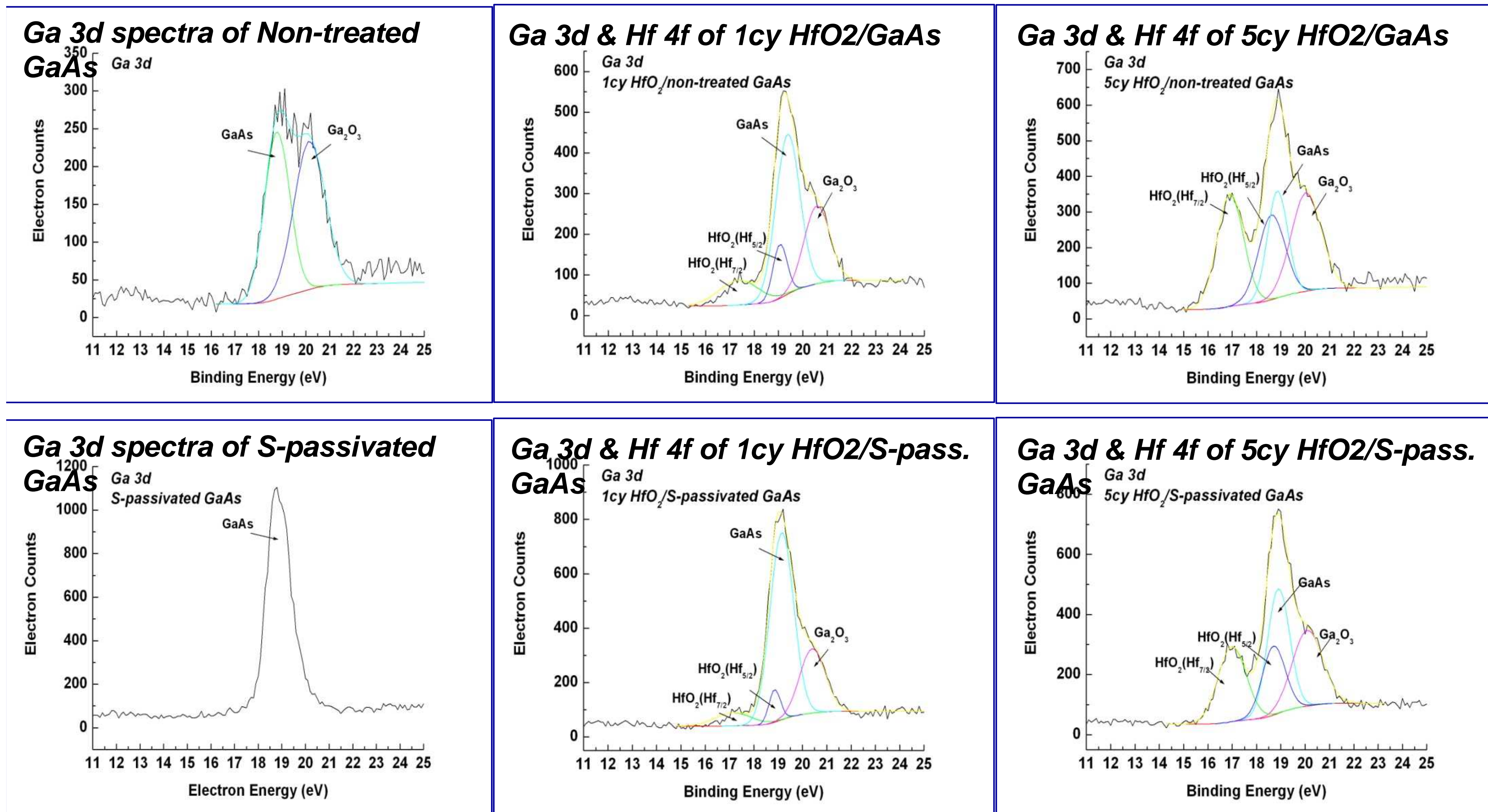

- **S-passivation partly suppresses re-oxidation of the GaAs surface during ALD.**

Highlight of Results: S-passivation

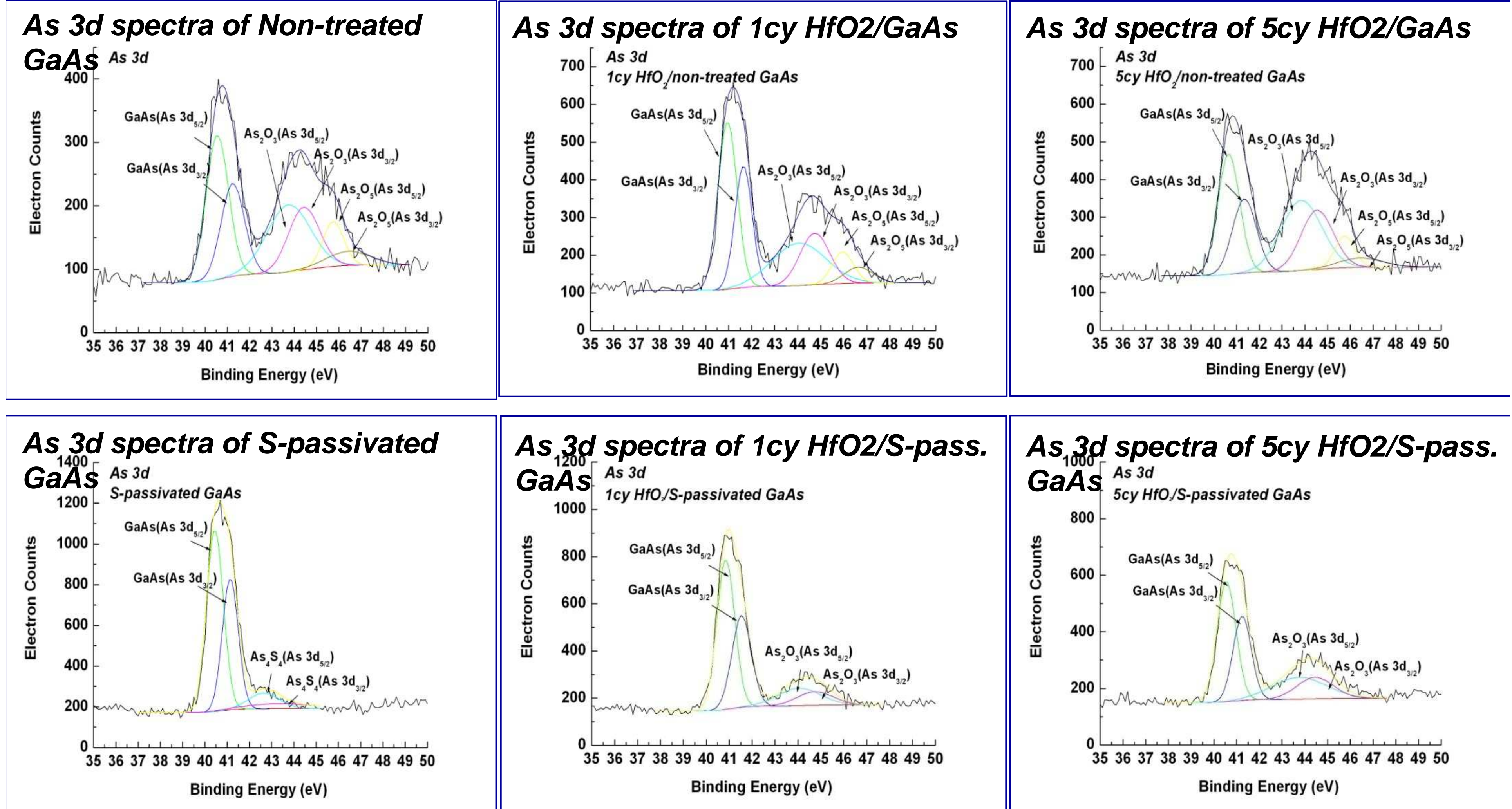

• S-passivation partly suppress As oxide formation of the GaAs surface during ALD.

Highlight of Results: S-passivation

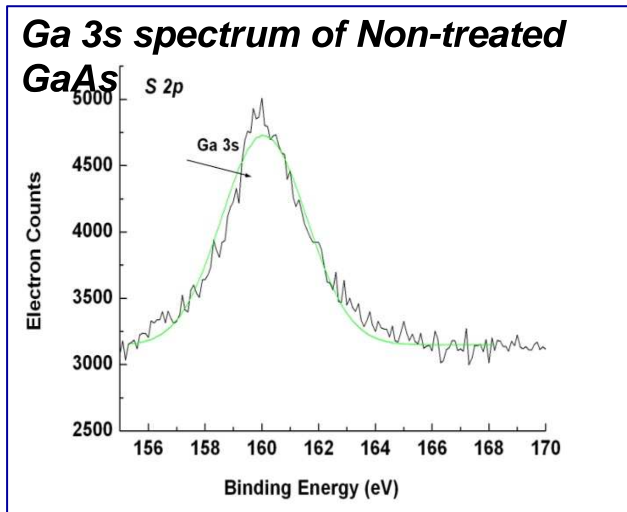

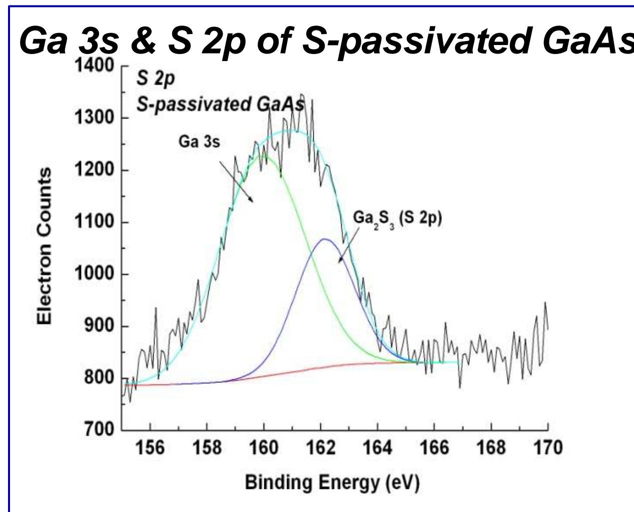

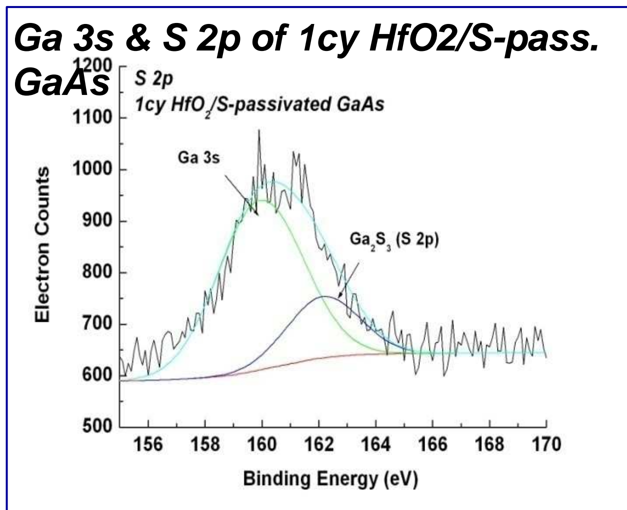

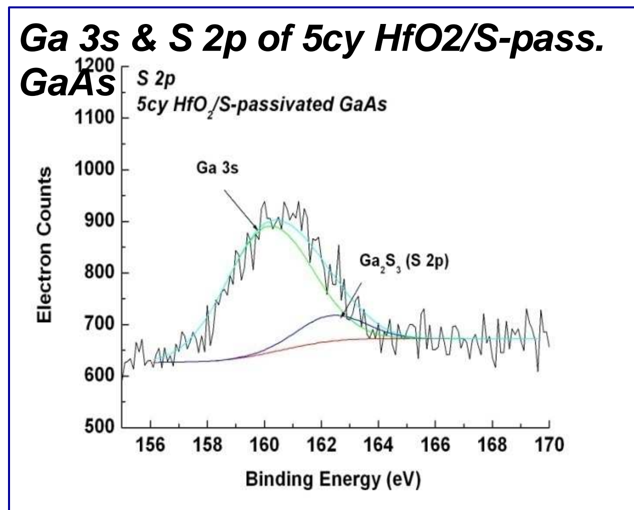

- **Ga_2S_3 was clearly shown after S-passivation and was still observed until 5 cycles of HfO_2 deposition.**

Highlight of Results: High Temp. Anneal

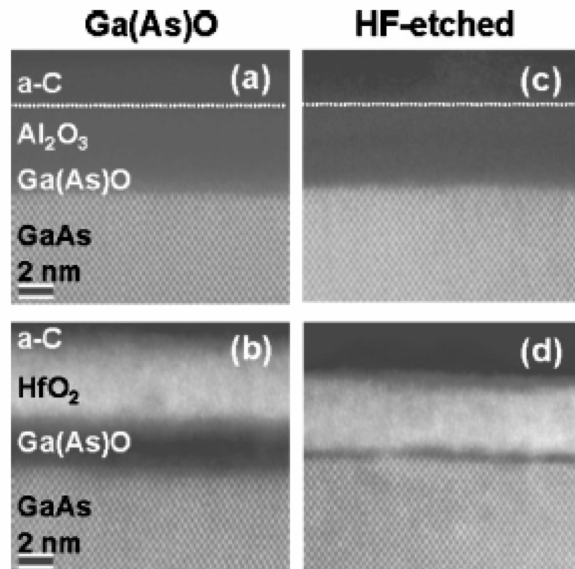

M.M. Frank et al., APL 86, 152904 (2005).

Capacitance -Voltage of high-temp. annealed

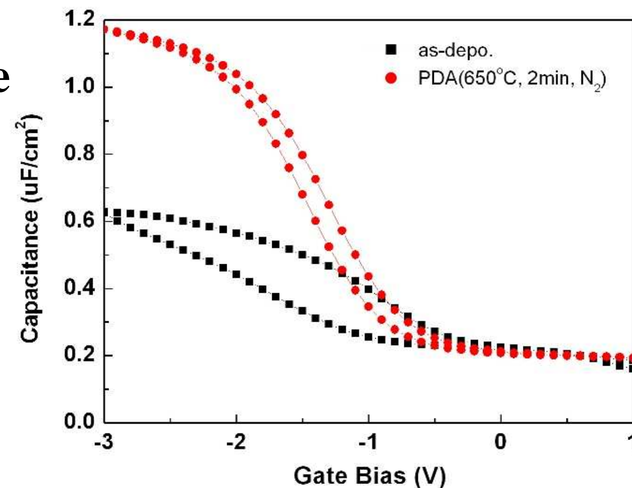

Gate Leakage Current

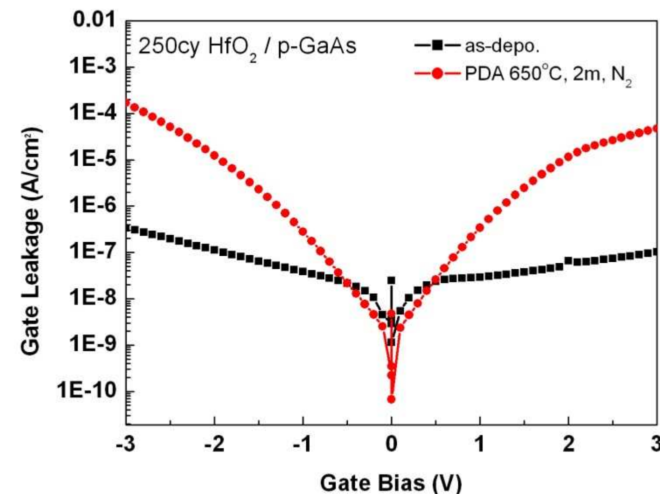

- Post-ALD anneals at 480 - 650°C were found to produce desorption of arsenic and gallium oxides through the high-k film, improving device performance.

- Improved C-V characteristics, higher gate leakage current consistent w/ reduced EOT.

Highlight of Results: High Temp. Anneal

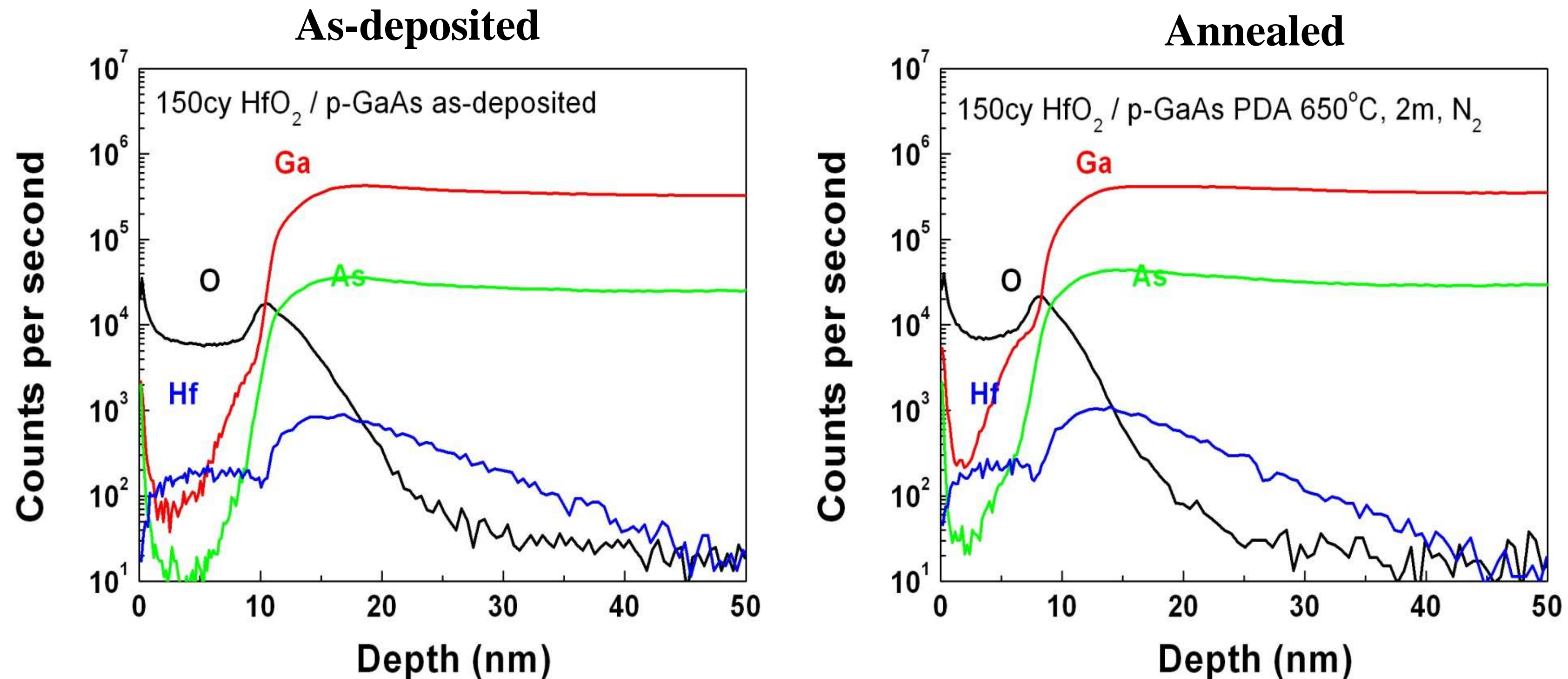

- SIMS data suggest that there may be Ga diffusion into the HfO_2 layer after the 650°C anneal; further work is needed to confirm.
- Evidence for As diffusion is not obvious.
- Apparent concentration tail for Hf in GaAs is likely a SIMS artifact.

Highlight of Results: High Temp. Anneal

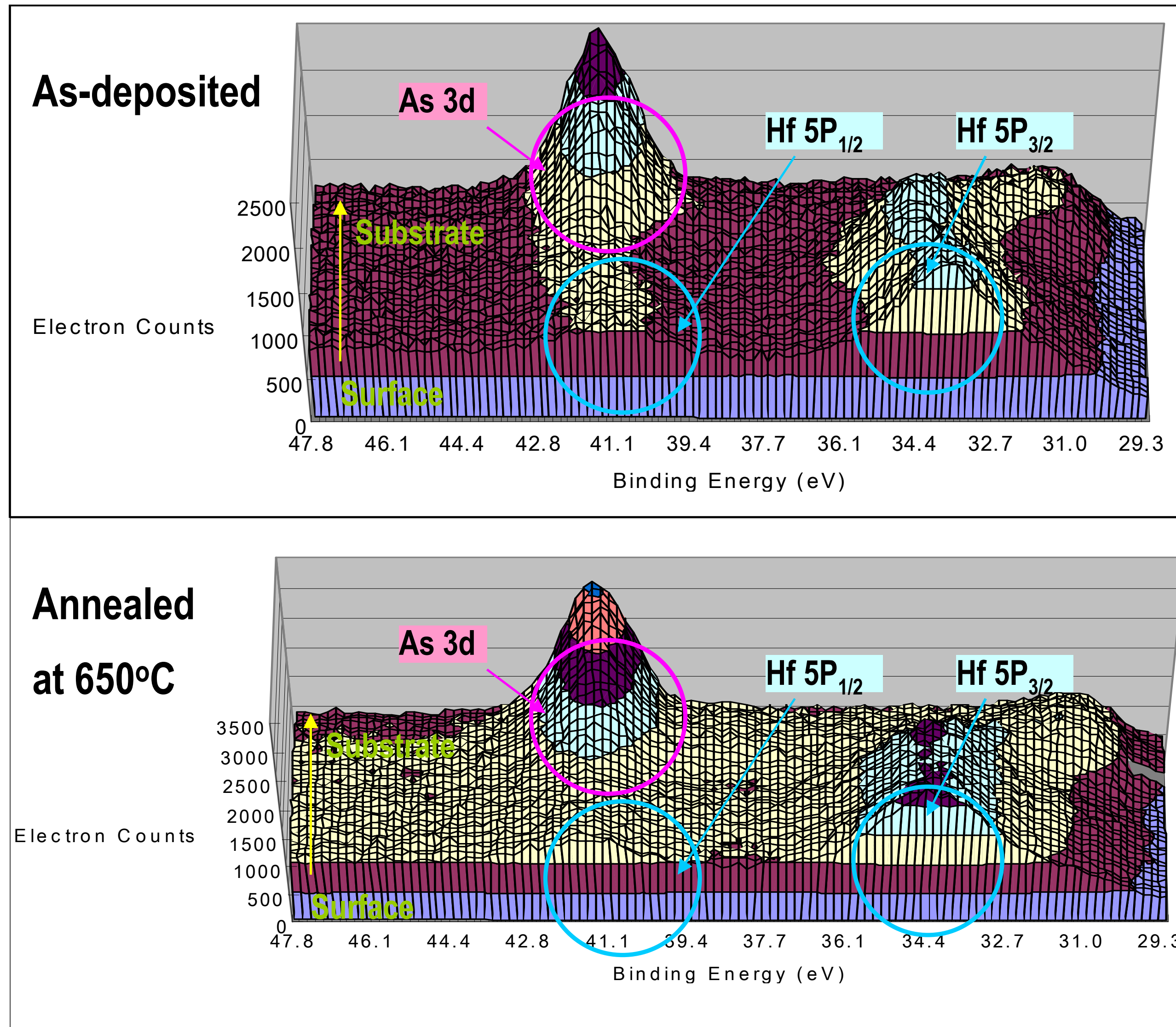

XPS depth profiling

(150cyc HfO_2 on p-GaAs)

- **No evidence of oxide features for As within the HfO_2 layer in the expected binding energy range of 44.9~46.2eV (As oxides)**

InGaAs: Native oxide removal, wet-etching

- Preparation of clean native oxide free $In_{0.2}Ga_{0.8}As$ surface for subsequent high k film deposition: wet-etching and pre-ALD anneal
- Choice of wet etchant? A: HCl (30%), B: HCl (30%) + $NH_4(OH)$ (4%), C: HCl (30%) + $NH_4(OH)$ (30%), D: $NH_4(OH)$ (30%)

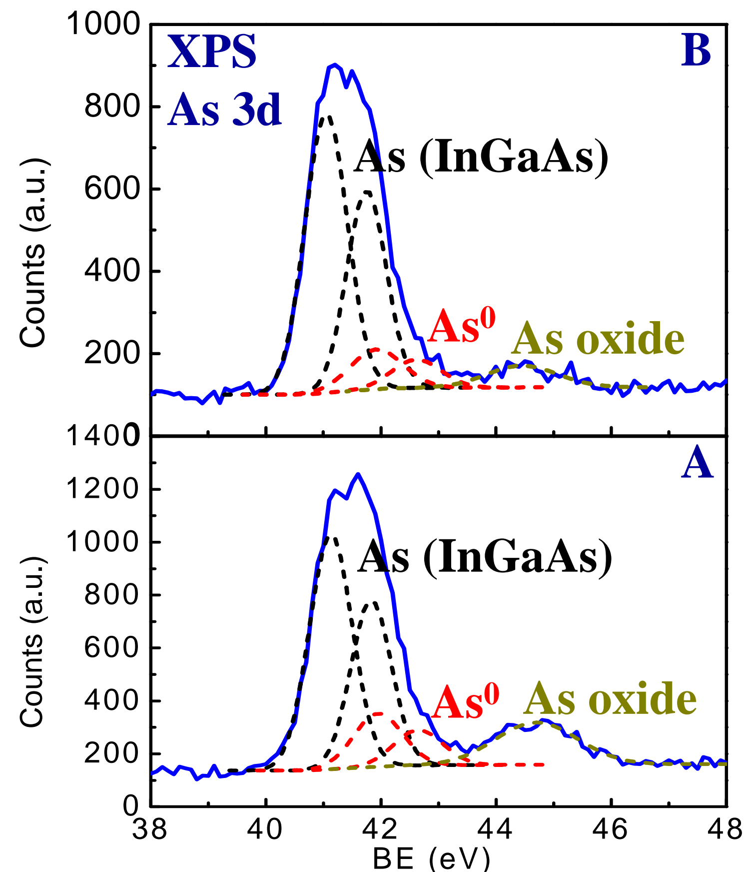

Compositional analysis by XPS

	In oxide*	Ga oxide**	As^0	As oxide
A	1.26	0	5.62	4.96
B	2.39	0	2.66	1.68
C	2.56	0	2.57	3.73
D	2.49	0	2.02	4.91

* Most likely In-hydroxide

** From Ga 3p spectra (BE ~105eV), Ga oxide seen in Ga 2p spectra (BE ~1167eV)
=> existence of very thin surface Ga oxide layer

Ultrathin Al_2O_3 on wet-etched $In_{0.2}Ga_{0.8}As$

- Chemical removal of native oxides by HCl and $NH_4(OH)$
- Pre-ALD anneal at 360 °C for thermal desorption of remaining oxides
- ALD-Al_2O_3 : 30 cycles (2.8 nm) at 310 °C

XPS on 2.8 nm Al_2O_3 / $In_{0.2}Ga_{0.8}As$: confirmation of no In-, Ga-, As- oxide

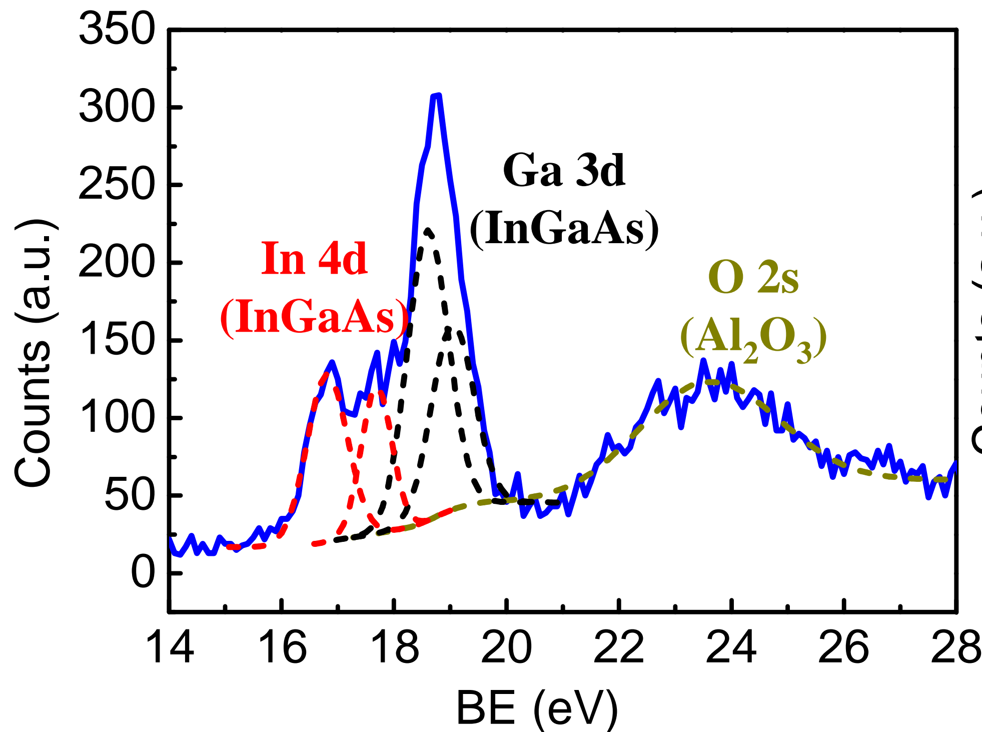

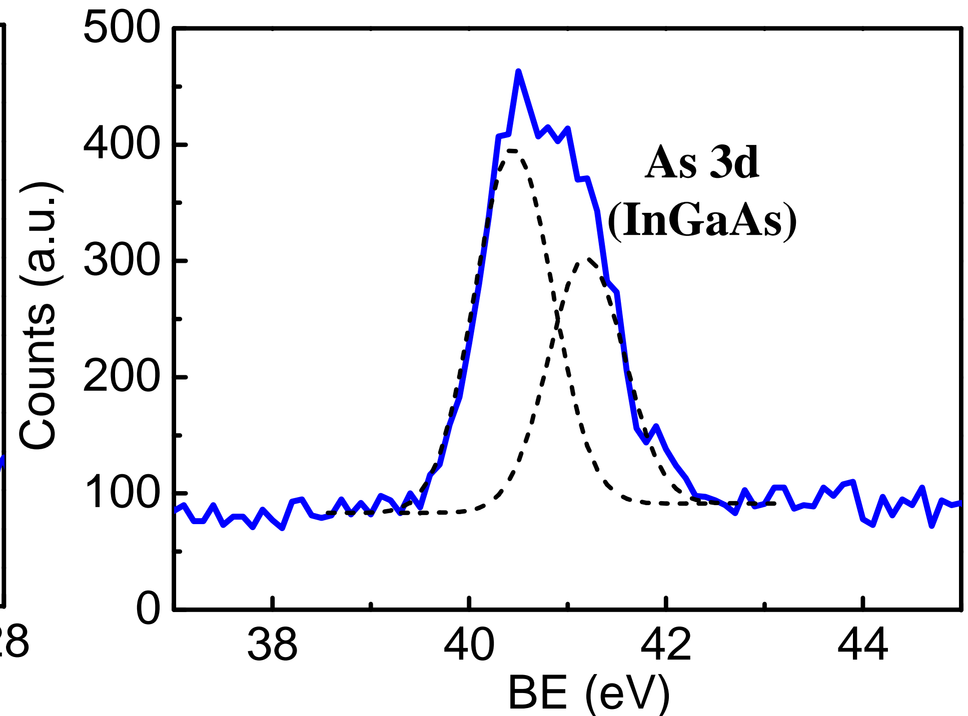

Ultrathin Al_2O_3 on wet-etched $In_{0.2}Ga_{0.8}As$

- **Demonstration of scaling down EOT to 1.8 nm**

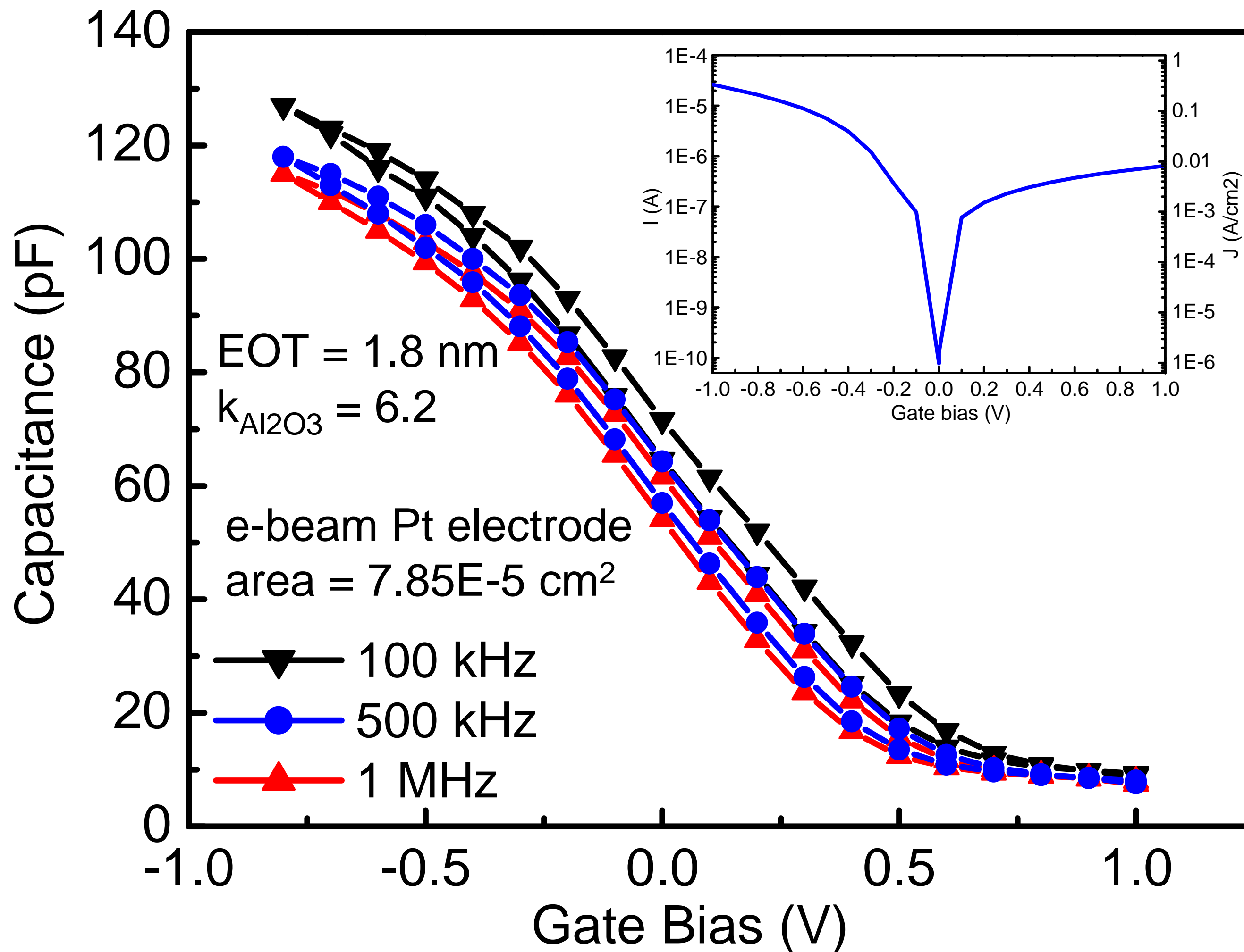

Industrial Interactions and Technology Transfer

- **ALD-HfO_2 growth mechanism study in collaboration with Dr. Wilman Tsai (Intel) and David P. Brunco (Intel & IMEC)**

Future Plans

Next Year Plans

- **Optimization of pre-ALD wet clean and vacuum anneal procedures for reduced charge-trapping inAl_2O_3/InGaAs gate stacks**
- **D_{it} measurements using MOSCAPs (low-T conductance) and MOSFETs (collaboration w/ UCSB)**
- **Comparison of electrical behavior and ESH trade-offs for wet-cleaned InGaAs channels vs. decapping of protective As layer prior to high-k ALD**

Long-Term Plans

- **Explore HfO_2/Al_2O_3 and TiO_2/Al_2O_3 bilayer gate insulators for thinner (~ 1 nm EOT) gate stacks on $In_{0.53}Ga_{0.47}As$ channels**

Publications, Presentations, and Recognitions/Awards

- **E. Kim, P-T. Chen, D. Choi, J. Harris, Y. Nishi, K. Saraswat, and P. McIntyre, "Atomic Layer Deposition of HfO_2 on III-V Semiconductors: Effects of Surface Treatment and Post-Deposition Anneals," TMS Electronic Materials Conference (EMC 2007), University of Notre Dame, IA, June 20-22, 2007. (oral presentation)**

- **E. Kim, J. Chen, D. Choi, N. Goel, C.O. Chui, W. Tsai, J. Harris, Y. Nishi, K. Saraswat and P.C. McIntyre "Electrical and Physical Characterization of ALD-Grown HfO_2 Gate Dielectrics on GaAs (100) Substates with Sulfur Passivation," Spring MRS Meeting, San Francisco, CA, April 9-13, 2007. (poster)**

Section 2

Seed and Customized Projects

Biologically Inspired Nano-Manufacturing (BIN-M)

(*Seed Project*)

PIs:

- Anthony Muscat, Chemical and Environmental Engineering, UA
- Megan McEvoy, Biochemistry and Molecular Biophysics, BIO5 Institute, UA
- Masud Mansuripur, College of Optical Sciences, UA

Graduate Students:

- Amber Young, PhD candidate, College of Optical Sciences, UA
- Sam Jayakanthan, PhD candidate, Biochemistry and Molecular Biophysics, UA
- Shawn Miller, PhD candidate, College of Optical Sciences, UA
- Rahul Jain, PhD candidate, Chemical and Environmental Engineering, UA

Undergraduate Student:

- Ben Mills, Chemical and Environmental Engineering, UA

Other Researchers:

- Zhengtao Deng, Postdoctoral Fellow, ChEE & Optical Sciences, UA
- Babak Imangholi, Postdoctoral Fellow, ChEE & Optical Sciences, UA
- Gary Fleming, Postdoctoral Fellow, Chemical and Environmental Engineering, UA

Cost Share (other than core ERC funding):

- $825k Science Foundation Arizona, ASM, SEZ, Arizona TRIF

Objectives

- **Minimize costs of materials, energy, and water to fabricate nanoscale devices using bio-based strategy**
- **Exploit homogeneity, mild reaction conditions, and specificity of active biological molecules**
- **Grow 3D structures to achieve scalable architecture**
- **Employ additive, bottom up patterning methods**

ESH Metrics and Impact

Sustainability metrics			
Process	Water l/bit/masking layer	Energy J/bit/masking layer	Materials g/bit/masking layer
Subtractive 32 nm*	$3.3x10^{-10}$	$1.5x10^{-12}$ EUV	$2.9x10^{-16}$
Additive	$3.6x10^{-13}$	$9.2x10^{-17}$	$1.8x10^{-19}$

*D. Herr, Extending Charge-based Technology to its Ultimate Limits: Selected Research Challenges for Novel Materials and Assembly Methods. Presentation at the NSF/SRC EBSM Engineering Research Center Review Meeting: February 24, 2006.

Process Goal: Deposit Array of Metal Dots

Biochemistry of metal transport proteins
Megan McEvoy/UA

Characterize bio & inorganic structures using scanning probe and optical techniques
Masud Mansuripur/UA

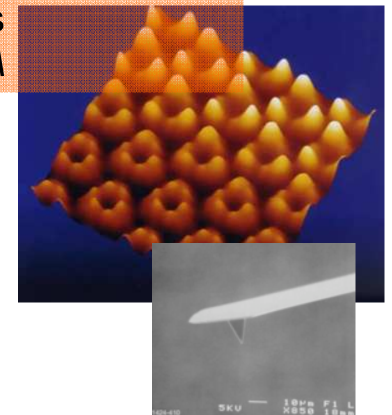

Selective deposition
Glen Wilk, Eric Shero, Christophe Pomarede Steve Marcus/ASM

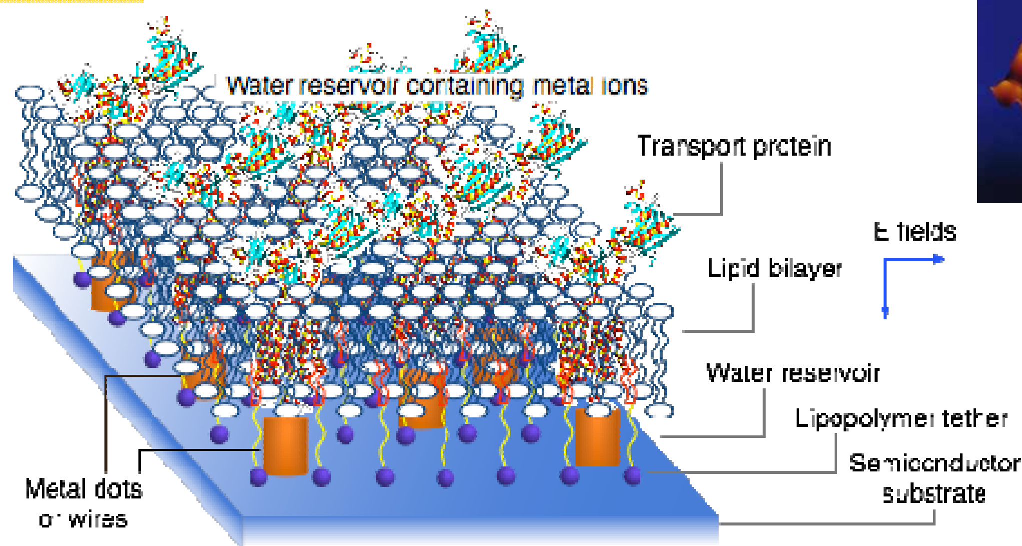

Pattern surfaces and build structures
Anthony Muscat/UA

Semiconductor surface preparation
Harald Okorn-Schmidt, Zach Hatcher, Jeremy Klitzke/SEZ

Methods and Approach

Metal Transport Proteins:
CopB from *Archaeoglobus fulgidus*

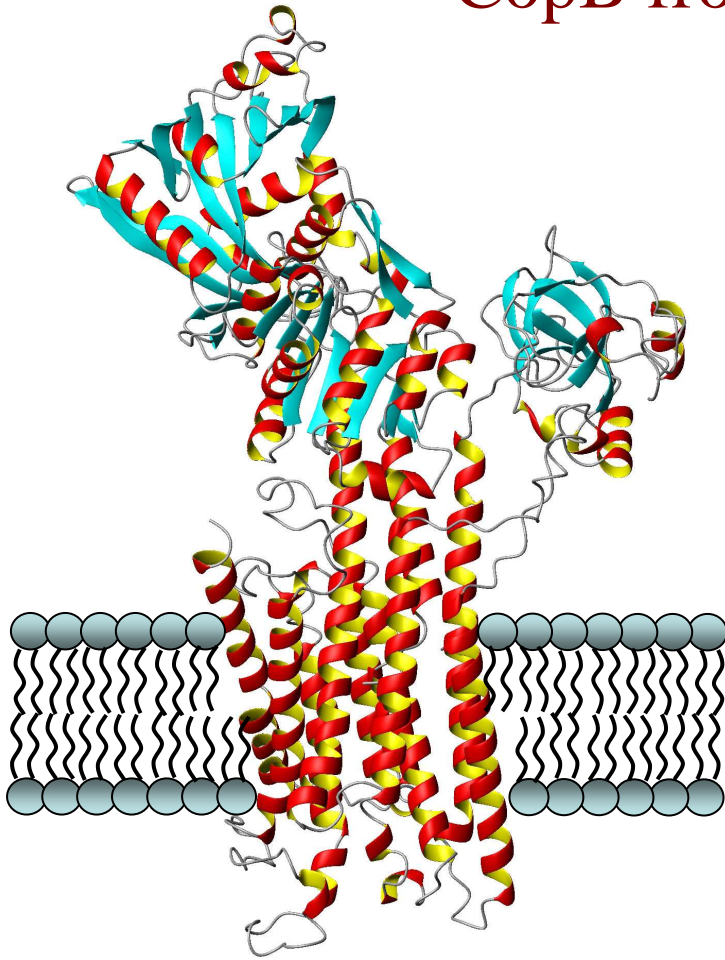

- Recombinant protein purified from *E. coli*
- Cu(II) transport activity in artificial membranes
- Energy source: Adenosine triphosphate (ATP)
- Enhanced stability at room temperature

Preparation of CopB

copB gene

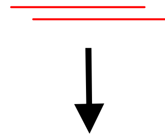

E. coli expression plasmid

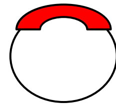

CopB protein expression in *E. coli*

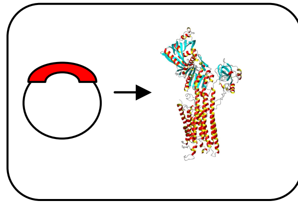

Affinity chromatography to isolate CopB protein

- The *copB* gene from *Archaeoglobus fulgidus* has been isolated using the polymerase chain reaction (PCR)
- The *copB* gene has been inserted into a plasmid for expression in *E. coli*
- CopB will be expressed in *E. coli* and purified using an affinity tag
- CopB containing vesicles will be fused with lipid bilayers

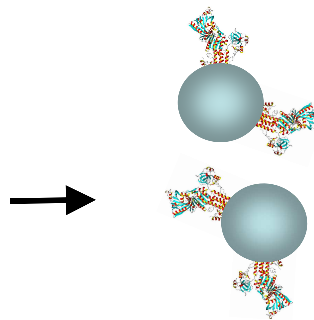

Purified CopB in vesicles

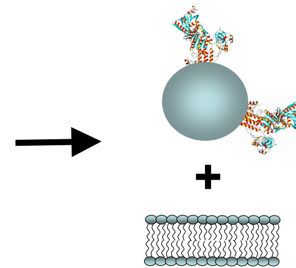

Fusion of vesicles and lipid bilayer

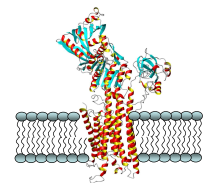

CopB incorporated in lipid bilayer

Surface Patterning

(i) Surface Preparation

Cleaning performed by chemical etching.

Characterised via XPS, AFM,TPD.

Possible Substrates for Use

Si, Ge, GaAs, InAs, InP, InSb

Tertiary Materials.

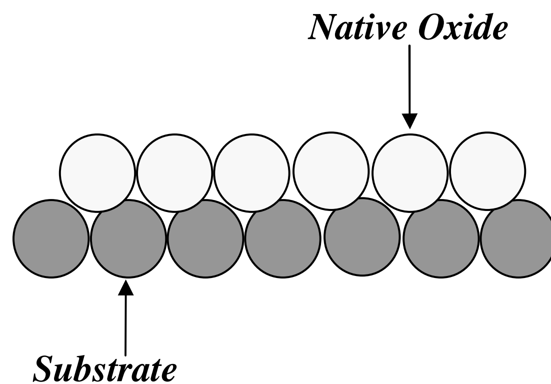

(ii) Surface Functionalisation

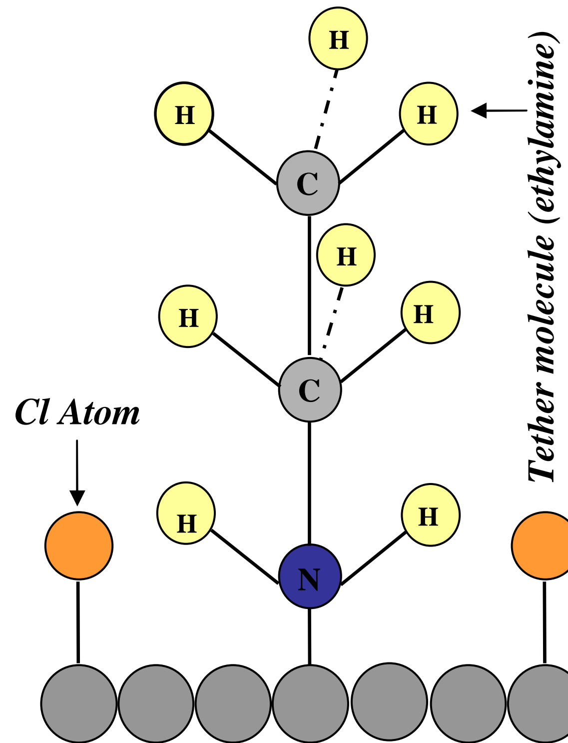

Surface chemistry used to modify surface and to introduce patterning and tether molecules to attach lipid bilayer

Types of Chemistry

Patterning Step: UV/Cl_2, NH_3

Tethers = Amines (dibutylamine, ethylamine), Benzene, Pyridine.

(iii) Lipid Bilayer Addition

Attachment of lipid bilayer to surface.

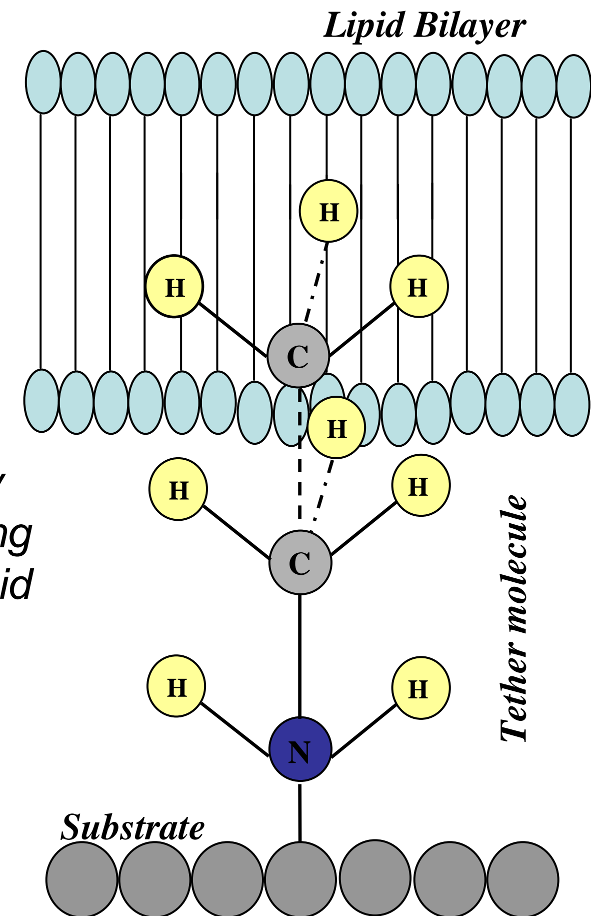

GaAs Surface Preparation

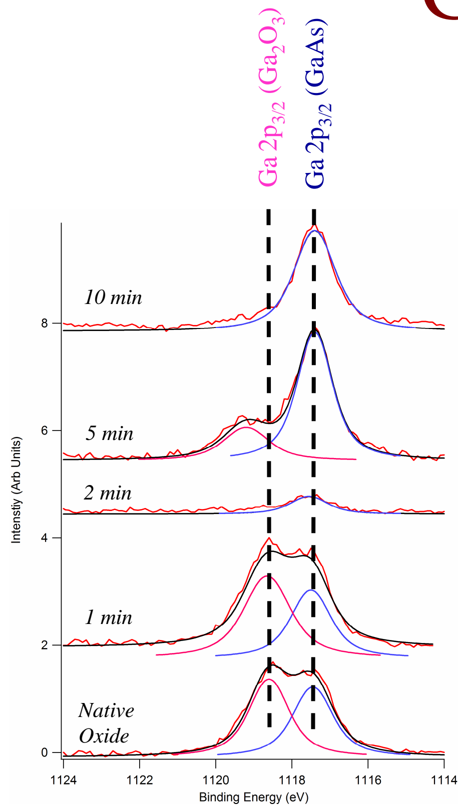

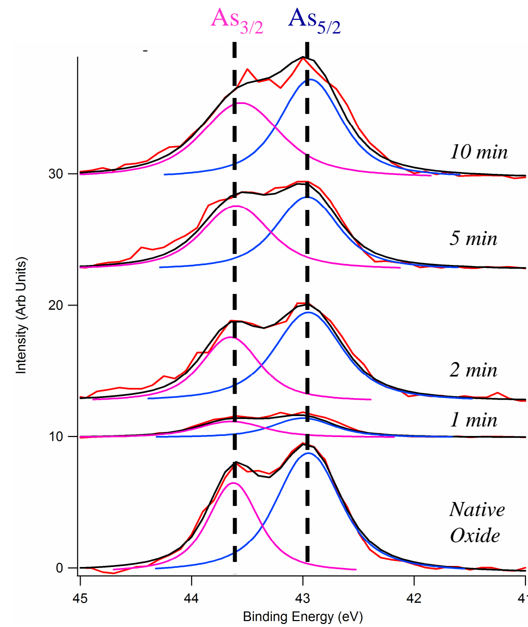

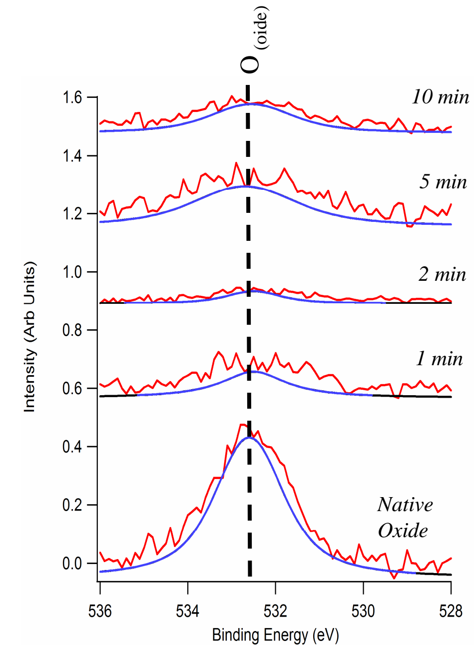

Ga oxides removed but regrow with time

Possible presence of elemental As in the bulk

$$Ga_2O_3 + 4GaAs \rightarrow 3Ga_2O + 2As_2$$

$$Ga_2O_3 + 4GaAs \rightarrow 3Ga_2O + As_4$$

Bilayer Deposition

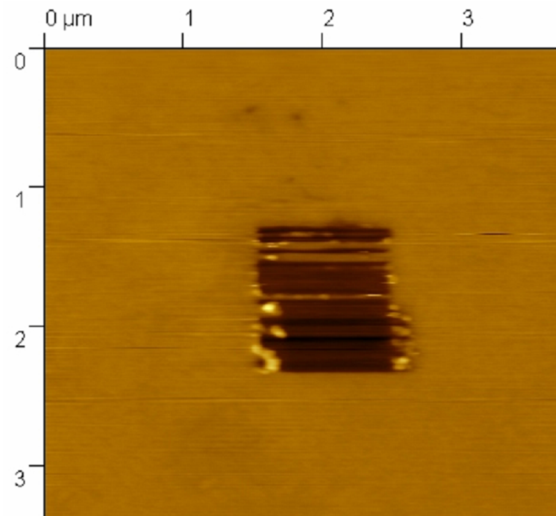

1um square hole dug in lipid membrane. Observe smooth bilayer surface. Note excess material piled at edge of hole.

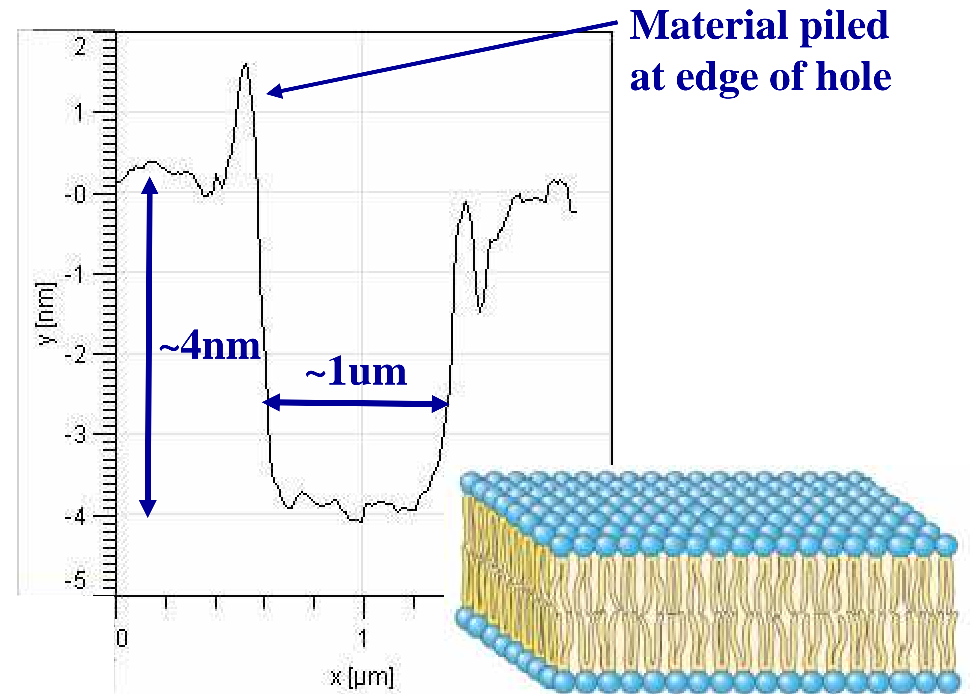

Material piled at edge of hole by AFM tip

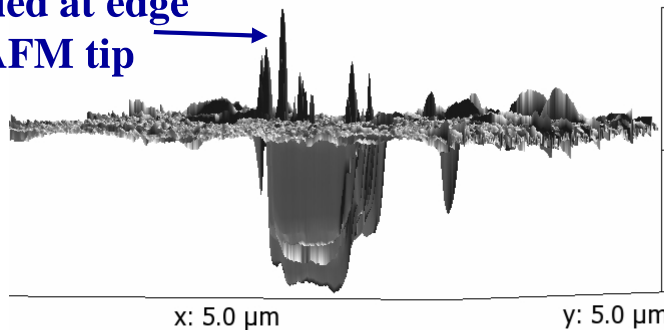

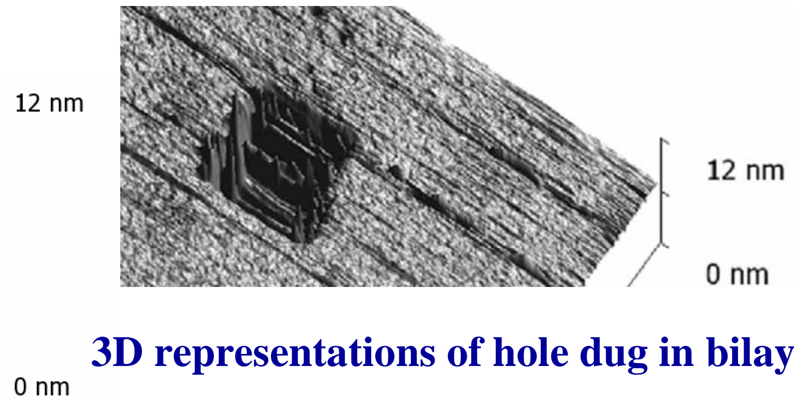

3D representations of hole dug in bilayer.

Link Quantum dots to proteins

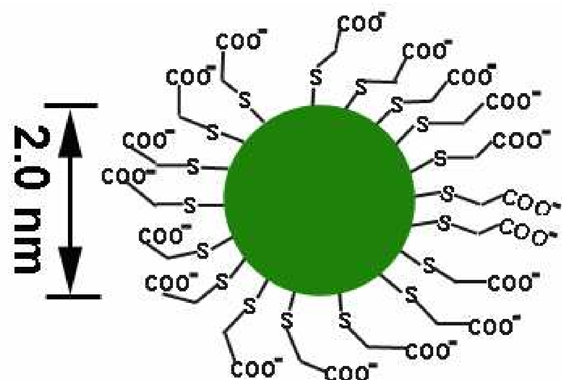

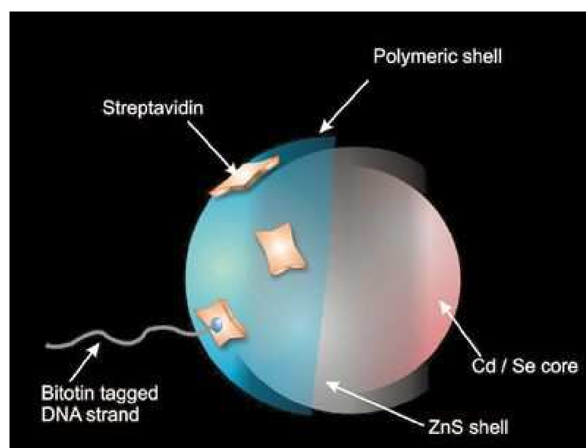

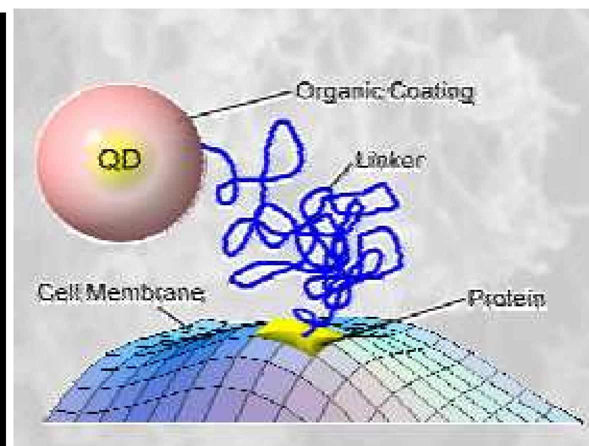

(Left) Single quantum dot terminated with COOH groups
(Middle) Functionalized quantum dot
(Right) Quantum dot attached to protein with linker

Image Q-dots with Confocal Fluorescent Microscope

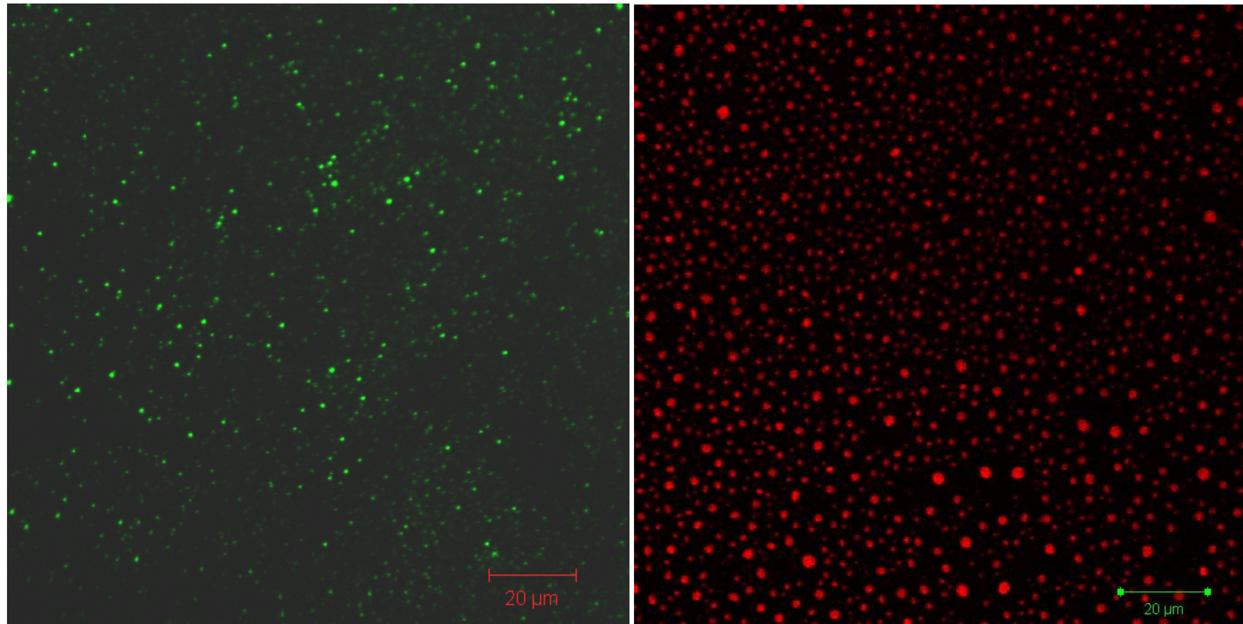

(Left) Confocal fluorescent microscopy image of the green emission from CdSe quantum dots.
(Right) Confocal fluorescent microscopy image of the red emission from CdTe quantum dots.

Industrial Interactions and Technology Transfer

- **Presentation on liquid and gas phase cleaning of high mobility substrates to SEZ**
- **Jeremy Klitzke from SEZ visiting scientist at UA**
- **ALD film growth development with ASM**

Future Plans

Next Year Plans

- Liquid and gas phase cleaning of high mobility substrates
- ALD film nucleation on high mobility substrates
- Express CopB protein
- Demonstrate chemically patterned surface
- Attach membrane to patterned surface and build structures
- Characterize proteins and structures using q-dots

Long-Term Plans

- Develop characterization techniques for nanostructures
- Demonstrate patterned nanostructures over cm length scale

Publications, Presentations, and Recognitions/Awards

- **Z. Deng, et al., "*A Simple Open-to-Air Water-Based Route to Ligand-Selective Synthesis of ZnSe and $Zn_xCd_{1-x}Se$ Quantum Dots with Finely Tunable UVA to Blue Photoluminescence*," under consideration by the Journal of Physical Chemistry**

Lowering Material and Energy Usage during Purging Gas Distribution Systems

(Customized Project: Sponsored by Intel)

PI:

- **Farhang Shadman, Chemical and Environmental Engineering, UA**

Co-PI:

- **Carl Geisert Intel**

Graduate Students:

- **Harpreet Juneja: PhD candidate, Chemical and Environmental Engineering, UA**
- **Junpin Yao: PhD candidate, Chemical and Environmental Engineering, UA**
- **Asad Iqbal: PhD, Graduated 2007, Chemical and Environmental Engineering, UA**

Undergraduate Students:

- **Paul Swift, Chemical and Environmental Engineering, UA**

Objectives and ESH Impact

1. **Determine the effect of temperature and flow rate on moisture removal during purging of gas distribution lines.**
2. **Compare effects of moisture removal in main transfer line and in laterals during purge processes.**
3. **Develop a method to determine the effect of dead legs and stagnant lines.**
4. **Design criteria for stopping back diffusion and cross contamination caused by laterals.**
5. **Develop a process model for application to minimize gas usage during purging and cleaning processes at the start up or during the operation of gas distribution systems.**

Background

1. **Moisture removal on stainless steel tubing is a slow process.**

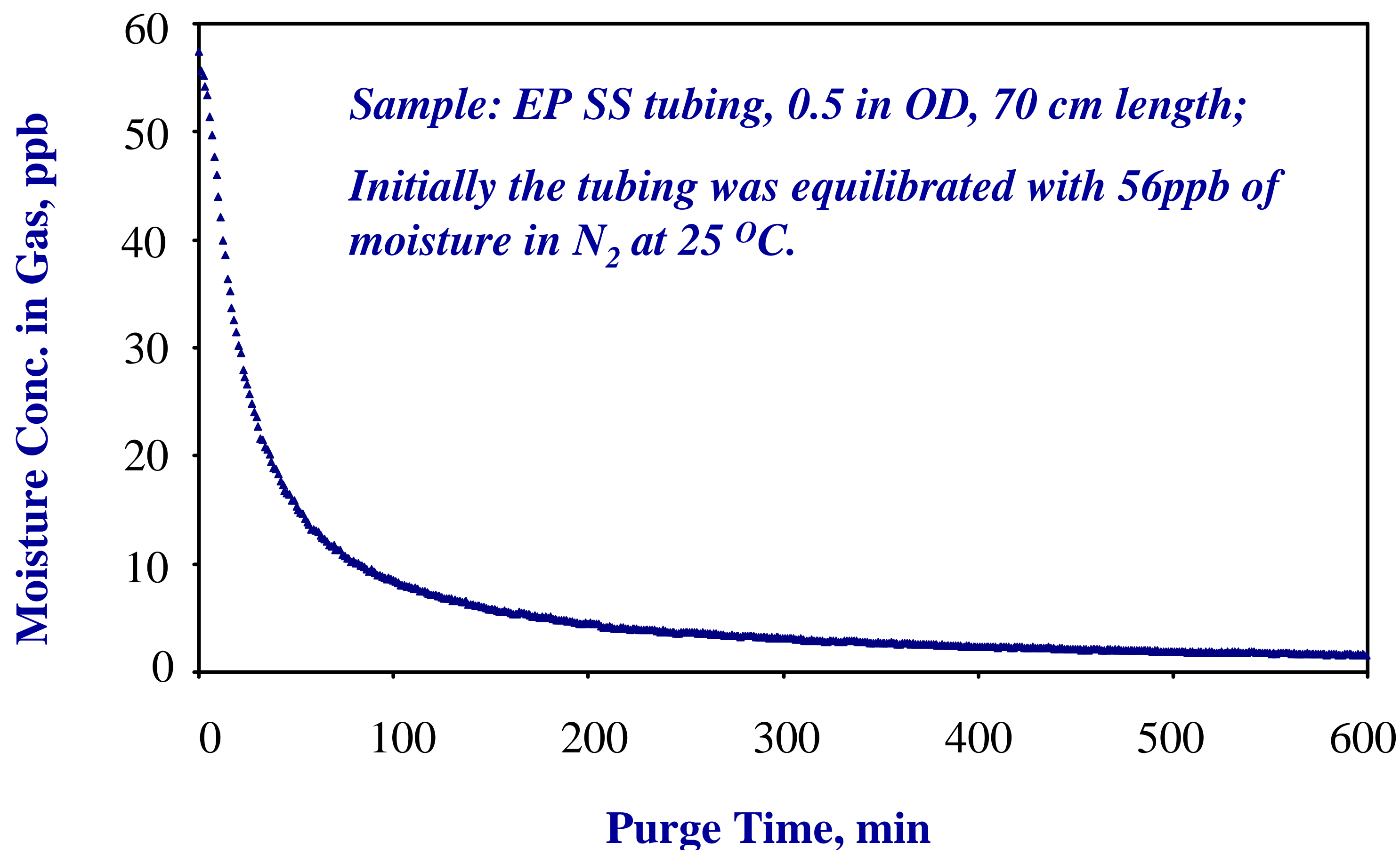

Background

1. Surface adsorption/desorption, back diffusion from dead legs, and stagnant sections can cause significant contamination in ultra-pure gas distribution systems.
2. Once moisture contamination in gas distribution systems reaches a critical level (due to contamination accidents) the system needs to be purged by UHP nitrogen for a long time. Significant reduction in purge time and gas usage can be accomplished by applying programmed purge and cleaning processes that are based on process model and key point monitoring.
3. In order to block back diffusion from laterals and open ports, a methodology is needed to determine the optimum flow rate and geometry to minimize gas usage that is wasted for stopping the back-diffusion.

Experimental Setup

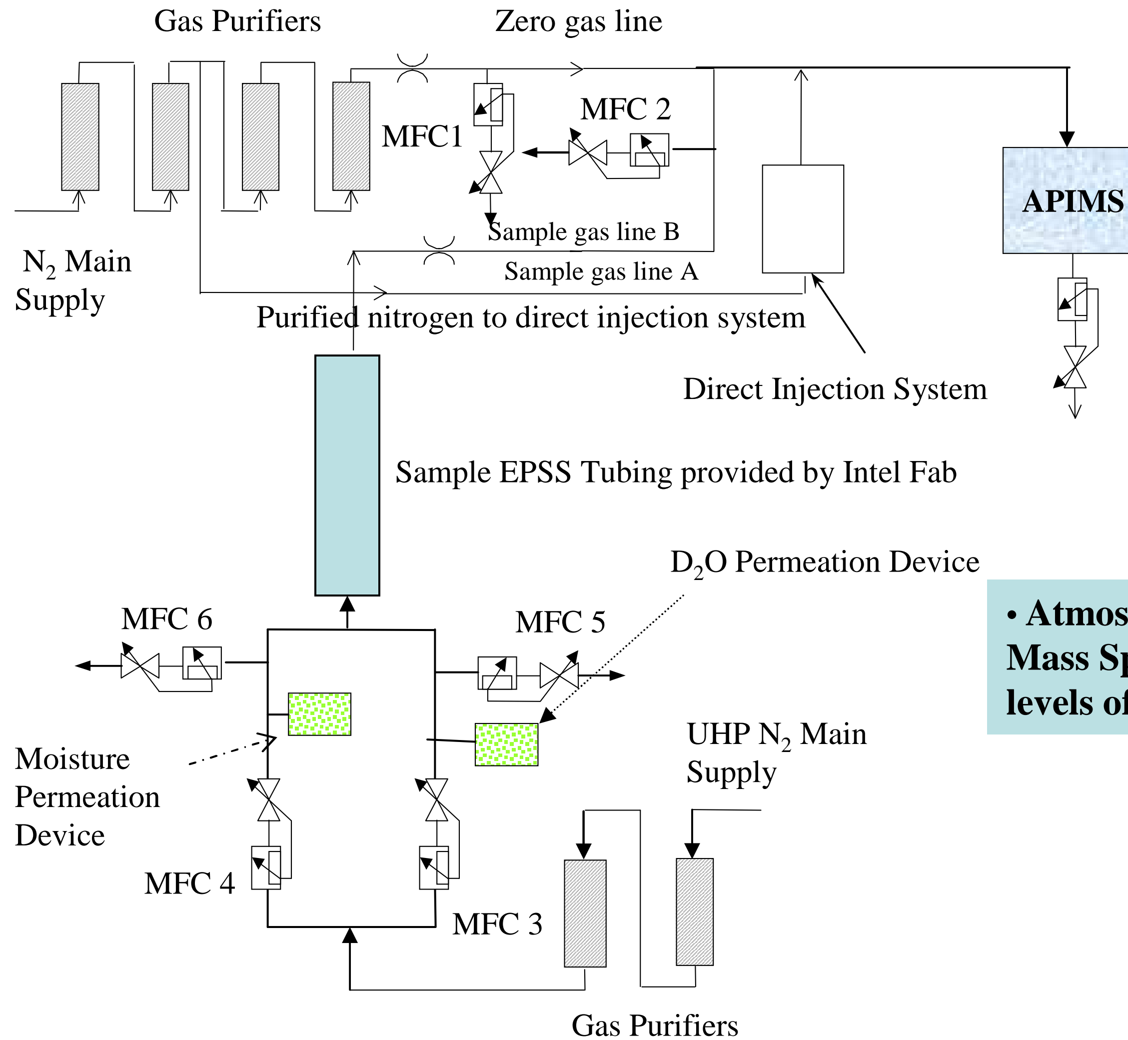

- **Atmospheric Pressure Ionization Mass Spectrometer (APIMS) – ppb levels of impurities**

Model Development for Mass Transport in Cylindrical Tubing

Moisture adsorption on tubing wall:

$$\frac{\partial C_S}{\partial t} = k_{ads} C_g (S_0 - C_S) - k_{des} C_S$$

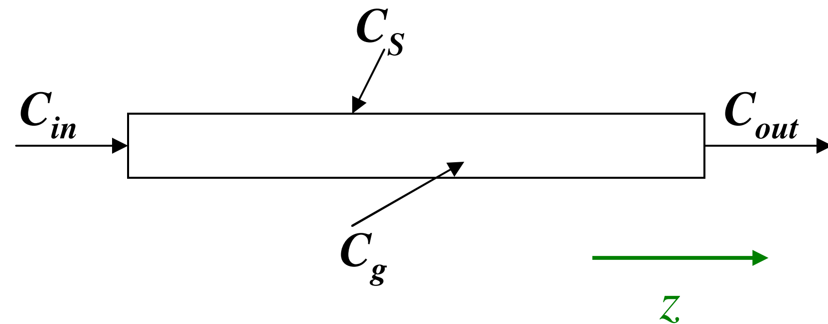

Governing equation for gas phase:

$$\frac{\partial C_g}{\partial t} = D_L \frac{\partial^2 C_g}{\partial z^2} - u \frac{\partial C_g}{\partial z} + \frac{A_S}{V}(k_{des} C_S - k_{ads} C_g (S_0 - C_S))$$

C_S: Moisture concentration on wall, mol/cm^2;

C_g: Moisture concentration in gas, mol/cm^3;

k_{ads}: Adsorption rate constant, cm^3/mol/s

k_{des}: Desorption rate constant, 1/s

S_0: Site density of surface adsorption, # of sites/cm^2;

D_L: Dispersion coefficient, cm^2/s;

u: Velocity, m/s; A_S: Surface area of wall, m^2; V: Volume of tubing, m^3

- **Surface adsorption/desorption**
- **Bulk convection**

Model Application: Back Diffusion at Laterals

Governing equation for bulk gas:

$$U = 2U_{\text{avg}}\left[1 - \left(\frac{r}{R}\right)^2\right] \quad [1]$$

$$2u_{\text{avg}}\left[1 - \left(\frac{r}{R}\right)^2\right]\frac{\partial C_g}{\partial z} + D_g\frac{\partial^2 C_g}{\partial z^2} + \frac{D_g}{r}\frac{\partial}{\partial r}\left(\frac{r\partial C_g}{\partial r}\right) = 0 \quad [2]$$

The boundary conditions used for Eq. 2 are

$$C_g = C_{go} \quad \text{at } z = 0, \quad 0 \le r \le R \quad [3]$$

$$C_g = C_{g-} \quad \text{at } z = L, \quad 0 \le r \le R \quad [4]$$

$$\frac{\partial C_g}{\partial r} = 0 \quad \text{at } r = 0, \quad 0 \le z \le L \quad [5]$$

$$-D_g\frac{\partial C_g}{\partial r} = k_a C_g - k_d C_s \quad \text{at } r = R, \quad 0 \le z \le L \quad [6]$$

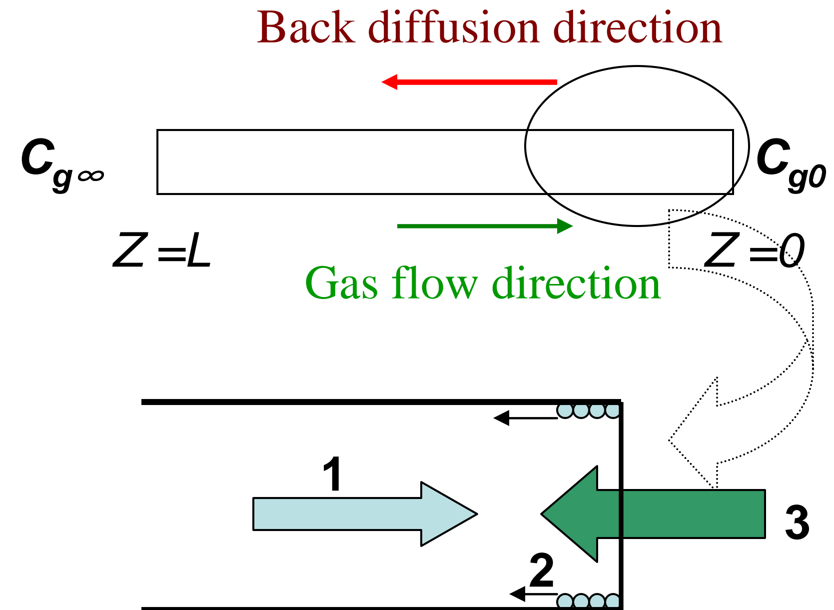

Governing equation for surface diffusion:

$$k_a C_g|_{r=R} - k_d C_s + D_s\frac{d^2 C_s}{dz^2} = 0 \quad [7]$$

$$C_s = \frac{k_a}{k_d}C_g \quad \text{at } z = 0 \quad [8]$$

$$C_s = \frac{k_a}{k_d}C_{g-} \quad \text{at } z = L \quad [9]$$

1: Bulk Convection

2: Surface diffusion

3. Bulk diffusion

Back Diffusion at Laterals-Simplified Model

Governing equation:

$$D_L \frac{\partial^2 C_g}{\partial z^2} - u \frac{\partial C_g}{\partial z} = 0$$

BC:

$$z = 0,\ C_g = C_{g0}$$
$$z = L,\ C_g = 1\,ppb$$

C_g: Moisture concentration in gas, mol/cm^3;

D_L: Dispersion coefficient, cm^2/s;

u: Velocity, m/s;

C_{g0}: Ambient moisture concentration

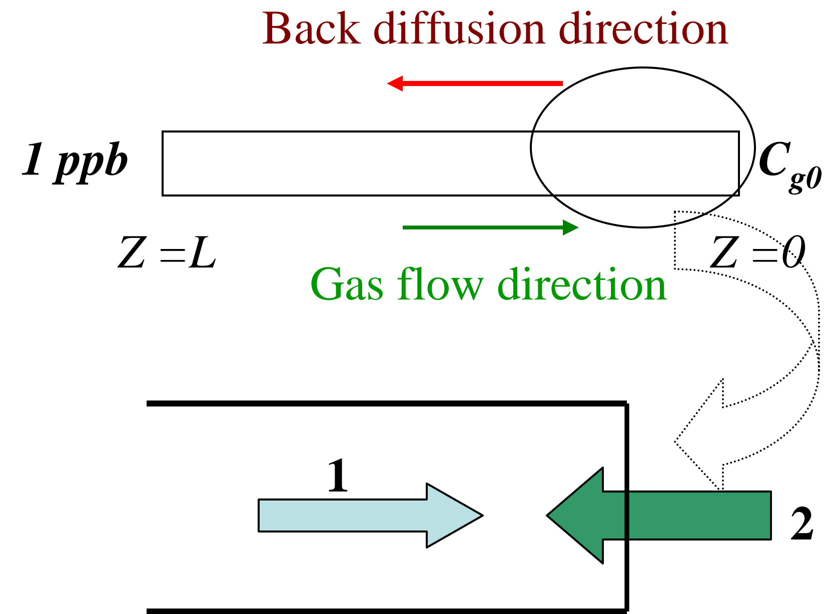

1: Bulk Convection

2. Bulk diffusion

Back Diffusion at Laterals

----Contd.

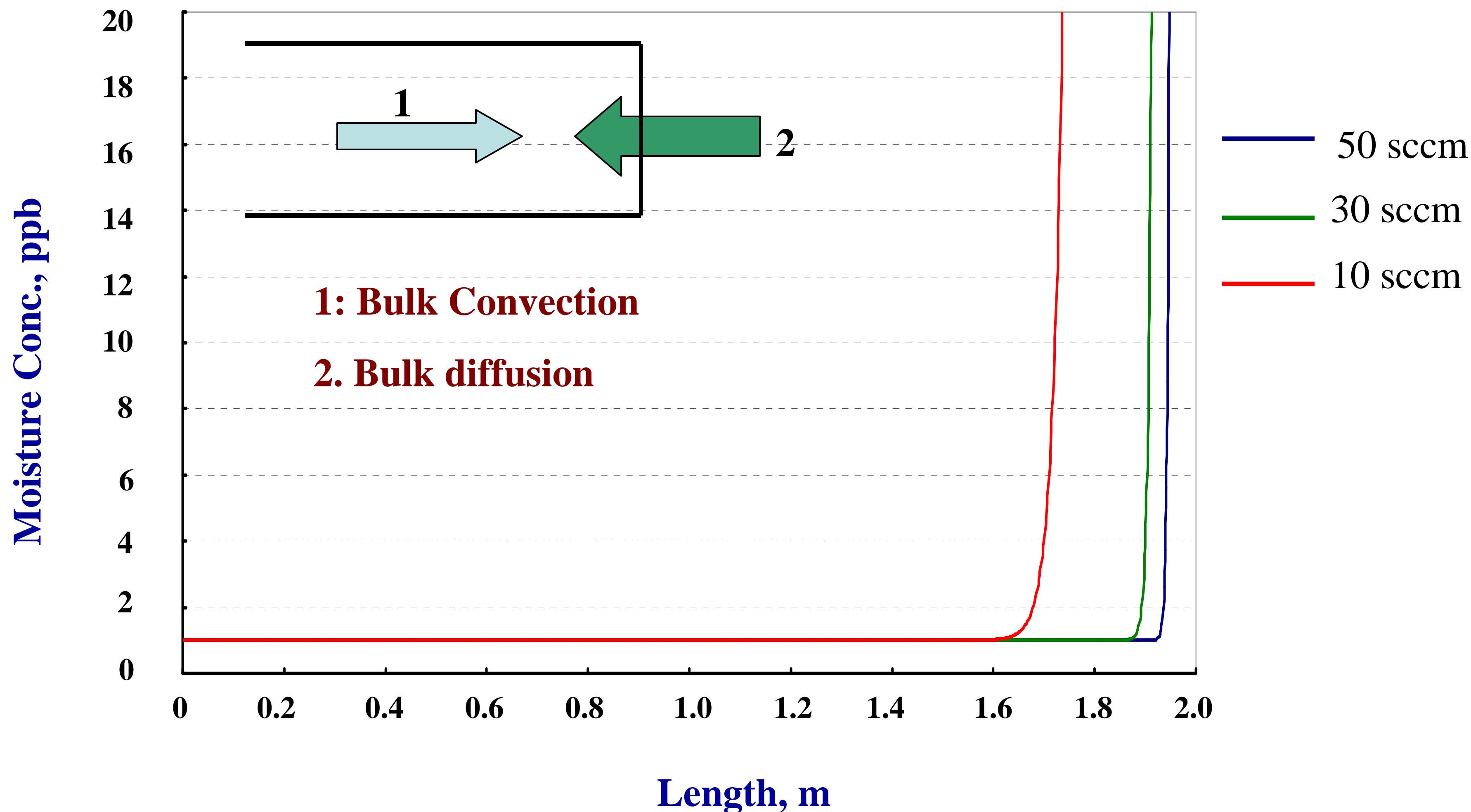

Interactions and Future Plans

- Continue working with Intel on this customized joint project; initiate similar applications and studies for other members.
- Experimentally compare cleaning of configurations that represent segments of a typical gas distribution network: single tubing without laterals, dead space or back-diffusion ports, etc.
- Complete the development of a comprehensive model.
- Prepare a software package for use in industry
- Study the positive and negative effects of transience in pressure and flow rate: negative effect on contamination and potential positive effect during purge.

Publications, Presentations, and Recognitions/Awards

- **J. Yao, A. Iqbal, H. Juneja, F. Shadman and Carl Geisert, "Lowering Purge Gas Consumption during Dry-down of Gas Delivery Systems ", Poster Presentation, 11th ERC Annual Review Meeting, Feb., 2007**

- **J. Yao, A. Iqbal, H. Juneja, F. Shadman, "Lowering Purge Gas Consumption during Dry-down of Gas Delivery Systems in Intel Chip Fabrication Factories", Presentation to gas engineers at Intel, Apr., 2007**

Post-Planarization Waste Minimization

(Customized Project)

PI:

- **Ara Philipossian, Chemical and Environmental Engineering, UA**

Graduate Student:

- **Ting Sun: Ph. D. candidate, Chemical and Environmental Engineering, UA**

Other Researcher:

- **Yun Zhuang, Research Associate, Chemical and Environmental Engineering, UA**

Cost Share (other than core ERC funding):

- **In-kind donation (PVA brushes) from ITW Rippey Corporation**

Objectives

- **Investigate how eccentric PVA brushes behave differently during post-CMP cleaning process in terms of brush contact pressure, contact area, variance of shear force, and shear force spectrum.**
- **Install a new motor to increase brush rotation rate and investigate the effect of brush rotation rate during post-CMP cleaning process.**

ESH Metrics and Impact

1. *Eliminates chemical, water, and energy consumption associated with qualifying PVA brushes that are eccentric for post-CMP cleaning processes.*

2. *Reduce PVA brush consumption by 20%.*

3. *Reduce post-CMP cleaning solution consumption by 20%.*

Method and Approach

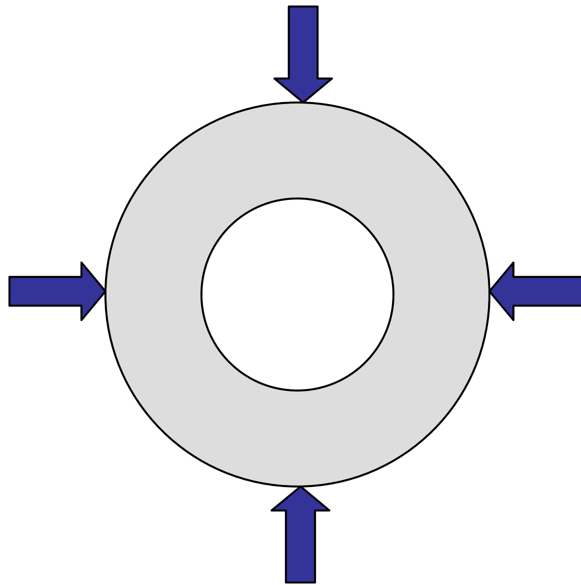

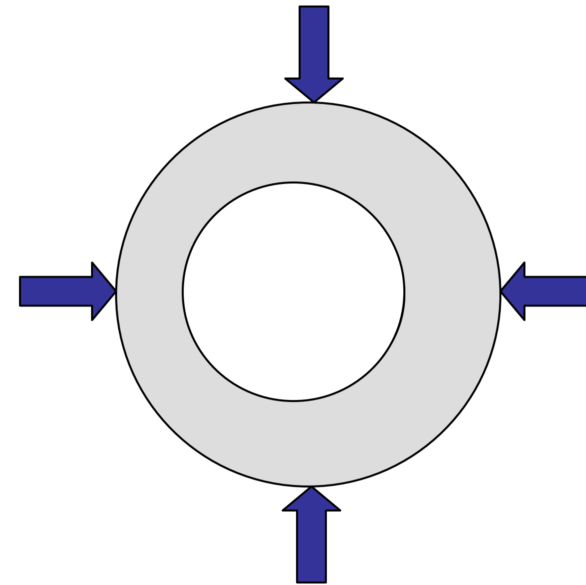

Good (i.e. perfectly concentric) Brush

Eccentric Brush

Good brushes were tested and compared with eccentric brushes when scrubbing under the same compression distance, *i.e.*, all brushes were compressed to the same point to generate a pressure of 0.5 PSI for the good brushes.

Multiple contact pressure and area measurements were performed by rotating brushes under four different orientations to investigate the effect of eccentricity.

Pressure Contour Map and Contact Area

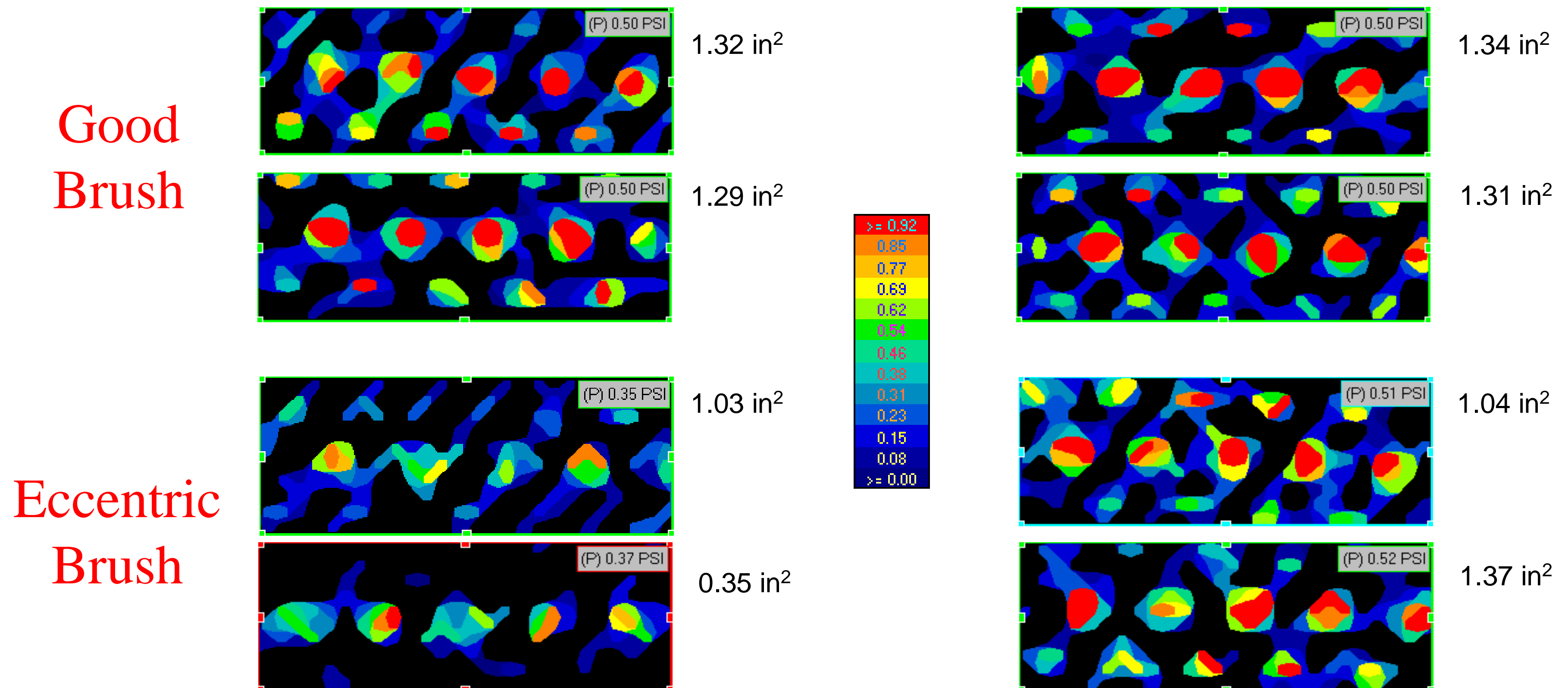

For the good brush, the contact pressure and contact area were consistent when rotating the brush. In comparison, for the eccentric brush, both the contact pressure and contact area varied significantly when rotating the brush.

Variance of Shear Force

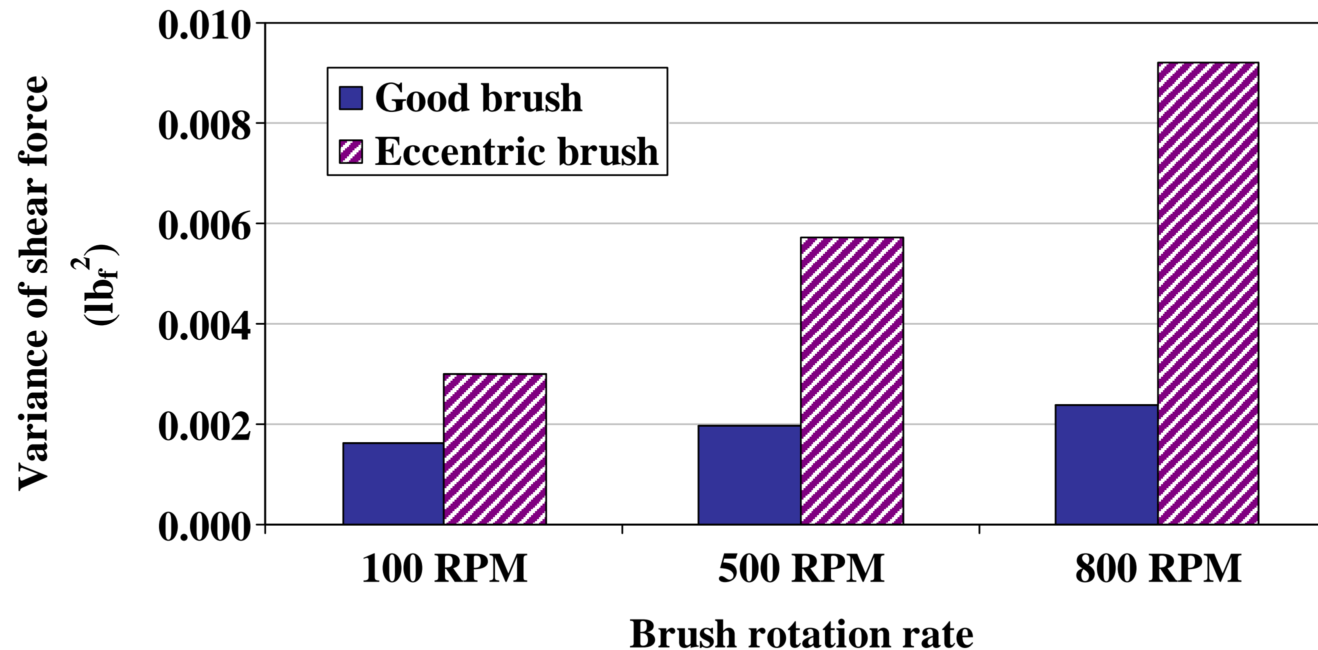

For both good and eccentric brushes, the variance of shear force increased with the brush rotation rate.

Under the same brush rotation rate, the eccentric brush had a significantly higher variance of shear force than a good brush.

Shear Force Spectral Analysis

Good Brush, 100 RPM

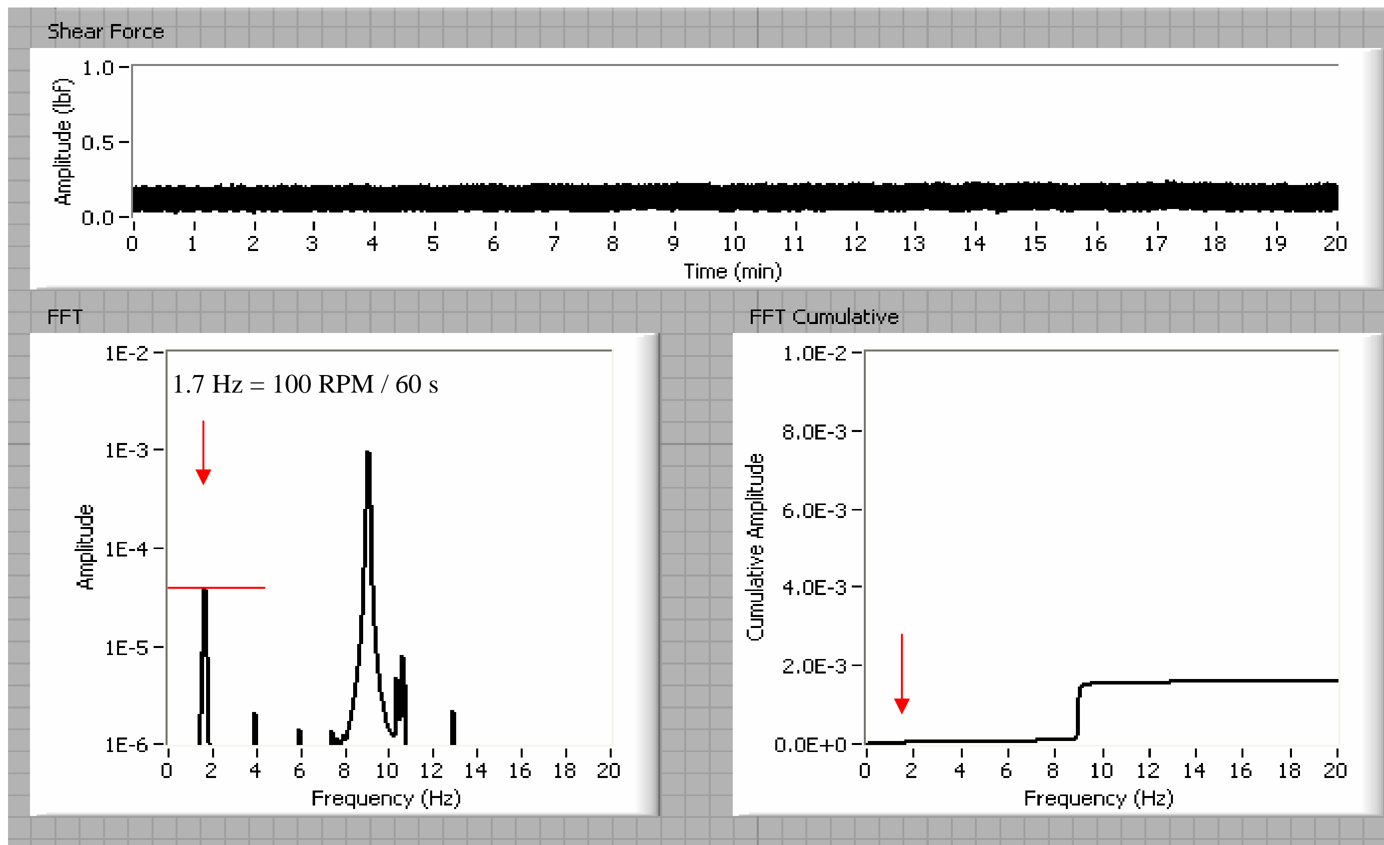

Shear Force Spectral Analysis

Eccentric Brush, 100 RPM

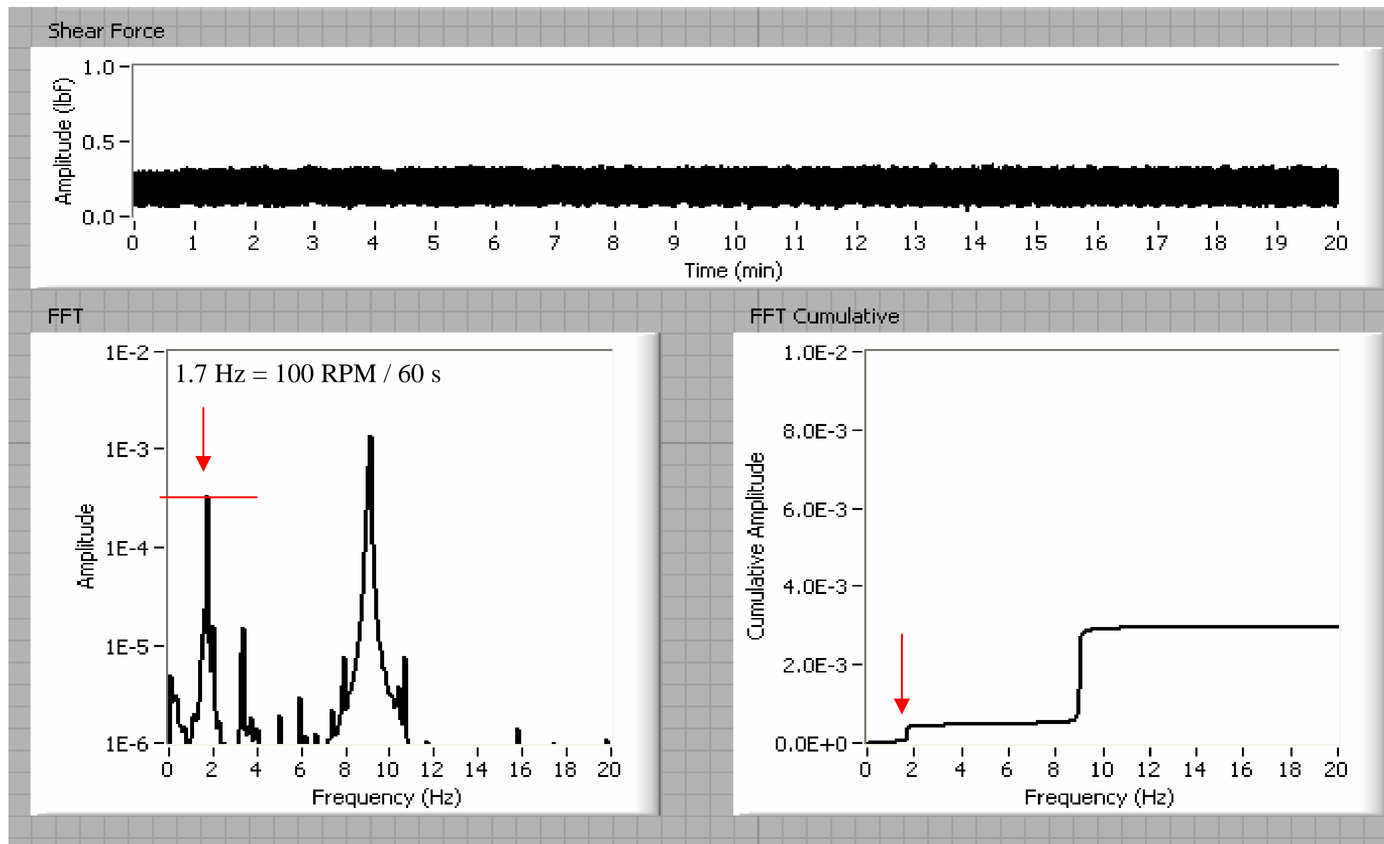

At 100 RPM, the eccentric brush showed higher spectral amplitudes at the frequency of 1.7 Hz.

Shear Force Spectral Analysis

Good Brush, 500 RPM

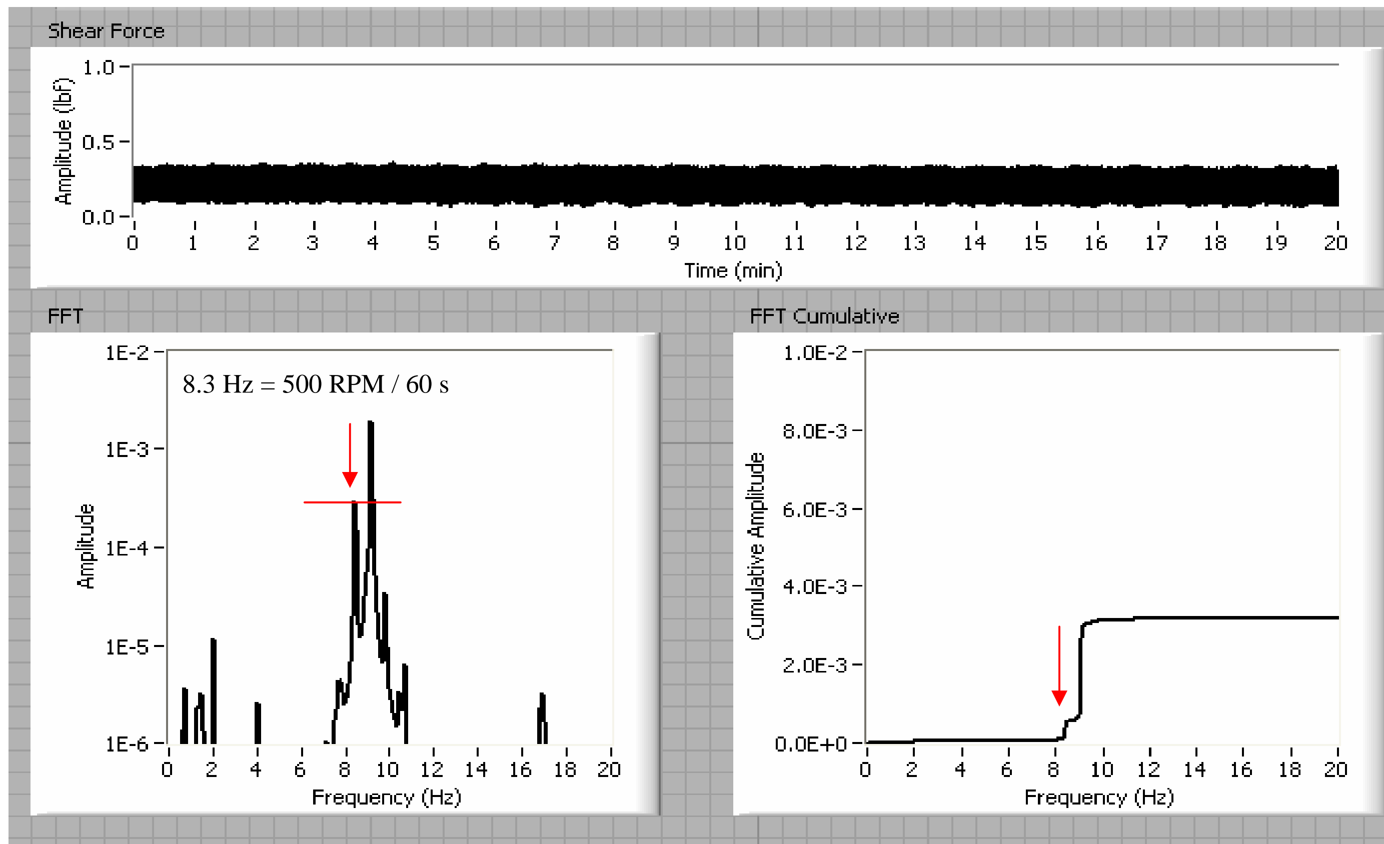

Shear Force Spectral Analysis

Eccentric Brush, 500 RPM

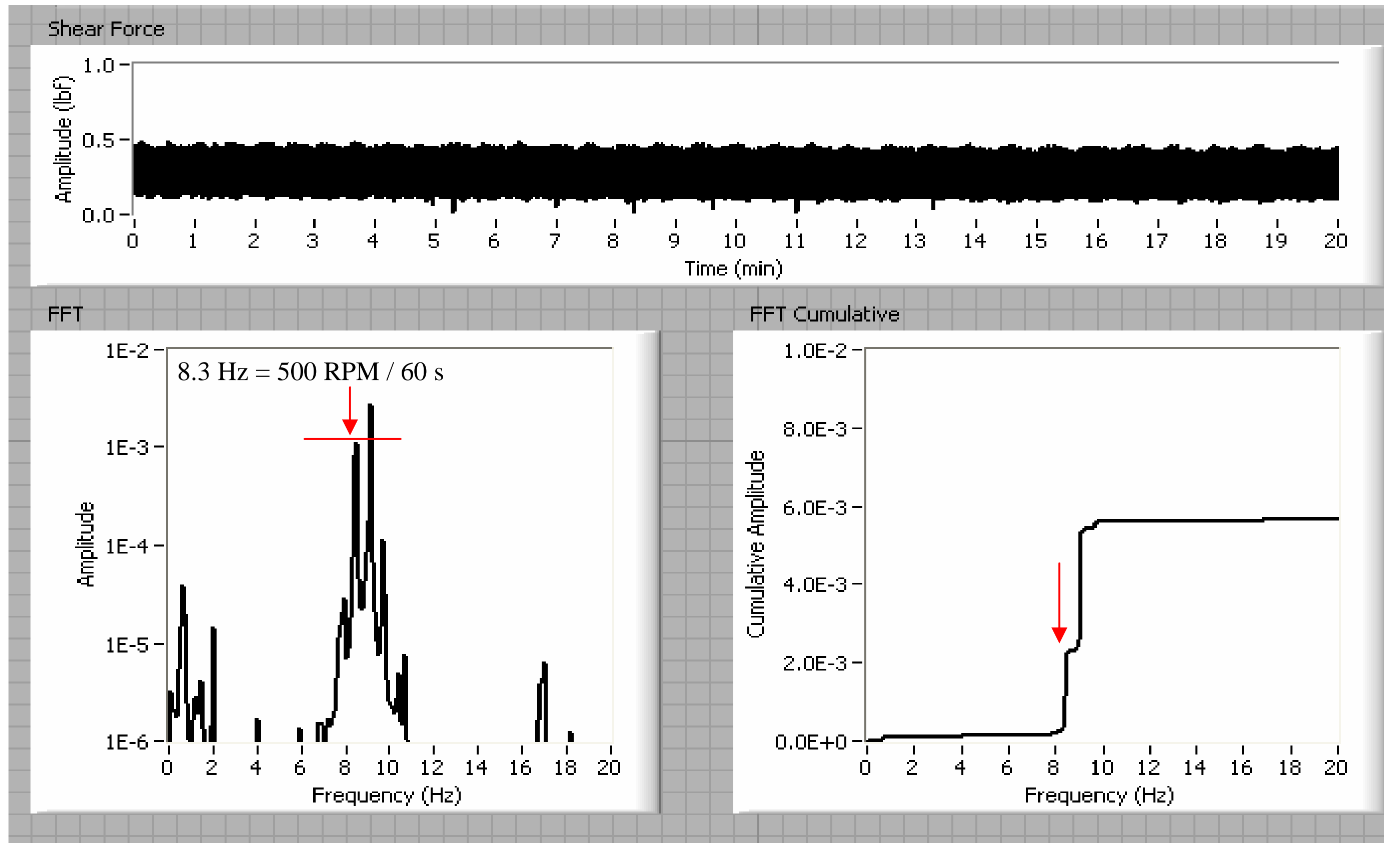

At 500 RPM, the eccentric brush showed higher spectral amplitudes at the frequency of 8.3 Hz.

Shear Force Spectral Analysis

Good Brush, 800 RPM

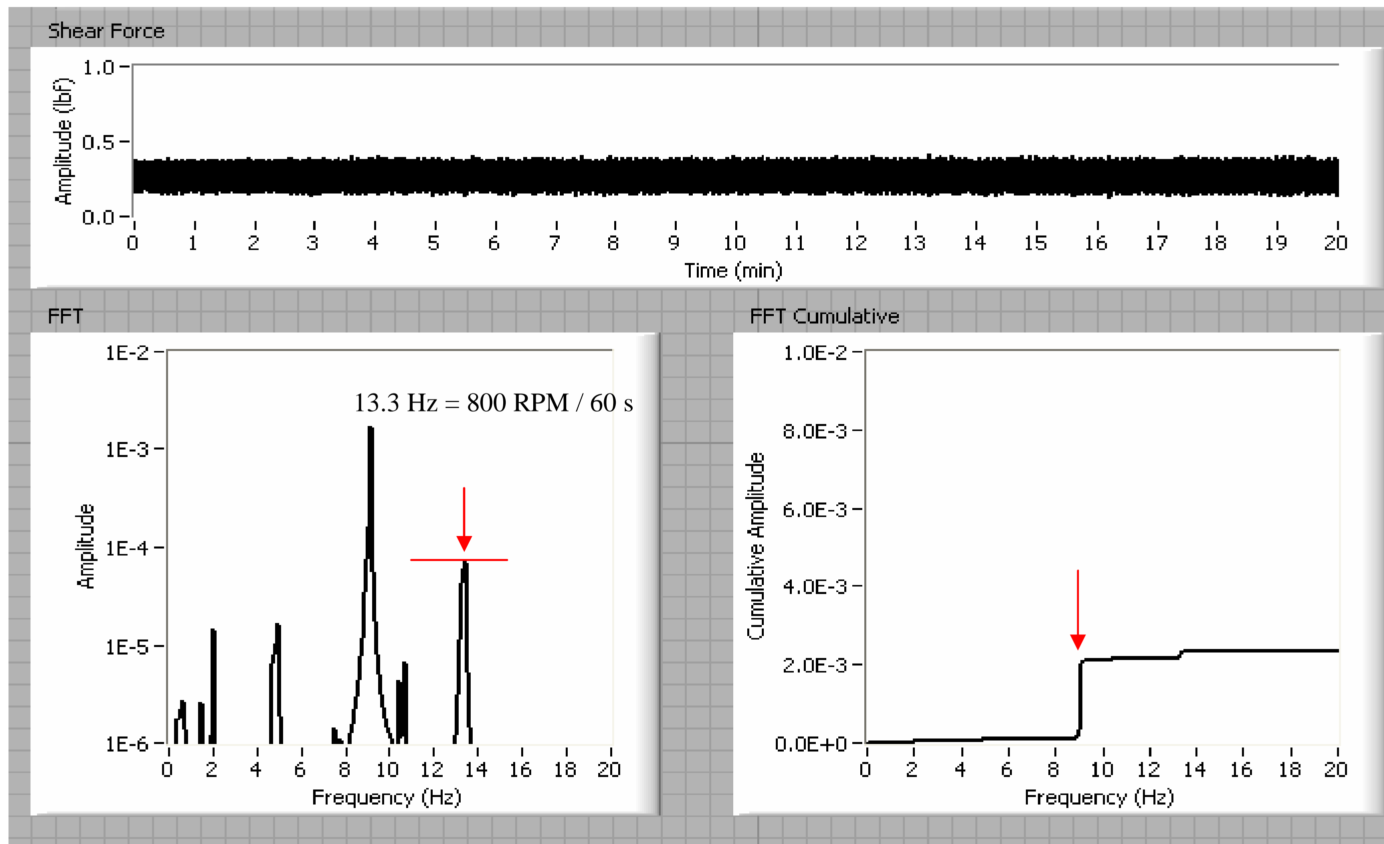

Shear Force Spectral Analysis

Eccentric Brush, 800 RPM

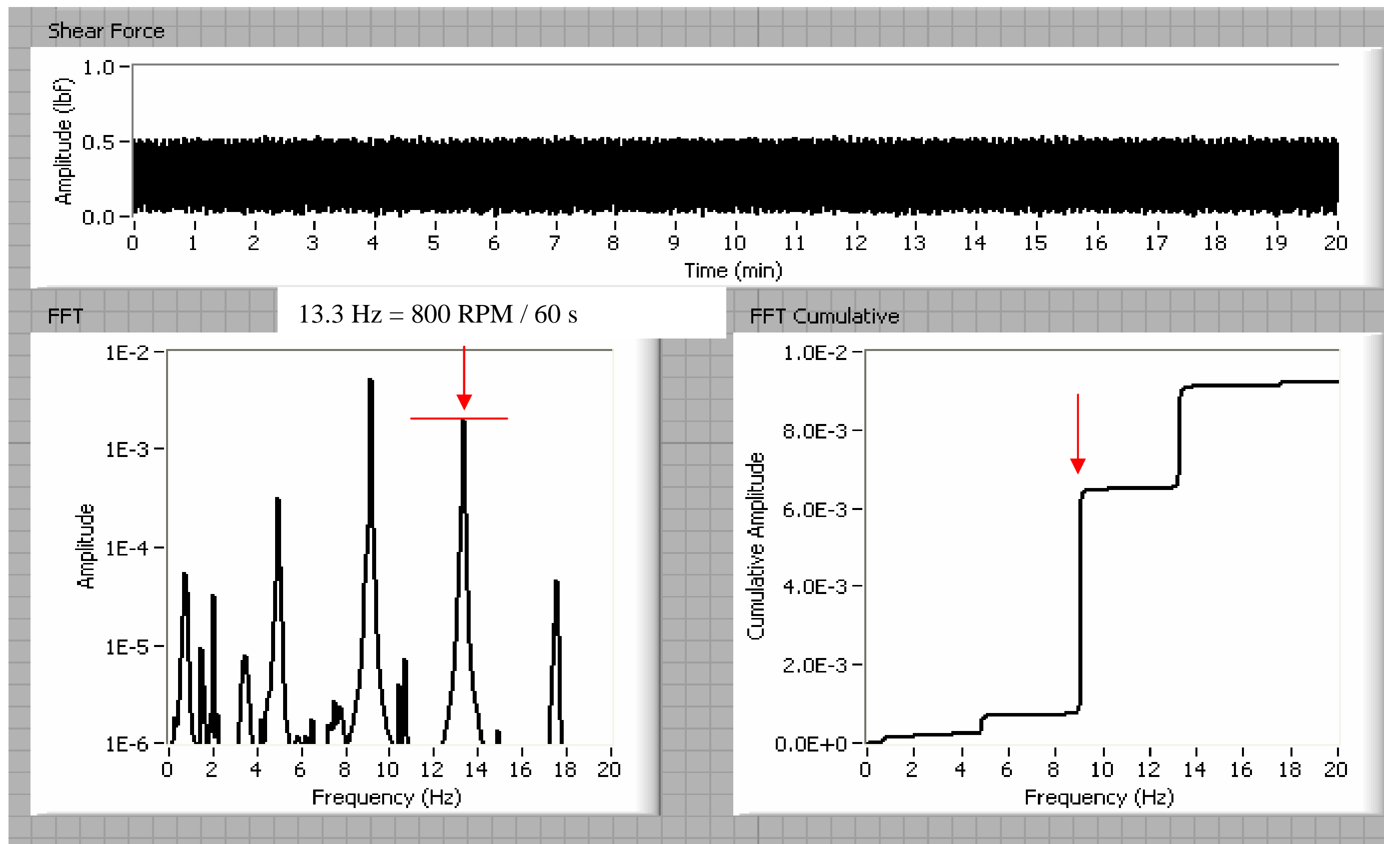

At 800 RPM, the eccentric brush showed higher spectral amplitudes at the frequency of 13.3 Hz.

Effect of Brush Rotation Rate on Shear Force

Good Brush

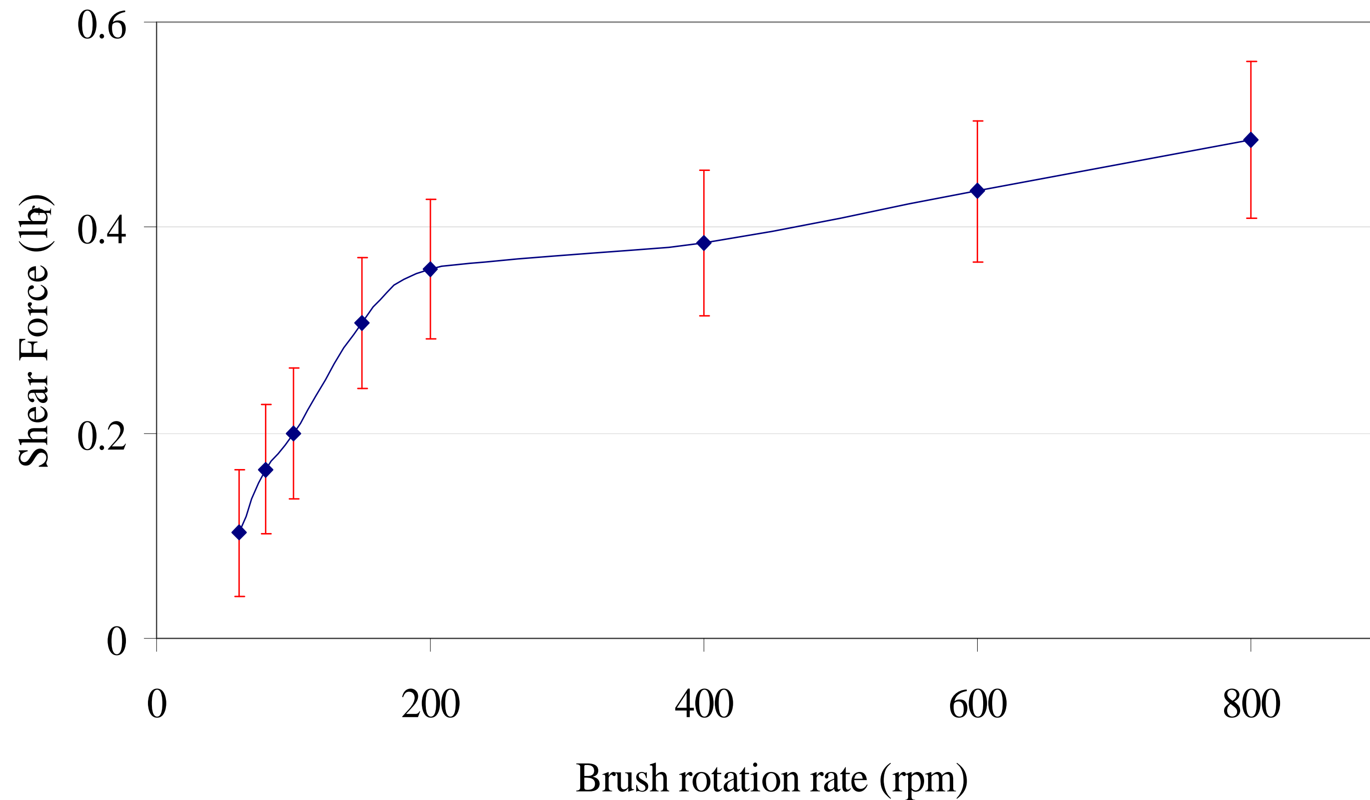

The shear force generally increased with the brush rotation rate.

Industrial Interactions and Technology Transfer

Industrial mentor / contact:

- **Weijin Li (ITW Rippey Corporation)**

Future Plans

Next Year Plans

- Investigate the effect of brush physical properties on the tribological behavior during post-CMP cleaning processes.
- Design, construct and qualify an incremental loading tool to investigate brush nodule deformation as a function of applied load and extended use.

Long-Term Plan

- Extend PVA brush life by better understanding the brush wear mechanism.

Simulation of Pad Stain Formation during Copper CMP

(Customized Project)

PI:

- **Ara Philipossian, Chemical and Environmental Engineering, UA**

Graduate Student:

- **Hyosang Lee: PhD candidate, Chemical and Environmental Engineering, UA**

Other Researcher:

- **Yun Zhuang, Research Associate, Chemical and Environmental Engineering, UA**

Cost Share (other than core ERC funding):

- **In-kind support from Araca, Inc.**

Objective

Develop 3-D fluid transport, thermal and kinetic models to simulate pad stains formed during copper CMP process.

ESH Metrics and Impact

1. *Reduce pad cleaning solution consumption by 25%*

2. *Reduce pad consumption by 25%*

Axisymmetric Polishing System

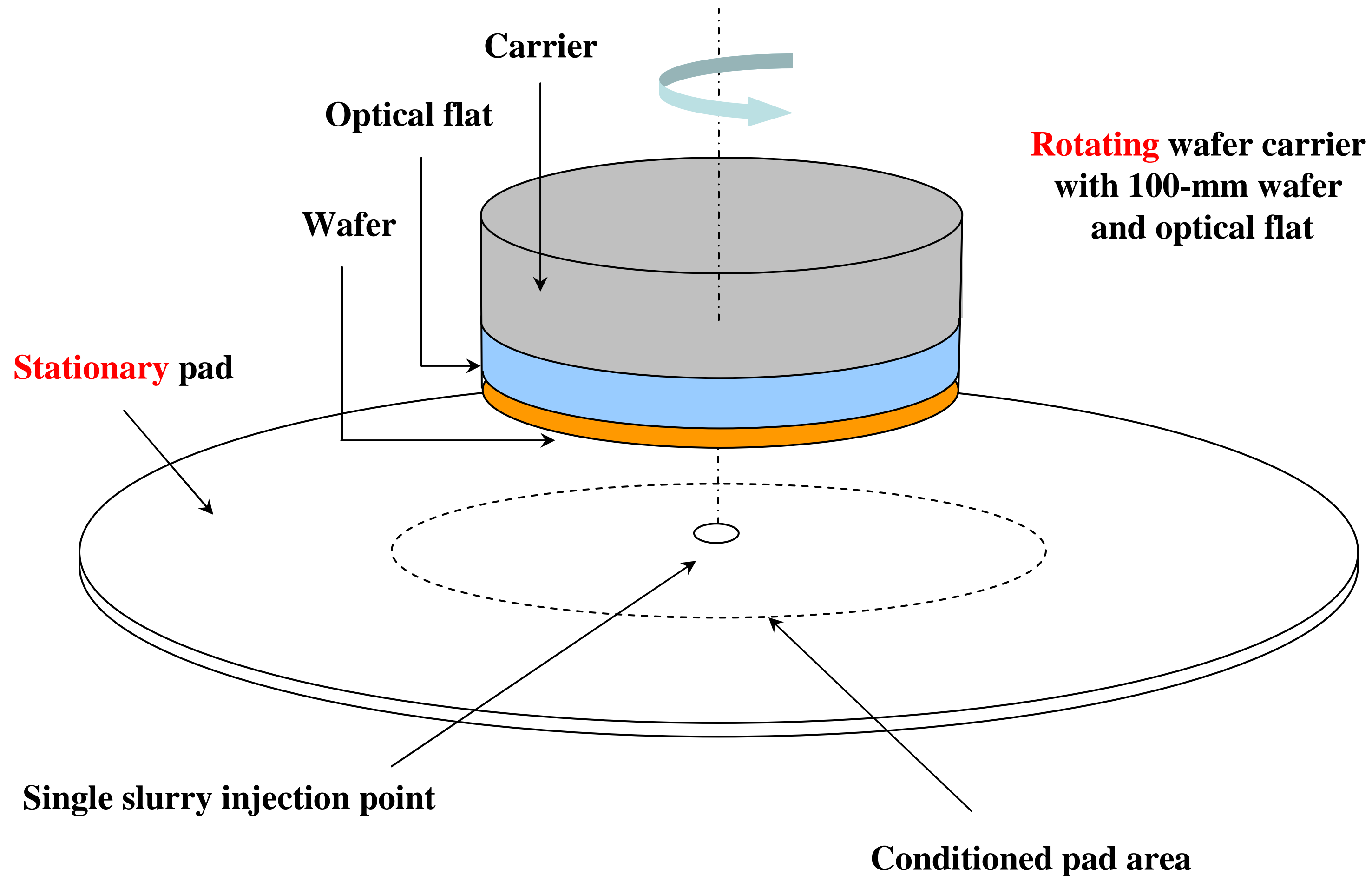

Stain Advection

Pad was rotating counter-clockwise.

The generated pad stain on each land area was darker following the direction of wafer rotation, suggesting the stain was affected by slurry advection.

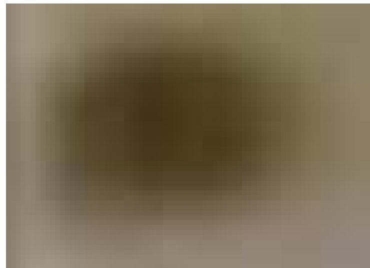

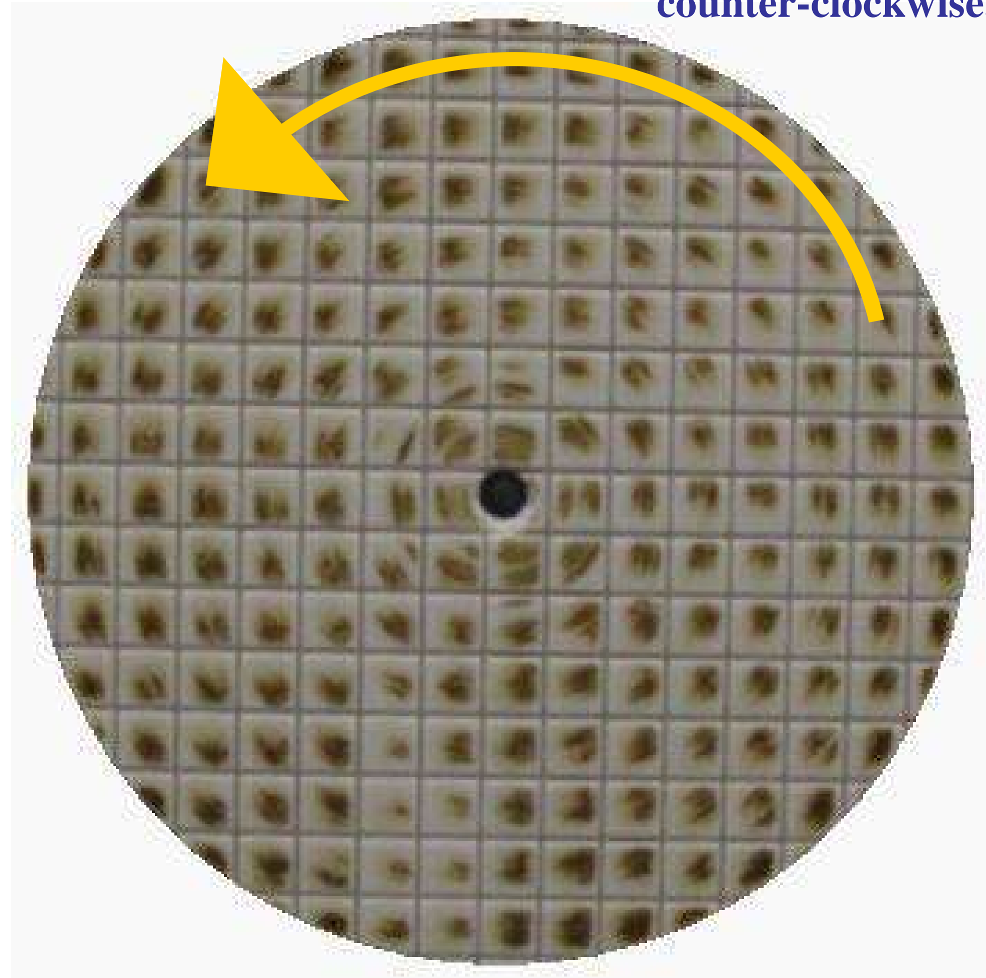

Simulation of By-Product Concentration on Pad Surface

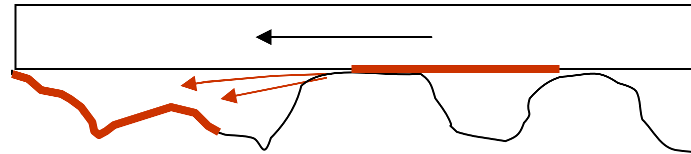

Governing equation:

$$\frac{\partial c_s}{\partial t} + \vec{V} \cdot \vec{\nabla} c_s = \nabla \cdot (D \nabla c_s)$$

Advection by the fluid with a velocity

C_s: Concentration of by-product

B.C. at wafer surface:

$$D \vec{\nabla} C_s \cdot \vec{n} = \frac{k_2 k_1}{k_1 + k_2}$$

$$k_1 = A_1 \cdot \exp\left(\frac{-E_1}{kT}\right)$$

T: extracted from copper surface

$$k_2 = c_p \text{ x } \mu_k \text{ x } p_s \text{ x } V$$

B.C. at pad surface:

$$-D \vec{\nabla} C_s \cdot \vec{n} = k_4 C_s$$

$$k_4 = A_4 \cdot \exp\left(\frac{-E_4}{kT}\right)$$

T: extracted from pad surface

Slurry Velocity Simulation

Conditions

- **20 micron slurry layer**
- **1 mm groove depth and width**
- **50 ml/min slurry flow rate**
- **150 RPM wafer rotation rate**

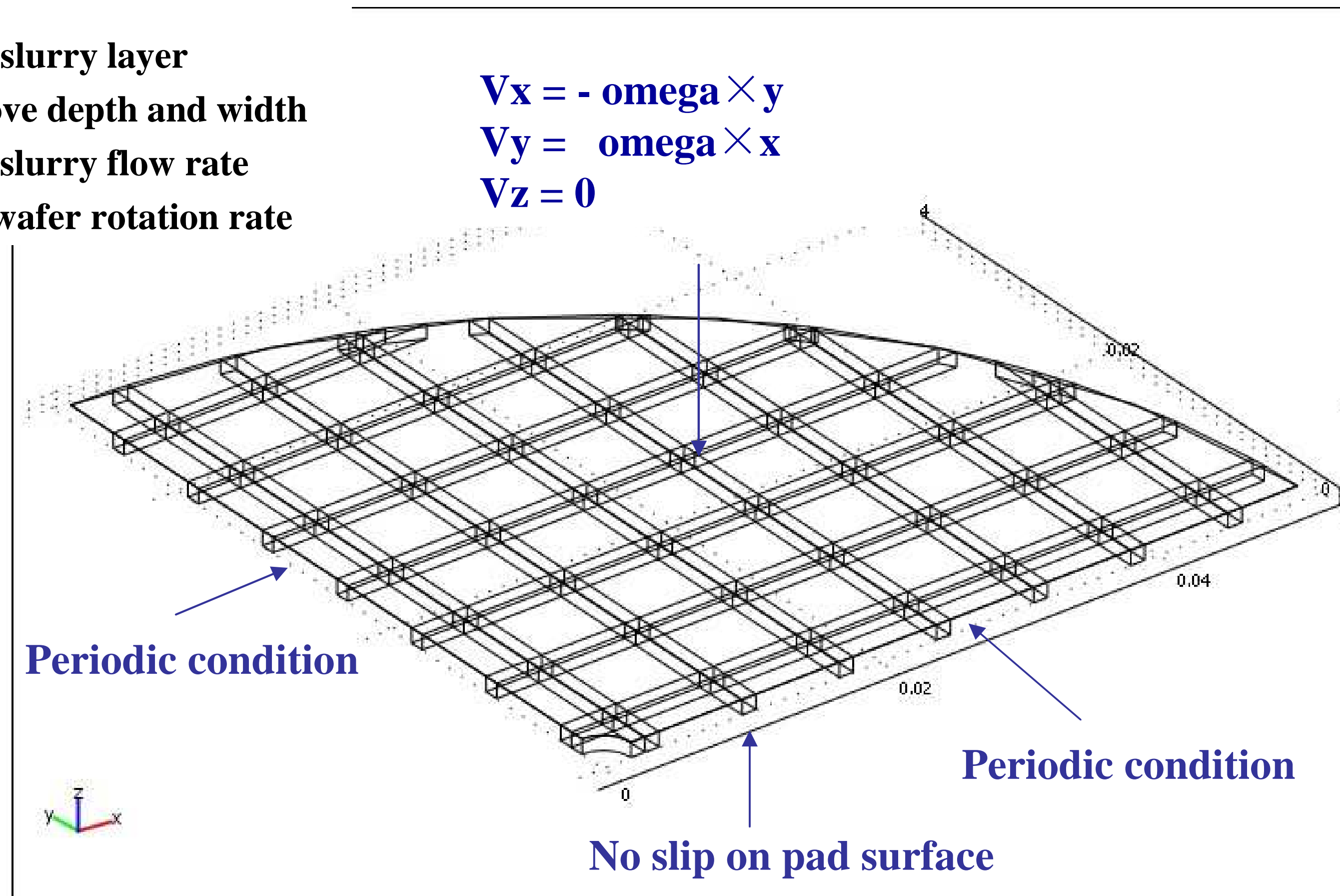

The Navier-Stokes equations for the slurry flow were solved only in the grooves and on the land areas.

Simulated Slurry Velocity on Wafer Surface

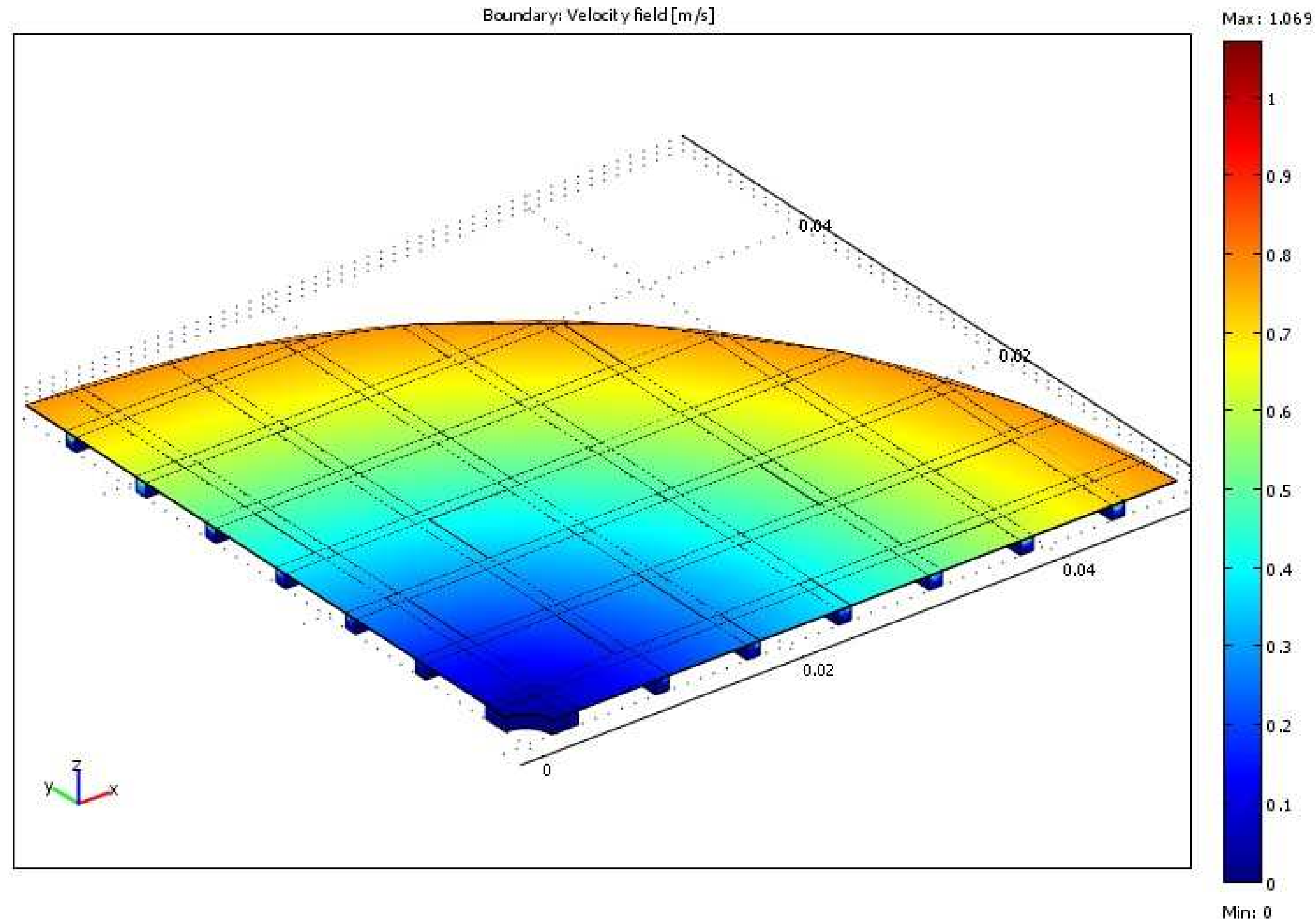

Slurry velocity increased gradually on wafer surface in the radial direction due to wafer rotation, thus affecting slurry velocity in the grooves.

Simulated Slurry Velocity in Grooves and on Land Area

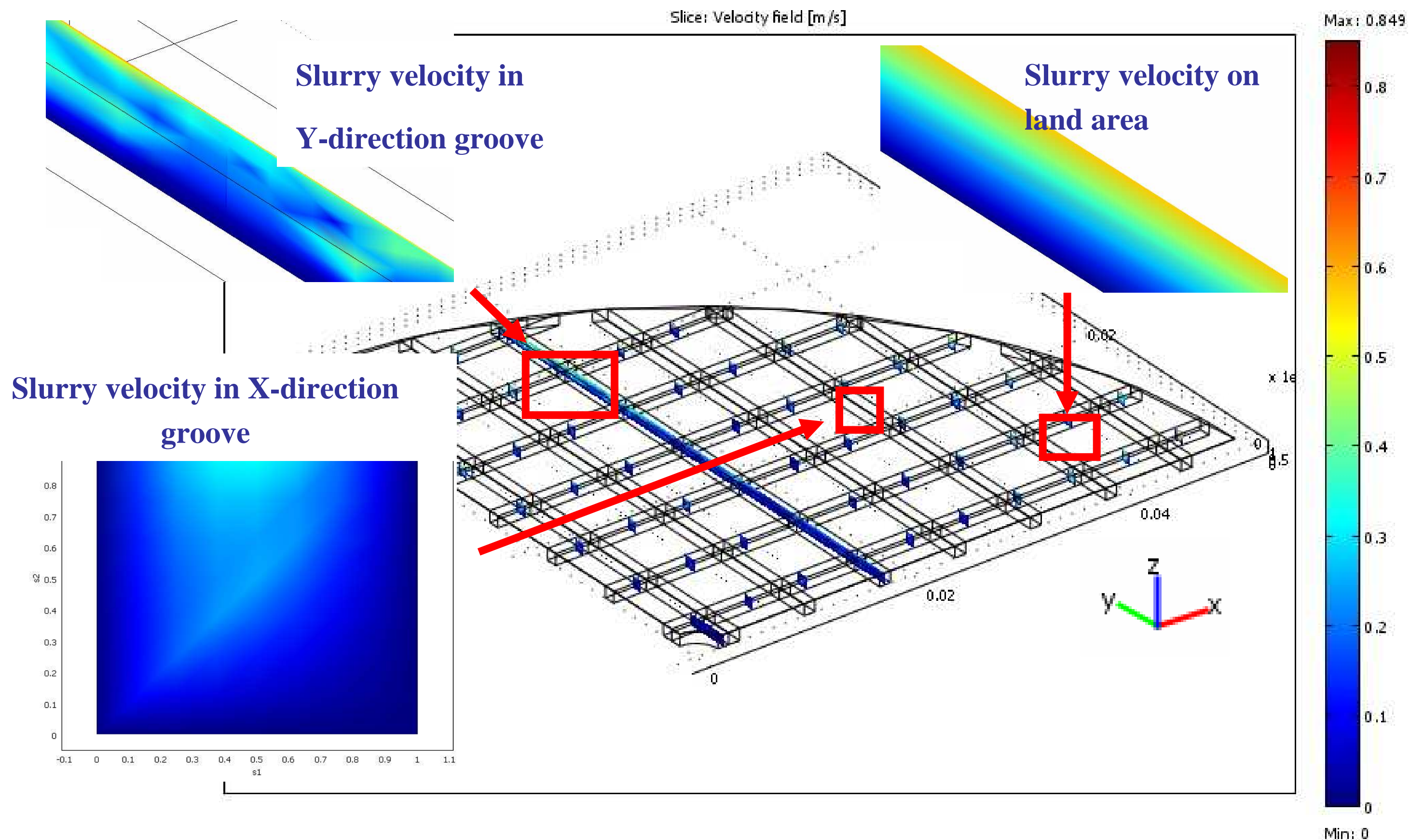

Results showed shear flow on the land areas and wafer-driven circulation in the grooves.

Thermal Model

Heat equation

$$\rho C_p\left(\frac{\partial T}{\partial t} + \vec{V}\cdot\vec{\nabla}T\right) = \vec{\nabla}\cdot(\kappa\vec{\nabla}T) + Q$$

$\vec{V}$:
- From Navier-Stokes in slurry layer
- Rigid body in wafer and above
- 0 in pad

Q : $\frac{\mu_k p_s V_s}{h}$ in slurry layer

μ_k : COF

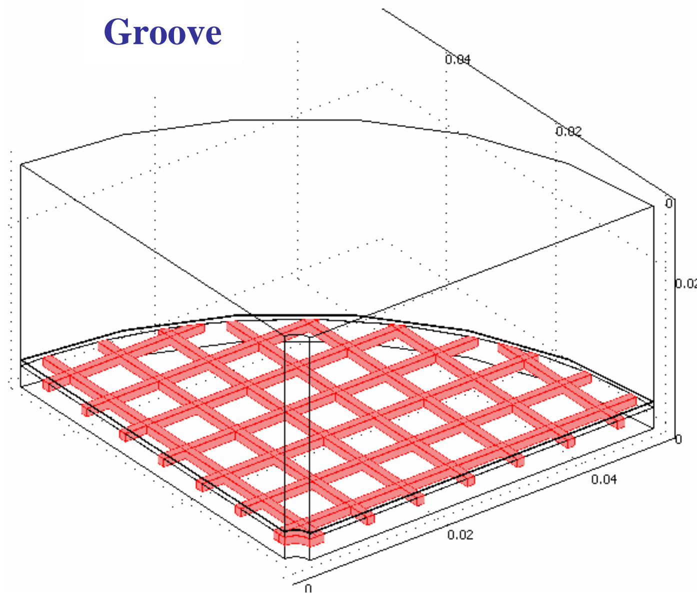

$$\rho C_p\left(\frac{\partial T}{\partial t} + \vec{V}\cdot\vec{\nabla}T\right) = \vec{\nabla}\cdot(\kappa\vec{\nabla}T)$$

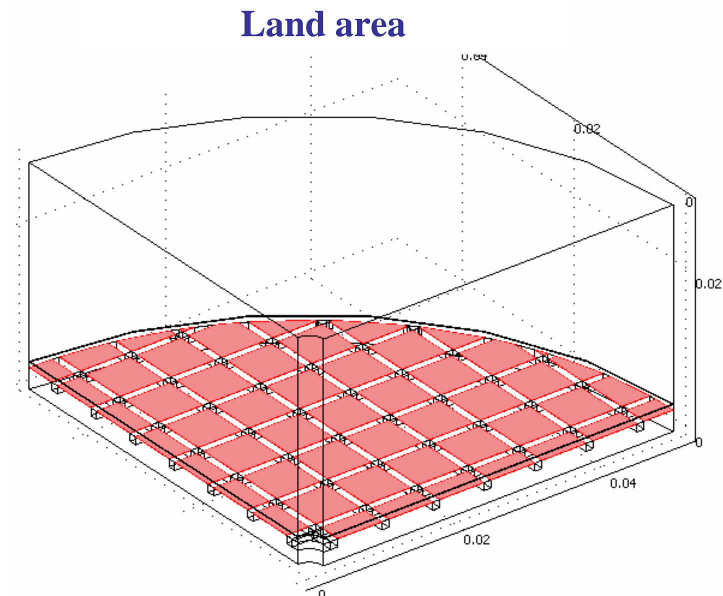

$$\rho C_p\left(\frac{\partial T}{\partial t} + \vec{V}\cdot\vec{\nabla}T\right) = \vec{\nabla}\cdot(\kappa\vec{\nabla}T) + \frac{\mu_k p_s V_s}{h}$$

Simulated Temperature Profile

Copper surface

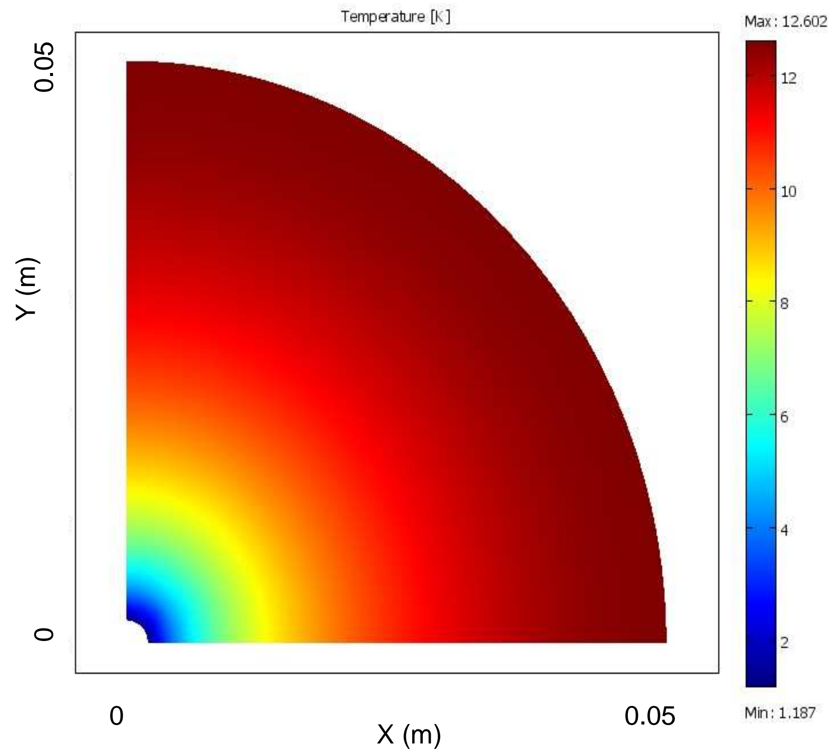

Pad land area

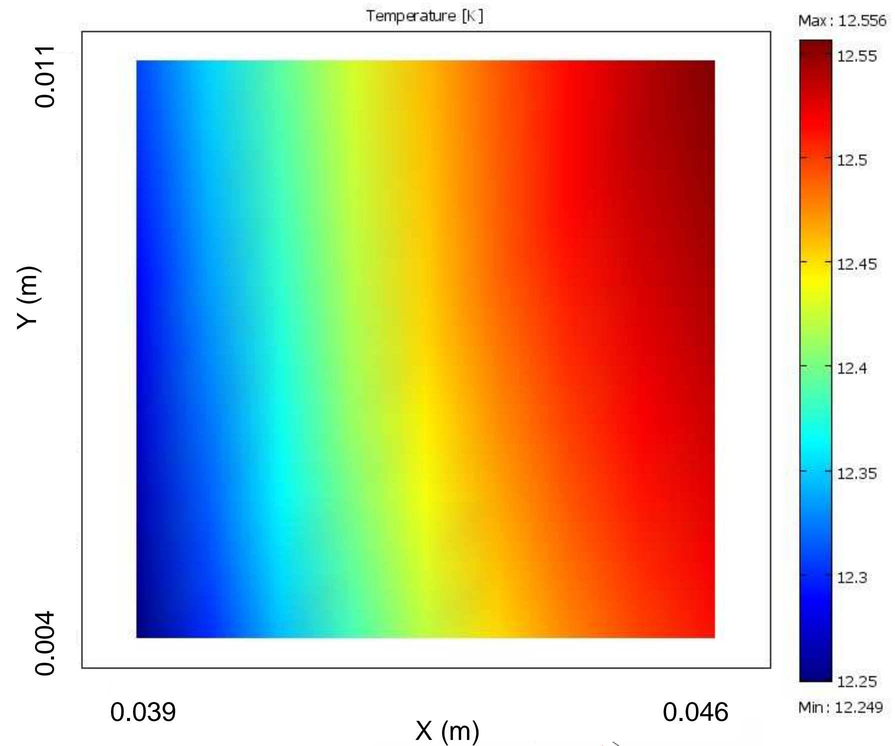

Simulated wafer and pad temperatures increased in the radial direction.

There was a 12 °C temperature rise at the wafer edge.

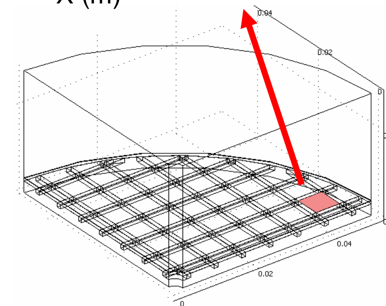

Boundary Conditions for Stain Formation

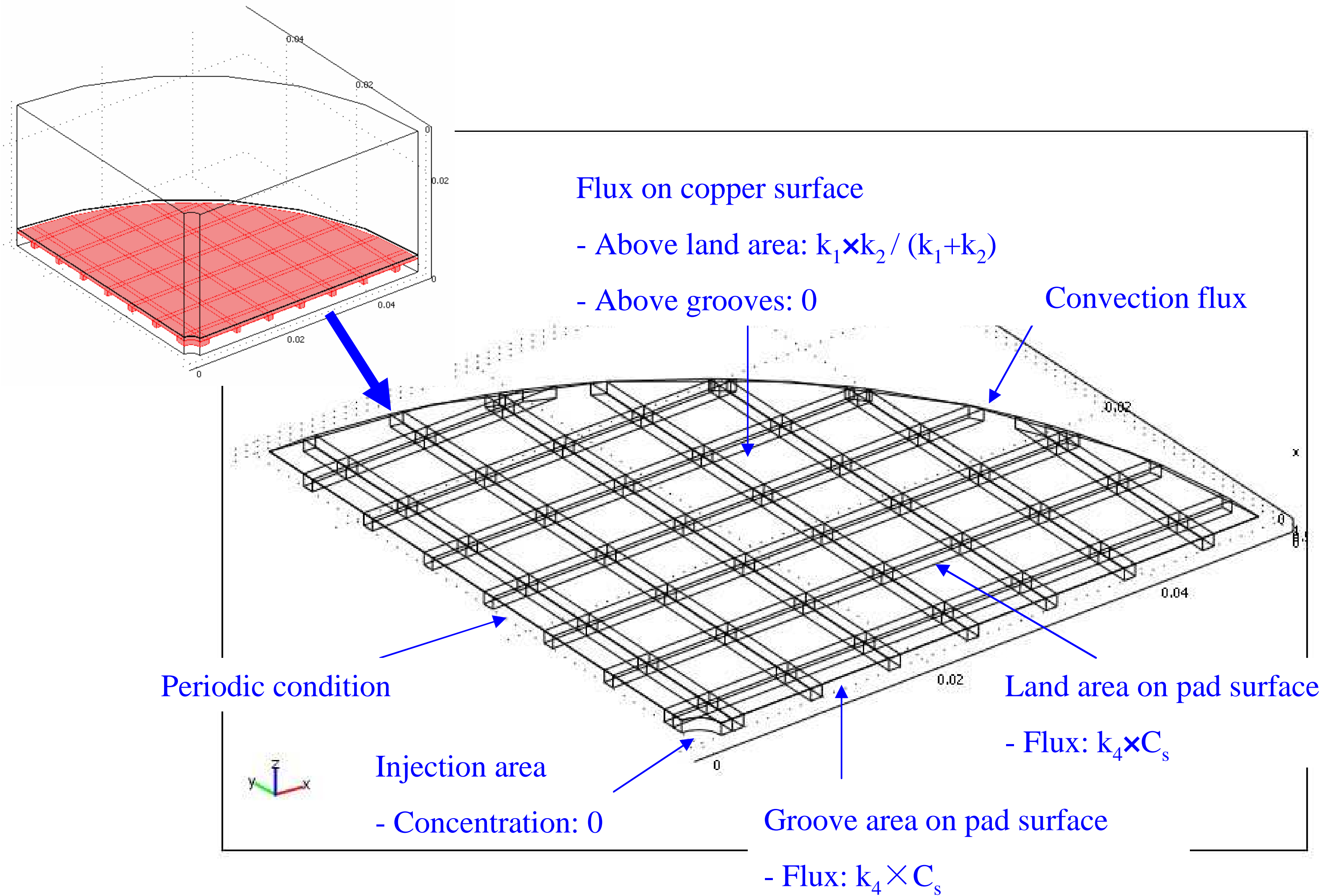

Simulated Stain Formation

Pad stain picture

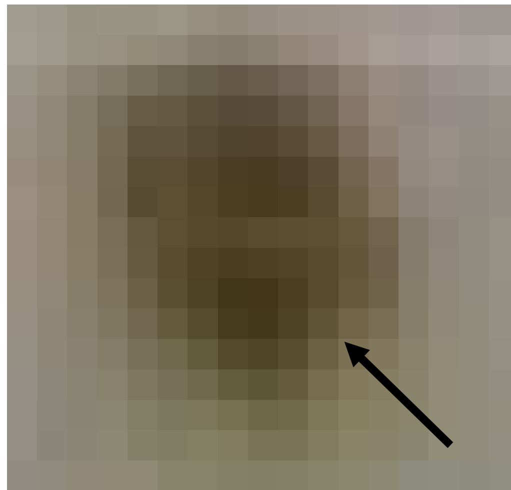

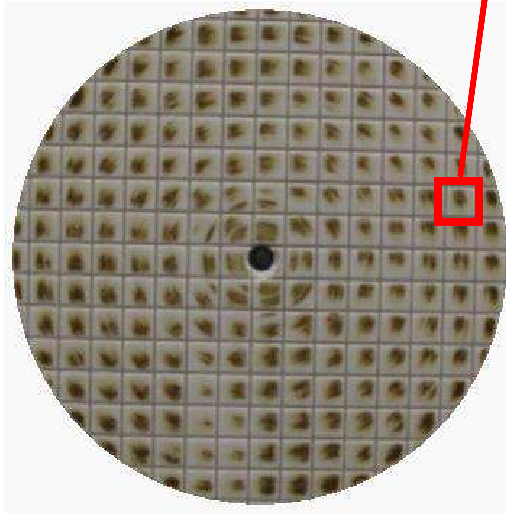

Simulated pad stain

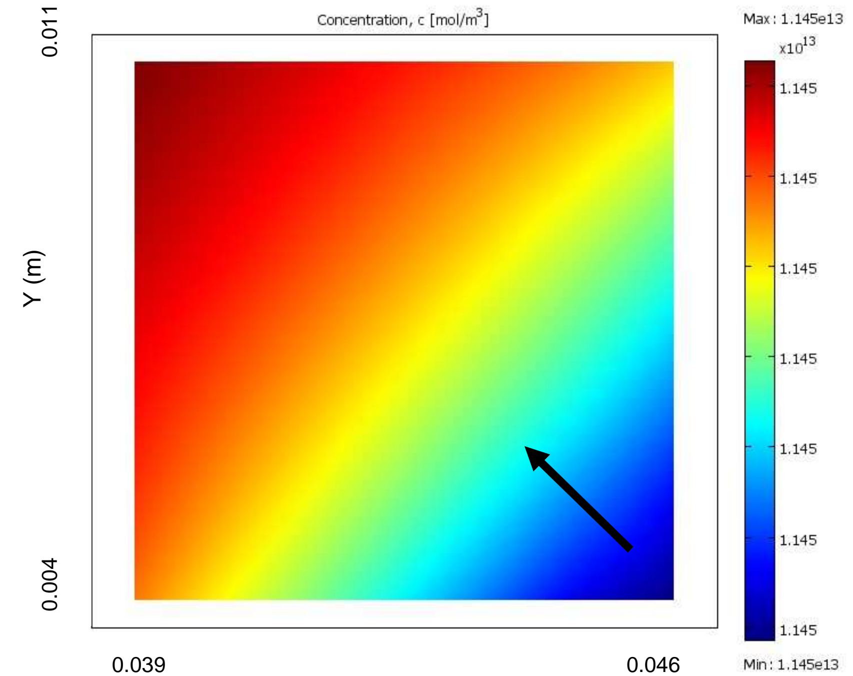

The simulated pad stain was darker following the direction of wafer rotation (black arrows indicated the direction of wafer rotation).

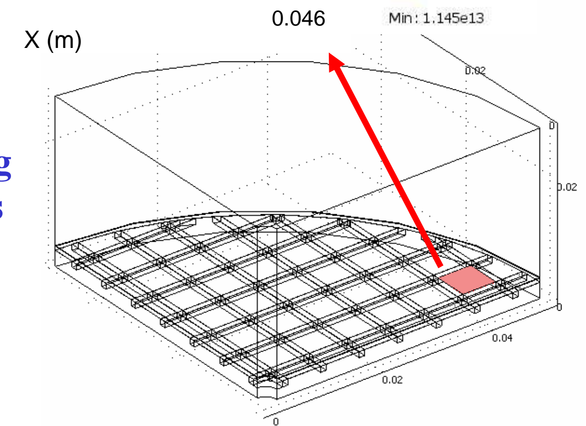

Industrial Interactions and Technology Transfer

Industrial mentors / contacts:

- **Fergal O'Moore (Novellus Systems, Inc.)**
- **Sooyun Joh (Novellus Systems, Inc.)**
- **Brian Brown (Novellus Systems, Inc.)**
- **Leonard Borucki (Araca, Inc.)**

Publications and Presentations

Publication:

- **Experimental Investigation and Numerical Simulation of Pad Stain Formation during Copper CMP. H. Lee, Y. Zhuang, L. Borucki, F. O'Moore, S. Joh and A. Philipossian. Materials Research Society Symposium Proceedings, Vol. 991, C06-02 (2007).**

Presentation:

- **Experimental Investigation and Numerical Simulation of Pad Stain Formation during Copper CMP. H. Lee, L. Borucki, Y. Zhuang, F. O'Moore, S. Schultz, S. Joh and A. Philipossian. 2007 Materials Research Society Spring Meeting, San Francisco, California, April 9-13 (2007).**

Effect of Concentric Slanted Groove Patterns on Slurry Flow during Copper CMP

(Customized Project)

PI:

- Ara Philipossian, Chemical and Environmental Engineering, UA

Graduate Students:

- Daniel Rosales-Yeomans: Chemical and Environmental Engineering, UA, graduated with Ph. D. degree in December 2007
- Hyosang Lee: Ph. D. candidate, Chemical and Environmental Engineering, UA

Undergraduate Student:

- Roy Dittler, Chemical and Environmental Engineering, UA

Cost Share (other than core ERC funding):

- In-kind support (pad grooving service) from Toho Engineering

Objective

Determine the effects of concentric slanted groove design, wafer pressure, sliding velocity, and slurry flow rate on slurry film thickness between pad and wafer interface.

ESH Metrics and Impact

1. *Reduce slurry consumption by 33%*

2. *Extend pad life and reduce pad consumption by 33%*

Concentric Slanted Groove Design

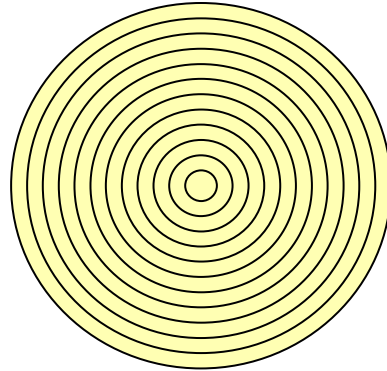

Wafer and pad rotate counter – clockwise.

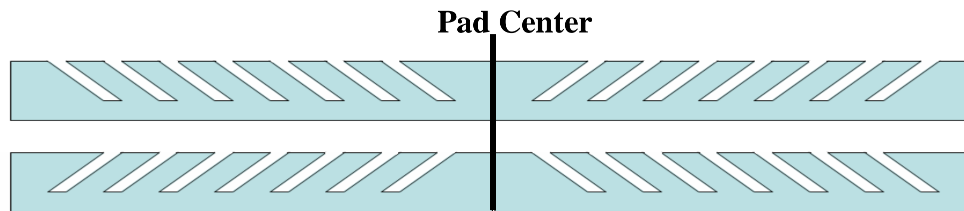

Positive Direction

Negative Direction

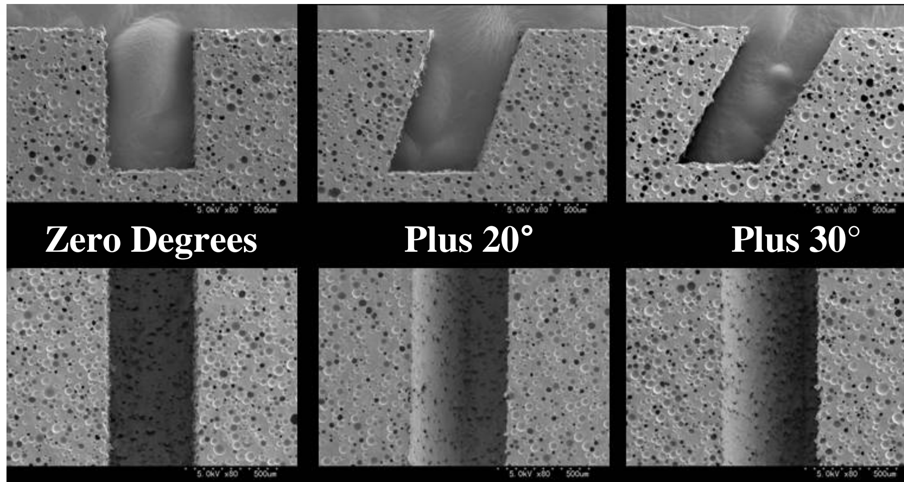

Side View

Top View

The Effect of Slanted Grooves on Slurry Flow

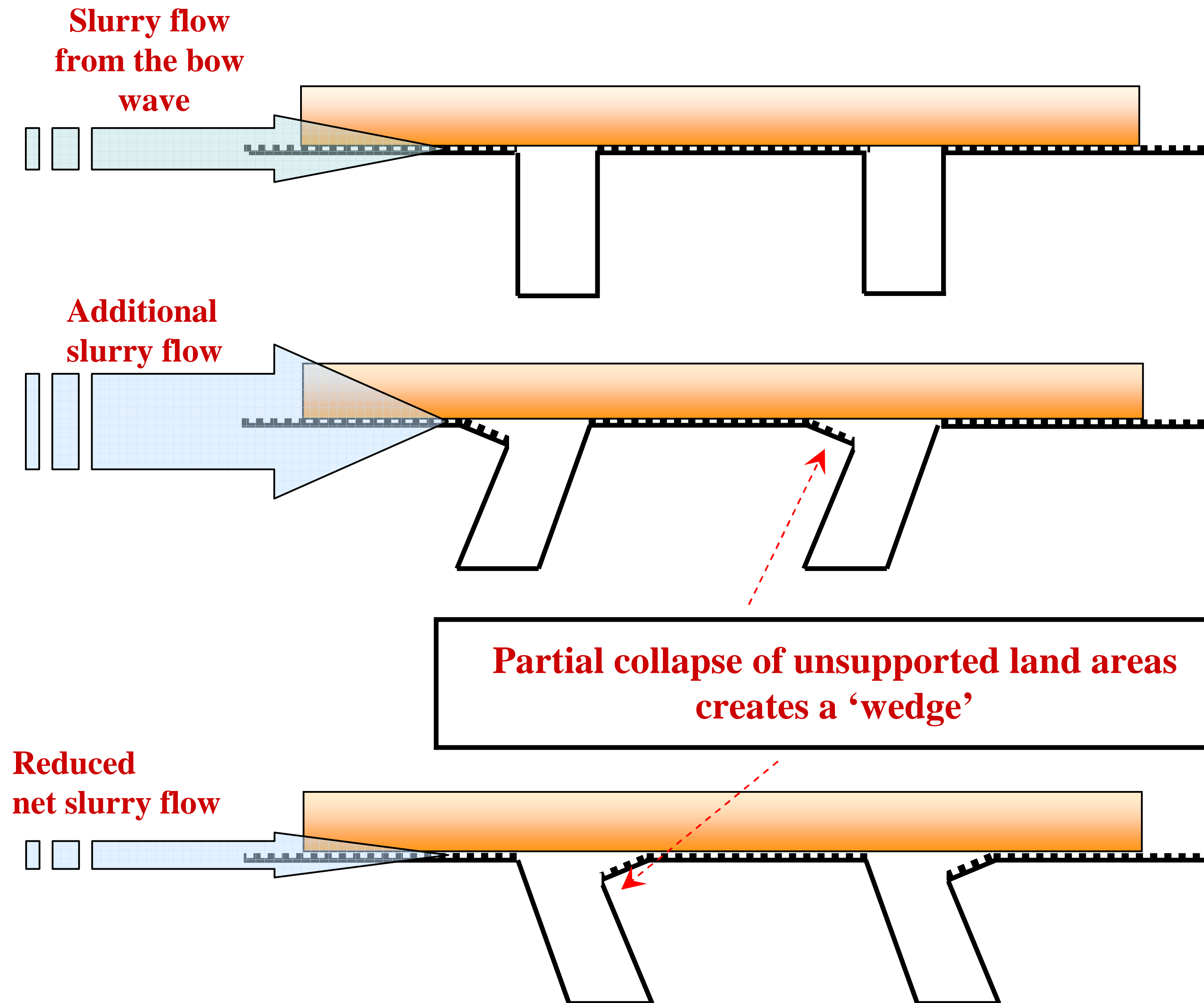

Wafer load is supported by pad land areas.

Wafer load is partially supported by pad land areas and by the slurry.

Slurry must flow continuously INTO the wedge of the 'land area' to balance hydrodynamic forces.

Dual Emission UV Enhanced Fluorescence

Slurry is tagged with 2 different fluorescent dyes:

Coumarin at 0.25 g/l

Calcein at 1.00 g/l

When excited by UV, each dye emits fluorescent light at a different wavelength.

Two CCD cameras capture emitted light.

During the excitation process:

1) **UV excites Coumarin**
2) **Coumarin emits fluorescent light**
3) **The light emitted by Coumarin, is absorbed by Calcein**
4) **Calcein then emits fluorescent light**
5) **The intensity ratio of Calcein-to-Coumarin is related to fluid film thickness**

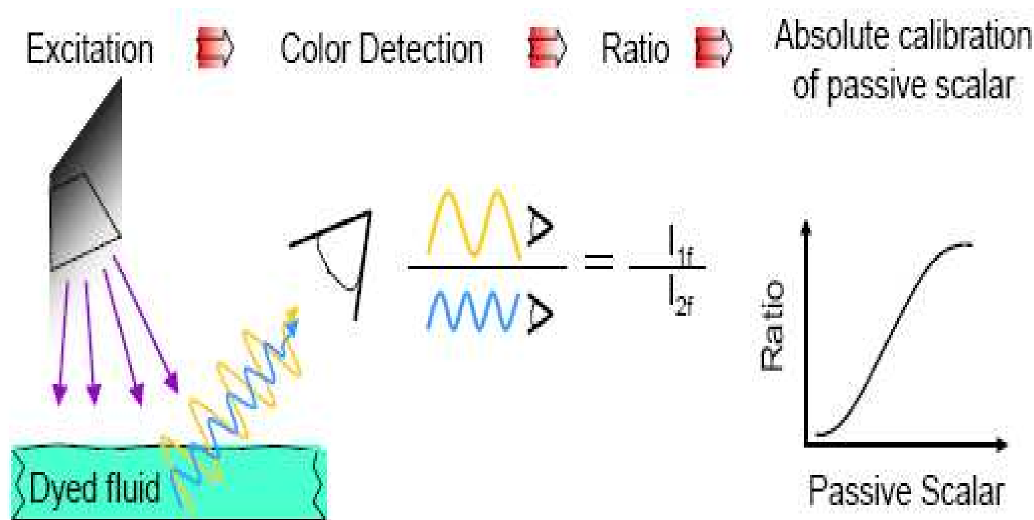

Amount of light (intensity) emitted is proportional to:

- **Extent of UV radiation**
- **Ability of a dye to convert UV light into fluoresced light**
- **Amount of UV light absorbed**
- **Dye concentration**
- **Amount of dye exposed**

200-mm Polisher Equipped with DEUVEF

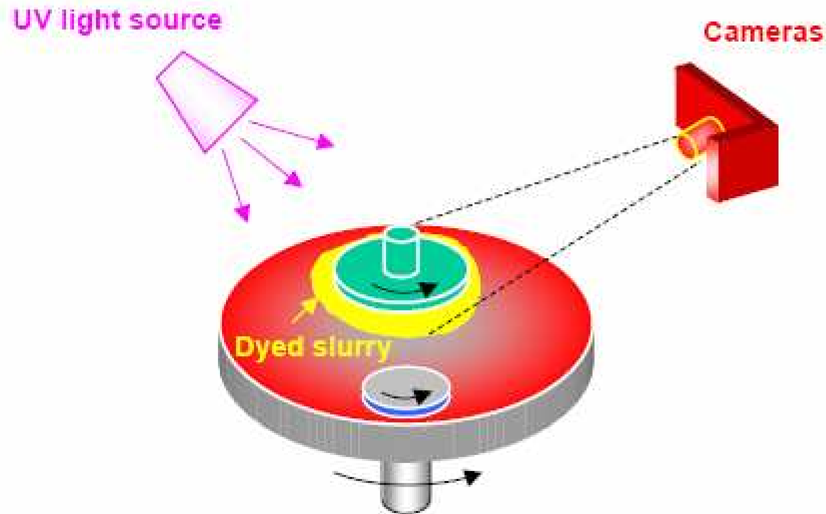

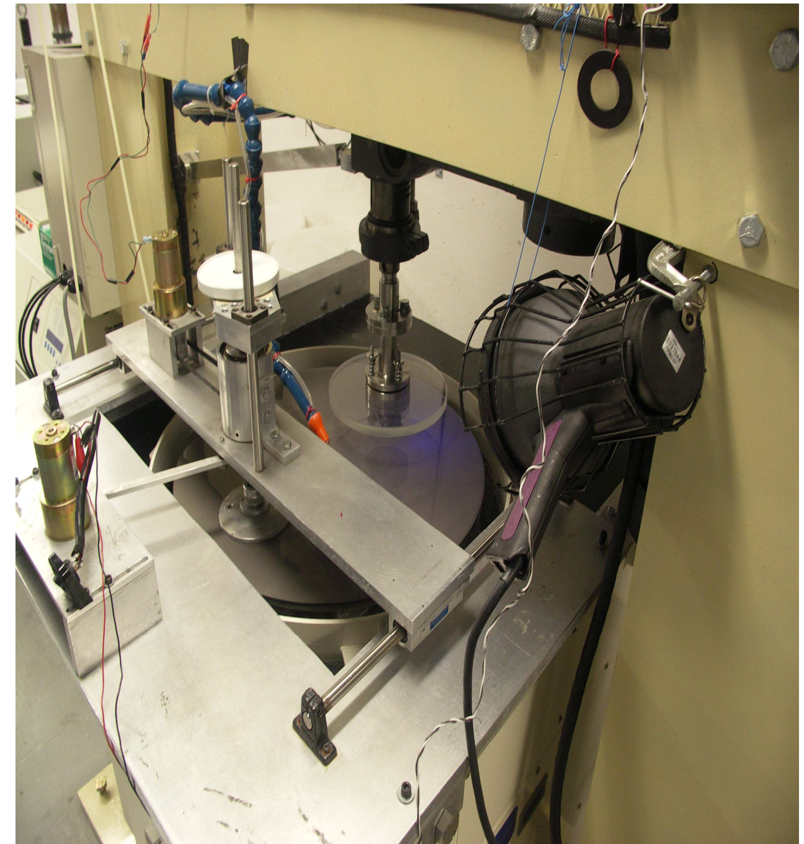

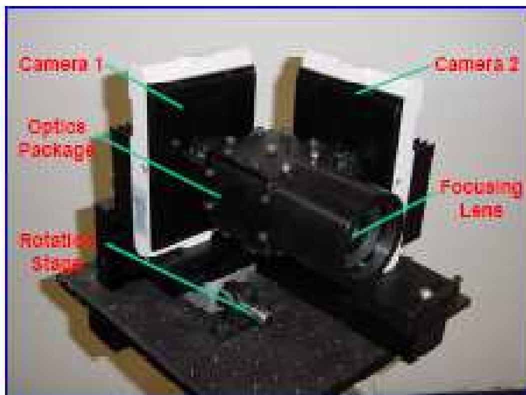

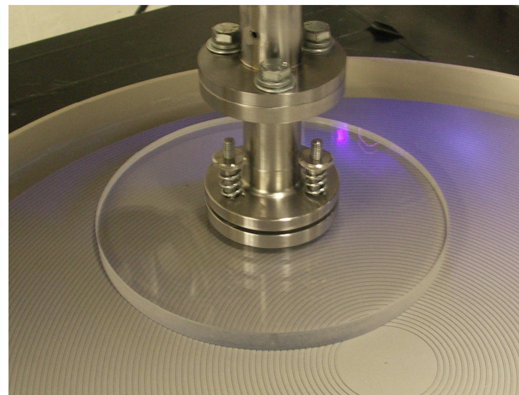

Two CCD cameras are aligned orthogonally and rotationally.

The optics configuration allows each camera to record the exact same spatial image, but in a different color (i.e. different ranges of wave lengths).

Experimental Conditions

- **Constants:**
  - **Pad break-in**
    - **100-grit TBW diamond disc conditioner**
    - **30 min with UPW at 30 rpm disc speed and 20 times per min sweep frequency**
  - **Slurry**
    - **Fujimi PL-7102 slurry with coumarin and calcein dyes**
  - **Wafer**
    - **200-mm quartz wafer**

- **Variables:**
  - **Sliding velocity (m/s)**
    - **0.30**
    - **1.20**
  - **Wafer pressure**
    - **1.0 PSI (6,894 Pa)**
    - **2.0 PSI (13,780 Pa)**
    - **3.0 PSI (20,684 Pa)**
  - **Slurry flow rate**
    - **220 cc/min**
    - **165 cc/min**
    - **110 cc/min**
  - **Pad groove design**
    - **Concentric Slanted (Minus 30°, Minus 20°, Plus 20° and Plus 30°)**
    - **Concentric (0°)**

Slurry Film Thickness Measurement Area

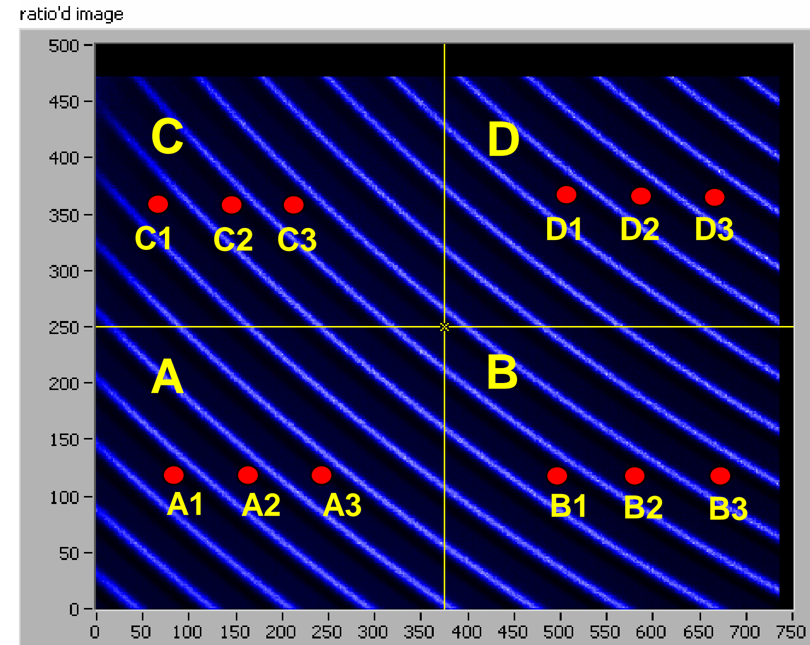

The area analyzed under the wafer is divided into four smaller regions: A, B, C and D.

Regions A & C are close to the wafer edge; Regions B & D are close to the wafer center.

In each region, three sub land areas are analyzed.

Values reported for each region (A, B, C and D) are an average of the three sub land areas.

Effect of Groove Slanting on Slurry Film Thickness

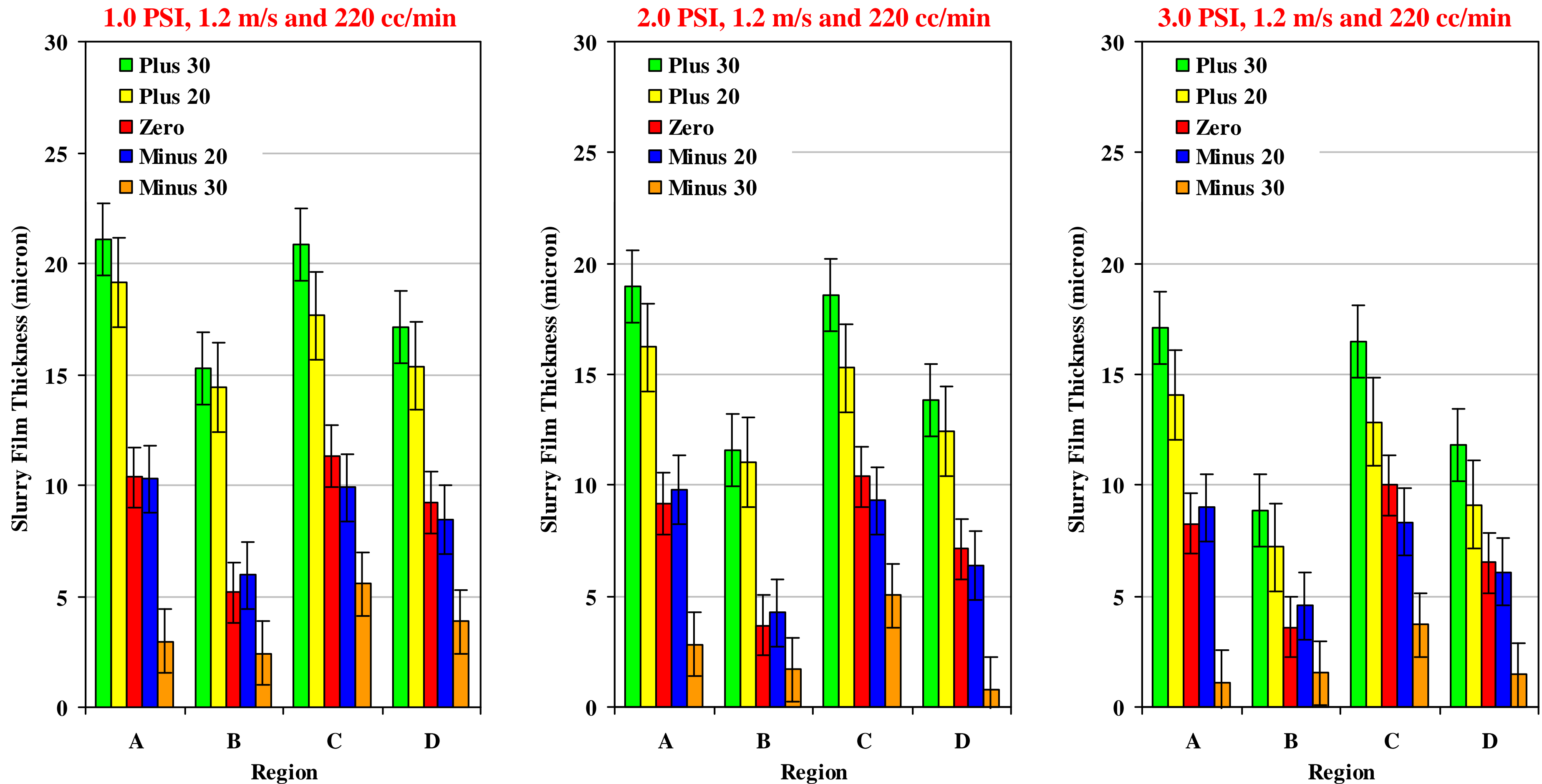

Slanting the grooves towards the edge of the pad (i.e. positive direction) facilitates slurry flow into the pad-wafer interface area.

Slanting the grooves towards the center of the pad (i.e. negative direction) reduces slurry flow into the pad-wafer interface area.

Slurry Film Thickness Contour Plot

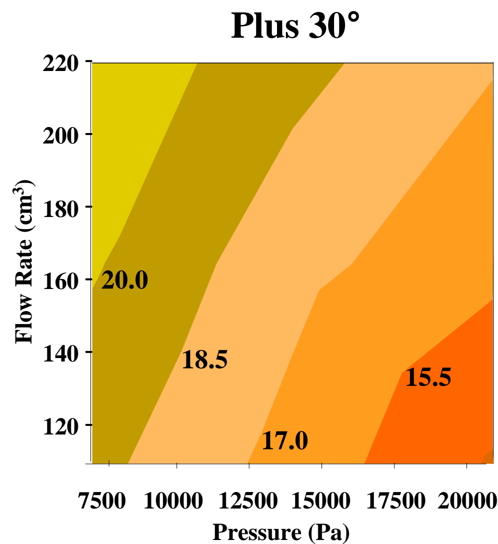

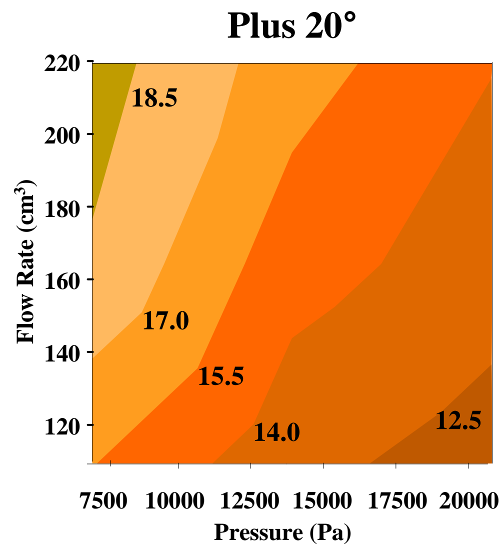

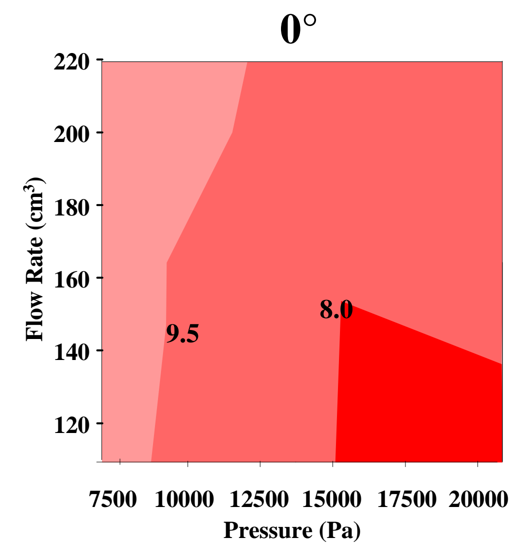

Sliding Velocity = 1.2 m/s

The slurry film thickness generally increases with the flow rate, showing evidence of saturation at higher flow rates.

Higher wafer pressures further compress pad asperities thereby diminishing the slurry flow into the pad-wafer interface area.

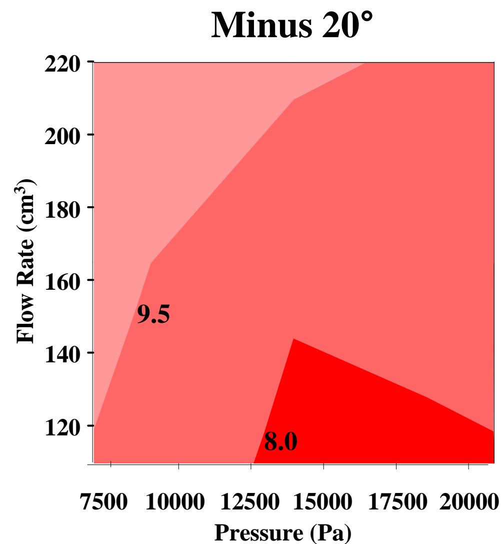

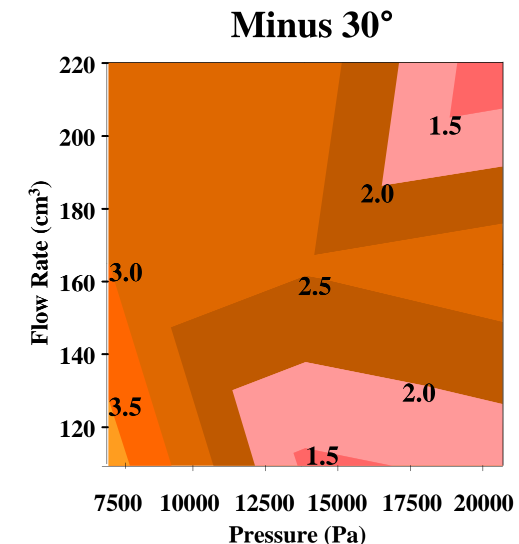

Slurry Film Thickness Contour Plot

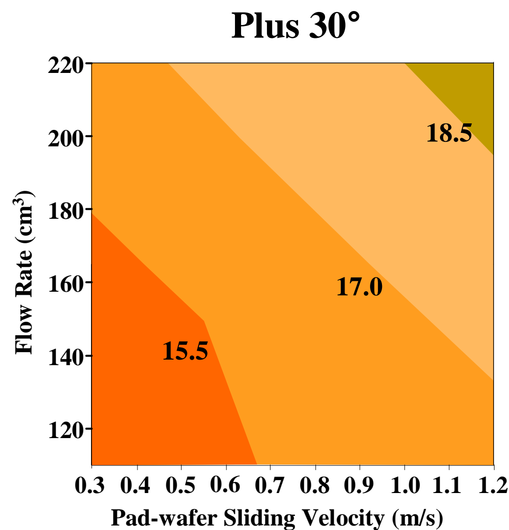

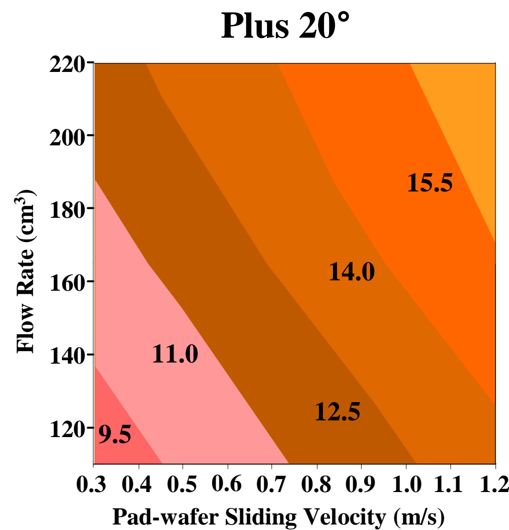

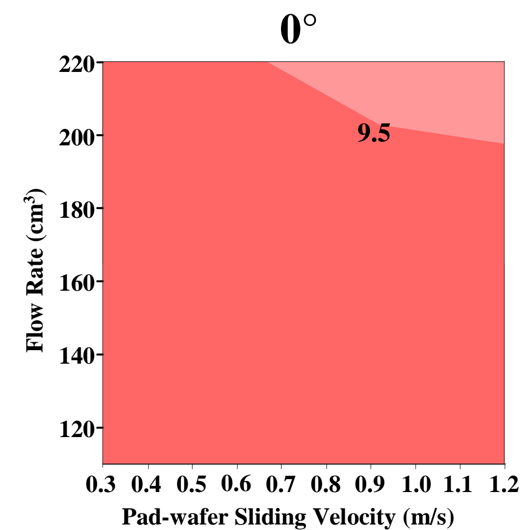

Pressure = 3 PSI

The slurry film thickness generally increases with the flow rate, showing evidence of saturation at higher flow rates.

The slurry film thickness generally increases with the sliding velocity.

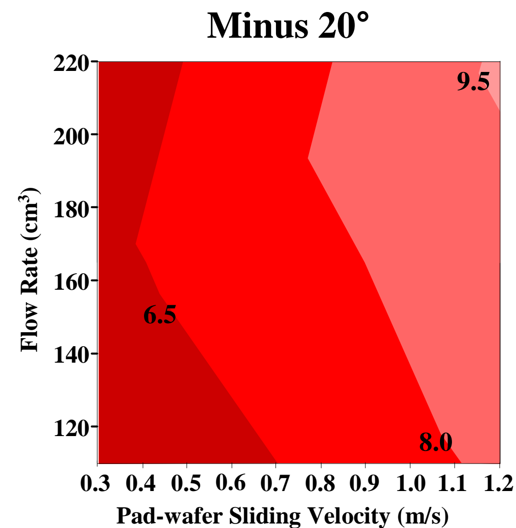

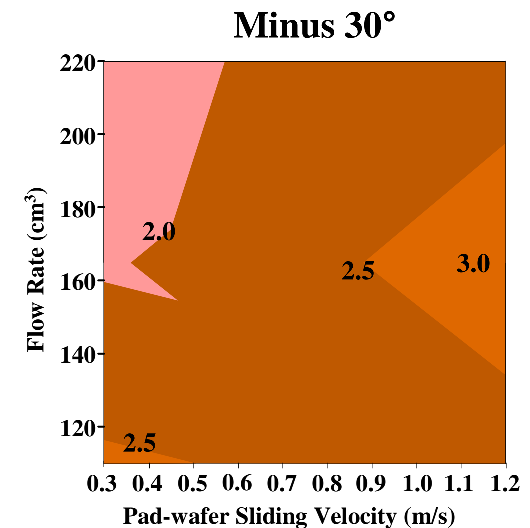

Effect of Groove Slanting on Removal Rate

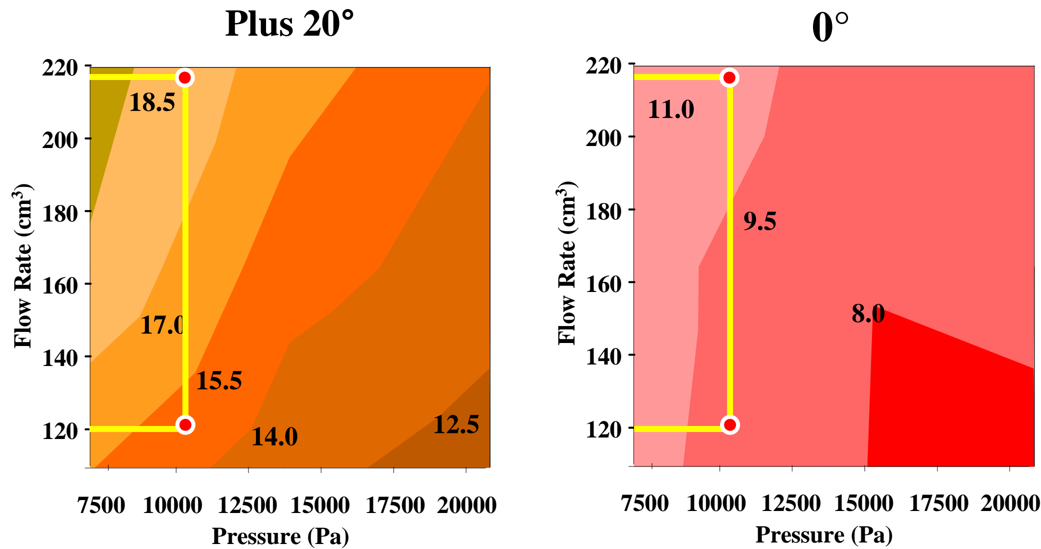

At any given sliding velocity, pressure, and flow rate, the Plus 20° pad shows a higher slurry film thickness at the pad land area compared to the 0° pad. This can have significant pad-wafer contact area ramifications that affect removal rate and defectivity.

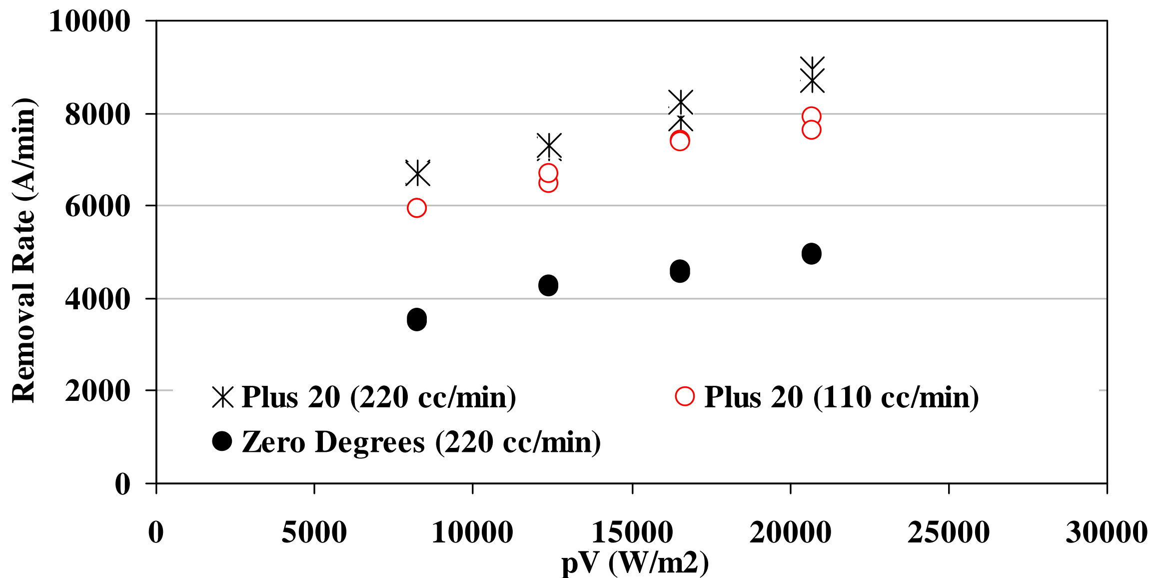

Removal rate slightly decreases as the flow rate is cut by 2X for the Plus 20° pad. However, even at this lower flow rate (110 cc/min), the Plus 20° pad has a significantly higher removal rate than the 0° pad at 220 cc/min.

Industrial Interactions and Technology Transfer

Industrial mentor / contact:

- **Tatsutoshi Suzuki (Toho Engineering)**

Presentation

Effect of Concentric Slanted Groove Patterns on Slurry Flow during Copper CMP. D. Rosales-Yeomans, H. Lee, T. Suzuki and A. Philipossian. SRC 9th Premier TECHCON, September 10-12, Austin, Texas, 2007.